UNIVERSITÄT ZU LÜBECK

FROM THE INSTITUTE OF SYSTEMIC INFLAMMATION RESEARCH

OF THE UNIVERSITY OF LÜBECK

DIRECTOR: PROF. DR. MED. JÖRG KÖHL

# Anaphylatoxin receptors as regulators of dendritic cell differentiation and function

Dissertation

for Fulfillment of

the Requirements

for the Doctoral Degree

of the University of Lübeck

from the Department of Natural Sciences

Submitted by

Alicja Anna Nowacka

From Bytów

Lübeck 2025

First referee: Prof. Dr. med. Jörg Köhl

Second referee: Prof. Dr. rer. nat. Kathrin Kalies

Date of oral examination: April 29, 2026

Approved for printing. Lübeck, April 30, 2026

# Contents

# Summary

Conventional dendritic cell type 1 (cDC1) and 2 (cDC2) are innate sentinels sensing pathogen-associated molecular patterns (PAMPs) or danger-associated molecular patterns (DAMPs) to instruct distinct T cell responses. They derive from distinct bone marrow (BM) residing progenitor cells through a sophisticated ontogenetic program orchestrated by different growth factors. The role of complement in this process has not been explored.

First, I determined the numbers of monocyte DC progenitor (MDP) and common DC progenitor (CDP) progenitors in BMs of wildtype (WT), C3aR and C5aR1-deficient mice. An important first result of my thesis was the significantly reduced number of MDPs and CDPs in BMs from *C5ar1*$^{-/-}$ but not *C3ar1*$^{-/-}$ mice, demonstrating a previously unrecognized role for C5aR1 as a regulator of MDP and CDP homeostasis. Single-cell transcriptomic analysis of MDPs showed the expression of several signature genes of MDPs and pre-cDC subsets. Importantly, I identified the upregulation of the *CD300c* gene in several MDP clusters from *C5ar1*$^{-/-}$ as compared to WT mice. This molecule defines a BM pro-cDC2 progenitor, exclusively generating a cDC2 subset critical for humoral immune responses to T cell-dependent antigens suggesting an important role for C5aR1 in cDC2 subset differentiation. In line with this view, combined GM-CSF and Flt3L stimulation of MDPs or CDPs resulted in differentiation of two CD11c$^{hi}$MHCII$^{hi}$CD11b$^{+}$ cDC subsets that were either CD172$^{+}$ or CD172$^{-}$. The cDC subsets showed as distinct autonomous C3 and C5 production, C3a and C5a generation as well as C3aR and C5aR1 expression. This was associated with the suppression of CD172$^{-}$ cDC generation from C5aR1-deficient and early CD172$^{+}$ cDC generation from C3aR-deficient as compared to WT CDPs suggesting an autocrine complement loop controlling the differentiation of the two DC subsets. Further, I found that CD172$^{-}$ and CD172$^{+}$ cDCs, differentiated from MDPs of *C3ar1*$^{-/-}$ or *C5ar1*$^{-/-}$ mice, differed in their frequency and expression levels of different costimulatory molecules and their production of pro-inflammatory cytokines in response to T cell-dependent antigen stimulation resulting in altered T cell responses. Together my findings uncover a novel autocrine, intracellular complement loop shaping the differentiation and function of two distinct cDC subsets differentiated from BM precursors.

To complement my research on the differentiation and function of cDCs from CPDs or MDPs in vitro, I assessed the influence of the C5a/C5aR1 axis on Flt3L-induced in vivo mobilization and function of splenic cDC subsets.

To address this question, I injected Flt3L expressing B16 melanoma cells into WT and *C5ar1*$^{-/-}$ mice. Flt3L induced a strong induction and mobilization of cDC1 and cDC2 cells into the spleen independent of C5aR1 expression. Ovalbumin stimulation ex vivo resulted in strong effector T cell (TEFF) and less effector memory T cell (TEM) generation by cDC2, which was markedly reduced in cDC2s from *C5ar1*$^{-/-}$ as compared to WT mice at low ovalbumin concentration. Surprisingly, TEFF and TEM generation was absent using cDC1 cells. Additional LPS or PAM3 challenge of cDC2 cells from either WT or *C5ar1*$^{-/-}$ mice increased the dominant TEFF cell differentiation. In contrast, TEM and TEFF induction was similar using cDC1 cells from WT or C5aR1-deficient mice. Strikingly, I found a strong and dominant IFN-γ production upon wildtype cDC2

cell stimulation with OVA ± TLR ligands and OT-II cell co-coculture, which was significantly reduced using *C5ar1*$^{-/-}$ cDC2 cells.

My findings suggest that cDC2 but not cDC1 cells are critical for antigen-driven T cell proliferation and TEFF differentiation in the absence of TLR ligands. Further, C5aR1 activation seems to be crucial for this effect at low but not at high antigen concentration. Also, while C5aR1 activation did not affect TEFF or TEM cell differentiation induced by cDC1 or cDC2 following OVA ± TLR ligand stimulation, it controlled the dominant Th1 induction mediated by cDC2 cells. Thus, I identified a novel role for C5aR1 in antigen-driven TEFF/Th1 differentiation by splenic cDC2 cells in response to pattern recognition receptor activation.

# Zusammenfassung

Konventionelle dendritische Zelltypen 1 (kDZ1) und 2 (kDZ) sind Wächterzellen des angeborenen Immunsystems, die pathogen- oder schadstoffassoziierte molekulare Muster (PAMPs bzw. DAMPs) erkennen und unterschiedliche T-Zell-Antworten steuern. Sie stammen aus unterschiedlichen Vorläuferzellen im Knochenmark (KM) und durchlaufen ein komplexes ontogenetisches Programm, das von verschiedenen Wachstumsfaktoren reguliert wird. Die Rolle des Komplementsystems in diesem Prozess wurde bisher nicht untersucht.

Zunächst habe ich die Anzahl der Monozyten-DC-Vorläuferzellen (MDP) und der gemeinsamen DC-Vorläuferzellen (CDP) im Knochenmark von Wildtyp- (WT), C3aR- und C5aR1-defizienten Mäusen bestimmt. Ein wichtiges erstes Ergebnis meiner Arbeit war die signifikant reduzierte Anzahl von MDPs und CDPs im Knochenmark von *C5ar1*$^{-/-}$ Mäusen, jedoch nicht von *C3ar1*$^{-/-}$ Mäusen, was eine bisher unbekannte Rolle von C5aR1 als Regulator der MDP- und CDP-Homöostase aufzeigt. Die Einzelzelltranskriptomanalyse von MDPs zeigte die Expression von mehreren Signaturgenen von MDP und prä-kDZ Subtypen. Nenneswerterweise konnte ich die Hochregulation von *CD300c* in mehreren Zellclustern von *C5ar1*$^{-/-}$ MDPs sehen, Dieses Molekül definiert eine KM-pro-kDZ2 Vorläuferpopulation, die entscheidend für die Entwicklung humoraler Immunantworten gegen T-Zell-abhängige Antigene ist, was auf eine wichtige Rolle des C5aR1 bei Differenzierung dieser kDZ Population hindeutet. Im Einklang mit dieser Sichtweis führte die gleichzeitige Stimulation von MDPs oder CDPs mit GM-CSF und Flt3L zur Differenzierung zweier CD11c$^{hi}$ MHCII$^{hi}$ CD11b$^{+}$ kDZ-Subsets, die entweder CD172a$^{+}$ oder CD172a$^{-}$ waren. Diese kDZ Subsets zeigten eine jeweils unterschiedliche autokrine C3- und C5-Produktion, Generierung von C3a und C5a sowie Expression von C3aR und C5aR1. Dies war verbunden mit der Suppression der CD172a$^{-}$ kDZ-Differenzierung aus C5aR1-defizienten und der frühen Differenzierung von CD172a$^{+}$ kDZ aus C3aR-defizienten im Vergleich zu WT CDPs, was für eine autokrinen Komplement-vermittelten Mechanismus spricht, der die Differenzierung der beiden kDZ-Subsets kontrolliert. Weiterhin konnte ich nachweisen, dass CD172a$^{-}$ und CD172a$^{+}$ kDZ, die aus MDPs von *C3ar1*$^{-/-}$ oder *C5ar1*$^{-/-}$ Mäusen differenziert wurden, sich in ihrer Häufigkeit, der Expression verschiedener kostimulatorischer Moleküle und der Produktion proinflammatorischer Zytokine auf T-Zell-abhängige Antigen-Stimulation hin unterschieden, was zu veränderten T-Zell-Antworten führte. Zusammengenommen zeigen meine Ergebnisse eine neue autokrine intrazelluläre Komplementaktivierung während der kDZ Differenzierung von MDPs und CDPs, die die Entwicklung zweier unterschiedlicher kDZ Subsets und ihrer Funktion reguliert.

Zur Ergänzung meiner Untersuchungen zur Differenzierung und Funktion der kDZ Subsets aus MDP oder CDPs in vitro, untersuchte ich zusätzlich den Einfluss der C5a/C5aR1-Achse auf die FLt3L-induzierte in vivo-Mobilisierung von kDZ Subsets in die Milz und ihre Funktion.

Zur Beantwortung dieser Fragestellung injizierte ich subkutan FLt3L-exprimierende B16-Melanomzellen in WT und *C5ar1*$^{-/-}$ Mäuse. Flt3L führte zu einer starken Induktion und Mobilisierung von kDZ1 und kDZ2 in die Milz unabhängig von der C5aR1-Expression. Die ex vivo OVA-Stimulation von WT kDZ2 führte zu einer starken Bildung

von Effektor T Zellen (TEFF) und einer geringeren Effektor-Gedächtniszellen (TEM) Differenzierung, welche bei kDZ von *C5ar1*$^{-/-}$ Mäusen bei niedriger Ovalbuminkonzentration deutlich vermindert war. Überraschenderweise blieb die TEFF- und TEM-Bildung bei Verwendung von kDZ1 völlig aus. Die zusätzliche LPS oder PAM3-Stimulation von kDZ2 aus WT- oder *C5ar1*$^{-/-}$ Mäusen steigerte die dominante TEFF-Differenzierung. Im Gegensatz dazu zeigte sich eine vergeleichbar starke TEM- und TEFF-Induktion bei Verwendung von kDZ1 von WT- oder C5aR1-defizienten Mäusen. Besonders auffällig war die starke und dominante IFN-γ-Produktion nach Stimulation von WT-kDZ2 mit OVA ± TLR-Liganden und OT-II Ko-Kultur, die bei Verwendung von *C5ar1*$^{-/-}$ im Vergleich zu WT kDZ2 deutlich reduziert war.

Meine Ergebnisse deuten darauf hin, dass kDZ2, nicht jedoch kDZ1 Zellen, für die antigengetriebene T-Zell-Proliferation und die TEFF-Differenzierung in Abwesenheit von TLR-Liganden entscheidend sind. Weiterhin scheint die C5aR1-Aktivierung bei niedrigen, nicht jedoch bei hohen Antigenkonzentrationen wesentlich für diesen Effekt zu sein. Während die C5aR1-Aktivierung die TEFF- oder TEM-Zelldifferenzierung durch cDC1 oder cDC2 nach OVA ± TLR-Ligand-Stimulation nicht beeinflusste, kontrollierte sie die dominante Th1-Induktion, die durch kDZ2 vermittelt wird. Somit konnte ich eine neue Funktion des C5aR1 in der antigen-vermittelten TEFF/Th1-Differenzierung durch kDZ2 der Milz als Reaktion auf die Aktivierung von Mustererkennungsrezeptoren identifizieren.

# 1. Introduction

## 1.1 The immune system

The term 'immunity' derives from the Latin word *immunis*, meaning 'exempt,' which in this context refers to exemption from infection. The earliest documented reference to the concept of protection from reinfection following a primary infection dates back to 430 BC, when Thucydides observed that individuals who had recovered from the Athenian plague were able to care for the sick without contracting the disease again[1]. Louis Pasteur is widely regarded as the father of immunology. His groundbreaking work in the late 19th century on the germ theory of disease, along with the notion that infectious diseases could be prevented through prophylactic vaccination, firmly established his legacy in the foundation of immunology[2].

The immune system comprises a diverse array of cell types, organs, proteins, and tissues distributed throughout the body, playing a fundamental role in maintaining physiological integrity. To fulfill this function, it must detect and eliminate potential threats through specialized recognition mechanisms. The immune system relies on pattern recognition receptors (PRRs), such as Toll-like receptors (TLR), to sense both, external pathogens and internal danger signals from injury or cell death. These receptors have likely co-evolved to detect diverse threats, enabling immune responses that not only eliminate pathogens but also clear damaged cells and support tissue repair[3-5].

Many of the immune cells not only arise from the bone marrow (BM) but also develop and mature there as well. The main immune cells are B and T lymphocytes, natural killer (NK) cells, macrophages, monocytes, dendritic cells (DCs), innate lymphoid cells (ILC), eosinophils, neutrophils, basophils, and mast cells (MC), which can be further divided into sub-categories[6].

After maturation, immune cells migrate from primary lymphoid organs to peripheral tissues, where some remain resident while others circulate through the blood and lymph. The lymphatic system, a specialized vessel network spanning the body, plays a key role in draining extracellular fluid and supporting immune cell trafficking[6].

During migration through the lymphatic system, immune cells accumulate in secondary lymphoid organs such as the lymph nodes and spleen. These organs act as key sites for antigen processing and immune coordination, enabling communication among diverse immune cell populations to mount effective protective responses.

Immune defense can be divided into three layers based on timing, duration, cell types, and specificity: (1) anatomical and physiological barriers, (2) the innate immune system, and (3) the adaptive immune system[7,8] (**Fig. 1.1**). The first line of defense consists of physical and chemical barriers, including the skin, mucosal surfaces of the respiratory and gastrointestinal tracts, secretions from sweat and saliva glands, acidic stomach pH, and antimicrobial molecules such as lysozyme in tears, saliva, and milk[9]. These mechanisms help prevent pathogen entry and eliminate residual threats at barrier sites. If pathogens breach these defenses, the innate and adaptive immune systems act in coordination through cellular and humoral responses to recognize and clear the invaders (**Fig. 1.1**).

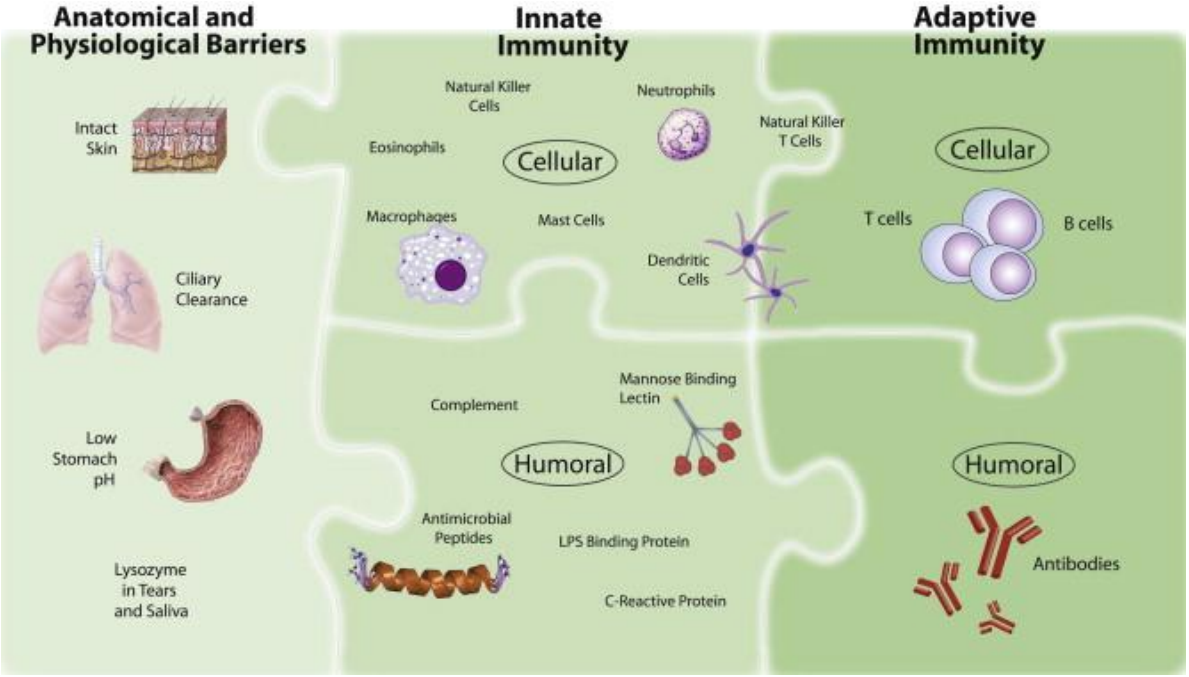


**Figure 1.1 Overview of the integrated human immune system.** This schematic illustrates the hierarchical organization of the human immune defense, which can be broadly divided into three interconnected layers: anatomical and physiological barriers, innate immune mechanisms, and adaptive immune responses. While this framework provides a useful structural overview, several immune cell populations exhibit overlapping characteristics that challenge strict categorization. In particular, natural killer T (NKT) cells and DCs display both innate and adaptive features, positioning them at the interface between these two branches of immunity and highlighting the integrated nature of host defense[10].

When faced with a threat, the immune system mounts a response through cellular and humoral mechanisms. Depending on the organism, this defense may consist solely of innate immunity, present across primitive and advanced species, or a combination of innate and adaptive immunity, which is characteristic of more evolutionarily advanced organisms. Innate immunity relies on germline-encoded receptors that recognize conserved pathogen-associated or damage-associated signals. In contrast, adaptive immunity depends on the somatic generation of clonally diverse lymphocytes, each expressing unique antigen receptors[11]. Despite these differences, both systems can establish immunological memory in response to exogenous threats, enabling faster and more specific responses upon re-exposure. This memory is particularly evident in long-lived immune cells such as microglia[12] and plasma cells[13]. The following sections will examine innate and adaptive immunity, as well as the mechanisms of immunological memory, in greater detail.

### 1.1.1 The innate immune system

Innate immunity represents the most ancient form of host defense, present in all multicellular organisms, whereas adaptive immunity arose later and is restricted to higher vertebrates[14]. The foundations of innate immunity were laid in 1884, when Élie Metchnikoff, studying starfish larvae, discovered phagocytes, cells that protect the host by engulfing foreign particles and microorganisms, thus establishing the foundation of our understanding of host defense[15]. This groundbreaking work earned him the 1908 Nobel Prize, recognizing the discovery of phagocytes and the process of phagocytosis as a cornerstone in the understanding of innate immunity[16,17].

The innate immune system is present from birth and can undergo antigen-specific modifications during infection[18]. It plays a fundamental role in preserving cellular integrity, tissue homeostasis, and overall survival[19,20]. Beyond maintaining homeostasis, innate immunity provides the first line of defense against pathogens, malignant cells, and toxins, acting before the adaptive response is engaged. Initially, it has been described as rapid, non-specific, non-adaptive, and lacking immunological memory[21].

The innate immune system is generally recognized to perform three essential functions: (1) detecting a wide range of threats, (2) neutralizing or mitigating them once recognized, and (3) maintaining tolerance to self-structures and non-pathogenic foreign entities[22,23]. Conceptually, it can be divided into two main components: the sensing (afferent) arm, responsible for detecting aggression such as pathogens, and the effector (efferent) arm, which mediates elimination or tolerance of the threat. Both arms rely on a combination of anatomical barriers, cellular elements, and humoral factors.

The innate immune system is composed of barrier structures, effector molecules, and innate immune cells. It comprises of four main components. (1) Physical and chemical barriers provide the first layer of defense and detect invading pathogens or abnormalities. (2) Cellular elements include macrophages, DCs, monocytes, NK cells, ILCs, granulocytes (eosinophils, neutrophils, basophils), and MCs. (3) Humoral factors such as the complement system contribute to pathogen clearance, and (4) cytokines and chemokines mediate communication and immune coordination. This multifactorial system is essential not only for recognizing danger signals but also for mounting the first line of defense. During infection or injury, inflammation is triggered by mediators released from resident or recruited immune cells, which both contain pathogen spread and promote pathogen clearance and tissue repair[3,6,24] (**Fig. 1.2**).

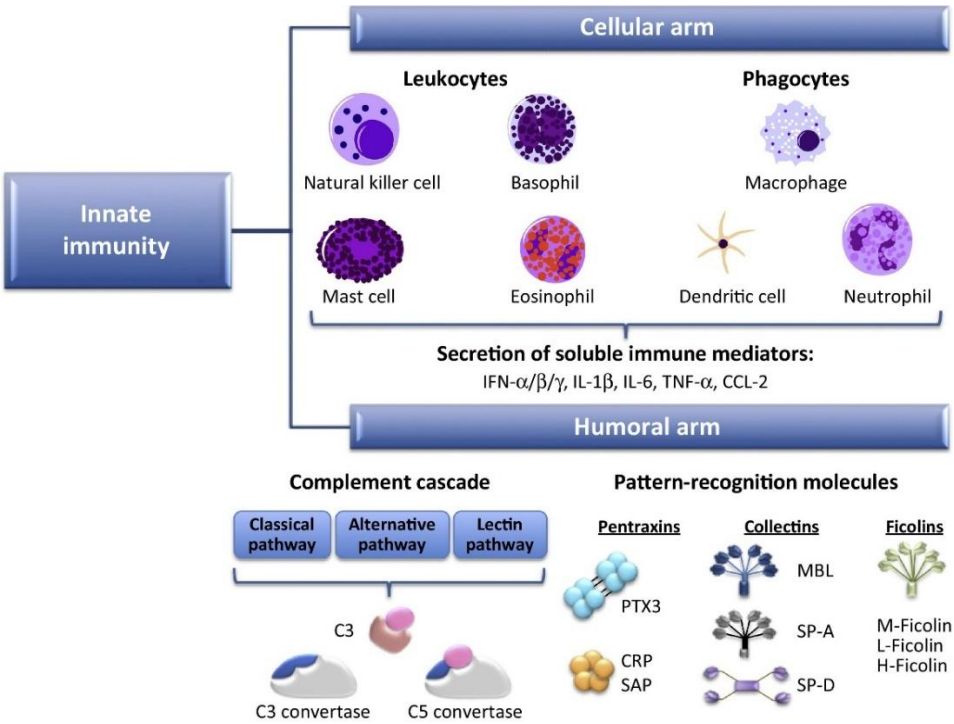

**FIGURE 1.2 Scheme of the two components of innate immunity: cellular and humoral responses.** The cellular component consists of immune cells such as leukocytes and phagocytes, along with the mediators they release. The humoral component includes the complement system and pattern-recognition molecules (PRMs). Interaction between these two components is essential for rapid response to threats and for facilitating the activation of adaptive immunity[25].

Acute inflammation is initiated by tissue-resident cells that express PRRs. These receptors detect PAMPs, conserved across microbes, as well as DAMPs released by injured cells. Four major PRR families have been identified: transmembrane receptors such as TLRs and C-type lectin receptors (CLRs), and cytoplasmic receptors including NOD-like receptors (NLRs) and RIG-I-like receptors[26]. PRRs are expressed not only on professional immune cells, such as DCs and macrophages, but also on nonprofessional immune cells, enabling broad pathogen and environmental sensing. Many PRRs also deliver potent maturation signals, though their role is complex since ligands are not exclusive to pathogens but may also derive from commensals or host tissues. How DCs interpret these signals to maintain immune homeostasis in steady state remains incompletely understood[24,26]. This dual capacity of PRRs, to induce activation while preserving tolerance, underscores the complexity of innate immune regulation[23].

Innate immunity, traditionally viewed as nonspecific and the first line of defense before the adaptive response in vertebrates, has been shown to be far more versatile than previously thought. Many organisms rely solely on innate immunity to combat diverse pathogens, and some can even develop a form of immunological memory. For instance, insects display immune priming, where exposure to non-lethal doses of bacteria confers protection against subsequent infections. This protection can range from broad-spectrum to highly pathogen-specific and may persist throughout the insect's lifespan[27].

The fruit fly *Drosophila melanogaster* has been instrumental in uncovering mechanisms of innate immune memory. During viral infection, haemocytes, circulating immune cells, phagocytose microbes, secrete antimicrobial peptides, and generate small interfering RNAs (siRNAs) from viral double-stranded RNA (dsRNA). Remarkably, they also produce circular viral DNA through a reverse-transcriptase-dependent process, which serves as a template for the amplification of virus-derived small RNAs (vsRNAs) in an Ago2-dependent manner[28,29]. These vsRNAs are packaged into exosome-like vesicles and distributed systemically, where they are processed into siRNAs and incorporated into RNA-induced silencing complexes. Importantly, exosomes from infected flies can transfer long-lasting, pathogen-specific protection to naïve flies, demonstrating a form of passive antiviral immunity[29,30].

This evidence highlights that even in the absence of an adaptive immune system, organisms like *Drosophila* can mount efficient, specific, and durable immune responses through alternative innate mechanisms.

### 1.1.2 The adaptive immune system

Adaptive immunity, the second arm of the immune system, was discovered around the same time as innate immunity. Paul Ehrlich, often regarded as the father of humoral adaptive immunity, demonstrated that immunization with foreign proteins, such as

animal-derived proteins or bacterial toxins, induces the production of protective antibodies detectable in the blood[16]. The earliest evidence of adaptive immunity comes from jawless vertebrates, which develop lymphocyte-like cells resembling T and B cells. Antigenic stimulation in these species significantly influences both humoral and cellular immune responses[31-33]. Compared to innate immunity, adaptive immunity, also called the acquired response, is slower to initiate but provides highly specific recognition and long-lasting memory. It is broadly divided into two branches: (1) the humoral response, mediated by antibodies produced by B cells, and (2) the cellular response, mediated by T and B lymphocytes and their antigen-specific receptors[7].

A defining feature of adaptive immunity is the capacity of T and B lymphocytes to undergo genetic rearrangements, enabling specific recognition of antigens[18]. These cells form the core of the adaptive immune system: T cells mediate cellular immunity by defending the body against pathogens such as viruses and bacteria, B cells drive humoral immunity, and together they generate long-lasting immunological memory, ensuring durable protection against future infections. T cells are characterized by their surface TCRs, which enable them to recognize specific antigens presented by other cells, a recognition critical for initiating and coordinating immune responses[6,13].

Both B and T lymphocytes carry specialized antigen receptors. In B cells, these receptors, known as B cell receptors (BCRs), take the form of immunoglobulins and can exist as either transmembrane receptors or secreted antibodies. T cells, in contrast, express T cell receptors (TCRs) exclusively as transmembrane proteins. These receptors enable lymphocytes to detect antigens in their environment. Antigen recognition is mediated by the variable (V) region of the receptor, which exhibits amino acid sequence diversity essential for high antigen specificity. The V region is linked to a constant (C) region, which provides effector and signaling functions. Each lymphocyte displays numerous copies of a receptor with a unique antigen-binding site. Lymphocytes are among the most abundant immune cells, with billions present in each individual, allowing the immune system to recognize a vast array of antigens. This immense receptor diversity is achieved through a sophisticated genetic mechanism, as it would be impossible to encode each receptor fully in the genome, given the number of receptor variants far exceeds the total number of genes in the genome[6,23,34-36].

To overcome the challenge of generating a vast repertoire of antigen receptors, lymphocytes employ a process called gene rearrangement. In this mechanism, the V region of the receptor is encoded in multiple gene segments, which are somatically recombined during lymphocyte development to form a complete V region sequence. This process occurs in both T and B cells. In B cells, however, the immunoglobulins undergo additional modifications to enhance the antibody response. One such modification is somatic hypermutation, in which point mutations are introduced into the V region of activated B cells. This results in progressively stronger antigen binding, a process known as affinity maturation, which develops as the immune response advances[6].

However, these modifications are not limited to the V region, at least in the case of antibodies. For TCRs, the primary role of the C region is to support the V region and

anchor the receptor in the cell membrane, so no further modifications are needed. In contrast, immunoglobulins have a more versatile function. As noted earlier, antibodies can exist either as membrane-bound receptors or as secreted molecules. In secreted antibodies, the C region plays a crucial role in mediating diverse effector functions. Antibodies are produced in multiple classes, and they acquire these functional differences through a process called class switching, which alters the C region while retaining the same antigen specificity. Class switching allows antibodies to maintain their target recognition while gaining distinct functional properties[6,34,36].

To generate specific immune responses, lymphocytes must first recognize antigens and become activated. Both B and T cells undergo activation in secondary lymphoid organs. T cells, however, can only recognize antigens that are presented on the surface of antigen-presenting cells (APCs), such as DCs. Importantly, T cells do not recognize the entire antigen, but rather small peptide fragments derived from the pathogen's proteins[37,38]. These peptide fragments are displayed on the cell surface bound to a family of glycoproteins called major histocompatibility complex (MHC) molecules, which are encoded by a large cluster of genes[39]. There are two main classes of MHC molecules: MHC-I and MHC-II[40]. MHC-I molecules present peptides derived from cytosolic proteins and are recognized by $CD8^+$ T cells. Nearly all nucleated cells can present antigens via MHC-I, with a few exceptions such as erythrocytes. In contrast, MHC-II molecules present peptides to $CD4^+$ T cells. $CD4^+$ and $CD8^+$ T cells carry out distinct functions, each specialized in defending the host against different types of pathogens[6,40,41].

However, T cell activation is not achieved solely through TCR recognition of MHC-bound peptides. A second signal, known as the co-stimulatory signal, is also required. This signal arises from interactions between co-stimulatory molecules on the surface of APCs and corresponding receptors on T cells. Key co-stimulatory molecules on APCs include CD40, OX40L, CD80, and CD86, which interact with CD40L, OX40, and CD28 on T cells to fully activate them[38].

B lymphocytes, as well as DCs, not only recognize intact antigens derived from pathogens but also function as APCs. When a BCR binds an antigen, the antigen is internalized, processed, and presented on the B cell surface as peptide fragments bound to MHC-II molecules**.** T helper (Th) cells recognize these MHC-II–peptide complexes through their TCRs. Following this recognition, T cells express CD40 ligand (CD40L) and secrete cytokines. CD40L provides a critical co-stimulatory signal by engaging CD40 on the B cell surface, promoting B cell activation. This interaction drives B cell proliferation, immunoglobulin class switching, somatic hypermutation and supports T cell growth and differentiation. Once these signals are received, B cells are fully activated[34] (**Fig. 1.3**).

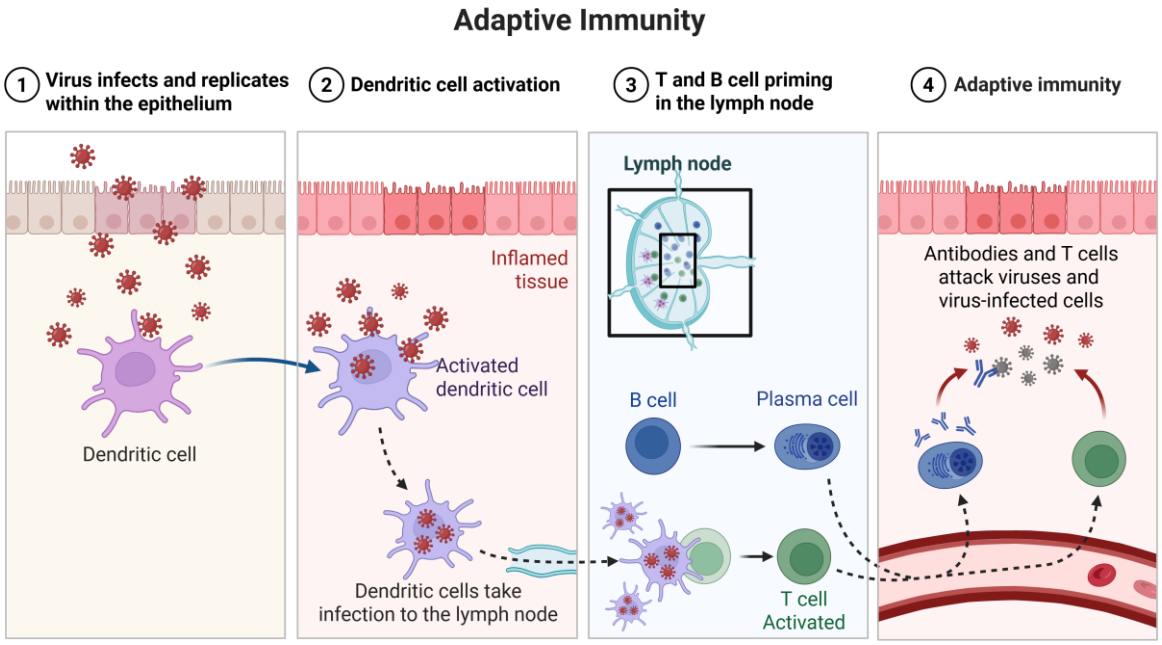


**Figure 1.3 Schematic illustration of the adaptive immune response to viral infection.** This illustration shows the stepwise progression of adaptive immune defenses that occur in response to viral infection. (1) The process begins when a virus infects epithelial cells and replicates within the tissue. (2) DCs capture viral antigens and become activated, migrating toward the lymphatic system. (3) Within the draining lymph node, antigen-bearing DCs interact with and prime naive T and B cells, leading to their activation and differentiation. (4) The final phase involves effector mechanisms, where activated T cells and antibody-producing plasma cells circulate to eliminate viruses and virus-infected cells, thereby providing targeted immune protection (adapted from *Biorender.com*).

## 1.2 Dendritic cells

DCs, named for their mature cells bearing numerous dendritic or pseudopodial processes, were identified as a distinct cell type within the peripheral lymphoid structures of mice, including the spleen, lymph nodes, and Peyer's patches[42,43] by Ralph Steinman in 1973. Steinman received the Nobel Prize in Physiology or Medicine in 2011 for the discovery of the DCs and their role in adaptive immunity. DCs are characterized by their irregular shape, large nuclei and star-like cellular extensions. DCs are BM-derived and produced by the lymphoid-myelopoietic system.

### 1.2.1 Dendritic cell development

The origin of DCs has been debated in immunology because they are an independent hematopoietic lineage, separate from monocyte-derived cells. Recent findings show that DCs develop from a series of limited-potential precursors that progressively differentiate into distinct subsets, each with unique phenotypic and functional traits, and are found in blood, secondary lymphoid organs and various tissues[44].

Several distinct subsets of DCs have been described that can differentiate from myeloid progenitors and lymphoid progenitors in the BM. The DC subsets migrate from the BM into the peripheral blood and then spread to various tissues throughout the body[45,46]. Depending on their location and stage of differentiation, they display different

phenotypes and functional traits. This widespread presence is crucial for their role in immune surveillance and initiating immune responses upon pathogen detection[6,47].

$CD34^+$ hematopoietic stem cells (HSC) give rise to lymphoid–myeloid progenitors, which retain the capacity to differentiate into both lineages[48,49]. These progenitors further develop into common myeloid progenitors (CMPs) and serve as a source of different myeloid cells [48,49]. The CMPs in turn produce granulocytes, monocytes, and DC precursors (GMDPs). DCs share a common BM progenitor with monocytes, known as the MDP[49,50], which further gives rise to a CDP[51,52]. The CDP differentiate into committed precursors for the conventional DC1 (pre-cDC1) and cDC2 (pre-cDC2) subsets (see below), both of which differentiate in the BM but complete their terminal differentiation in the peripheral tissues[53-56]. Recent studies have shed light on the remarkable diversity within the cDC2 compartment. Multiple subpopulations have been described, with differing nomenclature across studies, such as cDC2A and cDC2B[57-59], or as cDC2 and cDC3[60-65]. The relationship between these subsets remains a topic of debate. While some researchers argue that cDC2B and cDC3 may share overlapping features and markers[63,64], others provide evidence suggesting that DC3s emerge from $Ly6C^+$ MDPs, distinguishing them developmentally from cDCs that arise via CDPs[58,61,63,64]. Another DC subsets, i.e. plasmacytoid DCs (pDCs) originate from CDP[51,52,55] or common lymphoid progenitors (CLP)[66]. Recent findings suggest that pDCs may share a developmental origin with cDCs via a $CX3CR1^+$ $Ly6D^+$ pro-pDC precursor[67]. Another progenitor derived from MDPs, the common monocyte progenitor (cMoP), is specifically committed to differentiate into monocytes and macrophages but not into DCs (**Fig. 1.4**).

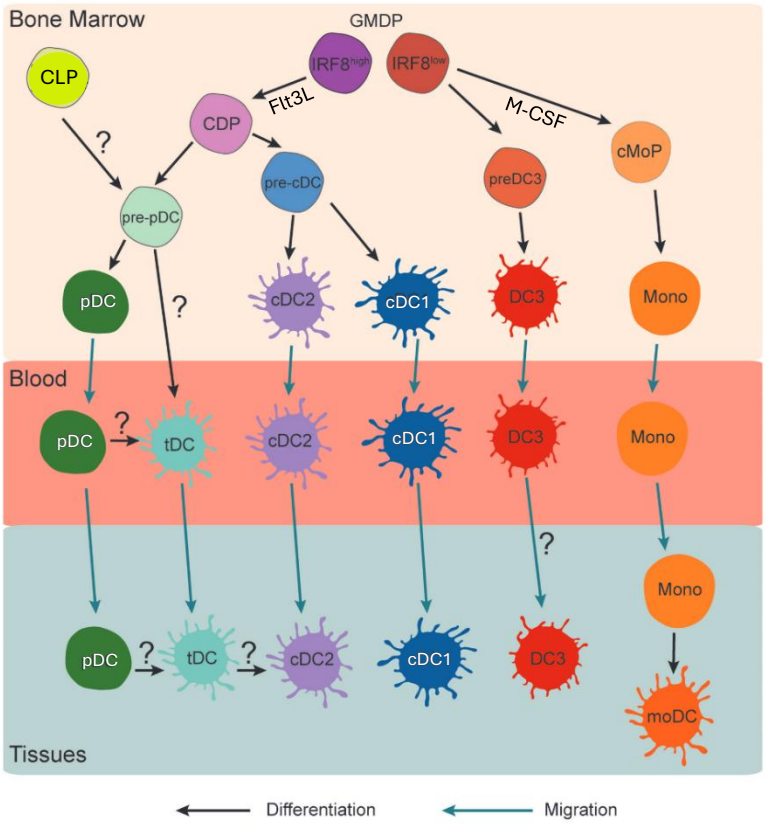


**FIGURE 1.4 Ontogeny of DC subsets.** DC precursors originate in BM and give rise to pDCs, cDC1, cDC2, and DC3 subsets. In contrast, monocyte-derived DC (moDCs) differentiate from

monocytes within peripheral tissues. The developmental pathway of transitional DCs (tDCs) remains poorly defined. Black arrows indicate cell differentiation, while blue arrows represent cell migration. Question marks highlight areas that are not yet fully understood. CDP, common DC progenitor; CLP, common lymphoid progenitor; cMoP, common monocyte precursor; GMDP, granulocyte-monocyte and DC progenitor, mono, monocyte; tDC, transitional DC[68].

The differentiation of DCs is critically dependent on the cytokine Fms-like tyrosine kinase 3 ligand (Flt3L). Studies have shown that mice deficient in either Flt3L[69] or its receptor Flt3[70] exhibit a marked reduction or complete absence of steady-state DC subsets. Conversely, administration of exogenous Flt3L has been demonstrated to significantly expand both the frequency and diversity of DC populations[71]. Administration of Flt3L in both healthy individuals and patients significantly increases the frequency of various DC subsets, with reported expansions of 6–16-fold in pDCs, 48-fold in cDC1, and 130-fold in cDC2[72,73]. Humanized mouse models further confirm Flt3L's essential role in promoting human DC subset differentiation and proliferation[74].

Another cytokine, which is critical for DC survival is granulocyte-macrophage colony stimulating factor (GM-CSF). While GM-CSF–deficient mice exhibit normal levels of lymphoid-resident DCs, mice lacking the GM-CSF receptor (GM-CSFR/CD115) show a threefold reduction in steady-state DCs, a phenotype potentially linked to the absence of the shared β-chain with IL-3 and IL-5 receptors. Elevated GM-CSF levels enhance DC frequencies in the spleen, thymus, and lymph nodes[75].

DC development and associated signature genes expressed in different progenitors such as MDP, CDP, cMoP as well as pre-pDC, pre-cDC subsets, pro-DC3 and monocytes are outlined in **Fig. 1.5**.

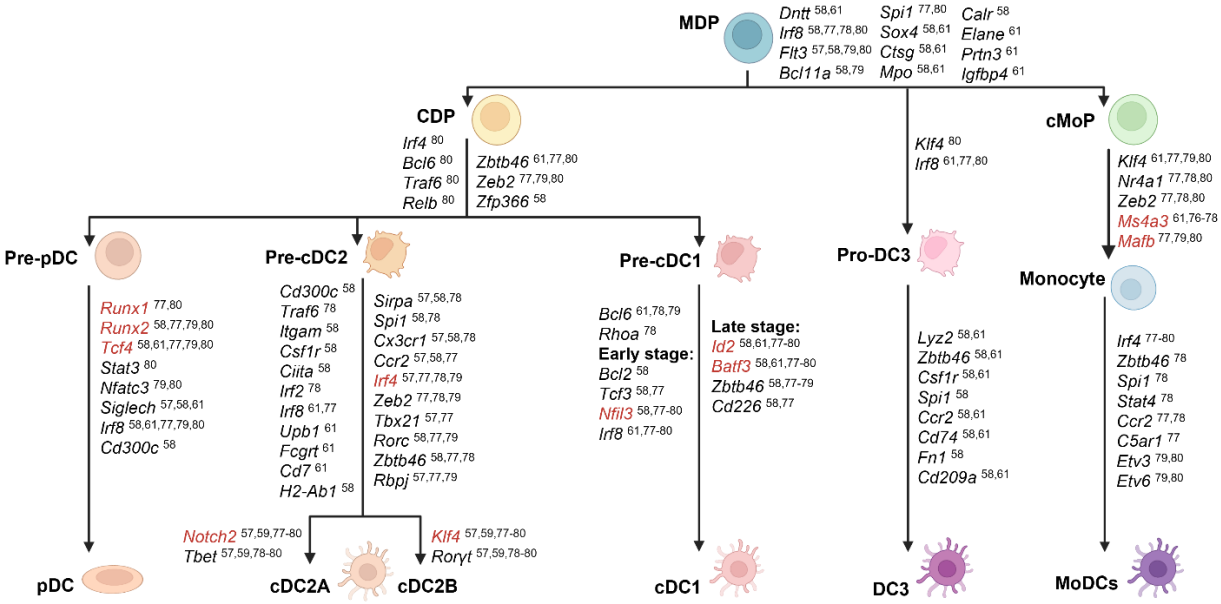


**FIGURE 1.5 Signature genes expressed in different progenitors such as MDP, CDP, cMoP as well as pre-pDC, pre-cDC subsets, pro-DC3 and monocytes[57-59,61,76-80]**. Signature genes exclusively expressed in pre-pDC, pre-cDC1, pre-cDC2 or cMoP are marked in red. The cartoon and the diagram were created with *Biorender.com*.

### 1.2.2 Dendritic cell subtypes

DCs can be divided into two primary subsets: cDCs, which include cDC1 and cDC2, and pDCs[81]. Studies of hematopoietic progenitor and stem cells indicate that both pDCs and cDCs derive from the same progenitor cells, and that their differentiation is controlled by Flt3L[67,82]. DC maturation is driven by Flt3 involving $CX3CR1^{+}$precursors that rapidly differentiate into all DC subsets. Although these progenitors are common, commitment to specific DC lineages is heterogeneous and can occur at multiple stages of hematopoiesis[67].

#### 1.2.2.1 Conventional dendritic cell type 1

Mouse cDC1s are defined by high expression of MHC-II, CD11c and co-expression of either CD8a or CD103, but lack the expression of CD11b and B220. In lymphoid tissues such as the spleen, CD8α marks the lymphoid-resident cDC1 subset[83]. Conversely, CD103 is predominantly expressed by cDC1 in non-lymphoid tissues, including skin, lung, liver and kidney, and is widely regarded as a marker of the migratory cDC1 population[84-88]. Murine cDC1s further express CADM1, Clec9a, and XCR1[83,89]. Of note, Clec9a is present on cDC progenitors and pDCs[90]. Murine cDC1 lack expression of macrophage markers such as F4/80, CD64, CD11b and SIRPα (CD172a)[91], which helps distinguish bona fide cDC1s across different tissues. CD11c expression in cDC1s can vary across tissues and organs; therefore, additional markers such as CD26 and CD24 are valuable for precise identification of this subset in diverse anatomical sites[91].

The differentiation of cDC1s from CDPs is regulated by a network of transcription factors, notably interferon regulatory factor 8 (IRF8)[61,77-80], inhibitor of DNA binding 2 (ID2)[58,61,77-80], and Basic Leucine Zipper ATF-Like Transcription Factor 3 (BATF3)[53,57,58,61,77-80,92]. Recent studies highlight the pivotal role of the Spi-1 proto-oncogene (SPI1 or PU.1) in regulating the DC-SCRIPT gene, thereby influencing and modulating cDC1 differentiation[93,94]. PU.1 is a key transcription factor in early hematopoiesis and in the development of both myeloid and lymphoid lineages. It is an important inducer of Flt3 receptor expression, critical for the DC subset development[95]. cDC1s are characterized by low expression of IRF4 and Zinc Finger E-Box Binding Homeobox 2 (Zeb2), but high expression of Zinc Finger and BTB Domain Containing 46 (ZBTB46)[96]. Further, Notch signaling is essential for the functional maturation of murine cDC1s[97].

While PRR are important for DC maturation, cDC1s exhibit low expression of TLRs as compared with other DC populations, in particular in the circulation[98]. Mouse splenic cDC1s can produce IL-12 in response to TLR3 ligand, Poly (I:C). Interestingly, cDC1s do not express TLR8 but do express TLR4, allowing them to produce inflammatory cytokines upon LPS stimulation[47]. NOD-like receptor family pyrin domain-containing proteins (NLRPs) are key components of innate immunity, mediating inflammasome-driven inflammatory responses. Inflammasome activation triggers caspase-1, which in turn promotes the maturation of IL-1β and IL-18 and induces a form of inflammatory cell death called pyroptosis. Notably, cDC1s exhibit very low expression of several NLRP components, including NLRP1, NLRP2, and NLRP4[99,100].

cDC1s also express high levels of indoleamine 2,3-dioxygenase 1 (IDO1) and IDO2, enzymes involved in immune tolerance and the generation of regulatory T cells

(Tregs)[89]. They exhibit high expression of TLR3 and produce type III interferon (IFN) upon stimulation with Poly (I:C) or natural TLR3 ligands, such as dsRNA[101]. Additionally, cDC1s display a specific repertoire of Fc receptors, which contribute to antigen uptake and the modulation of immune responses. Several in vitro reports have demonstrated that Fc receptor-mediated antigen uptake by DCs enhances cross-presentation in cDC1s.

### 1.2.2.2 Conventional dendritic cell type 2

cDC2s are characterized by high expression of MHC-II, CD11c, CD11b and CD172a. They lack any cDC1-specific markers, including CD8α, XCR1, Clec9a, and CD24, as well as pDC markers such as CD45RA. In contrast, cDC2s can express additional markers, including CD26 and CD4.

cDC2s can exhibit tissue-specific marker expression, such as CD103 in the gut[102-106] and CADM3 in the spleen. Splenic cDC2s can be further subdivided into two subsets based on Clec12A and ESAM expression: Clec12A$^{low}$ESAM$^{high}$ cDC2A and Clec12A$^{high}$ ESAM$^{low}$ cDC2B. Notably, the ESAM$^{low}$ cDC2B subset shows strong similarities to moDCs and displays IRF8-dependent development, a feature not typically associated with cDC2s[78,107,108]. Extensive single cell RNA sequencing (scRNA-seq) studies, including the comprehensive review by Chen et al. (**Fig. 1.6**)[109], have revealed profound heterogeneity within the cDC2 population. This subset can be further divided into distinct lineages, including cDC2A, cDC2B, and the closely related DC3 subset[109]. ScRNA-seq has significantly advanced the understanding of cDC2 heterogeneity. Villani et al.[64] highlighted distinct gene expression profiles within the CD1c$^+$ DC compartment, identifying DC3s that express CD14 and display a "monocyte-like" transcriptional signature characterized by genes associated with both acute and chronic inflammation. In contrast, classical cDC2s shared greater similarity with cDC1s. Building on this, Dutertre et al.[63] proposed that CD14$^+$CD1c$^+$ DC represent a subset within the cDC2 population, distinguishing CD5$^+$ cDC2s as true DC2s and CD5$^-$ cDC2s as DC3s through integrated single-cell protein and RNA analyses. This separation by CD5 expression is supported by findings from Yin et al.[110] and Korenfeld et al.[111]. In murine splenic DC, scRNA-seq similarly revealed two cDC2 subtypes segregated by exclusive expression of the transcription factors T-bet and RORγt, associated with pro- and anti-inflammatory functions, respectively[59]. Beyond intrinsic cellular heterogeneity, significant interindividual variability in cDC2 phenotypes and subset distribution was documented through single-cell transcriptomics, differing more markedly compared to other DC subsets. Moreover, these heterogeneities and variations complicate the comprehensive understanding of the cDC2 lineage family (**Fig. 1.6**).

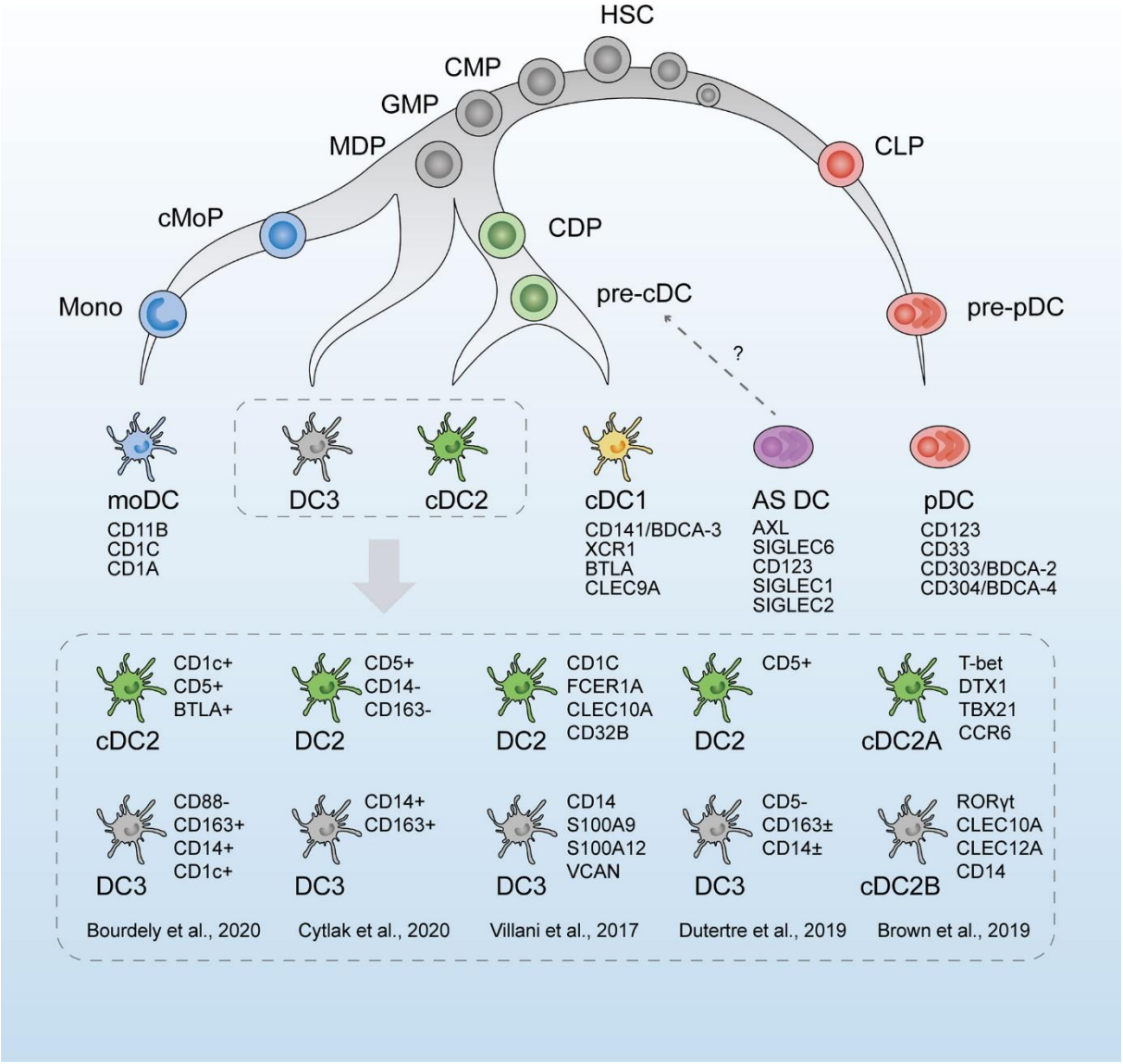


**Figure 1.6 Developmental model and classification of human DCs.** A model that describes DC development as a continuous differentiation pathway, in which early progenitors already exhibit lineage priming toward distinct DC types. The primary DC populations include moDCs, cDC1s and cDC2s, pDCs. Recent scRNA-seq analyses by Villani et al.[64], Brown et al.[59], and Dutertre et al.[63] have revealed that the previously unified cDC2 compartment is composed of phenotypically and transcriptionally diverse subsets identifiable by distinct marker profiles. Findings from Bourdely et al.[65] and Cytlak et al.[62] introduced DC3s as a separate population that originates independently from MDPs. The developmental source of pDCs has been reattributed to the lymphoid progenitor lineage. The identity and function of AXL$^{+}$SIGLEC6$^{+}$ DCs (AS DCs) remain under investigation, particularly regarding their potential role as cDC intermediates[109].

In the murine spleen, cDC2 subsets have been classified based on their dependence on transcription factors such as NOTCH2 and KLF4[97,112]. NOTCH2-dependent cDC2s constitute a relatively homogeneous group characterized by expression of CD4 and the adhesion molecule ESAM. In contrast, KLF4-dependent cDC2s display greater heterogeneity, comprising mostly ESAM$^{low}$ cells with variable expression of markers including CD4, CLEC10A, and CLEC12A[59,97,113]. More recently, these subsets have also been described in terms of transcription factor expression as T-BET$^{+}$ cDC2A and RORγt$^{+}$ cDC2B populations[59,97,112], though the precise overlap with NOTCH2- and

KLF4-dependent cells remains unclear. Whereas NOTCH2 and the GTPase RhoA tightly regulate the homeostasis of cDC1s and ESAM$^{high}$ cDC2s, ESAM$^{low}$ cDC2s are maintained independently of these factors[114]. Importantly, splenic ESAM$^{high}$ cDC2s require retinoic acid and lymphotoxin beta receptor (LTβR) signaling for their maintenance, while ESAM$^{low}$ cDC2s exhibit high LTβR expression and are unaffected by LTβ signaling[115].

The differentiation of mouse cDC2s is dependent on Notch2, Klf4 signaling and is largely regulated by IRF4- and Zeb2-mediated transcriptional programs. Several transcription factors, including CEBPB, SPI1, RUNX3, NFKB1, and BHLHE40, are specifically enriched in cDC2s, supporting their functional specialization[116]. Functionally, mouse cDC2s express a variety of cytosolic nucleic acid sensors such as RIG-I and MDA-5, as well as NOD-like receptors including NOD1 and NLRX1, enabling them to detect cytosolic nucleic acids and trigger inflammatory responses[117]. They also express a broad array of TLRs, with subset- and tissue-specific patterns. Splenic cDC2s predominantly express TLR3 and TLR12[117], and they are also known to express TLR5, TLR7, and TLR9, enabling the production of various inflammatory cytokines[118].

Recent work by Rodríguez et al.[58] identified CD300c as a reliable marker of a BM–resident cDC2 progenitor that also retains pDC differentiation potential. Using single-cell transcriptomics, fate-mapping, and in vitro differentiation assays, Rodríguez and colleagues demonstrated that CD300c$^{+}$ progenitors arise directly downstream of MDPs and represent a developmentally flexible population capable of generating multiple cDC2 subsets and pDCs. Transcriptomic profiling revealed that these CD300c$^{+}$ progenitors express intermediate levels of IRF4, KLF4, and TCF4, while maintaining low IRF8 and ID2 expression, situating them between classical CDP and pre-cDC2 states[58]. This population thus represents a critical point in DC ontogeny, integrating signals that determine whether cells commit to the cDC2 or pDC lineage.

### 1.2.2.3 Plasmacytoid dendritic cells

pDCs were first identified in human lymph nodes in the early 1950s[119]. They were initially referred to as “IFN-producing cells” because of their robust type I IFN secretion, and as “plasma cells” due to their morphological resemblance to B cells[120]. pDCs are characterized by an extensive rough endoplasmic reticulum, which contributes to their distinctive cellular morphology.

Mouse pDCs lack conventional lineage-specific markers but display high expression of MHC-II. They are characterized by the expression of CD11c, BM stromal cell antigen 2 (BST2), and sialic acid–binding Ig-like lectin H (SiglecH). Unlike cDCs, pDCs do not express markers such as XCR1, CD172a, CD11b, CD24, or CD26. Peripheral mouse pDCs additionally express CCR9, SCA-1, and Ly49Q, which are not detected on BM–resident pDCs[119]. SiglecH expression is downregulated during pDC maturation. Evidence of pDC heterogeneity has been reported, with subsets identified based on markers such as CX3CR1 and CD8[121,122] or the presence of a surface receptor tyrosine kinase AXL$^{+}$ population[123]. Notably, deletion of AXL in murine models has been demonstrated to increase type I IFN levels, while concurrently reducing IL-1β production and diminishing T cell activation during viral infections[124,125]. Additional

heterogeneity has been described in pDC subsets differentially expressing CD4 or CD8[126] and CCR2[127]. Mouse pDCs also exhibit heterogeneity in surface marker expression, with subsets distinguished by CD4 and, in some cases, low levels of CD8 in splenic populations. Functionally, pDCs express high levels of TLR7 and TLR9, enabling robust type I IFN production in response to their respective ligands[119,120,128,129] in particular upon viral stimulation[130].

Their differentiation and function are governed by a network of transcription factors, including IRF7, IRF8, IRF4, E2-2/TCF4, SpiB, Runx2, BCL11A, and ZEB2[120]. The development of pDCs is also dependent on Flt3L[131], and type I IFN have been shown to upregulate Flt3 in CLPs, thereby synergizing with Flt3L to promote pDC differentiation[132]. A central determinant of pDC fate is the balance between E2-2 and ID2. E2-2 plays a central role, with high expression favoring pDC commitment, while its deletion drives transdifferentiation into cDC-like cells capable of T cell priming[133,134]. IRF8 is essential for mononuclear phagocyte development from the HSCs[135,136]. While not intrinsically required for pDC lineage commitment, IRF8 is essential for the functional integrity and survival of both pDCs and cDC1s[137]. Terminally differentiated pDCs lacking IRF8 fail to produce type I IFNs upon TLR stimulation, underscoring its additional role in regulating antiviral responses. In contrast, studies in the BXH2 mouse model revealed that a point mutation in IRF8 results in a profound loss of the cDC1 compartment, while pDC development remains largely unaffected[138]. Together, these findings highlight the multifaceted role of IRF8 in shaping DC subset development, maintenance, and effector function. Zeb2 and SpiB are also critical for pDC differentiation and survival, while Runx2, and BCL11A regulate pDC trafficking and functional competence[139,140]. In contrast, PU.1 favors cDC development and represses the pDC lineage[141].

### 1.2.3 Dendritic cell functions

The primary function of DCs as APCs is to capture, process, and present antigens to initiate immune responses. Immature DCs internalize antigens through mechanisms such as macropinocytosis, phagocytosis, and receptor-mediated endocytosis. Processed antigens are then displayed as peptide–MHC complexes (pMHC) to naïve T cells, driving their activation. In addition, DCs secrete a range of cytokines and chemokines that regulate immune cell differentiation, activation, and effector functions, thereby shaping the immune responses. Beyond immune activation, DCs also play a critical role in maintaining tolerance. In the thymus, DCs contribute to central tolerance by mediating the negative selection of self-reactive T cells. Peripherally, immature DCs promote tolerance by lacking costimulatory signals, thereby inducing T cell anergy, and by stimulating the differentiation of Tregs. Through the secretion of inhibitory cytokines such as IL-10 and TGF-β, they further suppress immune activation and help preserve self-tolerance[142].

DC maturation is tightly linked to their function as key mediators between innate and adaptive immunity[143,144]. DC maturity is typically defined by three features: reduced endocytic capacity, increased ability to stimulate T cell proliferation, and enhanced responsiveness to chemokines such as CCL19 and CCL21, which guide migration to lymph nodes[145,146]. As outlined above in detail, DCs originate in the BM and circulate to peripheral tissues, where they remain in an immature state. Immature DCs efficiently

capture antigens but express low levels of antigen-presenting and co-stimulatory molecules, limiting their ability to activate T cells. Upon encountering antigens, they undergo maturation and migrate to lymph nodes, where they present processed antigens to T lymphocytes[145,147] (**Fig. 1.7**). The maturation process progresses through three stages: precursor, immature, and mature DCs[148]. Precursors differentiate into immature DCs in tissues, and following antigen uptake or signals in lymphoid organs, they mature into potent APCs equipped with high expression of MHC and co-stimulatory molecules, enabling robust T cell activation[149].

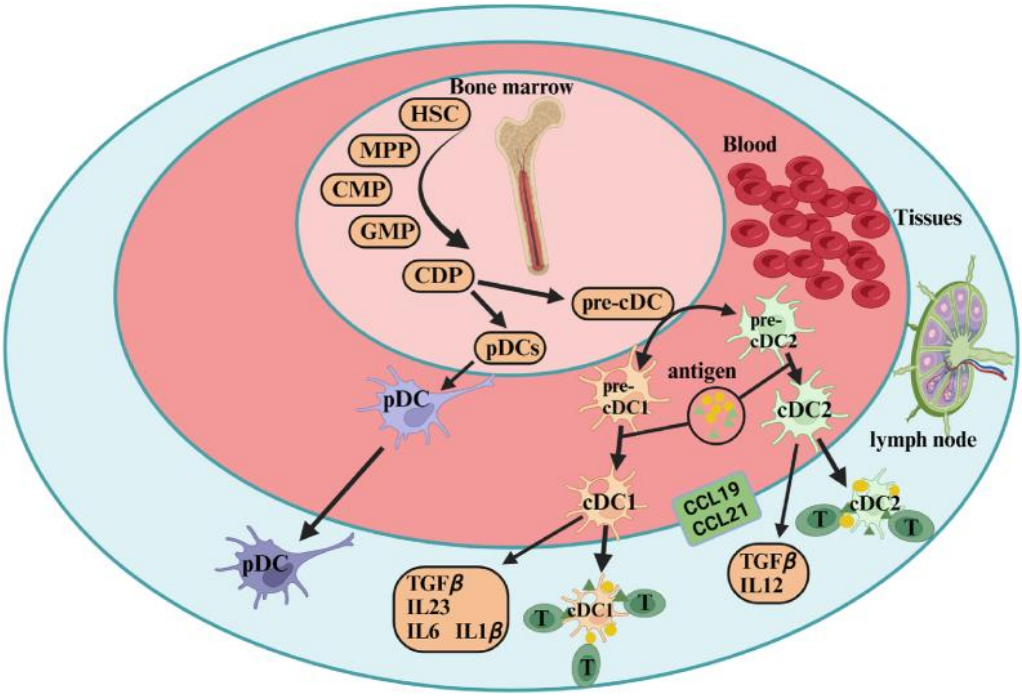


**FIGURE 1.7 DC development and function in immune response.** DC maturation is a multistep process beginning in the BM, where HSCs give rise to multipotent progenitors (MPPs). MPPs branch into CLPs and CMPs, the latter further differentiating into GMPs. From these lineages arise both monocytes and CDPs. Unlike monocytes, CDPs are committed to the DC lineage and give rise to pDCs and pre-cDCs. Pre-cDCs exit the BM and enter circulation, where they segregate into pre-cDC1 and pre-cDC2 subsets. Upon antigen encounter, pre-cDCs mature into cDCs with enhanced antigen presentation capacity. Functionally, cDC1 cells mainly secrete TGFβ, IL-23, IL-6, and IL-1β, whereas cDC2 cells produce TGFβ and IL-12. Guided by the chemokines CCL19 and CCL21, mature cDCs migrate into lymphoid tissues, where they play a central role in antigen presentation and T cell activation[43].

DCs are marked by the expression of CD11c, a transmembrane protein known as integrin alpha X. Although its role in DCs is not fully understood, Wu et al. suggested that CD11c may help DCs recognize and engulf cells lacking CD47[150]. DCs are also defined by their expression of costimulatory molecules, which reflect their maturation status. Members of the B7 family, particularly CD80 (B7.1) and CD86 (B7.2), interact with CD28 on T cells. This interaction is essential for T cell activation, proliferation, cytokine production, and for preventing T cell anergy[151]. B7 molecules can also bind CTLA-4 on T cells, leading to inhibition of T cell effector functions. This pathway is crucial for regulating T cell activity, as evidenced by mouse models lacking CTLA-4,

which develop severe autoimmunity and lymphoproliferative disorders[152,153]. CD40 is another key costimulatory molecule on DCs, belonging to the TNF receptor superfamily. Its ligand, CD40L (CD154), is expressed on activated $CD4^+$ and $CD8^+$ T cells[154]. Interaction between CD40 and CD40L enhances DC maturation, upregulates CD80 and CD86, and stimulates IL-12 production, promoting Th1 differentiation in naïve T cells[154]. CD83, a glycoprotein of the IgG superfamily, is a classical marker of DC maturation, expressed primarily on mature DCs[155]. Its soluble form can inhibit DC maturation and DC-driven T cell proliferation[155]. However, CD83-deficient mice exhibit reduced peripheral $CD4^+$ T cells, highlighting its essential role in T cell development[156,157].

It has been recognized that DCs specialize in priming antigen-specific T cells, with cDC1s being particularly effective at inducing $CD8^+$ cytotoxic T lymphocyte (CTL) responses. Early *ex vivo* studies showed that cDC1s drive CTL responses through cross-priming[158,159], whereby exogenous, cell-associated antigens are processed and presented on MHC-I molecules to $CD8^+$ T cells in lymphoid tissues[160-162]. The first in vivo evidence came from *Batf3*$^{-/-}$ mice, which lack cDC1s and display impaired CTL responses, increased susceptibility to viral infections, and uncontrolled tumor growth[163]. Since then, the essential role of Batf3-dependent cDC1s in CTL induction has been confirmed across diverse models[164-170].

Interestingly, cDC1 development in *Batf3*$^{-/-}$ mice can be partially restored in certain tissues by factors such as mycobacterial infection, IL-12 treatment, or irradiation, through compensatory activity of other BATF family members (BATF, BATF2)[171,172]. Deletion of a BATF3-bound enhancer prevents this compensation, indicating that BATF and BATF2 maintain *Irf8* expression in BATF3's absence[173]. Moreover, transgenic *Irf8* expression in *Batf3*$^{-/-}$ mice restores cDC1 populations, but only a subset of BATF3-regulated genes is required for cDC1-mediated rejection of immunogenic tumors[174,175]. Identifying the precise genetic targets of BATF3 that define cDC1 identity and function remains an ongoing area of research.

cDC1s also regulate innate immunity through unique receptor expression and cytokine production. They selectively express TLR11, which recognizes *Toxoplasma gondii* profilin and induces IL-12 production[176]. *Batf3*$^{-/-}$ mice revealed that cDC1-derived IL-12 is indispensable for resistance to acute *T. gondii* infection[177], as it drives IFN-γ production by NK cells and primes regulatory functions in monocytes[178]. cDC1s also express TLR3, whose activation by ds-RNA (e.g., Poly(I:C)) promotes cDC1 maturation and enhances antiviral and antitumor immunity[179,180].

Conditional gene-deletion models, particularly those based on *Xcr1* expression, have clarified cDC1-specific functions[168,181-185]. For instance, deletion of *Vegfa* in cDC1s reduces neutrophil infiltration and skin inflammation in *Propionibacterium acnes* infection[186], whereas CLEC9A suppresses CXCL2 production, thereby limiting neutrophil-driven inflammation[187]. These findings highlight context-dependent crosstalk between cDC1s and neutrophils.

Several receptors underpin cDC1 regulation of adaptive immunity. The XCR1–XCL1 axis orchestrates the positioning of cDC1s and $CD8^+$ T cells within lymphoid tissues [183,185,188], while DEC-205 (LY75) and CLEC9A have been utilized to deliver antigens and enhance vaccine responses[189-194]. Targeting cDC1s through XCR1 similarly improves antitumor and antiviral immunity[195,196].

Mouse models highlight the pivotal role of cDC1s in cancer immunotherapy. Effective responses to checkpoint blockade (anti-PD1, anti-PDL1, anti-CTLA4, anti-CD137) and certain adoptive T cell therapies require Batf3-dependent cDC1s[165,197,198]. Intratumoral adjuvants, Flt3L administration, or XCL1 delivery can expand or recruit cDC1s[199-202], facilitating tumor rejection. NK cell–derived XCL1 has likewise been shown to attract cDC1s into tumors, reinforcing their non-redundant role in antitumor immunity[203].

Although cDC1s are the primary cell type mediating cross-presentation of cell-associated antigens in vivo, most mechanistic insights into this process have been derived from in vitro systems using GM–CSF and IL-4–driven monocyte- or BM–derived DCs (GMDCs)[204]. While informative, these models do not fully reflect the intrinsic properties of cDC1s. Recent in vivo studies have identified several genes uniquely required for cross-presentation by cDC1s.

WDFY4, a large integral membrane protein selectively expressed in cDC1s, is essential for cross-presentation to $CD8^+$ T cells. Although cDC1 development is unaffected in *Wdfy4*$^{-/-}$ mice, these mice display immunological defects similar to those of *Batf3*$^{-/-}$ animals, highlighting its non-redundant role[205]. WDFY4 is thought to regulate vesicular trafficking critical for antigen processing, but its size has hindered detailed functional characterization. Another vesicular trafficking regulator, RAB43, is also required for cross-presentation by cDC1s in vivo[206]; however, GMDCs from *Rab43*$^{-/-}$ mice do not exhibit defects, reinforcing that cross-presentation mechanisms in GMDCs differ from those in bona fide cDC1s (**Fig. 1.7**).

Multiple functional subsets of cDC2s have been identified, all defined by relatively high expression of IRF4[91]. Ontogenetically distinct from cDC1s, cDC2s perform specialized functions that cannot compensate for cDC1 deficiencies. Much of our understanding of their roles has come from the analysis of *Irf4*-deficient mice. A limitation of this model is that *Irf4* deficiency affects cDC2 subsets in a tissue-specific manner[207,208]. Nevertheless, extensive characterization of these mice has revealed the importance of cDC2s in orchestrating type II immune responses against allergens and parasites, type III immune responses against extracellular pathogens and commensal microbiota, and humoral responses to blood-borne antigens[209-215] **Fig. 1.8**).

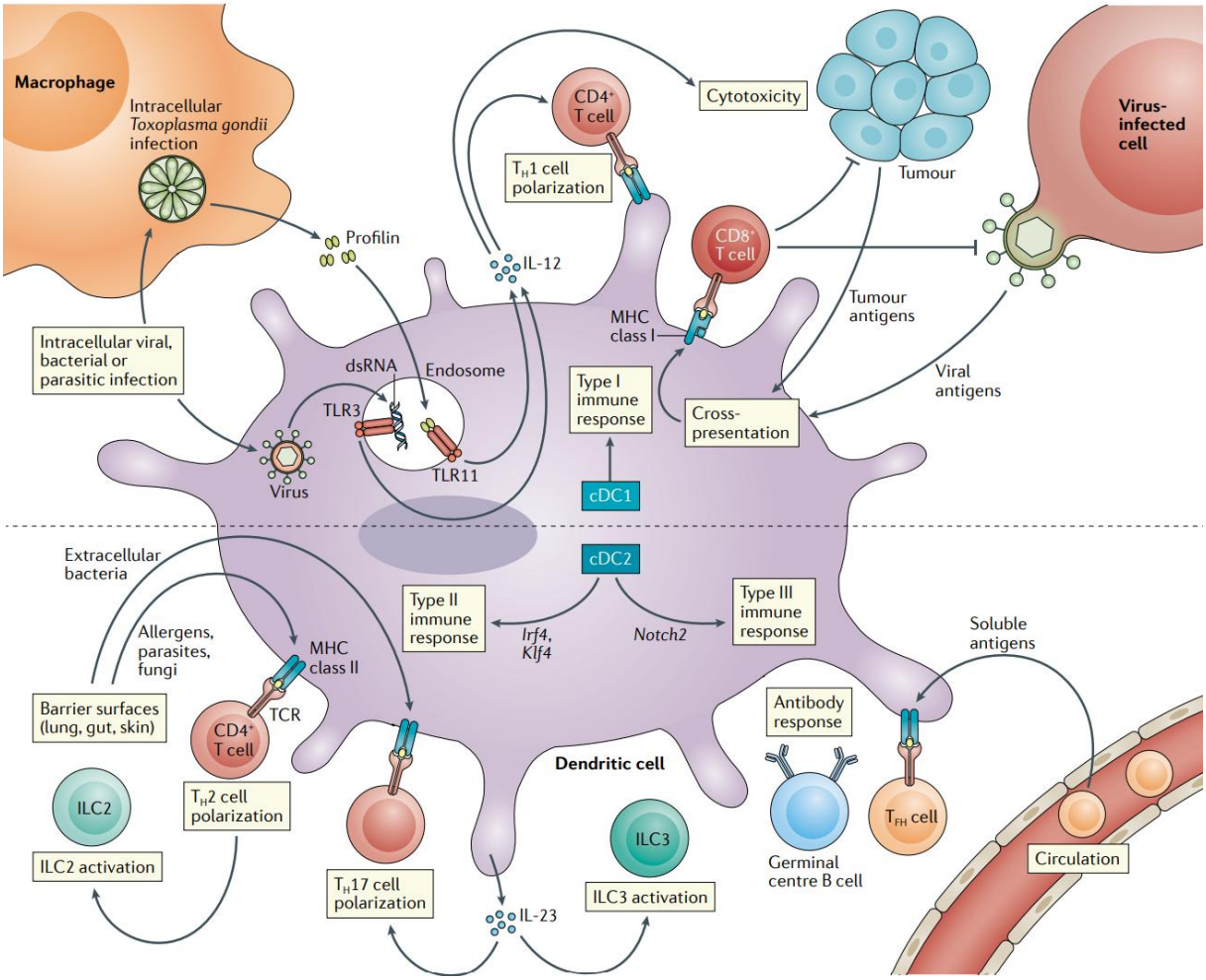


**FIGURE 1.8 Specialized functions of cDC subsets**. cDC1s regulate type I immunity by priming $CD8^+$ CTL and $CD4^+$ $T_H1$ cells. They uniquely express TLR3 and TLR11 (which recognize dsRNA and the *Toxoplasma gondii* antigen profilin, respectively), produce IL-12, and are essential for resistance to intracellular viral, bacterial, and parasitic infections. cDC1s are specialized for cross-presentation of host cell–associated antigens, critical for pathogen clearance and antitumor immunity. cDC2s regulate type II and III immune responses and antibody responses to soluble antigens. At barrier surfaces (lung, gut, skin), *Klf4*-dependent cDC2s drive $T_H2$ and ILC2 responses to parasites, fungi, and allergens via IRF4. *Notch2*-dependent cDC2s produce IL-23 during *Citrobacter rodentium* infection, activating ILC3s and inducing $T_H17$ cells. In lymphoid organs, these cDC2s also support humoral immunity by inducing $T_{FH}$ cells and germinal center B cells[77].

Dissection of cDC-intrinsic transcription factor requirements has further enabled the assignment of functions to discrete cDC2 subsets. *Notch2*-dependent cDC2s, found in the spleen, lung, and gut-associated lymphoid tissues[113], also rely on *Ltbr* and *Rbpj*[97]. In the gut, this subset regulates type III immune responses to extracellular pathogens such as *Citrobacter rodentium*[113]. Here, cDC2-derived IL-23 activates ILC3s, which promote epithelial resistance through IL-22 production[216]. In the spleen, *Notch2*-dependent cDC2s capture soluble antigens from the circulation and are essential for germinal center (GC) formation and antibody production; in their absence, immunization with sheep red blood cells (RBC) or heat-killed *Listeria* fails to elicit T follicular helper (Tfh) cell expansion or GC B cell responses[217]. By contrast, the *Klf4*-

dependent cDC2 subset migrates from barrier surfaces to draining lymph nodes, where they regulate type II responses to allergens and parasites[112].

Both $CD8^+$ and $CD4^+$ T cell responses are critical for effective antitumor immunity and checkpoint blockade[198,218]. While cDC1s may contribute to $CD4^+$ T cell priming via MHC-II presentation, cDC2s play a clearly non-redundant role in initiating $CD4^+$ T cell responses[219]. Supporting this, tumor antigen–bearing cDC2s isolated from the tumor microenvironment can prime antigen-specific $CD4^+$ T cells *ex vivo*. Moreover, ablation of $CD11b^+$ cDC2s in tumor-draining lymph nodes of *Cx3cr1*$^{LSL–DTR}$ *Itgax*$^{Cre}$ mice impairs the priming and differentiation of naïve $CD4^+$ T cells[220]. These findings underscore that certain anticancer immunotherapies depend on cDC2 activity to achieve full efficacy[221].

Recently discovered, cDC2A subset plays a crucial role in initiating Th17-driven immune responses by producing IL-23, and it has been linked to anti-inflammatory processes essential for tissue repair[57]. Conversely, cDC2B share functional characteristics with cDC1, such as promoting Th1 responses, generating IL-12, and effectively cross-presenting antigens to $CD8^+$ T cells[59].

pDCs are uniquely equipped to produce high levels of type I IFN upon activation, triggered by recognition of unmethylated CpG DNA or viral stimuli. This capacity remains robust across pDC subsets in mice and is critical for antiviral defense, as demonstrated by impaired viral control following pDC depletion in murine cytomegalovirus infection. In addition to type I IFN, pDCs secrete type III IFNs, TNF-α, and other cytokines[120]. Single-cell analyses reveal functional heterogeneity within pDCs, distinguishing IFN-producing subsets from those primarily involved in antigen presentation[222]. The functional state of pDCs can be shaped by the nature of the stimulus, with some ligands and viruses promoting an IFN-producing phenotype, while others drive antigen presentation. Beyond TLR7/9 signaling, pDCs utilize cytosolic sensors like cGAS and RIG-I to detect various viral infections[223-225] and TLR2 activation in pDCs modulates adaptive immunity by inducing IL-10 production in $CD4^+$ T cells[226]. Although less efficient antigen presenters compared to cDCs, pDCs are pivotal in orchestrating antiviral and antitumor responses through type I IFN secretion and recruitment of effector cells such as $CD8^+$ T cells, NK cells, and γδ T cells via CXCR3 ligands[227].

DC3s, as a last DC subset, were first identified in the human bloodstream through scRNA seq[64], showing a hybrid transcriptomic and phenotypic signature of cDC2 and monocytes. These cells coexpress CD1c and CD163[62,63] and have been identified in BM[62], oropharyngeal cancers[228], and psoriatic skin lesions[229]. However, their presence and characteristics in lymphoid organs and peripheral tissues remain underexplored. Elevated frequencies of circulating DC3 have been observed in systemic lupus erythematosus and melanoma patients[63,230], as well as in severe COVID-19 cases[231,232], though their precise pathogenic role is unclear. Ex vivo, blood-derived DC3 efficiently activate naive $CD4^+$ T cells[63-65] and have been reported to preferentially drive either Th17[63] or Th1[65] differentiation contingent on experimental conditions. DC3 can also induce naive $CD8^+$ T cell proliferation and promote maturation marker expression[65], but their capacity for antigen cross-presentation is yet to be confirmed. They are implicated in fostering tissue-TRM by upregulating CD103[65] and expressing

high levels of the costimulatory molecule GITRL upon type I IFN stimulation[233], essential for establishing TRM. In terms of cytokine secretion, DC3 produce IL-12p70 and IL-23 comparable to cDC2, alongside considerable amounts of IL-1β similarly to monocytes[62,65]. In mice, DC3 are frequently considered alongside cDC2B, exhibit a distinct developmental origin from Ly6C$^+$ MDP, in contrast to the classical DC2s derived from CDP, suggesting both developmental and functional divergence from canonical cDC2 lineages. Although DC3s share surface and transcriptional features with cDC2 and moDCs, their precise physiological roles remain under exploration[61].

Taken together, cDCs play a pivotal role in orchestrating immune responses by directing the differentiation of CD4$^+$ T cells into specialized subsets such as Th1, Th2, Th17, and Tregs. These distinct T cell lineages, characterized by their unique cytokine profiles and transcriptional programs, mediate tailored immune functions essential for pathogen clearance and immune regulation. The mechanisms and implications of CD4$^+$ T cell differentiation will be explored in greater depth in the following chapter.

## 1.3 T lymphocytes

T lymphocytes (T cells) are central mediators of adaptive immunity, playing an essential role in the elimination of pathogens such as viruses and bacteria, as well as in the surveillance and eradication of malignant cells. They are defined by the expression of surface TCRs, which recognize MHC molecules on APC. The recognition triggers T cell activation, clonal expansion, and the orchestration of downstream immune responses[6,142,234,235].

This thesis will explore some cell subsets, their proliferation, and differentiation pathways, with a particular focus on CD4$^+$ T cells. This subset will receive in-depth attention throughout this chapter, reflecting its central role in coordinating immune responses and providing the foundation for the experimental research presented.

### 1.3.1 T lymphocyte subtypes

T cells originate from progenitors in the BM that migrate to the thymus for maturation. In the thymus, these progenitors differentiate into distinct T cell lineages, including the prevalent αβ T cells subdivided into CD4$^+$ and CD8$^+$ subsets, as well as smaller populations of γδ T cells and natural killer T (NKT) cells. The αβ T cells recognize antigenic peptides presented by MHC molecules on APC[236]. This section of thesis presents an overview of three important T cell subsets: Tregs, CD8$^+$ cytotoxic T cells, and CD4$^+$ helper T cells.

Tregs, characterized by the expression of CD4, CD25, and the transcription factor Foxp3, are essential mediators of immune tolerance. They play a vital role in maintaining peripheral tolerance, preventing autoimmune diseases, and limiting chronic inflammation[237-240]. Tregs constitute a significant subset of T cells with potent anti-inflammatory capabilities and specialized involvement in tissue remodeling[241]. Due to their phenotypic and functional diversity, classifying Tregs into universally comprehensive subpopulations remains challenging. Based on their origin, Tregs are divided into thymus-derived[242], which are Foxp3$^+$ and consistently suppressive, and peripherally induced Tregs[243-246], which display more plasticity with variable Foxp3 expression and potential effector functions[247]. Additional Treg subsets have been identified based on markers, cytokine profiles, and regulatory roles[246,248], including

resting ($rT_{regs}$), activated ($aT_{regs}$), non-suppressive (non-$T_{regs}$), helper-like (Th-$T_{regs}$), and Foxp3$^-$ Tregs. The importance of Tregs in immune regulation was recognized in 2025 by the Nobel Assembly at Karolinska Institutet, honoring discoveries of their role in preventing autoimmunity through Foxp3 regulation, following key findings by Sakaguchi, Brunkow, and Ramsdell in the late 1990s and early 2000s[249,250].

CD8$^+$ T cells, commonly referred to as CTLs, are part of the adaptive immune system responsible for targeting and eliminating cells infected with intracellular pathogens as well as malignant cells[251]. They recognize antigenic peptides presented by MHC-I molecules[252,253], with CD8 serving as a co-receptor to stabilize the interaction. Upon antigen recognition, naive CD8$^+$ T cells rapidly proliferate and differentiate into effector cells that induce apoptosis of target cells through mechanisms such as Fas/Fas ligand interaction and the release of cytolytic molecules like perforin and granzymes. These effector cells also secrete cytokines, including IFN-γ and TNF-α, which enhance immune activation and target cell susceptibility. Following antigen clearance, a subset of these cells transitions into memory populations that provide long-lasting protection by mounting swift responses upon re-exposure to the antigen. The CD8$^+$ T cell compartment is heterogeneous, comprising various effector and memory subsets, such as short-lived effector cells (TEFF), exhausted cells, memory precursors (TMP), central memory (TCM), effector memory (TEM), and tissue-resident memory T cells (TRM), distinguished by their phenotypic markers, functional capabilities, and tissue localization[254,255]. The differentiation and maintenance of these subsets are regulated by specific transcription factors, epigenetic changes, and metabolic pathways, with their development timed and spatially coordinated in response to immune challenges.

The final major T cell subset previously mentioned, which I will now discuss in detail, is the CD4$^+$ T cell population. The subsequent section of this thesis will be dedicated to a thorough exploration of this subset. CD4$^+$ Th cells is a heterogeneous population of T cells that serve as central regulators of the immune system, influencing multiple aspects of host defense. CD4 T-cell activation is initiated when the TCR specifically recognizes an antigen presented on MHC-II molecules on APCs[252,253,256-258].

Effective activation of T cells requires TCR engagement but also a costimulatory signal, typically provided by CD28 on T cells interacting with CD80 or CD86 on activated APCs. This costimulation supports T cell survival, proliferation, and metabolic activity through pathways enhancing glucose metabolism and anti-apoptotic protein expression (such as Bcl-X). T cells also express regulatory receptors such as CTLA-4 and PD-1, which modulate immune responses. CTLA-4 competes with CD28 for ligand binding, inhibiting T cell activation by disrupting APC interactions and promoting immunosuppressive cytokines like IL-10 and TGF-β. PD-1 engagement with its ligands PDL1/PDL2 induces T cell exhaustion or apoptosis, often through SHP2-mediated inhibition of signaling pathways. While CTLA-4 acts early to checkpoint activation, PD-1 functions later to limit immune responses[259-261]. When signaling through the CD28 receptor predominates, T cells become activated and differentiate into primarily CD8 and CD4 T cells. CD4 Th cells subsequently differentiate into a range of specialized subsets, including Th1, Th2, Treg, Tfh, Th17, Th9, Th22, and CD4$^+$ CTLs[262-264]. CD4$^+$ T-cells can be categorized into principal subsets: Th1 cells predominantly produce IFN-γ, TNF-α, IL-2, facilitating cell-mediated immunity by activating macrophages, promoting defense against intracellular pathogens, and aiding B cell maturation. Th2

cells secrete IL-4, IL-5, and IL-13, primarily driving humoral immunity by supporting IgE-producing B cells and recruiting MC and eosinophils. Th17 cells produce IL-17 family cytokines, playing pivotal roles in chronic inflammatory processes and persistent infections[252,253,265,266] (**Fig. 1.9**).

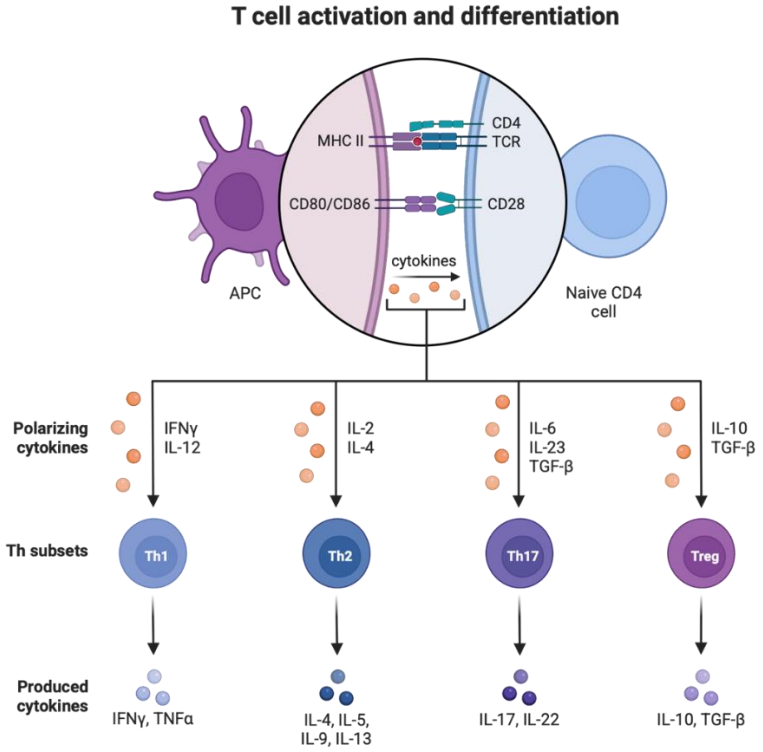


**FIGURE 1.9 Schematic representation of CD4⁺ T cell activation and differentiation by an APC**. TCR engages the peptide-MHC-II complex on the APC, while the CD4 coreceptor binds to the MHC-II molecule, together delivering the first activation signal. Costimulatory signal arises from the interaction between CD28 on the T cell and CD80/CD86 on the APC, which amplifies T cell activation and supports proliferation. Finally, cytokines released by the APC provide a third signal, guiding T cell activation, clonal expansion, and differentiation into distinct effector subsets[267].

### 1.3.2 T lymphocyte proliferation and differentiation

T cells arise from hematopoietic precursors in the BM and complete their maturation in the thymus. During development, they undergo rigorous selection processes to shape a functional and self-tolerant repertoire. In positive selection, thymocytes that can recognize self-MHC molecules with sufficient affinity are retained, while negative selection removes those with strong reactivity to self-antigens, thus preventing autoimmunity. The mature T cell pool consists of several subsets with distinct immunological roles[6,142].

A key function of all T cell subsets is the production of cytokines, which orchestrate diverse immune responses (**Fig 1.10**). T cells can be categorized into conventional and unconventional groups. Conventional T cells possess a highly diverse TCR repertoire composed of α and β chains, which determine their antigen specificity. These cells are further subdivided based on expression of CD4 or CD8 co-receptors. Upon encountering their specific antigens, naive CD4⁺ and CD8⁺ T cells differentiate into effector subsets tailored by their differentiation programs. CD4⁺ Th cells are classified according to transcription factors and cytokine profiles, such as T-BET, IFN-

γ and TNF-α in Th1 cells, GATA3, IL-4 and IL-13 in Th2 cells, IRF 4, IL-9 in Th9 cells, RORγt, IL-17A, and IL-17F in Th17 cells, AHR, and IL-22 in Th22 cells, and BCL-6 with IL-21 in Tfh cells (**Fig. 1.10**).

Tregs expressing FOXP3 exert immunosuppressive roles primarily via IL-10 and TGF-β. $CD8^+$ Tc cells demonstrate less clearly defined functional subsets yet parallel $CD4^+$ lineages such as Tc1 and Tc17[268,269]. Emerging single-cell sequencing and epigenetic analyses reveal extensive heterogeneity and plasticity within these subsets[270,271], indicating that classical classification systems only partially capture the complex landscape of T-cell differentiation.

Distinct Th subsets are characterized by their cytokine profiles: Th1 cells secrete IFN-γ, thereby activating macrophages and enhancing their phagocytic activity; Th2 cells release IL-4, which promotes B cell activation and antibody production; and Th17 cells produce IL-17, a cytokine that recruits neutrophils to sites of infection. Tregs contribute to immune homeostasis by producing suppressive cytokines such as IL-10 and TGF-β, thereby dampening excessive immune activation[272] and maintaining tolerance. In addition to cytokine secretion, direct cytotoxicity represents a critical effector function of cytotoxic $CD8^+$ T cells. These cells identify infected or transformed cells displaying antigens on MHC-I molecules and induce target cell death either by releasing perforin and granzymes or by triggering apoptosis via the FasL–Fas pathway. Furthermore, cytotoxic T cells can amplify their effector activity through the secretion of pro-inflammatory cytokines such as TNF-α[6,142].

In addition to conventional T cells, specialized unconventional subsets, including γδ T cells, NKT cells, and mucosal-associated invariant T cells, play distinct roles in immunity. These populations are defined by semi-invariant TCRs, recognition of atypical antigens, and innate-like properties. Notably, they are enriched at barrier sites and contribute to frontline immune defense against microbial challenge[273] (**Fig. 1.10**).

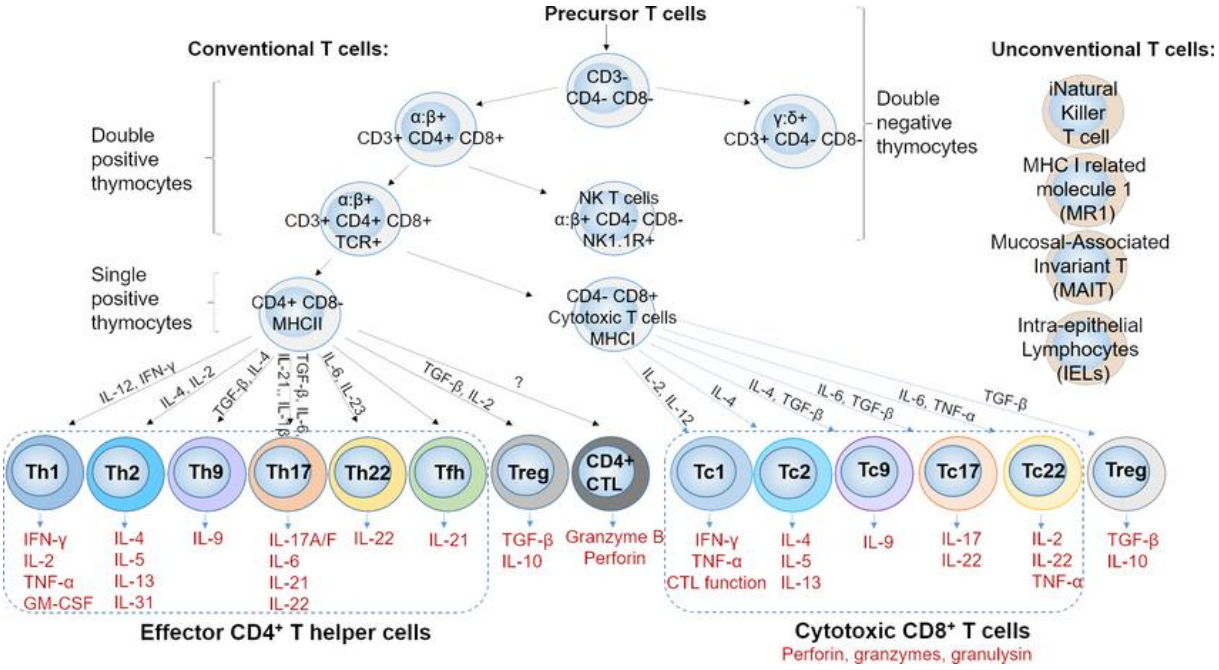


**FIGURE 1.10 Developmental pathways and major subtypes of T cells.** During maturation, T cells undergo sequential selection processes accompanied by stage-specific expression of

surface molecules. Following thymic egress, naive T cells further differentiate under the influence of local cytokines and signaling cues, giving rise to functionally specialized effector and regulatory subsets. The diagram also includes both conventional and unconventional T-cell lineages to highlight their distinct origins and immune roles[274].

Some activated CD4 and CD8 T cells transition into memory T cell populations that persist long-term, providing rapid recall responses upon antigen re-exposure. The antigen-specific T cell response can be broadly segmented into several phases (**Fig. 1.11**): an initial expansion phase (days 0–7), characterized by rapid proliferation of T cells; a peak phase at day 8, when effector T cells reach their highest numbers and cease division; a contraction phase (days 8–15), during which the majority of effector cells undergo programmed cell death; and a memory phase (beyond 30 days), where a small subset of cells persists as distinct memory populations including $CD44^{+}CD62L^{-}$ effector memory (TEM), $CD44^{+}CD62L^{+}$ TCM, and $CD69^{+}CD103^{+}$ TRM cells[275]. TCM circulate through blood and secondary lymphoid tissues, while TEM permeate peripheral compartments such as skin[276]. Increasing evidence demonstrates that a portion of memory T cells become stably retained within non-lymphoid tissues, forming TRM[277]. These TRM cells serve as local sentinels, in situ, they continually survey for pathogens and mount immediate protective responses[278,279].

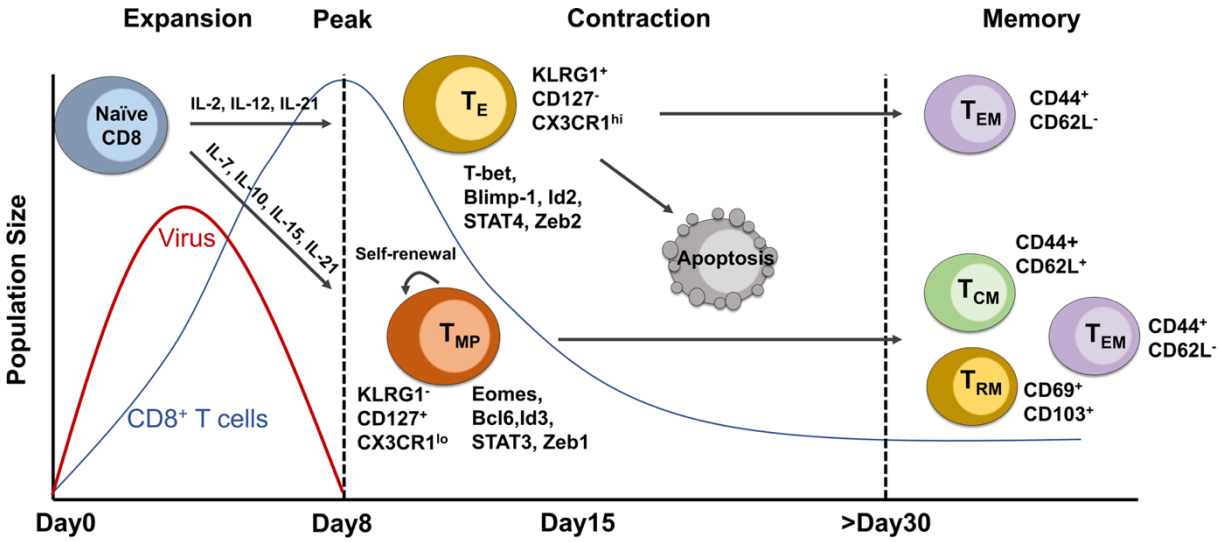


**FIGURE 1.11 Temporal progression of the $CD8^{+}$ T cell response during an acute infection.** The graph presents viral load (red line) alongside the $CD8^{+}$ T cell population size (blue line) throughout the course of infection. Following pathogen entry, $CD8^{+}$ T cells rapidly expand, peaking around day 8, coinciding with efficient clearance of the virus. At this critical expansion point, $CD8^{+}$ T cells diverge into effector ($T_E$) and memory precursor ($T_{MP}$) subsets, distinguished by unique surface markers and differentiation capacities. The development of effector and memory $CD8^{+}$ T cells is governed by distinct transcription factors and cytokines. Most $T_E$ cells undergo apoptosis during the contraction phase (days 8–15), while a $T_{MP}$ subset persists, self-renews, and subsequently gives rise to effector memory ($T_{EM}$), central memory ($T_{CM}$), and tissue-resident memory ($T_{RM}$) populations extending beyond 30 days post-infection[236].

While TEFF are crucial for eliminating primary infections, long-term protection against reinfection relies on the formation of durable TCM and TEM cell populations. TEM can mount rapid responses upon encountering DCs that present their cognate pMHC[280]. In addition, TEM cells can actively shape innate immunity[281]: once they recognize their specific antigen, they provide direct instructions to myeloid cells, prompting the

production of proinflammatory cytokines such as IL-1β, IL-6, and IL-12[282,283]. Although memory CD4$^+$ T cell-driven inflammation shares many features with innate immune responses triggered by microbial signals[283], it operates independently of conventional PRR pathways[284,285]. For instance, during secondary influenza infection, antigen-specific CD4$^+$ TEM can engage DCs directly, initiating innate-like inflammation without requiring PRR or type I interferon receptor (IFNAR) signaling[281]. While this mechanism contributes to protective immunity, it has also been implicated in pathology[286-288]. In autoimmune contexts, autoreactive CD4$^+$ TEM cells rapidly activate myeloid cells that present self-antigens, leading to an intense cytokine surge that exacerbates tissue damage[282,283]. This activation is mediated through multiple tumor necrosis factor receptor superfamily (TNFRSF) interactions. Specifically, T cell-derived TNF and Fas ligand (FasL) bind TNFR and Fas on DCs, promoting IL-1β production and processing[282]. In parallel, TNF and CD40L engage TNFR and CD40 on DCs, initiating a broad transcriptional program that drives release of proinflammatory cytokines, including IL-6 and IL-12[283]. Blocking TNF–TNFR and CD40L–CD40 signaling significantly reduces the cytokine storm and associated autoimmune pathology; however, it does not eliminate innate cytokine production, indicating that additional pathways contribute to TEM cell-mediated inflammatory responses.

## 1.4 The complement system

A key component of innate immunity is the complement system, first identified over a century ago as a **heat-sensitive factor in blood** that mediates bacterial killing and the lysis of foreign erythrocytes. In 1891, Hans Buchner demonstrated that heating serum to 55 °C for 30 minutes abolished its bactericidal activity. He termed this labile serum component alexin, derived from the Greek word meaning “to ward off.” A few years later, in 1895, Jules Bordet confirmed these observations and further showed that alexin could lyse RBC[289]. It was Paul Ehrlich, however, who clarified the mechanism by distinguishing between the heat-stable component of immune serum (antibodies) and the heat-labile factor (now recognized as complement)[16]. Ehrlich described how the latter “complemented” the action of antibodies, thereby laying the foundation for the discovery of the classical complement pathway. In recognition of these pioneering contributions, Ehrlich and Élie Metchnikoff were jointly awarded the Nobel Prize in 1908 for their groundbreaking work on immunity[16].

Today, complement is recognized as much more than a simple amplifier of antibody responses. It forms a complex network of soluble and membrane-bound proteins, consisting of over 50 plasma and membrane-bound proteins, most of which are produced by the liver[290,291]. Complement serves as a critical sensor system of innate immunity for DAMPs or PAMPs resulting in a sequential enzyme cascade in which the proteolytic cleavage of one component activates the next. This cascade ultimately generates effector molecules that either translates the fluid phase sensing into a cellular response leading to pathogen clearance and destruction or directly kills pathogens as the final step of terminal pathway activation. Complement activation occurs via both canonical (classical, lectin, and alternative pathways) and non-canonical routes. Canonical activation in the bloodstream proceeds through three major pathways: the classical pathway (CP), the first identified, which is initiated by

different subsets of antibodies; the alternative pathway (AP), discovered later, which is triggered by spontaneous hydrolysis of C3 followed by its deposition on microbial, foreign or altered cell surfaces; and the lectin pathway (LP), most recently described, which recognizes carbohydrate patterns on pathogen surfaces[6,292-294].

A central feature of complement activation is that all three canonical pathways ultimately converge on a common step: the generation of the C3 convertase. When one of the pathways is activated on the surface of a pathogen, a C3 convertase complex is assembled. Although its composition varies depending on the initiating pathway, the C3 convertase is always a multi-subunit protease responsible for cleaving C3. Once formed, it stably associates with the microbial surface, where it drives the production of large amounts of C3b, a major effector molecule of the complement system, and smaller quantities of C3a, a pro-inflammatory and regulatory peptide. This cleavage of C3 is the critical step in complement activation, as it initiates most downstream effector functions.

C3b plays two key roles. First, it can covalently bind to the pathogen surface and act as an opsonin, facilitating recognition and uptake by phagocytes via several complement receptors, leading to efficient microbial clearance[295]. Second, C3b can associate with existing C3 convertases (from either the CP or LP) to form the C5 convertase. This enzyme cleaves C5 into two fragments: C5a, a potent inflammatory mediator, and C5b, which serves as the initiating subunit for the terminal complement pathway. C5b recruits additional complement proteins to assemble the membrane attack complex (MAC), a pore-forming structure that disrupts microbial membranes and induces pathogen lysis[6,296-303] (**Fig. 1.12**).

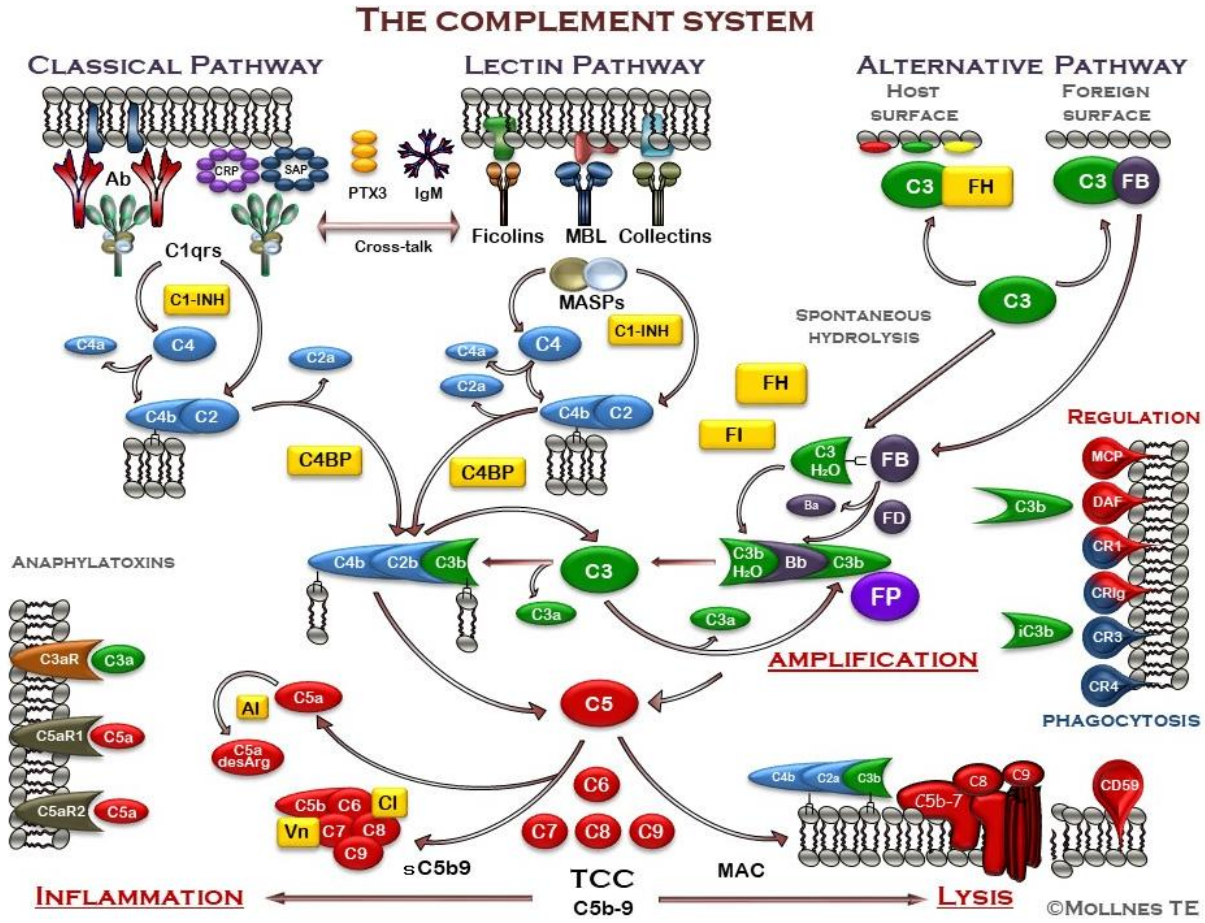


**FIGURE 1.12 Overview of the complement system activation and regulation**. The complement system can be initiated through three pathways (top): the CP, triggered primarily by antibody-antigen complexes but also by pentraxins such as CRP, SAP, and PTX3; the LP, activated by recognition of microbial carbohydrates via MBL, ficolins, or collectins, and in some cases by IgM bound to altered self-antigens; and the AP, driven by spontaneous C3 hydrolysis on foreign or damaged surfaces. The AP further acts as an amplification loop, largely stabilized by properdin (factor P), the only known positive regulator. All three pathways converge on the cleavage of C3 into C3a and C3b (center). C3a and C5a, generated by subsequent C5 cleavage, act as anaphylatoxins that bind to C3aR, C5aR1, and C5aR2, inducing inflammatory mediator release (lower left). C5b initiates formation of the terminal complement complex (C5b-9, TCC), which inserts into membranes as the MAC to induce cell lysis, or at sublytic levels, promotes cell activation (bottom). Cleavage of C3b to iC3b enables binding to CR3 (CD11b/CD18) and CR4 (CD11c/CD18), thereby enhancing phagocytosis, oxidative burst, and inflammatory responses (right). To prevent excessive activation, the system is tightly controlled by soluble inhibitors (yellow), including C1 inhibitor (C1-INH), factor H (FH), factor I (FI), C4b-binding protein (C4BP), anaphylatoxin inhibitor (AI), vitronectin (Vn), and clusterin (Cl). In addition, host cells express membrane-bound regulators such as MCP (CD46), CR1 (CD35), decay-accelerating factor (CD55/DAF), and CD59, which protect against C3/C4 convertase activity and block final MAC assembly (right)[304].

## 1.4.1 Activation of the complement system

### 1.4.1.1 The classical pathway

Although the CP is classified as part of the innate immune system, it is functionally important for both innate and adaptive immunity. The initiating component is C1q, a recognition protein that bridges the adaptive humoral response and complement activation by binding to IgM, IgG or IgA antibodies attached to antigens. Importantly,

C1q can also directly recognize and bind microbial surfaces, allowing complement activation to occur independently of antibodies. In physiological settings, C1q does not act alone but operates as part of the C1 complex, which consists of C1q associated with two zymogens, C1r and C1s, in a $(C1r:C1s)_2$ configuration[305]. Structurally, C1q is composed of six globular heads linked by a collagen-like tail, around which the C1r and C1s molecules are arranged[306,307].

When multiple globular heads of C1q simultaneously engage ligands on a pathogen surface, a conformational change is induced within the $(C1r:C1s)_2$ complex. This conformational rearrangement activates the autocatalytic activity of C1r, which then cleaves and activates its partner protease C1s[308,309]. Activated C1s subsequently cleaves complement component C4 into C4a and C4b, with C4b covalently attaching to the microbial surface[310,311]. C4a has antimicrobial activity[312]. Surface-bound C4b then recruits C2, which is cleaved by C1s into C2a and C2b. The C4b–C2a complex remains membrane-associated and constitutes the C3 convertase of the CP[313,314].

This C3 convertase has a crucial role: it cleaves numerous C3 molecules, generating large amounts of C3b that coat the pathogen surface, thereby facilitating opsonization. Concurrently, the smaller fragment C3a functions as a potent inflammatory mediator, contributing to the recruitment and activation of immune cells at the site of infection[315].

### 1.4.1.2 The lectin pathway

Unlike the CP, activation of the LP relies on pattern recognition molecules (PRMs), such as MBL, ficolins (ficolin-1, -2, and -3), and collectins-10/-11, which detect carbohydrate motifs on microbial surfaces. These PRMs are soluble proteins composed of a collagen-like region and a carbohydrate-recognition domain. Their ligand specificity includes sugar moieties such as mannose, N-acetylglucosamine, and β-glucan. Based on structural features, the PRMs are divided into two groups: C-type lectins (MBL, collectin-10, and collectin-11) and fibrinogen-like proteins (ficolin-1, -2, and -3)[316].

The effector activity of PRMs is mediated through MBL-associated serine proteases (MASPs), namely MASP-1, MASP-2, and MASP-3. Initially, MASP-2 was thought to be auto-activated and solely responsible for proteolytic activity in the LP. However, more recent evidence has shown that MASP-1 activates MASP-2 and is required for efficient pathway activation. Once PRMs assemble with MASP-1 or MASP-2, the complex catalyzes the cleavage of C4 and C2, generating the C4b2a complex that functions as the C3 convertase, analogous to the CP. The functional similarity between the two pathways is further reflected in the strong homology between MASP-1/2 and the CP proteases C1r and C1s.

The role of MASP-3 is less well characterized, as it remains the least studied MASP. Recent findings suggest that MASP-1 activates MASP-3, which in turn cleaves pro–factor D into factor D, thereby linking the LP to the initiation of the AP. Thus, through PRM recognition and MASP activity, the LP activates complement in a mechanism closely resembling that of the CP[317-320].

### 1.4.1.3 The alternative pathway

The AP was the second complement pathway to be identified, which explains the origin of its name. Unlike the CP and LP, it is initiated by the spontaneous hydrolysis ("tickover") of the internal thioester bond in C3, generating C3(H2O). Because C3 is present at high concentrations in plasma, tickover ensures a constant, low-level production of C3(H2O). This hydrolyzed form of C3 can bind factor B, which is subsequently cleaved by factor D to produce the short-lived fluid-phase C3(H2O)Bb convertase. This enzyme cleaves native C3 into C3a and C3b. While much of the C3b is rapidly inactivated through hydrolysis, a fraction covalently attaches to microbial surfaces via its thioester bond. Once deposited, C3b associates with factor B, which after cleavage by factor D generates the membrane-bound C3 convertase, thereby amplifying C3b production at the pathogen surface in the absence of complement regulators[321].

The AP convertase has a short half-life, but its activity can be prolonged by properdin, which binds and stabilizes the complex. Interestingly, properdin has additional functions: it can directly bind to microbial surfaces, acting as a PRR, thereby targeting complement activation specifically to pathogens. Owing to this dual role, both stabilizing the C3 convertase[322,323] and serving as a PRR, properdin is considered a key regulator of AP activity[324,325].

Beyond its role in direct activation, the AP also acts as an amplification loop for the CP and LP, significantly boosting complement responses once C3b is deposited. Moreover, ligand-bound pentraxins have been implicated in mediating crosstalk between all three pathways, further integrating their activity[6,296,297,320] (**Fig.1.13**).

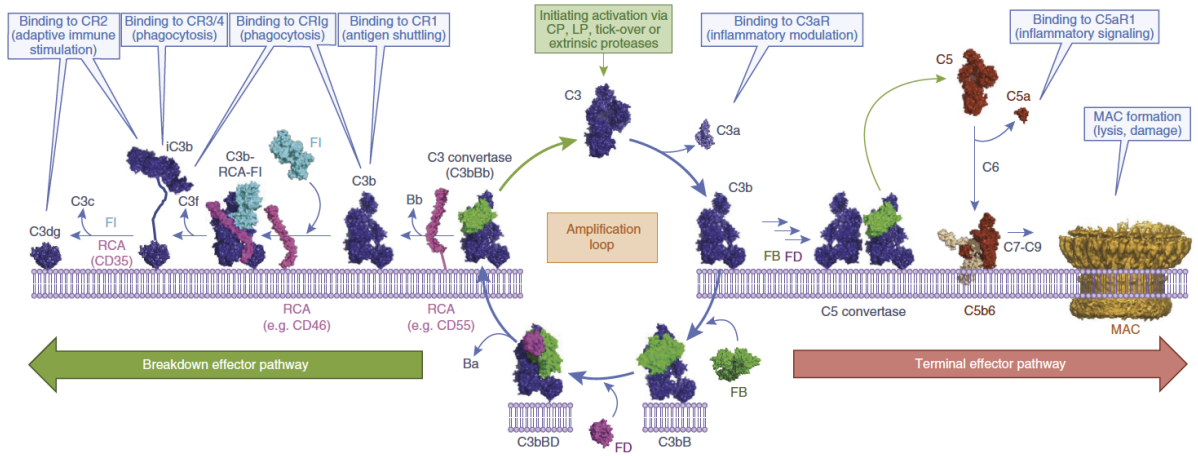


**FIGURE 1.13 Molecular processes underlying C3-driven complement activation, amplification, and effector generation.** This diagram illustrates the sequence of molecular events involved in complement activation initiated at the level of C3. Activation may occur through the CP, LP, or AP, leading to the deposition of C3b fragments on cellular surfaces. C3b associates with FB to form the C3bB, which is cleaved by FD to produce the active AP C3 convertase (C3bBb). In the absence of regulatory control, repeated formation of C3bBb establishes an amplification cycle that enhances overall complement activity and drives progression toward the terminal pathway (TP), culminating in the activation of C5, release of the C5a, and assembly of the MAC. Host tissues are protected by complement regulatory

proteins belonging to the regulators of complement activation (RCA) family, which promote disassembly of C3 convertases and facilitate FI-mediated inactivation of C3b to iC3b and C3dg. These degradation products function as opsonins, interacting with distinct complement receptors (CRs) to mediate diverse immunological effects[326].

### 1.4.1.4 The terminal pathway

The terminal complement pathway is initiated when the C5 convertase of either pathway cleaves C5 into the potent anaphylatoxin C5a and the larger fragment C5b. In contrast to the CP, AP and LP assembly of C5b-9 occurs without proteolytic cleavage of C7-9. In fact, C5b undergoes structural rearrangements that allow sequential assembly with C6, which stabilizes C5b and exposes a binding site for C7. The resulting C5b–7 complex associates with nearby lipid bilayers, anchoring to the membrane without yet disrupting its integrity[327,328]. Incorporation of C8 follows, in which the β-chain of C8 binds C7, creating the C5b–8 complex. At this stage, the complex inserts more deeply into the membrane, generating small pores and rendering the cell partially permeable.

The final step involves the recruitment of C9. Binding of the first C9 molecule to C8α induces a dramatic conformational change, shifting C9 from a compact globular form into an elongated structure that inserts into the bilayer. This initial insertion exposes additional binding sites, promoting polymerization of multiple C9 molecules. A complete MAC may incorporate up to ~22 C9 subunits, which together form a transmembrane pore. These pores allow the uncontrolled passage of ions and small molecules, ultimately leading to osmotic imbalance and the lysis of target cells[327,328].

To prevent host damage, MAC formation is tightly controlled. The membrane-bound regulator CD59 inhibits the final assembly of the C5b-9 complex, protecting host cells from complement-mediated injury. Nonetheless, when MAC inserts into eukaryotic membranes, cells may additionally internalize the complex through endocytosis, offering another layer of regulation[329].

### 1.4.1.5 Non canonical pathways of complement activation

While the canonical pathways of complement activation (CP, LP, AP) rely on convertase formation and sequential proteolytic cascades, complement can also be activated through non-canonical mechanisms. These routes bypass the formation of convertases and instead depend on various proteases that directly cleave C3 and C5 into their active fragments, C3a/C3b and C5a/C5b, respectively. Importantly, non-canonical complement activation is rapid and energetically less demanding compared with canonical pathways.

It is well established that almost all cell types can synthesize complement proteins and locally regulate their activation[330]. Several proteases with distinct tissue and cellular origins contribute to this process. For example, the kallikrein-related peptidase 14, present in tissues and biological fluids, efficiently cleaves C3[331]. The coagulation protease thrombin can generate biologically active C5a, thereby establishing a mechanistic link between the coagulation and complement system[332]. Furthermore,

phagocytic cells such as alveolar macrophages and Kupffer cells can produce and cleave C5, enabling them to generate C5a independently of the canonical C5 convertase[330,333]. Recent studies have further demonstrated that the lymphocyte-derived tryptase Granzyme K can activate the complement cascade by cleaving multiple complement components, including C2, C3, C4 and C5, resulting in the activation of the complement cascade[334,335].

The recognition that immune cells harbor a diverse set of intracellular complement proteins, receptors, and regulators led to the coining of the term “complosome”, reflecting its functional resemblance to other intracellular regulatory networks such as the inflammasome. Current evidence suggests that the complosome plays a key role in regulating cellular metabolism. Intriguingly, its functions extend beyond immune cells. For example, intracellular C3 activation in intestinal epithelial cells has been linked to ischemia/reperfusion injury[336], while neuronal fitness has been shown to depend on complosome regulation: mesenchymal stem cells suppress intracellular C3 expression in neurons to enhance survival under hypoxic stress[337].

The complosome also interfaces with intracellular pathogens, and its influence can be context-dependent. Depending on the pathogen and host cell type, complosome activation may either support pathogen clearance or, conversely, facilitate pathogen persistence[338-340]. These diverse and sometimes paradoxical outcomes underscore the complexity of intracellular complement biology and highlight the need for further investigation across a broader range of cell types and infection models.

Historically, complement activation was believed to occur exclusively in the extracellular space, whether systemically in plasma or locally in tissues. However, this dogma was increasingly questioned as evidence accumulated suggesting that complement could also be activated within cells[341,342]. A landmark study from the Kemper laboratory demonstrated the presence of large intracellular stores of C3 in resting human $CD4^+$ T cells, along with intracellular expression of C3aR and Cathepsin L (CTSL). They showed that CTSL constitutively cleaves intracellular C3 into C3a and C3b, within the lysosomes of resting human T cells, contributing to a form of intracellular complement activation[291,342] (**Fig. 1.14**). Binding of the intracellularly generated C3a to intracellular C3aR sustains T cell survival by maintaining low-level mammalian target of rapamycin (mTOR) signaling in the periphery[342]. Upon T cell activation, the intracellular complement machinery translocates to the cell surface, where C3a and C3b engage C3aR and CD46, respectively, to deliver autocrine signals that drive IFN-γ production and Th1 differentiation[291,343,344]. This dual role is striking: intracellular C3 activation is essential for T cell survival, whereas surface receptor engagement orchestrates Th1 responses. In line with this, T cells lacking C3aR fail to survive, underscoring the functional importance of compartment-specific complement activation. It is important to note that in mice, CD46 is not expressed on immune cells[345], leaving the role of intracellular complement in T cell regulation within the mouse model unclear. CD46 in mice is solely expressed primarily in spermatozoa[346] and retina[347] though recent evidence indicates its presence in the brain of CD1 mice[348].

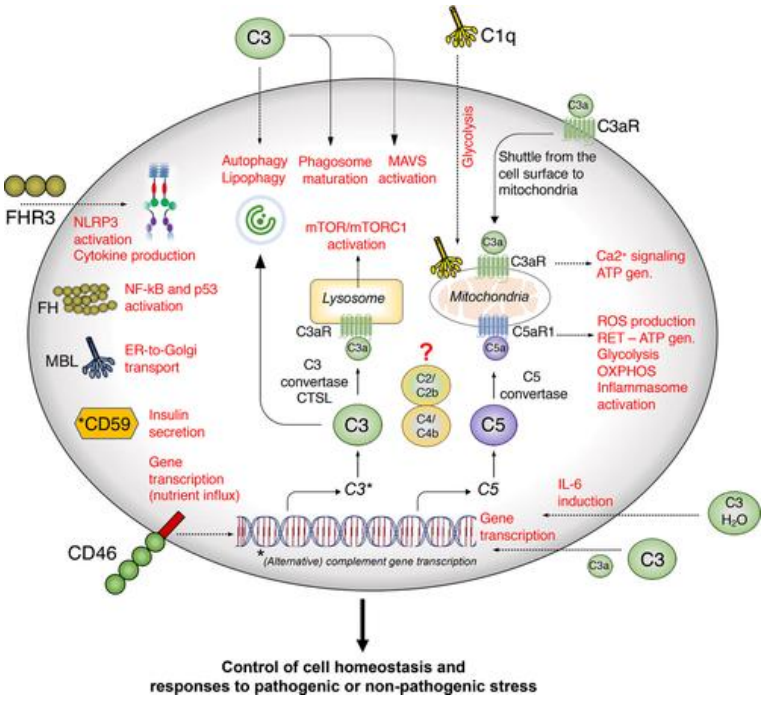


**FIGURE 1.14 Overview of human complosome activities presenting intracellular complement functions, highlighting both intrinsic and extrinsic sources of complement proteins.** Although displayed within a single cell for clarity, specific complosome roles can vary across different cell types, and retrograde C3 transport is omitted here. The diagram also illustrates selected regulatory components and signaling pathways reflecting diverse metabolic and immune functions influenced by the complosome. Note: Intracellular C3 and CD59 in pancreatic β-cells can be produced from alternative translation start sites, resulting in forms that remain within the cell, while the intracellular roles of C2 and C4 activation are still not fully understood[349].

Parallel findings established the existence of an intracellular C5 system in T cells, which is equally critical for human T cell activation[341]. T cells harbor intracellular stores of C5 that can be cleaved into C5a by an as-yet unidentified protease (**Fig. 1.14**). Intracellular C5a signals through C5aR1, leading to enhanced reactive oxygen species (ROS) production and subsequent activation of the NLRP3 inflammasome. This observation is consistent with earlier findings in myeloid cells, where C5aR1 also drives inflammasome activation[350]. Interestingly, T cells also express intracellular C5aR2, and signaling via C5aR2 in response to C5a or C5a-desArg provides a counter-regulatory mechanism that dampens C5aR1-driven inflammasome activation[341,351].

Murine T cells express the hybrid complement receptor CR1/2[352], but its functional role in vivo remains unexplored. Anaphylatoxin receptors, C3aR and C5aR, have emerged as key modulators of T cell responses. Engagement of these receptors on mouse $CD4^+$ T cells promotes IL-12 receptor expression, activates phosphatidylinositol-4,5-bisphosphate 3-kinase (PI3K) signaling, and inhibits protein kinase A by lowering cAMP levels, resulting in protein kinase B (PKB) phosphorylation and activation of mTORC1 and rbS6 pathways essential for producing IFN-γ and IL-2[353,354] (**Fig. 1.15**). Consequently, $CD4^+$ T cells deficient in both C3ar and C5ar1 show impaired Th1 responses and decreased severity in autoimmunity models[354]. Additionally, double-knockout T cells secrete higher levels of anti-inflammatory cytokines IL-10 and TGF-

β1[351], with an increase in suppressive Foxp3⁺ Tregs, indicating that blocking anaphylatoxin receptor signaling fosters regulatory functions[351,355]. Pharmacological inhibition of C3aR and C5aR1 similarly prevents Th1 induction and enhances regulatory capacity in naive human CD4⁺ T cells[356]. Moreover, C5aR1 contributes to T cell survival in mice by activating PKB and preventing apoptosis[353,357].

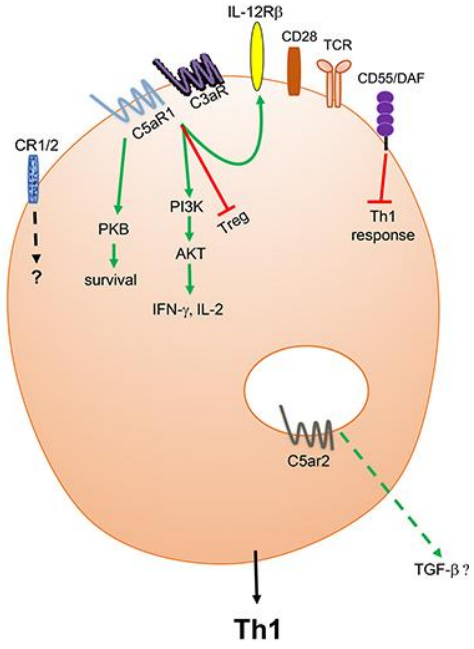


**FIGURE 1.15 Impact of complement receptor signaling on mouse T cells.** In mice, activated T cells express surface C5aR1 and C3aR, though the presence of C5aR1 remains debated, while C5aR2 is restricted to intracellular compartments. Activation of C5aR1 and C3aR triggers PI3K and PKB pathways, enhancing IFN-γ and IL-2 secretion, upregulating IL-12Rβ, promoting Th1 effector functions, and reducing FoxP3⁺ Tregs development. Additionally, C5aR1 supports T cell survival through PKB activation. Conversely, C5aR2 and CD55 serve as negative regulators of Th1 responses, with C5aR2 potentially inducing TGF-β release, and CD55 inhibiting complement convertase formation. Mouse cells also express a hybrid CR1/2, though its function is not yet defined. This figure focuses solely on complement receptor signaling; TCR and CD28 pathways are not depicted. Red arrows indicate inhibitory effects, while dashed lines represent observed but mechanistically unresolved interactions[358].

Complement plays a dual role in modulating T cell responses by both promoting their activation and facilitating contraction[291,359-361] (**Fig. 1.16**). This regulatory influence operates directly on T cells and indirectly through effects on APCs, which possess a broad array of complement receptors and regulators[5,362,363]. Engagement of these complement components modulates APC maturation and their cytokine and chemokine secretion profiles, ultimately shaping the quality and type of T cell responses triggered during antigen recognition. Early proof of complement's regulatory function came from studies using mice depleted of C3, which showed diminished CD4⁺ and CD8⁺ T cell responses and increased mortality in viral infection models[364,365]. Further research revealed that mice lacking C5aR exhibit reduced virus-specific CD8⁺ T cell responses during influenza[366], whereas double-deficient C3aR and C5aR1 mice are vulnerable to infections like herpes keratitis and Toxoplasma gondii due to impaired T cell immunity[354,367]. Studies with knockout mice for complement components such as C3, complement FB and FD, C5aR1 or C3aR demonstrated that these molecules are vital for DC maturation, effective T cell priming, and IFN-γ production, as deficiencies resulted in decreased MHC-II and costimulatory molecule expression[353,354,368]. Other findings indicate that complement fragments bound to apoptotic cargo and influence DC lysosomal trafficking, thereby enhancing antigen presentation and T cell expansion without biasing toward a specific effector subset[369]. Moreover, cytosolic detection of pathogen-derived C3b activates mitochondrial antiviral pathways and promotes proinflammatory cytokine secretion, revealing that intracellular complement receptor engagement in DC modulates their function distinctly from surface receptor activation[370].

Activation of anaphylatoxin receptors C3aR and C5aR1 on DCs triggers signaling cascades involving cyclic AMP (cAMP)[371], extracellular signal-regulated kinases (ERKs)[372], and nuclear factor kappa B (NF-κB)[373]. These pathways promote the release of cytokines such as IL-12, IL-23, IL-6, and TGF-β, which are key for driving Th1, Th2, and Th17 immune responses[374,375]. C5aR1 signaling enhances IL-12 production by DCs[376], and deficiency of C5 in mouse macrophages leads to impaired IL-12 secretion and decreased Th1 induction after *Staphylococcus aureus* challenge[377]. Furthermore, C5 knockout mice exhibit elevated Th2 responses in allergic asthma models, possibly due to reduced Th1 activity, suggesting that C5 via C5aR1 also negatively regulates Th2 lineage commitment[377,378].

Signals mediated by C3aR and C5aR1 are also crucial regulators of Th17 cell responses, primarily through their influence on TLR signaling in APCs. For instance, splenic DCs lacking C5aR1 produce significantly higher levels of IL-6 and IL-23 upon stimulation with the TLR ligand Pam3Cys compared to C5aR1-sufficient cells[379]. Supporting this, Lajoie et al. demonstrated that C5a inhibits IL-23 secretion induced by house dust mites in BMDCs within an asthma model[380]. Contrarily, BMDCs from C5aR1-deficient mice fail to produce IL-1β, IL-6, and IL-23 in response to OVA and LPS[375], highlighting that the effect of C5aR1 activation on Th17 differentiation depends on the DC subtype and TLR engagement. Parallel findings in humans show that *Candida albicans* stimulates IL-6 release from monocytes in a C5a-dependent manner[381], and C3aR activation induces IL-1β production in monocytes, specifically promoting Th17 differentiation in activated $CD4^+$ T cells without influencing Th1 or Th2 cytokines[382]. The human complement regulator CD46, engaged by C3b or C4b, enhances IL-23 expression in myeloid DCs[383] and stimulates IL-12 and nitric oxide (NO) generation in macrophages[384]. Moreover, monocytes from mice engineered to express human CD46 differentiate more rapidly into proinflammatory M1 macrophages, producing elevated IL-1β, IL-6, IL-12, and TNF[385].

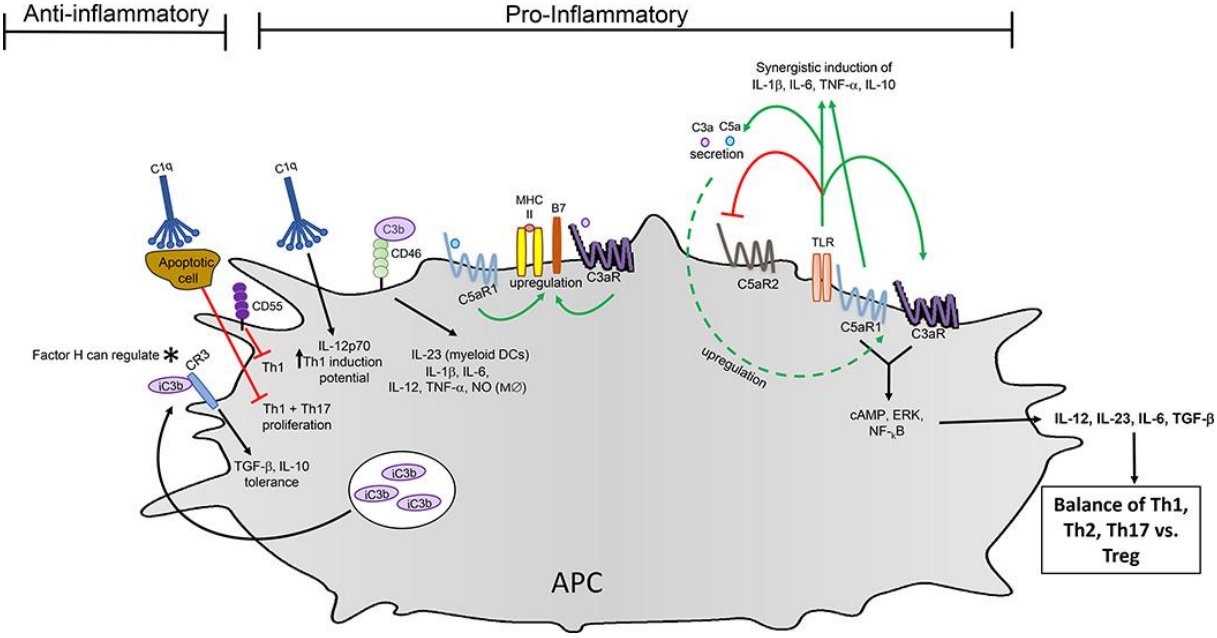


**FIGURE 1.16 Complement receptor activation effects on APC.** In DCs, engagement of C5aR1 and C3aR by their respective ligands enhances MHC-II and B7 costimulatory molecule expression, and activates signaling pathways including cAMP, ERK, and NF-κB. This results

in secretion of cytokines such as IL-12, IL-23, IL-6, and TGF-β. TLR activation amplifies C3a and C5a production, which bind their receptors and promote receptor upregulation in a positive feedback loop. Combined TLR and complement receptor signaling synergistically induces cytokines including IL-1β, IL-6, TNF-α, and IL-10, supporting Th1 and Th17 differentiation. In human DC and macrophages, CD46 activation stimulates proinflammatory cytokines and NO production. Complement component C1q exerts dual regulatory effects depending on context, enhancing Th1 responses via increased IL-1β and IL-12p70, while inhibiting IL-1β secretion and Th1/Th17 proliferation when bound to apoptotic cells. Additional anti-inflammatory signals derive from CD55/DAF, which limits Th1 induction by APCs, and iC3b-CR3 interaction, promoting TGF-β and IL-10 production and tolerance. FH and intracellular iC3b pools further modulate these processes. Inhibitory activities are indicated by red arrows[358].

### 1.4.2 Regulation of the complement system

All three complement activation pathways culminate in strong pro-inflammatory and cytotoxic effects. Given their amplification capacity, particularly through the AP, uncontrolled activation could be highly detrimental to the host. For this reason, strict regulation of complement activity is essential. The immune system ensures such regulation through two main strategies. First, activated complement proteins are rapidly inactivated unless they are bound to the pathogen surface where activation was initiated. Second, multiple inhibitory proteins act at various checkpoints in the cascade to prevent inappropriate complement activation on healthy host cells, thereby protecting them from accidental injury. Importantly, these regulators not only safeguard host tissues but also help terminate complement activity once pathogens have been cleared.

Two major mechanisms of complement regulation are recognized: decay-accelerating activity, which enhances the dissociation of C3 convertases (C4b2a and C3bBb), and factor I cofactor activity, which enables factor I to cleave and inactivate covalently bound C3b and C4b, preventing their participation in new convertase formation[292]. Regulation is achieved through both soluble (plasma) and membrane-bound inhibitors, which together maintain complement homeostasis.

Among the plasma regulators, C1-INH is a key molecule that irreversibly inactivates the initiating proteases C1r and C1s of the CP, as well as MASP-1 and MASP-2 of the LP, thereby blocking the earliest steps of activation (**Fig. 1.12**). Two other critical plasma regulators are FH and FI, which control the AP. In the absence of either protein, uncontrolled complement activation occurs, leading to excessive consumption of C3 and secondary complement deficiency. FI is a plasma serine protease that permanently inactivates C3b to iC3b by proteolysis, but this reaction requires cofactors. iC3b can be further cleaved into C3dg and C3c in a similar cofactor-dependent manner. FH serves as competitor with FB for C3b binding, acts as a cofactor for FI, and destabilizes the AP C3 convertase (C3bBb), thereby accelerating its dissociation (**Fig. 1.12**). FI also contributes to the regulation of the CP and LP by cleaving C4b, with C4BP serving as the required cofactor. C4BP itself further enhances regulation by accelerating decay of the C4b2a convertase and by promoting C3b inactivation, albeit less efficiently[292,293].

Membrane-bound regulators provide additional, localized protection to host cells. One of the RCA, membrane cofactor protein (MCP/CD46) serves as a cofactor for FI-mediated cleavage of C3b and C4b, thereby protecting the cells on which it is expressed[386]. Other RCA, DAF/CD55 accelerates the dissociation of C3 convertases across all three pathways, destabilizing both C3bBb (AP) and C4b2a (CP and LP)[387]. The other RCA, complement receptor 1, CR1 (CD35), expressed on circulating cells, primarily functions as an immune adherence receptor, facilitating the clearance of C3b/C4b-opsonized immune complexes and pathogens. In addition, CR1 exerts regulatory effects by serving as a cofactor for FI in the stepwise cleavage of C3b to iC3b and further to C3c and C3dg, as well as for the inactivation of C4b[292,293,388-390] (**Fig. 1.13**).

### 1.4.3 The anaphylatoxins and their receptors

Two important fragments generated during complement activation are the small peptides C3a and C5a, collectively referred to as anaphylatoxins. They are produced through the proteolytic cleavage of complement proteins C3 and C5, respectively, and exert their biological activity by binding to specific receptors, thereby triggering localized inflammatory responses[391-393]. Among all complement-derived fragments, C5a is considered the most potent inflammatory mediator. Once generated, anaphylatoxins can drive a wide range of effector functions[391].

The complement system requires strict regulation to prevent excessive inflammation. Given the potent pro-inflammatory properties of anaphylatoxins, the immune system has evolved mechanisms to restrict their activity via enzymatic degradation. This is mediated by carboxypeptidases, which remove the C-terminal arginine from C3a and C5a, generating C3a-desArg and C5a-desArg[394,395]. While C3a-desArg lacks receptor-mediated inflammatory function, C5a-desArg retains partial activity (1–10%), thereby maintaining limited pro-inflammatory potential[396,397].

The biological activities of anaphylatoxins are mediated through their interaction with specific receptors, collectively referred to as anaphylatoxin receptors. Three such receptors have been identified: C3aR, C5aR1, and C5aR2. All three belong to the superfamily of G-protein–coupled receptors (GPCRs), sharing high sequence homology and close structural similarity to chemotactic receptors. Despite this relatedness, each receptor displays unique ligand specificity, signaling properties, and functional roles[398].

The C3a receptor (C3aR), first cloned in 1996, shares 37% identity with C5aR1. C3aR binds exclusively to C3a, with no recognition of its degradation product C3a-desArg or of C5a[399,400]. C3aR is characterized by a short N-terminal segment and an extensive second extracellular domain consisting of 175 amino acids, which is highly conserved across species[399,400]. The murine version of C3aR shares 65% overall sequence identity with human C3aR and includes a unique 165-amino acid insertion. C3aR undergoes various post-translational modifications, including significant glycosylation and sulfation, which contribute to its molecular diversity[398]. Upon ligand binding, intracellular signaling is initiated through heterotrimeric G proteins, with responses

varying depending on cell type. Specifically, C3aR signaling can involve either pertussis toxin-sensitive or -insensitive G proteins[401,402] (**Fig. 1.17 A**).

The C5a receptor 1 (C5aR1) is the most extensively studied anaphylatoxin receptor, first cloned in 1991[403,404]. This membrane glycoprotein binds both C5a and C5a-desArg, though its affinity for the latter is 10–100 times weaker[396,403,404]. In humans, C5aR1 is encoded by the C5AR1 gene on chromosome 19 (chromosome 7 in mice) and forms a seven-transmembrane domain protein. Post-translational modifications modulate its function: N-terminal glycosylation does not affect receptor expression or ligand binding[405], whereas sulfation of the N-terminus enhances ligand binding[406-408]. C5a binding occurs through a dual-site interaction: a recognition site within the receptor's N-terminal extracellular domain engages the disulfide-linked core of C5a, while a second binding region involving Asp191/Glu199 and Arg206 in the second transmembrane loop interacts with Lys68 and the C-terminal carboxylate group of C5a[408]. Ligand engagement induces extensive phosphorylation of the C-terminal tail[398] **(Fig. 1.17 B)**.

C5a receptor 2 (C5aR2), first cloned by Ohno et al.[409] shares 38% sequence identity with its paralog C5aR1. C5aR2 binds C5a, but with a 20-fold higher affinity for its des-arginated form, C5a-desArg[410,411]. Positioned on chromosome 19 near the C5aR1 gene, C5aR2 is encoded by two exons. Its protein structure contains distinctive glycosylation and sulfation sites that influence C5a-desArg binding, plus a putative S-acylation motif in the C-terminal region, as well as multiple phosphorylation sites, some of which are modified in response to ligand engagement[398]. Unlike classical GPCRs, C5aR2 lacks key intracellular motifs such as DRY and NPXXY, preventing G-protein coupling. For this reason, it was initially classified as a non-signaling "decoy receptor", thought to scavenge excess C5a and thereby regulate C5aR1 activity[411,412]. However, more recent studies challenge this concept, revealing that C5aR2 can exert context-dependent pro- or anti-inflammatory effects[372,393,413] (**Fig. 1.17C**).

A

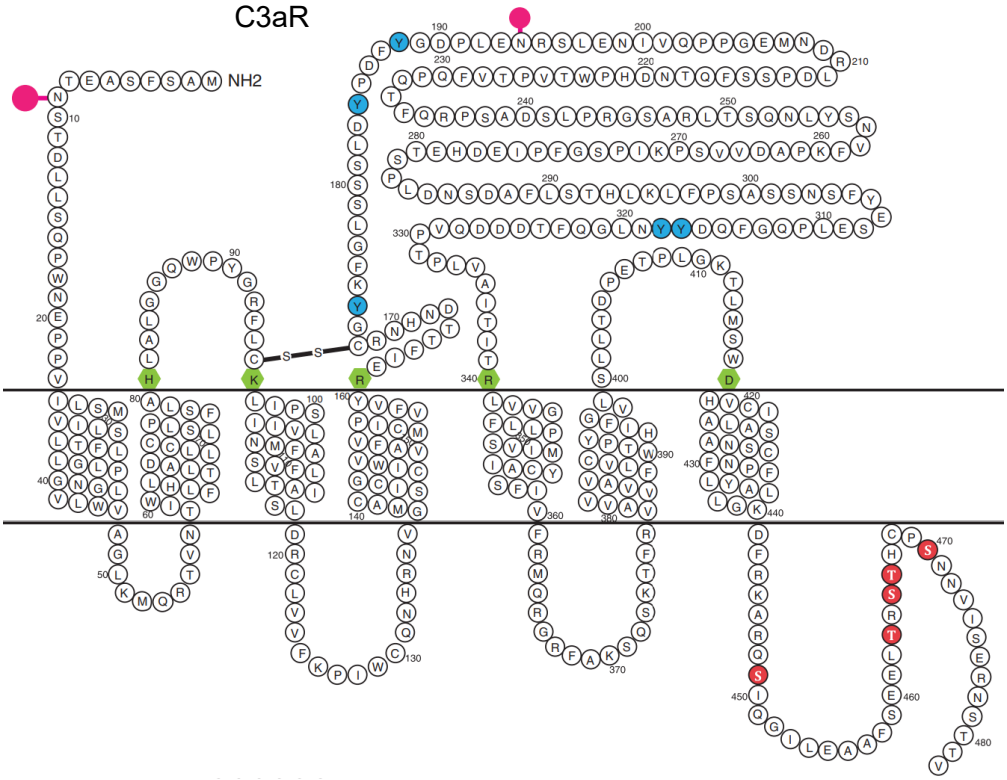


B

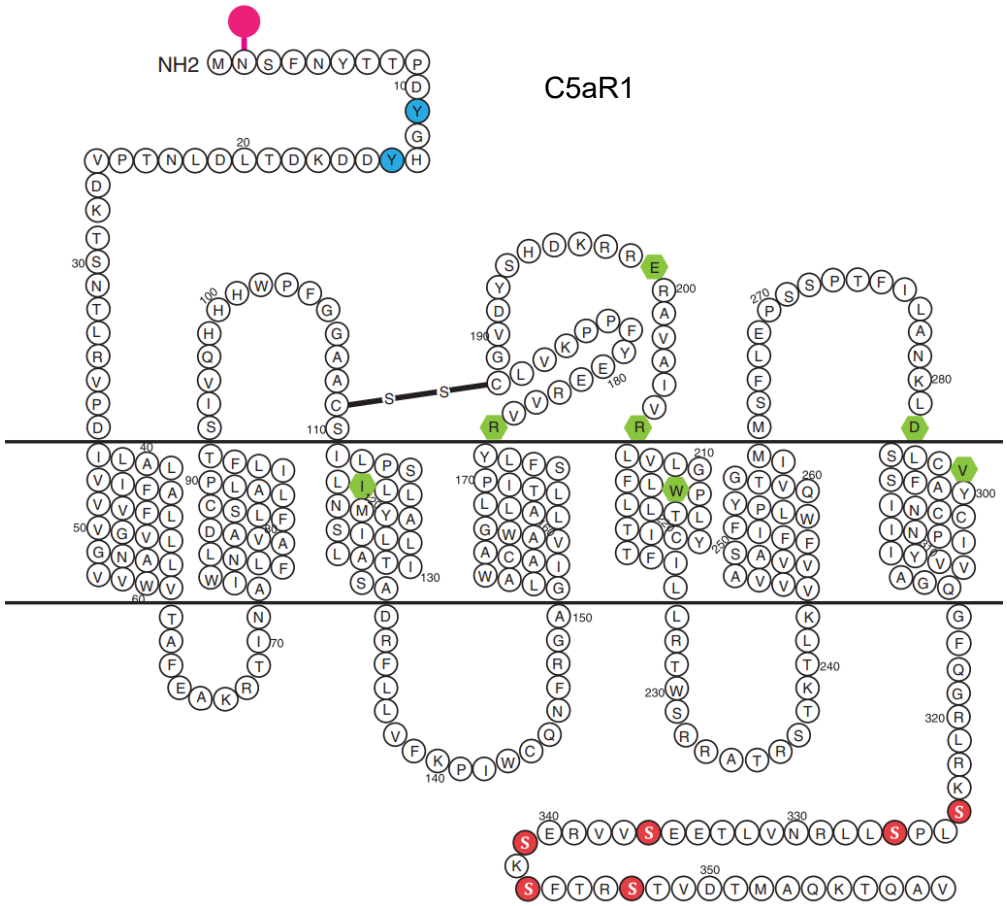

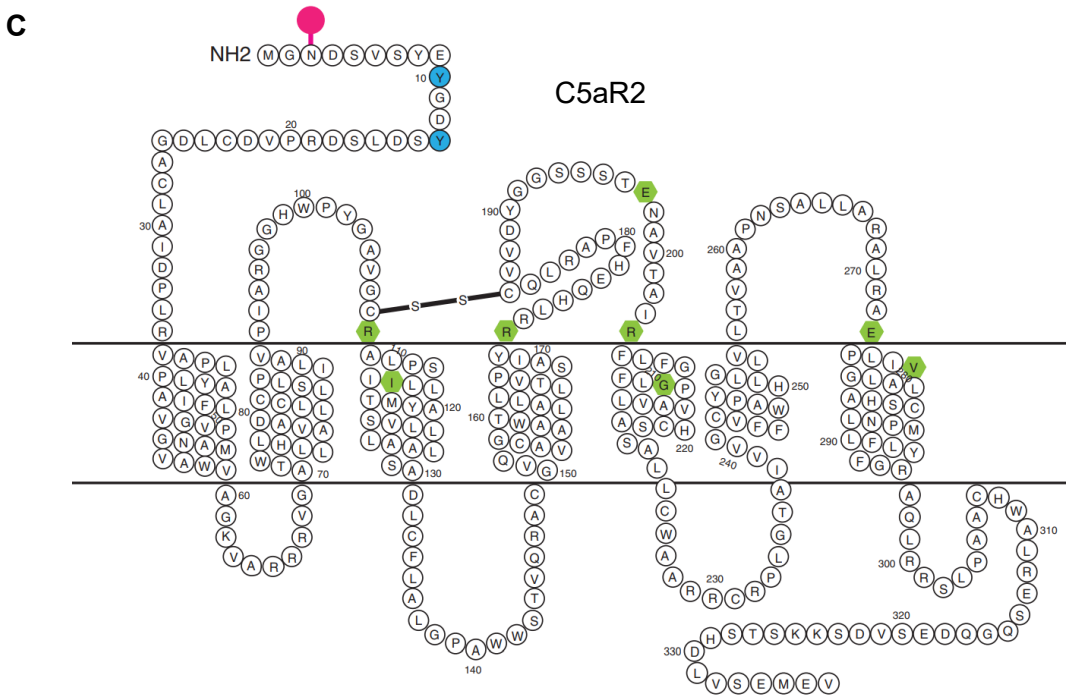


**FIGURE 1.17 Sequence and domain structure of C3aR, C5aR1 and C5aR2.** Illustrated are the amino acid sequences and structural domains of (A) C3aR, (B) C5aR1 and (C) C5aR2. For C5aR2 and C3aR, potential intracellular loops resulting from S-acylation of cysteine residues are indicated. Pink circles represent predicted glycosylation sites, while phosphorylation sites within the intracellular domains are marked in pink, and tyrosine sulfation sites in the extracellular regions are shown in blue. The ligand-binding regions located on the extracellular domains are indicated in green[398].

At the molecular level, C5aR1 signaling involves multiple G-proteins, kinases, and adaptor proteins. Both pertussis toxin–sensitive (Giα2, Giα3) and insensitive (Gαs, Gα16) G proteins can mediate signaling[414,415]. Engagement of C5aR1 triggers calcium mobilization from intracellular stores and extracellular influx[416]. Activated receptors are phosphorylated by GPCR kinases (GRKs), promoting the recruitment of β-arrestins 1 and 2, which regulate receptor internalization and desensitization. Beyond their classical roles, GRKs also interact with downstream signaling proteins such as Akt, MAPK/ERK, and PI3K-γ. Consequently, C5aR1 activation induces multiple intracellular cascades, including PI3K-γ[417,418], phospholipase C β2[419], phospholipase D[420], and Raf-1/B-Raf–dependent MEK-1 activation[421].

### 1.4.3.1 Cellular expression

The three anaphylatoxin receptors, C3aR, C5aR1, and C5aR2, exhibit distinct patterns of cellular expression that shape their biological functions.

C3aR expression is widespread among myeloid lineage cells, including basophils, eosinophils, MC, monocytes, macrophages, DCs, and microglia[422-427]. Evidence for C3aR on neutrophils and BM-derived DC varies between species, with some reports supporting expression in mice but remaining controversial in humans. In humans, strong C3aR mRNA expression is detected in the lung, spleen, small intestine, BM, and brain. Conversely, mouse tissues show high C3aR mRNA in the lung, but low level in brain and not expressed in spleen. Human platelets lack C3aR expression, unlike

guinea pig platelets. A useful tool to define C3aR expression in vivo is the *tdTomato-C3ar1*$^{fl/fl}$ reporter mouse model generated by the Köhl group. This strain encodes a self-processing polyprotein of tdTomato fused to C3aR, flanked by loxP sites[428]. This tool has enabled precise characterization of AT receptor expression in mice, providing valuable insights into their distribution and regulation under both steady-state and inflammatory conditions. In mice, Quell et al., confirmed that C3aR is expressed in multiple myeloid subsets: eosinophils exhibit intracellular expression, mucosal DCs are positive for C3aR, neutrophils upregulate the receptor only upon activation, and SiglecF– macrophages also express it[428]. Beyond myeloid cells, C3aR is also found in mice in non-hematopoietic tissues, such as astrocytes within inflamed brain tissue[429], endothelial cells[430], epithelial and smooth muscle cells, as well as the submucosal and parenchymal vessels of asthmatic lungs[431]. Reports on human lymphocytes remain inconsistent: little to no surface C3aR, though activation via CD3/CD28 upregulates surface expression[291,432] and intracellular C3aR also translocates to the membrane upon stimulation, whereas murine CD4$^+$ T cells appear to lack C3aR expression under both naïve and activated conditions[428]. Messenger RNA for C3aR has been detected in naive human Tregs with expression levels rising upon stimulation through CD3 and CD28. Additionally, C3aR is present on human tonsillar B cells.

C5aR2 mRNA is found in multiple tissues derived from both myeloid and non-myeloid sources, including the brain, placenta, ovary, testis, spleen, and colon. Karsten et al. found the strongest C5aR2 expression in the brain, BM, and airways[433]. Protein expression of C5aR2 has been identified on the surface of cells in lung, liver, heart, kidney, and adipose tissue, as well as in skin fibroblasts, neutrophils, and immature DC (but not mature DCs). Expression of C5aR2 has been documented in eosinophils, mucosa-associated DCs, NK cells, and B cells, with tissue-dependent expression patterns observed in macrophages; notably, no expression is found in murine T cells[433]. C5aR2 expression in neutrophils is consistently high and uniform, but varies according to tissue and cell type in eosinophils, macrophages, and DC subsets[433]. Naive and activated T cells did not show expression of C5aR2, while B cells from various tissues consistently displayed homogeneous C5aR2 expression[433]. In contrast, C5aR2 expression has been shown in human CD4$^+$ T cells[341]. Additionally, NK cell subsets in blood and spleen exhibited strong C5aR2 expression[433]. C5aR2 is often co-expressed with C5aR1 in myeloid-derived cells within solid tissues, such as tissue macrophages like Kupffer cells. C5aR2 is predominantly located intracellularly, with evidence suggesting it cycles between intracellular stores and the cell surface. Its expression is regulated by cytokines including IFN-γ and TNF-α; for instance, IFN-γ increases C5aR2 levels in HL-60 and U-937 cells, while in HeLa cells, both IFN-γ and TNF-α downregulate its expression, indicating cell- and context-dependent control mechanisms. The function of C5aR2 depends on the cell type: it can serve as a nonsignaling decoy receptor that antagonizes C5aR1, or act as an active receptor transmitting either pro-inflammatory or anti-inflammatory signals[391,434,435].

C5aR1 expression is widespread among myeloid cells such as neutrophils, macrophages, eosinophils, and DCs[408,436]. C5aR1 is broadly expressed in multiple tissues, including the central nervous system, connective tissue, eye, heart, kidney, liver, lung, and skin. Its presence spans various cell types such as endothelial,

epithelial, neural, and smooth muscle cells[408]. Using GFP-reporter mice, Karsten et al. demonstrated that C5aR1 is selectively expressed in CD11b$^+$ cDCs and moDCs, but absent from CD103$^+$ cDCs[436]. C5aR1 has been detected on human tonsillar B cells and peripheral T cells[291,341]. However, its presence on mouse T cells remains unclear[436]: some studies showed expression on T cells[354], while others report no expression[353,436,437]. The expression of C5aR1 is influenced by several cytokines and signaling molecules, including IFN-γ, IL-6, TNF, IL-4, phorbol esters, cAMP, and prostaglandin E2.

### 1.4.3.2 Regulation of innate immune cells

Once generated, anaphylatoxins can drive a wide range of effector functions[312]. Both C3a and C5a induce smooth muscle contraction and enhance vascular permeability. Their effects vary depending on the cell type they activate. For example, in macrophages[438], neutrophils[439], and eosinophils[439], they can trigger an oxidative burst, thereby regulating the production of ROS. In addition, anaphylatoxins stimulate the release of histamine from basophils[440] and MC[441]. In eosinophils, C3a and C5a further control the production of eosinophil cationic protein, promote adhesion to endothelial cells, and regulate migration[401,442]. C3a specifically enhances serotonin release from platelets[443].

C5a is particularly notable for its role as a potent chemoattractant, recruiting macrophages[444], neutrophils[445], as well as basophils[446] and MCs. Beyond their classical pro-inflammatory functions, anaphylatoxins have also been implicated in tissue regeneration[447,448], fibrosis[448-450], and even neurodevelopment[451].

The activities of anaphylatoxins are tightly regulated to avoid excessive inflammation. Carboxypeptidases degrade anaphylatoxins by removing the terminal arginine, generating C3a-desArg and C5a-desArg, with the latter retaining partial agonistic activity[394,396,397]. Functional diversity is further refined by receptor distribution. Functionally, C5a–C5aR1 interaction triggers cytoskeletal reorganization, upregulation of adhesion molecules and complement receptors (CR1, CR3/4), chemotaxis, apoptosis, granule exocytosis, neutrophil extracellular trap (NET) formation, and reactive oxygen metabolites production[391,401,418,444,452-454]. In DCs, C5aR1 regulates co-stimulatory molecule expression and the production of cytokines such as IL-12 family members, IL-6, and TGF-β, thereby shaping T cell activation and differentiation[455-458]. C5aR2, initially described as a non-signaling decoy receptor, is now recognized as a context-dependent modulator, either dampening or fine-tuning inflammatory signaling, particularly in neutrophils and macrophages[410,411,433,459]. Its preferential binding to C5a-desArg highlights its regulatory role in balancing C5a-driven inflammation[412]. C5aR2 can exert context-dependent pro- or anti-inflammatory effects[372,393,413]. For instance, C5aR2 deficiency in neutrophils alters cytokine responses to C5a, enhancing IL-6, TNF-α, and CR3 expression[413]. Moreover, C5aR2 knockout mice show improved survival in the cecal ligation puncture model of sepsis, associated with reduced neutrophil and macrophage infiltration and diminished HMGB-1 release[459].

Taken together, anaphylatoxins and their receptors establish a highly dynamic signaling network within innate immune cells. While C3aR and C5aR1 mediate pro-inflammatory and immunomodulatory functions, C5aR2 provides a critical regulatory checkpoint, ensuring that complement activation enhances host defense without driving uncontrolled inflammation.

C5aR1 signaling platforms engage in extensive crosstalk with other innate immunity receptor pathways, such as TLRs, cytokine receptors, Fc receptors for IgG (FcγRs), growth factor receptors, WNT signaling, CLRs, the Notch pathway, and the NLRP3 inflammasome[426] (**Fig.1.18**). Key examples of this crosstalk involve thrombin-mediated cleavage of C5 to generate C5a[332,460], which suppresses TLR-driven IL-12 production by macrophages[456] and regulation of NLRP3 inflammasome activation by C3a and MAC[382,461,462].

C3aR activation triggers the NLRP3 inflammasome in human monocytes[382] by stimulating ERK1/2, which promotes ATP release and engages the P2X7 receptor to induce inflammasome assembly[382] and IL-1β production. Similarly, C5aR1 signaling enhances inflammasome activation via CP activation, increasing IL1B transcription and caspase-1 activity[350]. Sublytic MAC formation also activates NLRP3 by inducing calcium release from the endoplasmic reticulum in DC and epithelial cells[463]. C1q can both activate and suppress NLRP3 depending on context, highlighting complement's dual regulatory roles[464]. Moreover, crosstalk between FcγRs, complement, and carbohydrate receptors like dectin-1 modulate inflammatory responses via cooperative receptor signaling, influencing downstream pathways that regulate C5aR1-mediated activities[454,465]. Post-translational modifications of antibodies, such as IgG1 glycosylation, further fine-tune this interplay by affecting receptor signaling cascades and immune cell effector functions (**Fig.1.18**).

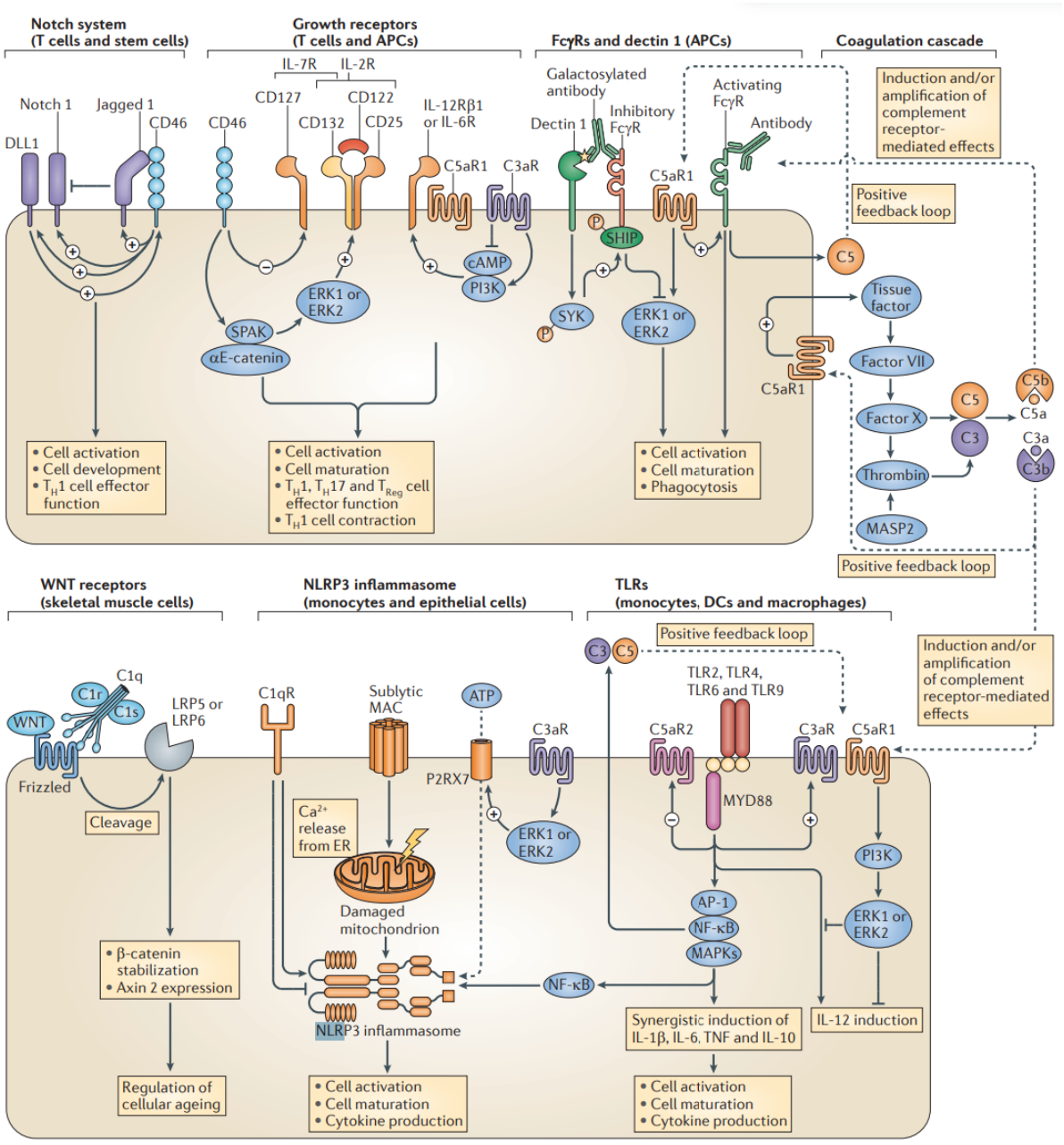


**FIGURE 1.18 Crosstalk between complement and cellular effector systems.** This figure illustrates the established and emerging crosstalk pathways between the complement system and TLR, the coagulation cascade, the NLRP3 inflammasome, CLRs, FcγRs, cytokine and growth factor receptors, as well as WNT and Notch signaling pathways. The diagram specifies the cell types involved and highlights the signaling pathways underlying these interactions[291].

### 1.4.3.3 Regulation of adaptive immune cells

C3a and C5a can shape adaptive immunity by signaling through C3aR, C5aR1, and C5aR2 expressed on T and B lymphocytes and on APCs. In $CD4^+$ T cells, autocrine and paracrine C3a/C5a signals integrate with intracellular ("complosome") complement activity to tune metabolism (mTOR, mitochondrial function), survival, and fate decisions, promoting effector differentiation (e.g., Th1/Th17) while restraining excessive cAMP/PKA pathways; conversely, dampened C3aR/C5aR1 signaling can bias toward regulatory programs. Emerging work also assigns C5aR2 a nonredundant,

T cell–intrinsic modulatory role that balances prostanoid and IL-1R2 axes to calibrate Th responses[290,358,466,467].

Human circulating CD4$^+$ T cells contain intracellular stores of C3 that are essential for maintaining basal mTOR activity, thereby supporting homeostatic cell survival, and for orchestrating both the induction and resolution phases of Th1 immune responses. Activation of these T cells through TCR engagement and CD28 co-stimulation promotes the rapid translocation of internally generated C3b to the cell surface, where it binds CD46[342]. This cell-autonomous activation of CD46 leads to nuclear signaling and metabolic shifts critical for IFN-γ production and Th1 differentiation[342,343,468]. The temporally controlled cleavage of CD46 is integral to terminating Th1 responses, partly by regulating cholesterol efflux[469-471]. Concurrently, intracellular generation of C5a interacts with mitochondrial C5aR1, triggering assembly of the NLRP3 inflammasome and stimulating IL-1β secretion[341], which supports Th1 responses at mucosal sites[341]. The alternative C5aR2, expressed on Th1 cells, appears to suppress NLRP3 activation and IL-1β production, contributing to Th1 response contraction via an as yet unclear mechanism[290,341].

Similarly, in human CD8$^+$ CTLs, CD46 engagement is crucial for metabolic adaptations, including increased glycolysis and fatty acid synthesis, which underpin optimal IFN-γ secretion, granzyme B expression, and cytotoxic activity[472,473]. Intriguingly, complement components can also modulate CTL functions negatively; for example, extracellular C1q acts on mitochondria in CD8$^+$ T cells to restrain glycolysis and dampen effector responses during infections, thereby limiting tissue damage[474].

Beyond T cells, C3a/C5a cues influence B-cell trafficking and activation and indirectly sculpt germinal-center quality by acting on DCs and other accessory cells. Collectively, anaphylatoxin–receptor circuits provide a rapid, complement-linked rheostat that amplifies or restrains adaptive responses depending on the context[290,358,466,467].

Further, C3a modulates IL-6 and TNF-α synthesis by B cells and monocytes[475,476]. Intracellular C3 stores are present in resting human and mouse B cells[342,477], but the necessity of cell-autonomous C3 for B cell survival and function remains unclear. Some evidence suggests that internalized C3 and C3a can enter the nucleus in human B cells, potentially regulating DNA packaging by modulating histone-DNA interactions[478]. While the impact of reduced C3 uptake on key B cell functions like cytokine production and antibody generation has not been fully explored, extracellular C3 is known to be important for proper memory B cell development[479]. B cell-expressed anaphylatoxin receptors contribute to GC formation[480], with systemic C3a being the main ligand for C3aR on B cells, though B cell-derived C3 may have a supplementary role.

## 1.5 Hypotheses and specific aims of the thesis

As outlined above, cDCs originate from BM precursors, which differentiate into pre-cDC1, -cDC2 or pro-DC3 in the BM. Based on previous findings that complement factors are expressed in hematopoietic stem and progenitor cells (HSPCs)[481], I hypothesized that C3 and/or C5 are expressed in BM precursor cells, such as MDPs and CDPs, and are cleaved into C3a and/or C5a, which bind to their cognate C3aR or C5aR1 in or on MDPs or CDPs. I further hypothesized that this loop of autocrine C3/C5

production, C3a and C5a generation and subsequent anaphylatoxin receptor activation is critical for MDP/CDP homeostasis, their appropriate DC differentiation and function of the different cDC subsets differentiated from MDPs and/or CDPs. To test these hypotheses, I pursued the following specific aims:

1. Determine the expression of C3/C3a, C5/C5a and the anaphylatoxin receptors (C3aR, C5aR1) in MDPs and CDPs from WT, *C3ar1*$^{-/-}$ and *C5ar1*$^{-/-}$ mice.

2. Assess the impact of C3aR or C5aR1-deficiency on MDP and CDP homeostasis in the BM.

3. Define the impact of C3aR or C5aR1-deficiency on Flt3L/ GM-CSF-driven differentiation of pDC, cDC1 and cDC2 subsets from MDPs or CDPs.

4. Define the impact of C3aR or C5aR1-deficiency on the function of Flt3L/ GM-CSF-differentiated cDC2 subsets from MDPs or CDPs.

5. Assess the impact of the C5a/C5aR1 axis on Flt3L-induced in vivo generation and function of splenic cDC subsets.

# 2. Materials and Methods

## 2.1 Materials

### 2.1.1 Chemicals

**TABLE 2.1 Used chemicals**

| Substance | Manufacturer | Cat. Number |
|---|---|---|
| Albumin from chicken egg white | Sigma-Aldrich Chemie GmbH, Steinheim | A5503 |
| Ambion Nuclease-Free Water | Invitrogen, Thermo Fisher Scientific, Waltham, USA | AM9937 |
| Bacillol | Hartmann, Heidenheim | 973389 |
| BD FACS Flow Sheath Fluid | BD Biosciences Europe, Erembodegem, Belgium | 342003 |
| Biozym LE Agarose, EEO | Biozym Scientific GmbH, Oldendorf | 840004 |
| Bovine Serum Albumin (BSA) | Sigma-Aldrich Chemie GmbH, Steinheim | A9418 |
| Dulbecco's Modified Eagle Medium (DMEM) | Invitrogen, Thermo Fisher Scientific, Waltham, USA | SH3008101 |
| Dulbecco`s Phosphate Buffered Saline (DPBS) | Gibco, Life Technologies Corporation, Carlsbad, USA | 14190-094 |
| DNase I | Roche Diagnostics | 10104159001 |
| Ethanol, 200 Proof Pure | Decon Labs, King of Prussia, USA | 2701 |
| Ethylenediaminetetraacetic acid (EDTA), ultrapure 0,5 M, pH 8,0 | Invitrogen, Thermo Fisher Scientific, Waltham, USA | 15575-038 |
| Fetal Calf Serum (FCS) | Sigma-Aldrich Chemie GmbH, Steinheim | F0926 |
| FCS ES Cell Pretested | Capricorn Scientific GmbH, Ebsdorfergrund, Germany | FBS-ES-12B |
| Fixation buffer | BioLegend, London, UK | 420801 |

| | | |
|---|---|---|
| Fluoroshield, histology mounting medium | Sigma-Aldrich Chemie GmbH, Steinheim | F6182 |
| HEPES 1 M | Gibco, Life Technologies Corporation, Carlsbad, USA | 15630-080 |
| Iscove's Modified Dulbecc's Medium (IMDM: +L-Glutamine, +25 mM HEPES, -Phenol Red) | Gibco, Thermo Fisher Scientific, Waltham, USA | 21056-023 |
| L-glutamine (200 mM) | Gibco, Thermo Fisher Scientific, Waltham, USA | 25030-081 |
| Liberase TL | Roche Diagnostics | 05401020001 |
| LPS *E. coli* O55:B5 | Sigma-Aldrich Chemie GmbH, Steinheim | L2880 |
| MACS BSA stock solution | Miltenyi Biotec GmbH, Bergisch Gladbach, Germany | 130-091-376 |
| Mouse CSF-2 (GM-CSF), recombinant protein | Peprotech Corporation, Rocky Hill, USA | 315-03 |
| Mouse Flt-3 Ligand (Flt3L) recombinant protein | Peprotech Corporation, Rocky Hill, USA | 250-31L |
| o-Phenylenediamine dihydrochloride (OPD) | Sigma-Aldrich Chemie GmbH, Steinheim | P6787 |
| Ovalbumin (OVA) Endofit | Invivogen, San Diego, USA | vac-pova |
| PAM3CSK4 | Invivogen, San Diego, USA | tlrl-pms |
| Penicillin, streptomycin | Thermo Fisher Scientific, Waltham, USA | 15140122 |
| RBC lysis buffer | Sigma-Aldrich Chemie GmbH, Steinheim | R7757 |
| Recombinant GM-CSF | BioLegend, London, UK | 576306 |
| Roswell Park Memorial Institute (RPMI) 1640 Medium | Gibco, Life Technologies Corporation, Carlsbad, USA | 11875093 |

| | | |
|---|---|---|
| RNase-ExitusPlus | AppliChem GmbH | A7153,0500 |
| Sodium pyruvate | Gibco, Life Technologies Corporation, Carlsbad, USA | 11360-039 |
| Streptavidin-HRP | VWR International GmbH, Darmstadt | 016-030-084 |
| TMB 1-step Ultra ELISA Substrate Solution | Thermo Fisher Scientific, Waltham, USA | 34028 |
| Trypan blue | Life Technologies Corporation, Carlsbad, USA | 15250-061 |
| Trypsin, 0,25% | Hyclone Laboratories Inc, Logan, USA | SH30042.01 |
| Tween 20 | Sigma-Aldrich Chemie GmbH, Steinheim | P1379 |

### 2.1.2 Antibodies used for flow cytometry and immunofluorescence staining

**TABLE 2.2 Antibodies used for flow cytometry and immunofluorescence staining**

APC = Allophycocyanin, AF = Alexa Fluor, Biot = Biotin, BUV = Brilliant Ultraviolet, BV = Brilliant Violet, Cy = Cyanin dye, eF = eFlour, FC = flow cytometry, FITC = Fluorescein isothiocyanate, IF = Immunofluorescence, PE = Phycoerythrin, PerCP = Peridinin chlorophyll protein, SB = Super Bright

| Antibody | Clone | Label | Manu-facturer | Isotype | Conc. mg/ml | Appli-cation | Dilution | Cat. Number |
|---|---|---|---|---|---|---|---|---|
| CD16/32 | 93 | – | eBioscience, Vienna, Austria | mAb IgG2a, κ | 1 | FC | 1:100 | 16-0161-86 |
| Fc shield CD16/32 | 2.4G2 | - | Tonbo | mAb IgG2b | | FC | 1:1000 | 70-0161 |
| CD19 | 6D5 | PE-Cy5 | BioLegend, London, UK | mAb IgG2a, κ | 0,2 | FC | 1:100 | 115509 |

| | | | | | | | | |
|---|---|---|---|---|---|---|---|---|
| CD3e | 145-2C11 | | BioLegend, London, UK | mAb Armenian Hamster IgG | 0,2 | FC | 1:200 | 100309 |
| CD4 | H129.19 | | BD Biosciences Europe, Erembodegem, Belgium | mAb IgG2a, κ | 0,2 | FC | 1:200 | 553654 |
| CD8a | 53-6.7 | | BioLegend London, UK | mAb IgG2a, κ | 0,2 | FC | 1:400 | 100709 |
| B220 | RA3-6B2 | | BioLegend, London, UK | mAb IgG2a, κ | 0,2 | FC | 1:100 | 103209 |
| GR1 | RB6-8C5 | | BioLegend, London, UK | mAb IgG2b, κ | 0,2 | FC | 1:100 | 108409 |
| TER119 | TER119 | | BioLegend, London, UK | mAb IgG2b, κ | 0,2 | FC | 1:200 | 116209 |
| CD49b | DX5 | | eBioscience, Vienna, Austria | mAb IgM, κ | 0,2 | FC | 1:100 | 15-5971-82 |
| CD11b | M1/70 | | BioLegend, London, UK | mAb IgG2b, κ | 0,2 | FC | 1:200 | 101209 |
| CD117 | 2B8 | APC | BioLegend, London, UK | mAb IgG2b, κ | 0,2 | FC | 1:200 | 105811 |
| | | PE-Cy7 | BioLegend, London, UK | mAb IgG2b, κ | 0,2 | FC | 1:200 | 105813 |
| CD135 | A2F10 | PE | eBioscience, Vienna, Austria | mAb IgG2a, κ | 0,2 | FC | 1:100 | 12-1351-81 |
| | | BV421 | BioLegend, London, UK | mAb IgG2a, κ | 0,05 | FC | 1:25 | 135313 |
| MHC-II | IA/IE M5/114.15.2 | FITC | BioLegend, London, UK | mAb IgG2b, κ | 0,5 | FC | 1:1500 | 107606 |
| | | AF700 | eBioscience, Vienna, Austria | mAb IgG2b, κ | 0,2 | FC | 1:660 | 56-5321-82 |
| | | AF700 | BioLegend, London, UK | mAb IgG2b, κ | 0,5 | FC | 1:1000 | 107622 |
| CD11c | N418 | APC | Invitrogen, Thermo Fisher Scientific, Waltham, USA | mAb Armenian Hamster IgG | 0,2 | FC | 1:200 (BMDC) 1:400 (splenic DC) | 17-0114-82 |

| | | | | | | | | |
|---|---|---|---|---|---|---|---|---|
| | | PerCp-Cy5.5 | Invitrogen, Thermo Fisher Scientific, Waltham, USA | mAb Armenian Hamster IgG | 0,2 | FC | 1:200 | 45-0114-82 |
| | | PE-Cy5 | BioLegend, London, UK | mAb Armenian Hamster IgG | 0,2 | FC | 1:200 | 117316 |
| | | PE-Cy7 | BioLegend, London, UK | mAb Armenian Hamster IgG | 0,2 | FC | 1:400 | 117318 |
| | | FITC | BioLegend, London, UK | mAb Armenian Hamster IgG | 0,5 | FC | 1:1000 | 117305 |
| | | BV650 | BioLegend, London, UK | mAb Armenian Hamster IgG | 0,2 | FC | 1:400 | 117339 |
| B220 | RA3-6B2 | AF700 | Invitrogen, Thermo Fisher Scientific, Waltham, USA | mAb IgG2a, κ | 0,2 | FC | 1:200 | 56-0452-82 |
| | | BV750 | BioLegend, London, UK | mAb IgG2a, κ | 0,2 | FC | 1:200 | 103261 |
| | | FITC | BioLegend, London, UK | mAb IgG2a, κ | 0,5 | FC | 1:1000 | 103205 |
| | | PE | BioLegend, London, UK | mAb IgG2a, κ | 0,2 | FC | 1:400 | 103207 |
| CD11b | M1/70 | PE | BD Biosciences Europe, Erembodegem, Belgium | mAb IgG2b, κ | 0,2 | FC | 1:800 | 557397 |
| | | BV785 | BioLegend, London, UK | mAb IgG2b, κ | 0,2 | FC | 1:800 (BMDC) 1:400 (splenic DC) | 101243 |
| | | APC | BioLegend, London, UK | mAb IgG2b, κ | 0,2 | FC | 1:400 | 101211 |
| CD172a | P84 | BV421 | BD Biosciences | mAb IgG1, κ | 0,2 | FC | 1:200 (BMDC) | 740071 |

| | | | | | | | | |
|---|---|---|---|---|---|---|---|---|
| | | | Europe, Erembodegem, Belgium | | | | 1:400 (splenic DC) | |
| | | APC-Cy7 | BioLegend, London, UK | mAb IgG1, κ | 0,2 | FC | 1:400 | 144018 |
| | | PE-Cy7 | BioLegend, London, UK | mAb IgG1, κ | 0,2 | FC | 1:400 | 144007 |
| XCR1 | ZET | APC-Cy7 | BioLegend, London, UK | mAb IgG2b, κ | 0,2 | FC | 1:400 | 148223 |
| | | BV421 | BioLegend, London, UK | mAb IgG2b, κ | 0,2 | FC | 1:400 | 148216 |
| | | PE | BioLegend, London, UK | mAb IgG2b, κ | 0,2 | FC | 1:400 | 148203 |
| PDCA1 | 927 | PE | BioLegend, London, UK | mAb IgG2b, κ | 0,2 | FC | 1:400 | 127009 |
| | | Biot. | BioLegend, London, UK | mAb IgG2b, κ | 0,5 | FC | 1:400 | 127006 |
| CD19 | 6D5 | Biot. | BioLegend, London, UK | mAb IgG2a, κ | 0,5 | FC | 1:400 (spleen) 1:300 (lungs) | 115504 |
| CD90.2 | 53-2.1 | | BioLegend, London, UK | mAb IgG2a, κ | 0,5 | FC | 1:300 | 140314 |
| NK1.1 | PK136 | | BioLegend, London, UK | mAb IgG2a, κ | 0,5 | FC | 1:300 | 108704 |
| F4/80 | BM8 | | BioLegend, London, UK | mAb IgG2a, κ | 0,5 | FC | 1:300 | 123105 |
| Ter119 | Ter119 | | BioLegend, London, UK | mAb IgG2b, κ | 0,5 | FC | 1:400 | 116204 |
| CD49b | DX5 | | BioLegend, London, UK | mAb IgM, κ | 0,5 | FC | 1:300 | 108904 |
| CD3e | 145-2C11 | | BioLegend, London, UK | mAb Armenian Hamster IgG | 0,5 | FC | 1:300 | 100303 |
| Ly6G | 1A8 | | BioLegend, London, UK | mAb IgG2a, κ | 0,5 | FC | 1:300 | 127604 |
| CD4 | H129.19 | Biot. | BD Biosciences Europe, Erembodegem, Belgium | mAb IgG2a, κ | 0,5 | FC | 1:400 | 553649 |
| CD44 | IM7 | BV785 | BioLegend, London, UK | mAb IgG2b, κ | 0,08 | FC | 1:400 | 103041 |

| | | | | | | | | |
|---|---|---|---|---|---|---|---|---|
| | | BV650 | BioLegend, London, UK | mAb IgG2b, κ | 0,2 | FC | 1:400 | 103049 |
| CD62L | MEL-14 | PE | BD Biosciences Europe, Erembodegem, Belgium | mAb IgG2a, κ | 0,2 | FC | 1:400 | 553151 |
| | | PE-Cy7 | BioLegend, London, UK | mAb IgG2a, κ | 0,2 | FC | 1:400 | 104418 |
| CD40 | 1C10 | SB436 | Invitrogen, Thermo Fisher Scientific, Waltham, USA | mAb IgG2a, κ | 0,2 | FC | 1:400 | 62-0401-82 |
| CD80 | 16-10A1 | biotin | Invitrogen, Thermo Fisher Scientific, Waltham, USA | mAb Armenian Hamster IgG | 0,5 | FC | 1:400 | 13-0801-82 |
| CD86 | GL1 | PE-Cy5 | Invitrogen, Thermo Fisher Scientific, Waltham, USA | mAb IgG2a, κ | 0,2 | FC | 1:400 | 15-0862-82 |
| Streptavidin | | PE | BD Biosciences Europe, Erembodegem, Belgium | - | 0,5 | FC | 1:400 | 554061 |
| | | PE | BioLegend, London, UK | | 0,2 | FC | 1:500 | 405203 |
| | | PE/Dazzle594 | BioLegend, London, UK | | 0,2 | FC | 1:160 | 405247 |
| | | FITC | BioLegend, London, UK | | 0,5 | FC | 1:1250 | 405202 |
| | | BV650 | BioLegend, London, UK | | 0,5 | FC | 1:1250 | 405232 |
| CD88 | 20/70 | PE-Cy7 | BioLegend, London, UK | mAb IgG2b, κ | 0,2 | FC | 1:400 | 135810 |
| | | AF488 | Thermo Fischer Scientific | mAb IgG2b, κ | 0,5 | IF | 1:1000 | 53-0882-82 |
| C3aR | 14D4 | BUV805 | BD Biosciences Europe, | mAb IgG2a, κ | 0,2 | FC | 1:100 | 753368 |

| | | | | | | | | |
|---|---|---|---|---|---|---|---|---|
| | | | Erembodegem, Belgium | | | | | |
| C3 | 11H9 | FITC | Hycult, Uden, Netherlands | mAb IgG2a, κ | 0,833 | FC/IF | 1:833 | HM1045B |
| C3a | 3/11 | AF647 | Hycult, Uden, Netherlands | mAb IgG2a | 0,417 | FC | 1:208 | HM1072 |
| C5 | BB5.1 | AF594 | Hycult, Uden, Netherlands | mAb IgG1, κ | 0,18 | FC/IF | 1:180 | HM1073 |
| | | AF647 | Hycult, Uden, Netherlands | mAb IgG1, κ | 0,2 | FC | 1:100 | HM1073 |
| C5a | I52-1486 | FITC | BD Biosciences Europe, Erembodegem, Belgium | mAb IgG1, κ | 0,417 | FC/IF | 1:208 | 558027 |
| isotype control | R35-95 | BUV805 | BD Biosciences Europe, Erembodegem, Belgium | Rat IgG2a, κ | 0,2 | FC | 1:100 | 612899 |
| isotype control | RTK2758 | FITC | BioLegend, London, UK | Rat IgG2a, κ | 0,5 | FC/IF | 1:500 | 400505 |
| isotype control | RTK2758 | AF647 | BioLegend, London, UK | Rat IgG2a | 0,5 | FC | 1:250 | 400526 |
| isotype control | RTK4530 | PE-Cy7 | BioLegend, London, UK | Rat IgG2b, κ | 0,2 | FC | 1:400 | 400617 |
| isotype control | RTK4530 | FITC | BioLegend, London, UK | Rat IgG2b, κ | 0,05 | FC/IF | 1:100 | 400634 |
| isotype control | RTK2071 | FITC | BioLegend, London, UK | Rat IgG1, κ | 0,5 | FC/IF | 1:250 | 400405 |
| isotype control | MOPC-21 | AF594 | BioLegend, London, UK | Mouse IgG1, κ | 0,5 | FC/IF | 1:500 | 400174 |
| CD90.2 | 30-H12 | Pacific Blue | BioLegend, London, UK | Rat IgG2b, κ | 0,5 | FC | 1:300 | 105323 |
| SiglecF | E50-2440 | PE | BD Biosciences Europe, Erembodegem, Belgium | Rat, IgG2a, κ | 0,2 | FC | 1:300 | 552126 |
| CD103 | 2E7 | APC | BioLegend, London, UK | mAb Armenian Hamster IgG | 0,2 | FC | 1:800 | 121413 |
| CD64 | X54-5/7.1 | BV421 | BioLegend, London, UK | mAb IgG1, κ | 0,2 | FC | 1:800 | 139309 |

### 2.1.3 Compounds used for flow cytometry

**TABLE 2.3 Compounds used for flow cytometry**

eF = eFlour, FC = flow cytometry

| Name | Label | Manufacturer | Application | Dilution | Cat. Number |
|---|---|---|---|---|---|
| LIVE/DEAD Fixable Viability Dye | eF780 | eBioscience, Vienna, Austria | FC | 1:1500 | 65-0865-14 |
| Zombie Yellow Fixable Viability Kit | Zombie Yellow | BioLegend, London, UK | FC | 1:1000 | 423104 |
| LIVE/DEAD Fixable Aqua Dead Cell Stain Kit | AmCyan | Invitrogen, Thermo Fisher Scientific, Waltham, USA | FC | 1:1000 | L34957 |

### 2.1.4 Compounds used for magnetic cell separation (MACS)

**TABLE 2.4 Compounds used for Lineage cell depletion (MACS)**

AF = Alexa Fluor, Cy = Cyanin dye

| Material | Manufacturer | Cat. Number |
|---|---|---|
| anti-Cy5/Anti-AF647 microbeads | Miltenyi Biotec GmbH, Bergisch Gladbach, Germany | 130-091-395 |
| $CD4^+$ T cell Isolation Kit mouse | Miltenyi Biotec GmbH, Bergisch Gladbach, Germany | 130-104-454 |
| MojoSort Streptavidin Nanobeads | BioLegend, London, UK | 480016 |
| MojoSort mouse Naïve CD4 T cell isolation kit | BioLegend, London, UK | 480040 |

### 2.1.5 Compounds used for transcription and q-PCR

**TABLE 2.5 Compounds used for transcription and q-PCR**

| Material | Manufacturer | Cat. Number |
|---|---|---|
| Anchored Oligo$(dT)_{20}$ Primer | Invitrogen, Thermo Fisher Scientific, Waltham, USA | 12577011 |
| SsoAdvanced Universal SYBR Green Supermix | Bio-Rad Laboratories, Hercules, California, USA | 1725270 |
| SUPERase in RNase Inhibitor | Invitrogen, Thermo Fisher Scientific, Waltham, USA | AM2694 |

### 2.1.6 Primers

**TABLE 2.6 Primers used for q-PCR**. All primers were manufactured by Eurofins Product Service GmbH, Reichenwalde. Shown are the sequences of forward (Fwd) and reverse (Rev) primers.

| Gene | Sequence | Source |
|---|---|---|
| *HPRT* | Fwd 5′-TCAGTCAACGGGGGACATAAA-3’ | own design |
| | Rev 5′-GGGGCTGTACTGCTTAACCAG-3’ | own design |
| *Actb* | Fwd 5′-GGCTGTATTCCCCTCCATCG-3’ | own design |
| | Rev 5′-CCAGTTGGTAACAATGCCATGT-3’ | own design |
| *IRF8* | Fwd 5′-CGGGGCTGATCTGGGAAAAT-3’ | own design |
| | Rev 5′-CACAGCGTAACCTCGTCTTC-3’ | own design |
| *IRF4* | Fwd 5′-TCCTCTGGATGGCTCCAGATGG-3’ | own design |
| | Rev 5′-CACCAAAGCACAGAGTCACCTG-3’ | own design |
| *Notch2* | Fwd 5′-CGTGCAAGTGTCAGAGGCTA-3’ | own design |
| | Rev 5′-GGGTCATCTTCCGACAGCAA-3’ | own design |
| *Id2* | Fwd 5′-GACAGAACCAGGCGTCCA-3’ | [482] |
| | Rev 5′-AGCTCAGAAGGGAATTCAGATG-3’ | [482] |
| *Nfil3* | Fwd 5′-GAGCAGAACCACGATAACCCA-3’ | own design |
| | Rev 5′-CCTCGTCCTACAGACCGGAT-3’ | own design |
| *Klf4* | Fwd 5′-ACTCACACAGGCGAGAAACC-3’ | [483] |
| | Rev 5′-AAGGCCCTGTCACACTTCTG-3’ | [483] |
| *Batf3* | Fwd 5′-ACTTTGTGCAGCTTCGGTCA-3’ | own design |
| | Rev 5′-CGGACAAAGGAGGAGTGAGC-3’ | own design |

### 2.1.7 Consumables

**TABLE 2.7 Consumables**

| Material | Manufacturer | Cat. Number |
|---|---|---|
| Biosphere filter tips 0,5-20 µl, 200 µl, 1250 µl | Sarstedt AD & Co., Nümbrecht | 70.1116.210 (0,5-20 µl), 70.1189.215 (200 µl), 70.1186.210 (1250 µl) |
| Cell strainer 40 µm | Th. Geyer GmbH & Co. KG Niederlassung Hamburg | 7.696 767 |
| Cell strainer 70 µm | Thermo Fisher Scientific, Waltham, USA | 22-363-548 |
| Cell strainer 100 µm | Th. Geyer GmbH & Co. KG Niederlassung Hamburg | 7.696 769 |
| Cover glasses (25x60 mm, thickness) | VWR International GmbH, Darmstadt | 14346 |
| ELISA-reservoir 25 ml | VWR International GmbH, Darmstadt | 613-1176 |
| ELISA plate: Costar Assay Plate 96 well | Corning inc., New York, USA | 9018 |
| FACS tube 5 ml | Sarsted AD&Co., Nümbrecht | 62.476.028 |
| 5 ml tubes FALCON | Corning inc., New York, USA | 352235 |
| Filter cards | Shandon Inc., Pittsburgh, USA | 190005 |
| Flask T75 | Greiner Bio-One, Kremsmünster, Austria | 658175 |
| Neubauer chamber | Brand GmbH + CO KG, Wertheim, Germany | 717805 |
| Hoechst33342 | Life technologies GmbH | 62249 |
| Individual PCR Tubes 8/tube strip, clear | Bio-Rad Laboratories, Hercules, California, USA | TLS0801 |
| LD, LS Column | Miltenyi Biotec GmbH, Bergisch Gladbach, Germany | LD: 130-042-901<br>LS: 130-042-401 |
| Liquid blocker PAP pen | Daido Sangyo Ltd., Tokyo, Japan | N71310-N |
| Microseal ’B’ seal | Bio-Rad Laboratories, Hercules, California, USA | MSB1001 |
| Microscope slide | Gerhard Menzel GmbH, Braunschweig | AAAA000001 12E |

| | | |
|---|---|---|
| Micro tube 0,5 ml; 1,5 ml; 2 ml | Sarstedt AD & Co., Nümbrecht | 72.699 (0,5 ml)<br>72.690.550 (1,5 ml)<br>72.695.500 (2 ml) |
| Multiplate PCR Plates 96-well, clear | Bio-Rad Laboratories, Hercules, California, USA | MLL9601 |
| Needle 26G | BD Biosciences Europe, Erembodegem, Belgium | 303800 |
| O'GeneRuler 50 bp DNA Ladder | Thermo Fisher Scientific, Waltham, USA | SM1133 |
| Optical Flat 8-Cap Strips for 0,2 ml tube strips/plates | Bio-Rad Laboratories, Hercules, California, USA | TCS0803 |
| Orange DNA Loading Dye (6X) | Thermo Fisher Scientific, Waltham, USA | R0631 |
| Parafilm | Parafilm Laboratory Sealing Film Bemis Inc., Neenah, USA | HS234526B |
| Pipette tip 10 µl, 100 µl, 1000 µl | Sarstedt AD & Co., Nümbrecht | 70.3021 (10 µl),<br>70.3031 (100 µl),<br>70.3050 (1000 µl) |
| Plate sealers | R&D Systems, Minneapolis, USA | DY992 |
| Protein low binding tube 0,5 ml, 1,5 ml | Sarstedt AD & Co., Nümbrecht | 72.704.600 (0,5 ml)<br>72.706.600 (1,5 ml) |
| Serological pipettes CELLSTAR, 5 ml, 10 ml, 25 ml | Greiner Bio-One, Kremsmünster, Austria | 606 180/5ml;<br>607 180/10ml;<br>760 180/25ml |
| Superfrost Plus Gold Adhesion Microscopic Slides | Epredia Netherlands B.V., Breda Netherlands | 48382-200 |
| Syringe 5 ml, 10 ml | BD Biosciences Europe, Erembodegem, Belgium | 309050 (5 ml)<br>309110 (10 ml) |
| Triton X-100 | Calbiochem, San Diego, USA | 648464 |
| Tubes 15 ml, 50 ml | Sarstedt AD & Co., Nümbrecht | 62.554.502 (15 ml)<br>62.547.254 (50 ml) |
| 6-well plate cell culture plate (F bottom), Costar | Corning inc., New York, USA | 3516 |
| 96-well V bottom plate (LEGENDPlex) | BioLegend, London, UK | 740446 – part 76883 |
| 96-well plate (F bottom) | Greiner Bio-One,<br>Kremsmünster, Austria | 655061 |

| | | |
|---|---|---|
| 96-well plate cell culture plate (U bottom), Costar | Corning inc., New York, USA | 7007 |
| 96 Well Cell Culture TC-Plate (F bottom), surface: suspension, flat base | Sarstedt AD & Co., Nümbrecht | 83.3924500 |

### 2.1.8 Kits

**TABLE 2.8 Used Kits**

| Kit | Manufactures | Cat. Number |
|---|---|---|
| AF594 Antibody Labeling Kit | Invitrogen, Thermo Fisher Scientific, Waltham, USA | A20185 |
| AF647 Antibody Labeling Kit | Invitrogen, Thermo Fisher Scientific, Waltham, USA | A20186 |
| AF647 Conjugation Kit Lightning-Link | Abcam, Cambridge, UK | ab269823 |
| BD Cytofix/Cytoperm Fixation/Permeabilization Kit | BD Biosciences Europe, Erembodegem, Belgium | 554714 |
| CellTrace CFSE, Cell Proliferation Kit | Invitrogen, Thermo Fisher Scientific, Waltham, USA | C34554A |
| ELISA MAX™ Standard Set Mouse IFN-γ | BioLegend, London, UK | 430801 – part 79069 |
| ELISA MAX™ Standard Set Mouse IL-17A | BioLegend, London, UK | 432501 – part 79109 |
| FITC Conjugation Kit - Lightning-Link | Abcam, Cambridge, UK | ab188285 |
| High-Capacity cDNA Reverse Transcription Kit | Applied Biosystems, Thermo Fisher Scientific, Waltham, USA | 4368814 |
| LEGENDplex™ Mouse Inflammation Panel (13-plex) | BioLegend, London, UK | 740150 |
| LEGENDplex™ Mouse Macrophage/Microglia Panel Detection Antibodies (2-plex; IL-12p40, TGF-β1) | BioLegend, London, UK | 740851 |
| Mouse IFN-γ DuoSet ELISA | R&D Systems, Minneapolis, USA | DY485 |
| Mouse IL-13 DuoSet ELISA | R&D Systems, Minneapolis, USA | DY413 |

| | | |
|---|---|---|
| Mouse IL-17 DuoSet ELISA | R&D Systems, Minneapolis, USA | DY421 |
| NovaSeq X Plus Series PE150, Pre-made libraries partial lane sequencing | Novogene GmbH, München, Germany | RSSQ01602 |
| Rneasy Plus Mini Kit | Qiagen GmbH, Hilden, Germany | 74104 |
| TURBO DNA-free Kit | Invitrogen, Thermo Fisher Scientific, Waltham, USA | AM1907 |

### 2.1.9 Buffers and Solutions

**TABLE 2.9 Buffers and solutions**

| Buffer /Solution | Substance |
|---|---|
| 10X TURBO DNase™ Buffer | Part of the TURBO DNA-free™ Kit |
| 10X Buffer | Part of the High-Capacity cDNA reverse transcription Kit |
| Assay Buffer | Part of the LEGENDplex™ Mouse Inflammation Panel (13-plex), LEGENDplex Mouse Macrophage/Microglia (2-plex) |
| Blocking buffer | 1% BSA (Sigma) in PBS |
| CFSE labeling buffer | pre-warmed DPBS with 2 µM CFSE |
| Complete DMEM medium | 2% FCS (Sigma)<br>100 U/ml penicillin<br>100 µg/ml streptomycin |
| Complete IMDM medium (BM-derived DCs) | IMDM medium |
| | 10% heat-inactivated FCS (Capricorn) |
| | 100 U/ml penicillin |
| | 100 µg/ml streptomycin |
| | 1 mM sodium pyruvate |
| | 20 ng/ml mGM-CSF (Peprotech) |
| | 100 ng/ml mFlt3L |
| Complete RPMI medium (B16-Flt3L cell line) | RPMI1640 medium |
| | 10% FCS (Sigma) |

| | |
|---|---|
| | 100 U/ml penicillin |
| | 100 µg/ml streptomycin |
| | 2 mM L-glutamine |
| | 1 mM sodium pyruvate |
| Digestion buffer | DMEM medium |
| | 10 nM HEPES |
| | 2% BSA (Sigma) |
| | 30 µg/ml Liberase TL |
| | 125 µg/ml DNase |
| Extraction buffer | 2% FCS (Capricorn) |
| | 20 mM HEPES in DPBS |
| GM-CSF DC medium | RPMI1640 medium |
| | 10% FCS (Sigma) |
| | 100 U/ml penicillin |
| | 100 µg/ml streptomycin |
| | 2 mM L-glutamine |
| | 1 mM sodium pyruvate |
| | 1% GM-CSF supernatant (BioLegend) |
| MACS buffer | 0,5% MACS BSA stock solution (Miltenyi Biotec) in DPBS |
| Perm/wash buffer | Part of the Cytofix/Cytoperm™ Fixation/Permeabilization Kit |
| RLT buffer | Part of the RNeasy Mini Kit, Qiagen |
| RW1 buffer | Part of the RNeasy Mini Kit, Qiagen |
| RPE buffer | Part of the RNeasy Mini Kit, Qiagen |
| Sort – collection buffer I | 20% FCS (Sigma) in DPBS |

| | |
|---|---|
| Sort – collection buffer II | 50% FCS (Capricorn) in IMDM |
| Staining buffer | 2% FCS (Capricorn) |
| | 2 mM EDTA in DPBS |
| Substrate solution | 0,1 M Citric acid |
| | 0,2 M $Na_2HPO_4$ |
| | 30% $H_2O_2$ |
| | OPD |
| Washing buffer | 0,05% Tween 20 in PBS |
| Wash buffer (WB) | Part of the LEGENDplex™ Mouse Inflammation Panel (13-plex), LEGENDplex Mouse Macrophage/Microglia (2-plex) |

### 2.1.10 Experimental Models: Mouse strains

**TABLE 2.10 Mouse strains**

| Name | Strain | Official name (symbol) | Breeder |
|---|---|---|---|
| *C5ar1*$^{-/-}$ | BALB/c | C5ar1$^{tm1Cge}$ | Internal breeding, ISEF, AG Köhl, Lübeck, Germany |
| *C3ar1*$^{-/-}$ | BALB/c | C3ar1$^{tm1Cge}$ | Internal breeding, ISEF, AG Köhl, Lübeck, Germany |
| DO11.10*Rag2*$^{-/-}$ | BALB/c | Tg(DO11.10)10Dlo | Internal breeding, ISEF, AG Köhl, Lübeck, Germany |
| Wildtype (BALB/c) | BALB/c | BALB/cAnNCrl | Charles River, Breeding Laboratories, Sulzfeld, Germany |
| | | | Internal breeding, ISEF, AG Köhl, Lübeck, Germany |
| *tdTomato-C3ar1*$^{fl/fl}$ | BALB/c | C3aR$^{tm1JKo}$ | Internal breeding, ISEF, AG Köhl, Lübeck, Germany |

| | | | |
|---|---|---|---|
| Wildtype (C57BL/6) | C57BL/6 | C57BL/6J | Jackson laboratory, USA |
| | | | Internal breeding, CCHMC, Pasare Lab, Cincinnati, USA |
| *C5ar1*$^{-/-}$ | C57BL/6 | B6.129S4-C5ar1$^{tm1Cge}$ | Internal breeding, CCHMC, Pasare Lab, Cincinnati, USA |
| OT-II | C57BL/6 | B6.Cg-Tg(TcraTcrb) 425Cbn/J | Jackson laboratory, USA |
| | | | Internal breeding, CCHMC, Pasare Lab, Cincinnati, USA |

### 2.1.11 Experimental Models: Cell Line

**TABLE 2.11 Cell lines**

| Name | Source | Identifier |
|---|---|---|
| B16-Flt3L mouse melanoma cell line | [484] | RRID:CVCL_IJ12 |

### 2.1.12 Equipment and Software

#### *2.1.12.1 Equipment*

**TABLE 2.12 Equipment**

| Equipment | Manufacturer |
|---|---|
| Autoflow IR direct heat CO2 incubator | NuAire Lab Equipment, IBS Integra Biosciences GmbH |
| Biological Safety Cabinets | Nuaire Inc., Plymouth, USA |
| Block heater Stuart | Cole-Parmer, Vernon Hills, USA |
| CASY TT -OLS OMNI | Life Science GmbH |
| C1000 Touch Thermal Cycler | Bio-Rad Laboratories, Hercules, California, USA |
| CFX96 Touch Real-Time PCR Detection System | Bio-Rad Laboratories, Hercules, California, USA |
| Cell Sorter BD FACSAria™ III | Beckton Dickinson GmbH, Heidelberg |
| Cell Sorter SH800S | Sony Corporation of America |
| Cell Sorter MA900 | Sony Corporation of America |
| Centrifuge 5424 | Eppendorf AG, Hamburg |
| Centrifuge 5424R | Eppendorf AG, Hamburg |

| | |
|---|---|
| Centrifuge 5810R | Eppendorf AG, Hamburg |
| Chemical hood | Waldner Laboreinrichtungen GmbH & Co KG, Wangen |
| Cytek Aurora N7-00020 | Cytek Biosciences, Fremont, USA |
| Cytospin centrifuge Cellspin I | Tharmac GmbH, Walsolms |
| Dissecting scissors | WPI Deutschland GmbH, Berlin |
| EasySep EasyEight Magnet | Stemcell Technologies,Vancouver, Canada |
| ELISA-Reader Fluostar Omega 0415 | BMG Labtech GmbH, Ortenberg |
| Forceps | WPI Deutschland GmbH, Berlin |
| Fridge, 4 °C and -20 °C combined | Liebherr-International Deutschland GmbH, Biberach an der Riß |
| Incubator | Heraeus, Hanau |
| IR Direct Heat $CO_2$ Incubator | Nuaire Inc., Plymouth, USA |
| Keyence BZ-X810 | Keyence, GmbH, Neu-Isenburg |
| MACS Multi Stand | Miltenyi Biotec GmbH, Bergisch Gladbach, Germany |
| Microscope Leica DM IL LED | Leica Mikrosysteme Vertrieb GmbH, Wetzlar, Germany |
| Microscope camera Leica EC3 | Leica Mikrosysteme Vertrieb GmbH, Wetzlar, Germany |
| Multichannel pipette | Eppendorf AG, Hamburg |
| Novocyte 2001 | Agilent Technologies, Santa Clara, USA |
| Neubauer counting chamber, improved | VWR International GmbH, Darmstadt |
| Orbital Plate Shaker | Ohaus, Parsippany, USA |
| Pipetboy | Integra Biosciences AG, Zizers, Schweiz |
| Pipette (0,1-2,5 µl; 0,5-10 µl; 10-100 µl; 20-200 µl; 100-1000 µl) | Eppendorf AG, Hamburg |
| PowerPac HC High-Current Power Supply | Bio-Rad Laboratories, Hercules, California, USA |
| Precision balance LC6200S | Sartorius AG, Göttingen |
| Pure water system Nanopure Diamond D11931 | Thermo Fisher Scientific GmbH, Bremen |
| Synergy LX Multi-Mode Plate Reader | BioTek, Vermont, United States |

| | |
|---|---|
| QuadroMACS Separator | Miltenyi Biotec GmbH, Bergisch Gladbach, Germany |
| QUANTUM CX5 | Vilber Lourmat GmbH, Eberhardzell |
| NanoDrop Spectrophotometer ND-1000 | Peqlab Biotechnologie GmbH |
| SomnoSuite Low-Flow Anesthesia System | Kent Scientific Corporation, Torrington, USA |
| Smartbox Prodigy Plus Lab Control Unit | Euthanex, Plexx B.V., Elst, Netherlands |
| Stain Tray Plate | Invitrogen, Thermo Fisher Scientific, Waltham, USA |
| Vacusip, portable aspiration system | Integra Biosciences GmbH, Biebertal, Germany |
| Vortex | Hassa Laborbedarf |
| Titramax 100 platform shaker | Heidolph, Schwabach, Germany |
| -80 °C freezer | Sanyo, Japan |

#### *2.1.12.2 Software*

**TABLE 2.13 Software used for data collection and analysis**

| Program | Company |
|---|---|
| BD FACSDiva 7.0 | BD Biosciences, San Jose, USA |
| CFX Maestro™ Software | Bio-Rad Laboratories, Hercules, California, USA |
| BioVision | Vilber Lourmat GmbH, Eberhardzell |
| EndNote X9 | Clarivate Analytics, Philadelphia, USA |
| FlowJo 10.10 | FlowJo, LLD, Ashland, USA |
| GraphPad Prism 10.0 | Graph Pad Software Inc., LaJolla, USA |
| Keyence, BZ-X800 analyzer | Keyence, Japan |
| LEGENDplex Data Analysis software Suite | BioLegend in agreement with Qognit, London, UK |
| Microsoft Office 2016 | Microsoft Corporation, Redmond, USA |
| ND-1000 V3.8 | Peqlab Biotechnologie GmbH |
| NovoExpress Software 1.6.3 | Agilent Technologies, Santa Clara, USA |

| | |
|---|---|
| SH800S, MA900 Cell Sorters software | Sony Corporation of America |
| SpectroFlo | Cytek Biosciences, Fremont, USA |
| R Studio 4.5.0, 2025.05<br><br>Packages: tidyverse v2.0.0; dplyr v1.1.4; Seurat 5.3.0; ggplot2 v3.5.2; viridis v0.6.5/viridisLite 0.4.2; EnhancedVolcano v1.26.0; VennDiagram v1.7.3; patchwork v1.3.0 | Posit, PBC, Boston, USA |

# 2.2 Methods

## 2.2.1 Mice

### *2.2.1.1 BALB/c background*

Wildtype (WT), *C3ar1*$^{-/-}$, *C5ar1*$^{-/-}$, *tdTomato-C3ar1*$^{fl/fl}$ mice were used at 8-12 weeks, and DO11.10*Rag2*$^{-/-}$ were used at 16-44 weeks of age due to the increasing number of splenic CD4$^{+}$ T cells with age. Animals of both sexes were used for organ removal. All mice were bred and maintained at the University of Lübeck facility under specific-pathogen-free conditions. All experiments were performed by institutional and national guidelines for animal care and were approved by the Animal Care and Use Committee from the Schleswig-Holstein state authorities (Ministerium für Landwirtschaft, Energiewende und ländliche Räume, Kiel, Germany; AZ:39_2018_11-27 and 39_2021-03-29). Mice were sacrificed by $CO_2$, followed by cervical dislocation.

### *2.2.1.2 C57BL/6 background*

WT, *C5ar1*$^{-/-}$ and OT-II mice were used at 8-12 weeks of age. WT and *C5ar1*$^{-/-}$ mice of both sexes were injected with the B16-Flt3L melanoma cell line. Animals were used for organ removal. All mice were bred and maintained at Cincinnati Children's Hospital Medical Center under specific pathogen-free conditions following protocols approved by Institutional Animal Care and Use Committee. Mice were inhaled with isoflurane and sevoflurane in a chamber and sacrificed by cervical dislocation. *C5ar1*$^{-/-}$ mice were a gift from Ian P. Lewkowich, PhD.

## 2.2.2 Expansion of splenic dendritic cells via Flt3L

The injection of B16-Flt3L melanoma cells is a strategy to increase the number of DCs. It has been previously shown that the CLPs and CMPs, which are required for the generation of DC subsets, express Flt3[485]. Robust expansion of DC populations was observed in mice bearing tumors generated from B16-melanoma cells secreting murine Flt3L, providing a reliable strategy for sustained systemic levels of Flt3L[484,486]. Karsunky et al. confirmed that within 10-14 days following subcutaneous implantation of the Flt3-secreting tumor, mice develop splenomegaly with marked enrichment of DCs, which constitute 40-60% of the total spleen cells[485]. This finding suggests that this model can be used for the purification of large numbers of functional DCs that can be used in cell transfer experiments to compare in vivo proficiency of different DC subsets[487].

To study the function of specific DC subsets, I isolated such DCs in sufficient numbers using B16-Flt3L melanoma cell injection that maintained their normal phenotype and functions.

The B16-Flt3L melanoma cell line was cultured in complete RPMI 1640 medium in T75 flasks. Cells were passaged and rinsed with DPBS. To detach them, the adherent layer of B16-Flt3L melanoma cells was covered with 2 ml of trypsin and incubated for one minute. Cells were collected in 20 ml RPMI 1640 medium and spun down to be reseeded afterwards at a 1:10 dilution.

For injection, B16-Flt3L melanoma cells were collected and washed 3 times with cold DPBS. $5x10^6$ cells in 100 µl DPBS were injected per WT or *C5ar1*$^{-/-}$ C57BL/6 mouse into the flank using a 27G needle. The tumor was visible from day 7. The spleen was ready for harvesting 10-21 days after s.c. B16-Flt3L melanoma cell injection (**Fig. 2.1**).

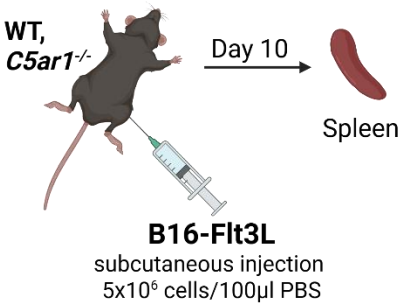


**FIGURE 2.1 Model of B16-Flt3L injection.** WT and *C5ar1*$^{-/-}$ mice were injected with $5x10^6$ B16-Flt3L melanoma cells in 100 µl DPBS into the flank. The spleen was harvested starting from day 10.

## 2.2.3 Organ removal and preparation of cell suspension

### *2.2.3.1 Isolation of splenic DCs and their in-vivo generation into cDC1, cDC2 and pDC after B16-Flt3L injection*

Cells were isolated from the spleen of B16-Flt3L melanoma cell- injected mice[484]. Single-cell suspension was prepared by mashing between frosted slides and then passing through a 70 µm cell strainer. After RBC lysis, single-cell suspensions were blocked with an Fc receptor anti-mouse CD16/32 (2.4G2; Tonbo), and then cells were stained with biotinylated anti-mouse CD90.2 (53-2.1), NK1.1 (PK136), CD19 (6D5), Ter119 (Ter119), and F4/80 (BM8) antibodies for 30 min. Cells were washed and subsequently incubated with MojoSort streptavidin nano beads. Unstained cells were obtained using MojoSort kit negative selection protocol. For negative selection, the untouched cells were collected by decanting the liquid in a clean tube. After lineage depletion by magnetic-activated cell sorting (MACS), the remaining cells were stained for DC subsets, pDC, cDC1, and cDC2. pDC identified as MHC-II$^+$CD11c$^+$B220$^+$PDCA-1$^+$ cells, cDC1 identified as MHC-II$^+$CD11c$^+$B220$^-$PDCA-1$^-$XCR1$^+$CD172a$^-$ cell and cDC2 identified as MHC-II$^+$CD11c$^+$B220$^-$PDCA-1$^-$XCR1$^-$CD172a$^+$ cells. Cells were sorted directly into collection buffer I and analyzed with Sony SH800S and MA900 cell sorters (Sony Corporation of America) (**Fig. 2.2**).

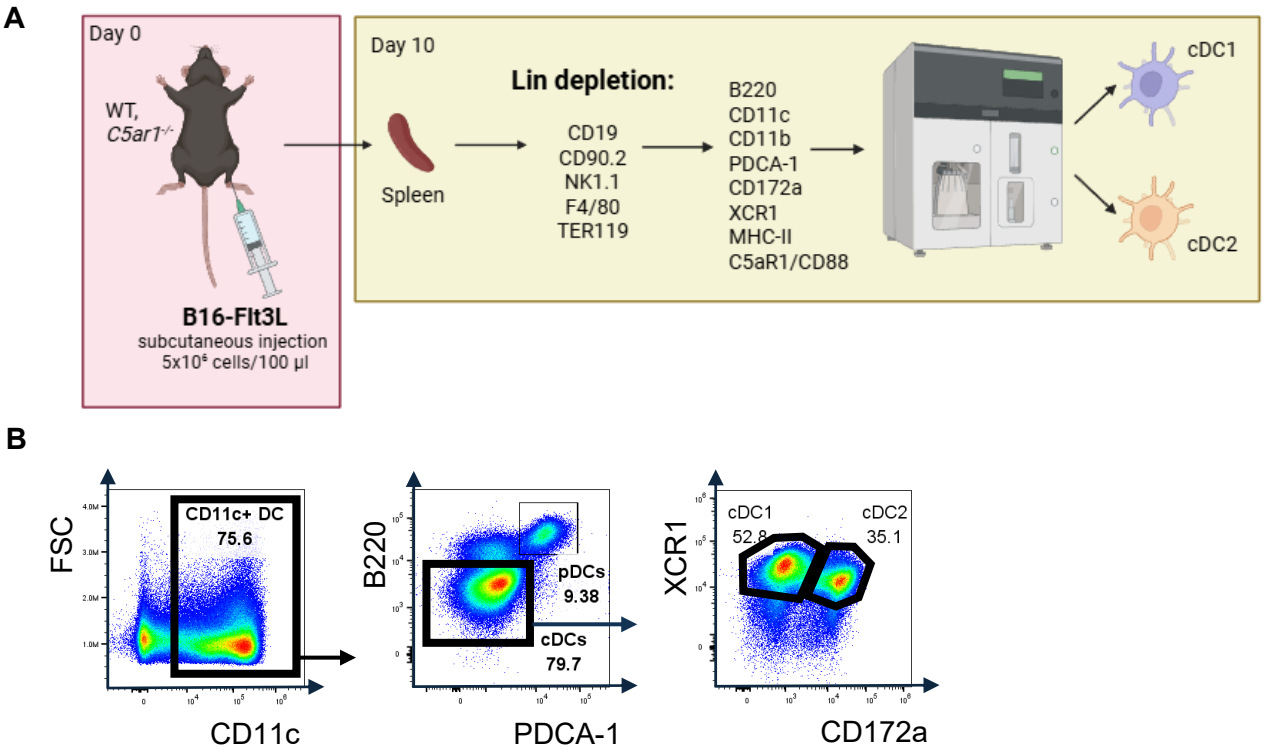


**FIGURE 2.2 Experimental setup and gating strategy to define splenic cDC1 and cDC2. A**. Experimental setup (created with *Biorender.com*). **B**. Gating strategy to define splenic cDC1 and cDC2 cells. cDC1 were identified as MHC-II$^+$CD11c$^+$B220$^-$PDCA-1$^-$XCR1$^+$CD172a$^-$ cell and cDC2 were identified as MHC-II$^+$CD11c$^+$B220$^-$PDCA-1$^-$XCR1$^-$CD172a$^+$ cells.

### *2.2.3.2 Isolation of bone marrow DCs precursors, MDP and CDP*

BM cells from two animals were isolated as described[488,489]. Briefly, the femurs, tibias, and humeri were removed, placed on ice in DPBS (**Fig. 2.3A**). Using forceps and small scissors, muscle and fibrous tissues were cut away from the bone, and the bone was wiped with 70% ethanol to remove any excess muscle fibers. Muscle-free femurs, tibias, and humeri were placed in the cold DPBS. The BM was isolated into extraction buffer. Flushing was performed by using a 21G needle attached to a 10 ml syringe through a 100 µm cell strainer. Cells were collected in a 50 ml tube, and the cell strainer was washed with an additional 8 ml DPBS. The cell suspension was centrifuged (5 min, 400xg, 4 °C) and the supernatant was discarded. The isolated BM cells were stained with PE-Cy5-conjugated antibodies to lineage antigens (CD3ε (145-2C11), CD4 (H129.19), CD8α (53-6.7), B220 (RA3-6B2), CD19 (6D5), CD11b (M1/70), Gr-1 (RB6-8C5), Ter119 (Ter119) and CD49b (DX5)) in staining buffer. Anti-Cy5/Anti-AF647 microbeads (Miltenyi Biotec) were used for secondary labeling according to the manufacturer's instructions for magnetic separation. After lineage depletion by MACS, the remaining lineage-negative (Lin$^-$) cells were stained with LIVE/DEAD® fixable viability dye, APC-conjugated antibody to CD117, and PE-conjugated antibody to CD135 in staining buffer. Subsequently, MDPs were identified as lin$^-$CD135$^+$CD117$^+$ cells and CDPs were identified as lin$^-$CD135$^+$CD117$^-$ cells[52,489]. Cells were sorted directly into collection buffer II and analyzed with the BD FACSAria III cell sorter (**Fig. 2.3B**) (BD Biosciences).

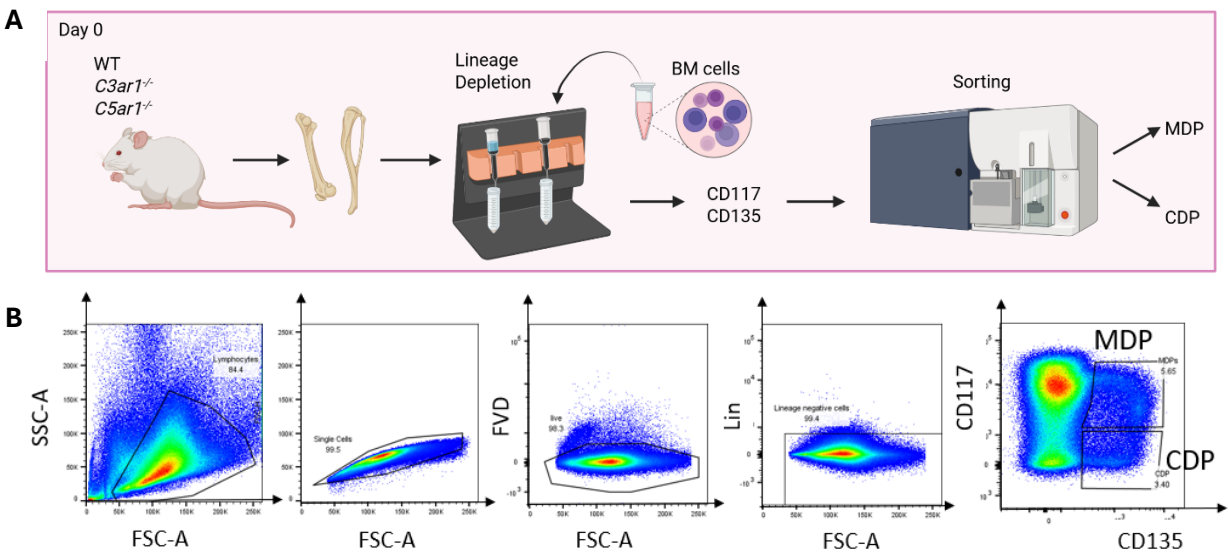


**FIGURE 2.3 Experimental setup and gating strategy to define MDP and CDP cells. A**. Experimental setup (created with *Biorender.com*). **B**. Gating strategy to define MDPs and CDPs. MDP cells were identified as Lin$^-$CD135$^+$CD117$^+$ cells. CDPs were identified as Lin$^-$CD135$^+$CD117$^-$ cells.

#### *2.2.3.3 Isolation of lung DCs*

Lung cells were isolated from B16-Flt3L melanoma-injected mice[484]. First, lungs were perfused with 10 ml DPBS into the right ventricle to clear blood from the pulmonary vasculature. All lobes were harvested from the thorax cavity and placed into 50 ml tube in complete DMEM medium. Lungs were placed on a 70µm cell strainer in a 6-well plate (Corning) with 2,5 ml digestion buffer. The lung tissue was minced with scissors to small pieces and was digested for 45 min at 37 °C on a shaker in the presence of freshly reconstituted 125 µg/ml DNase and 30 µg/ml Liberase TL. Subsequently, the lung tissue-containing cell strainer was transferred to a 50 ml Falcon tube. The single-cell suspension was prepared by mechanical disruption of the lungs using a 5 ml syringe stamp in complete DMEM medium. The cell suspension was centrifuged for 8 min at 400xg at 4 °C. The supernatant was discarded, and the pellet was resuspended in 1 ml RBC lysis buffer for 2 min at RT to lyse the erythrocytes. The lysis was terminated by adding 20 ml of DPBS and the cell suspension was centrifuged for 8 min at 400xg at 4 °C. Single-cell suspensions were blocked with an Fc shield anti-mouse CD16/32 (2.4G2; Tonbo) and then cells were stained with Zombie Yellow fixable viability dye, anti-CD19 (6D5)-biotin conjugated to streptavidin-FITC, CD49b (DX5), CD3e (145-2C11), Ly6G (1A8). PE-conjugated antibody to SiglecF (E50-2440), PE-Cy7-conjugated antibody to CD88/C5aR1 (20/70), APC-conjugated antibody to CD103 (2E7), AF700-conjugated antibody to MHC-II (IA/IE M5/114.15.2), BV421-conjugated antibody to CD64 (X54-5/7.1), BV650-conjugated antibody to CD11c (N418), BV785-conjugated antibody to CD11b (M1/70) for 30 min. DCs were identified as Lin$^-$SiglecF$^-$ CD11c$^+$MHC-II$^+$ cells (**Fig. 2.4**).

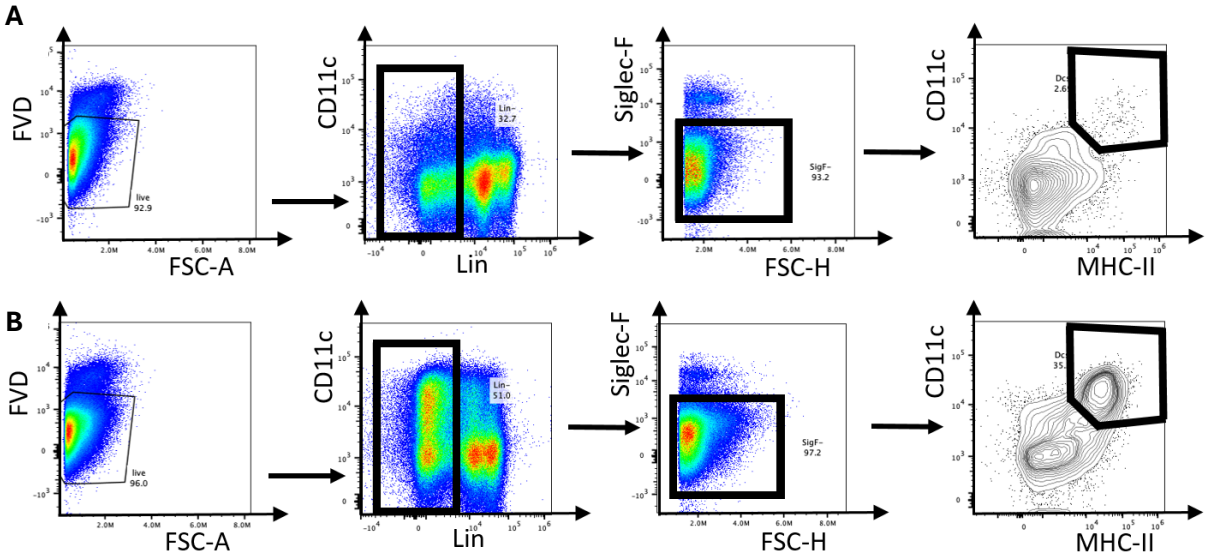


**FIGURE 2.4 Gating strategy to define pulmonary DCs.** Shown is the gating strategy to define DCs from noninjected (**A**) and injected (**B**) mice with B16-Flt3L melanoma cells. DCs were identified as $Lin^-SiglecF^-CD11c^+MHC\text{-}II^+$ cells.

#### *2.2.3.4 Determination of the cell number*

A hemocytometer was used to determine the cell number. To distinguish dead from living cells, an aliquot of 10 µl from the cell suspension was mixed with trypan blue at an 1:1 ratio. In the next step, 10 µl of the mixture was loaded on the hemocytometer and placed on the microscope stage of a transmitted light microscope. Only viable cells were counted, and the total cell number was calculated according to the following formula:

$$total\ cell\ count = \frac{counted\ cells}{number\ of\ counted\ big\ squares} \times dilution\ factor\ \times 10^4 \times V\ (ml)$$

Additionally, for BM cell suspensions characterized by a higher cell number, the electric field multi-channel cell counting system, CASY, was used to determine the total cell count.

The CASY system required counting a statistically sufficient number of cells to ensure accuracy and reproducibility. With the hemocytometer, this involved visual inspection and exclusion of debris. At the same time, the CASY counter achieved rapid, automated counts through electric current exclusion and provided multiparametric data on cell viability and size. These approaches allowed reliable assessment of the cell number for consecutive cell culturing.

### 2.2.4 Single-cell library preparation and sequencing

For the single-cell RNA-seq (scRNA-seq) experiments and analysis of the data, I collaborated with the Medical Systems Biology Group at the Institute of Experimental Dermatology at the University of Lübeck. More specifically, sections 2.2.4-2.2.7 have been written with support from Anke Fähnrich and members of her group.

Bones from four 12-week-old WT and *C5ar1*$^{-/-}$ mice were harvested and $lin^-CD135^+CD117^+$ MDPs were sorted as described (see 2.2.3.2). scRNA-seq was performed using the 10X Genomics Chromium Next Gem Single cell 3′ Reagents Kits

v3.1 (PN-1000121, CG000315 protocol rev A, 10X Genomics) and Dual Index kit TT set A (PN- 1000215, 10X Genomics) according to the manufacturer's instructions.

The target recovery was ~10000 cells. Briefly, the cell suspension barcoded gel beads and partitioning oil were loaded onto the 10X Genomics Chromium Chip (Next GEM chip G) to generate single cell Gel Beads In emulsion (GEMs). Captured cells were lysed and the transcripts were barcoded through reverse transcription inside individual GEMs. The constructed libraries were sequenced on Illumina Novaseq (FC S1 standard 200 cycles) (**Fig. 2.5**).

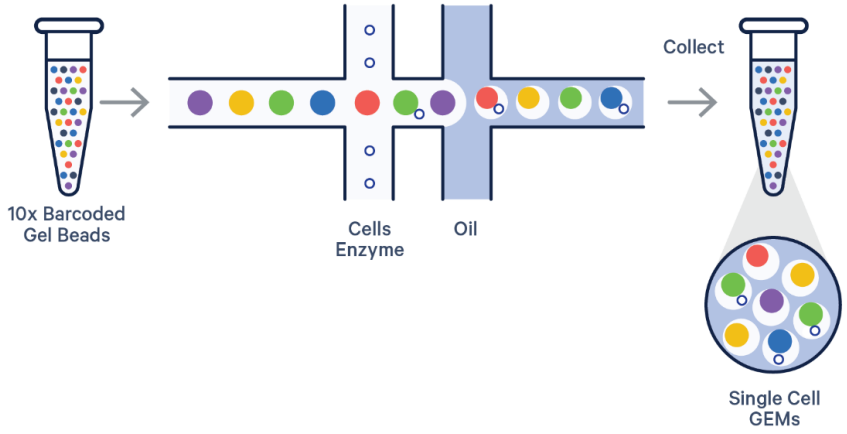


**FIGURE 2.5 A schematic representation of GEM generation and barcoding using the GEM-X chip workflow.** GEMs were formed by combining barcoded Gel Beads, a master mix with cells, and partitioning oil in a GEM-X 3′ or 5′ Chip. To enable single-cell resolution, cells were loaded at a limiting dilution so that most (~90-99%) GEMs contained no cell, while the rest primarily held a single cell (*https://www.10xgenomics.com/*).

### 2.2.5 Single-cell RNA-Seq analysis pipeline

Raw gene expression matrices were generated for each sample by a custom pipeline combining STAR (v.2.7.3a) using GRCm39 *mus musculus* reference genome. The output-filtered gene expression matrices were analyzed in 'R' (v.4.4.2), where empty droplets and doublets were removed for each sample using the packages 'DropletUtils'[490,491] (v.1.26.0) and 'scDblFinder'[492] (v.1.20.0), and further analysis was performed using the 'Seurat' (v.5.2.1)[493-497] package. Subsequently, cells were detected by ranking cell barcodes according to their number of unique molecular identifiers captured using the barcodeRanks function from DropletUtils. Low-ranked cells from this process were labelled as false positives and were discarded, yielding 24073 unique genes with an average of 3018 genes per cell. The criteria for filtering the dataset were as follows: (i) genes expressed in more than three cells; (ii) cells expressing more than 200 genes; (iii) low-quality cells were removed if they included more than 25% UMIs from the mitochondrial genome. Mitochondrial content can vary between humans and mice based on scRNA-seq technology. The frequency of mitochondrial (mt) DNA ranges from 5% in low-energy tissues to 30% in high-energy tissues[498]. The filter was set to 25% after calculating mitochondrial content for each sample. Gene expression matrices were normalized by the NormalizeData function, and 3,000 features with high cell-to-cell variation were calculated using the

FindVariableFeatures function. Data sets with multiple samples may be affected by technical effects such as batch effects, which should be addressed using data integration methods. In this study, Harmony was used[499], which has demonstrated strong performance for batch correction in simpler integration tasks with distinct batch structure. The dimensionality of the dataset was reduced to 100 principal components of the linearly scaled data using the ScaleData and RunPCA functions, respectively. Finally, cells were clustered using the FindNeighbors and FindClusters functions and performed nonlinear dimensionality reduction by uniform manifold approximation and projection for dimension reduction (UMAP) with the RunUMAP function, using 30 dimensions for all approaches. The FindAllMarkers function in Seurat was used to find markers for each unique cluster. Clusters were identified and annotated based on the expression of canonical markers.

### 2.2.6 Differential Gene Expression and Gene Set Enrichment

Differential gene expression (DGE) of the single-cell data was calculated per cell cluster and condition group via a statistical framework Model-based Analysis of Single-cell Transcriptomics considering and regressing the batch and gender confounder[500].

### 2.2.7 Pseudotime

Single-cell pseudotime trajectories were constructed using Monocle (version 2.6.4)[501]. Briefly, a set of ordering genes was selected that showed differential expression between the clusters. Subsequently, Monocle then uses reversed graph embedding, a machine learning technique, to generate a parsimonious principal graph and then reduces the given high-dimensional expression profiles to a low-dimensional space. Individual cells were projected onto this space and ordered along trajectories that were connected by branching points, which correspond to cell fate decisions. The resulting graph structure was then characterized for network centrality as a proxy of wild-type or impaired cell differentiation.

### 2.2.8 Quantitative PCR

#### *2.2.8.1 RNA isolation*

FACS-sorted MDP-derived CD172a$^{-}$ cDCs and CD172a$^{+}$ cDCs from *tdTomato-C3ar1$^{fl/fl}$* and *C5ar1$^{-/-}$*mice, were pelleted and washed once with DPBS. Total RNA was isolated using Qiagen RNeasy Mini extraction kit according to the manufacturer's protocol. First, it was important to determine the correct amount of starting material to avoid overloading of the RNeasy spin column, as this could significantly reduce RNA yield and purity. Pelleted cells were loosened by flicking the tube, and cells were disrupted with 350 µl RLT buffer with vigorous vortexing and mixing by pipetting. In the next step, 350 µl of 70% ethanol was added to the lysate and mixed well by pipetting. Up to 700 µl of the sample was transferred to a RNeasy spin column placed in a 2 ml collection tube. The sample was centrifuged for 15 s at ≥8000xg. The flow-through was discarded. Then, 700 µl of RW1 buffer were added to the RNeasy spin column and centrifuged for 15 s at ≥8000xg to wash the spin column membrane. The flow-through was discarded. In the next step, 500 µl of the RPE buffer were added to the RNeasy spin column and centrifuged for 15 s at ≥8000xg to wash the spin column membrane. The flow-through was discarded. Again, 500 µl of RPE buffer were added to the RNeasy spin column but centrifuged this time for 2 min at ≥8000xg to wash the spin column membrane. The long centrifugation dries the spin column membrane, ensuring

that no ethanol was carried over during RNA elution. Residual ethanol may interfere with downstream reactions. The flow-through was discarded. With the next step, the RNeasy spin column was placed in a new 1,5 ml collection tube. For RNA elution, 32 µl RNAse-free water were added directly to the spin column membrane and centrifuged for one minute at ≥8000xg. The final concentration was measured on NanoDrop with ND-1000 v3.8.1 software on RNA-40 sample type, monitoring optical density (OD) 260/280 and OD 260/230. The OD 260/280 ratio indicated the purity of RNA sample and should be around 2,0 to be considered pure. The OD 260/230 ratio indicates the presence of unwanted organic compounds (i.e. trizol, phenol, guanidine and guanidine thiocyanate) and should be in the range of 2,0 - 2,2. The A260/280 ratios of my samples ranged from 1.97 to 2.37, while the A260/230 ratios were between 0.34 and 1.02; these results suggest the presence of organic contaminants, most likely guanidine thiocyanate, a component of Buffer RLT and RW1 used during RNA isolation. This contamination arises because biological samples are lysed in guanidine thiocyanate-containing buffers, which effectively inactivate RNases to preserve intact RNA. However, if washing steps are insufficient, residual guanidine thiocyanate can remain in the eluate, leading to abnormally low A260/230 ratios and affecting sample purity.

#### *2.2.8.2 DNA digestion*

DNase treatment is important to remove contaminating DNA from RNA preparations and subsequently remove DNase and divalent cations from the sample using the TURBO DNA-free™ kit according to the manufacturer's protocol. The reaction was performed in 0,5 ml tubes. The reaction volume was 30 µl, i.e. 3,1 µl of 10X TURBO DNase™ Buffer were added and one µl of TURBO DNase™ Enzyme to the RNA sample, followed by gentle mixing. The sample was incubated at 37 °C for 30 min in a heating block. DNase Inactivation Reagent was resuspended by flicking or vortexing the tube before use. Five µl of resuspended DNase Inactivation Reagent were added to the sample and mixed well. The DNase Inactivation Reagent not only removes the DNase enzyme but also removes divalent cations, such as magnesium and calcium, which can catalyze RNA degradation when RNA is heated with the sample. The sample was incubated for 5 min at RT with flicking the tube 2-3 times during the incubation period to keep the DNase inactivation reagent suspended. The sample was centrifuged at 10000xg for 1,5 min; then the supernatant containing the RNA was transferred to a fresh tube with no disturbance of the DNase inactivation reagent pellet.

#### *2.2.8.3 Reverse transcription*

Complementary DNA (cDNA) synthesis was performed with the High-Capacity cDNA reverse transcription kit according to the manufacturer's protocol. As recommended, up to 2 µg of total RNA were used per 20 µl reaction. Two times master mix was prepared on ice and gently mixed; it was composed of 2 µl of 10X Buffer, 0,8 µL of 25X dNTP Mix (100 mM), 0,8 µL of anchored oligo(dT)$_{20}$ primers, 1 µl of MultiScribe™ Reverse Transcriptase, 1 µl of SUPERRase In RNase Inhibitor and 4,4 µl of Nuclease-free $H_2O$. Ten µl of 2X master mix were pipetted into a 0,2 µl tube together with 10 µl of RNA sample. The sample was pipetted up and down two times to mix. After briefly spinning down, the tube was loaded onto the C1000 touch thermal cycler and the reverse transcription reaction was performed using the conditions presented in table 2.14.

**TABLE 2.14 Conditions for reverse transcription**

| Settings | Step 1 | Step 2 | Step 3 | Step 4 |
|---|---|---|---|---|
| Temperature [°C] | 25 | 37 | 85 | 4 |
| Time [min] | 10 | 120 | 5 | hold |

#### *2.2.8.4 qPCR*

For the pPCR, I used the Sso7d fusion protein technology. The dsDNA-binding protein, Sso7d, stabilizes the polymerase-template complex without affecting PCR sensitivity, efficiency or reproducibility.

The qPCR was performed using the SsoAdvanced Universal SYBR Green Supermix. As recommended, 15 µL of Mastermix reaction was prepared as follows: 10 µL of 2X SsoAdvanced Universal SYBR Green Supermix, 1 µL of 100 µM primer mix (forward and reverse, in ratio 1:1), 1 µL of Nuclease-free $H_2O$. Fifteen µL of Mastermix reaction were pipetted into a PCR 96-well plate, together with 5 µL of template. The plate was spun briefly down and loaded into thermal cycler CFX96 Touch Real-Time PCR Detection System. For the DNA amplification, I used the program outlined in Table 2.15. The primers used in the thesis are shown in Table 2.6.

**TABLE 2.15 Thermal cycling protocol**

| | Amplification | | | | |
|---|---|---|---|---|---|
| Polymerase activation and DNA denaturation | Denaturation at 95 °C | Annealing/Extension + Plate Read at 60 °C | Cycles | Melt-curve Analysis | Hold at 15 °C |
| 30 s at 95 °C for cDNA | 15 s | 40 s | 35 | 65-95 °C increment 0.5 °C/cycle | |

### 2.2.9 Analysis and purification of cell populations by flow cytometry and fluorescence-activated cell sorting

#### *2.2.9.1 Differentiating distinct immune cell populations by flow cytometry*

Flow cytometry is a laser-based technology, in which both the physical and the molecular characteristics of cells can be measured. Single cells, that are passing the laser beam, can be distinguished by at least three factors; (i) their size, which is indicated by the forward scatter (FSC); (ii) their granularity, which relates to the side scatter (SSC); and (iii) expression of cell marker molecules, which can be visualized by fluorescently-labeled antibodies. Using different antibody panels allows to determine the frequency of a certain cell population in a cell suspension. Therefore, by using an antibody panel, the frequency of DC progenitors, MDPs and CDPs, or $CD172a^-$ and $CD172a^+$ cDCs within the BM population could be assessed. Using different antibody panels allowed me to identify pulmonary or splenic cDC1, cDC2 and pDC populations, On top of that, flow cytometry allows to perform the functional

analysis of the cell of interest. Cells were analyzed on a Cytek Aurora 5L 16UV-16V-14B-10YG-BR in Lübeck or on a Novocyte 2001 flow cytometer in Cincinnati.

#### *2.2.9.2 Immune cell purification by fluorescence activated cell sorting*

To perform functional studies with the different cDC subsets, I used Fluorescence Activated Cell Sorting (FACS). To sort MDP and CDP cells, BM from two mice was pooled. B16-Flt3L injection increased the number of pDCs and cDCs in vivo so that I was able to sort >1x$10^6$ cells from one mouse to set up all functional assays simultaneously. As dead cells, cell debris and doublets found in the cell suspension can give false-positive signal, such cells were gated-out. Sorts were performed with a flow-velocity of approximately 2-3000cells/s and a 100µm nozzle.

DC progenitors (MDPs and CDPs) as well as MDP-derived cDC subpopulations (CD172a$^-$ and CD172a$^+$ cDCs) were purified using a BD FACSARIA III cell sorter maintained by the CAnaCore (Cell Analysis Core Facility, University of Lübeck). The cells were sorted into collection buffer II.

Splenic DC subpopulations (pDCs, cDC1s and cDC2s) were purified using the Sony SH800S and MA900 cell sorters (Sony Corporation of America) maintained by the Research Flow Cytometry Core in the Division of Rheumatology at Cincinnati Children's Hospital Medical Center. The cells were sorted into collection buffer I.

#### *2.2.9.3 Fluorescence staining of cell surface markers*

For surface marker staining, IgG Fc receptor binding was first blocked with 100 µl anti-CD16/32 for 15 min at 4 °C to saturate unspecific binding sites. Then, the cells were resuspended in 100µl staining buffer including antibodies of interest (see Table 2.2) together with fixable viability dye for 20 min at 4 °C. The cells were washed with 1 ml DPBS to wash out unbound Abs and resuspended in 300 µl staining buffer for analysis on a Cytek Aurora or a Novocyte 2001 flow cytometer. Cells were gated on singlets, and dead cells were excluded. Data were analyzed using the FlowJo software (BD Biosciences).

#### *2.2.9.4 Intracellular fluorescence staining*

For intracellular staining of C3aR, C5aR1, C3, C5, C3a, and C5a, a formaldehyde-based fixation or a saponin-based permeabilization approach was used. Surface and live/dead staining were performed before the permeabilization step (see 2.2.9.1).

Briefly, cells were fixed and permeabilized with Cytofix/Cytoperm™ Fixation/Permeabilization kit (BD Biosciences). Cells were fixed for 30 min at RT in 100 µl 4,2% formaldehyde. After fixing, cells were washed in 1 ml Perm/wash buffer. Afterwards, cells were permeabilized in Perm/wash buffer for 30 min at RT. In next step, cells were incubated with an antibody cocktail in 100 µl Perm/Wash buffer for 20 min at 4 °C, using the antibodies depicted in Table 2.2 at the given concentrations. Afterwards, the cells were washed and resuspended in 300 µl staining buffer for the analysis on the Cytek Aurora flow cytometer. Cells were gated on singlets, and dead cells were excluded. Data were analyzed using the FlowJo software (BD Biosciences).

### 2.2.10 Immunofluorescence staining and image analysis

FACS-sorted MDP-derived CD172a$^-$ and CD172a$^+$ cDCs and CDP-derived CD172a$^-$ cDCs from WT, *C3ar1*$^{-/-}$, *tdTomato-C3ar1*$^{fl/fl}$, or *C5ar1*$^{-/-}$ mice were spun down for 5

min at 500xg at RT (1-5 x $10^4$ cells in 150 µl PBS) on glass slides in a cytocentrifuge Cytospin Cellspin I. The samples were air-dried, and circled on the glass slide with Liquid blocker, PAP pen. Samples were dried properly for the next step. Samples were fixed with 70 µl of Fixation buffer (BioLegend) for 20 min at RT, followed by 3X washing with 500 µl of PBS for 5 min. Subsequently, cells were permeabilized with 0.1% v/v Triton×100 in PBS for 5 min at RT, washed three more times with 500 µl of PBS and stained overnight at 4 °C with AF488-conjugated antibody to C5aR1/CD88 (20/70), FITC-conjugated antibody to C3 (11H9), AF594-conjugated antibody to C5 (BB5.1), FITC-conjugated antibody to C5a (I52-1486) together with Hoechst 33342 in 1% BSA (Sigma) in PBS. In some experiments, the tdTomato signal obtained in *tdTomato-C3ar1*$^{fl/fl}$ mice was used to assess C3aR expression as described [428]. After washing with 500 µl of PBS three more times, cells were air-dried, a coverglass was mounted using Fluoroshield (Sigma) and slides were stored at 4 °C in the dark until imaging. All PBS-containing steps were conducted at RT. Staining was evaluated using a Keyence BZ-X810 all-in-one fluorescence microscope and the BZ-X800 viewer software with identical settings for each cell type.

### 2.2.11 Expression of co-stimulatory molecules in MDP-derived CD172a$^-$ and CD172a$^+$ cDCs in response to antigen stimulation

FACS-sorted MDP-derived CD172a$^-$ and CD172a$^+$ cDCs were pulsed with 10 µM ovalbumin (OVA) (Sigma) for 24h, harvested, blocked with anti-CD16/32 (eBioscience) for 15 min and subsequently stained with LIVE/DEAD® fixable viability dye, anti-CD80-biotin (16-10A1) conjugated to streptavidin-PE-Dazzle594, PE-Cy5-conjugated antibody to CD86 (GL1), FITC-conjugated antibody to MHC class II (IA/IE M5/114.15.2) or SB436-conjugated antibody to CD40 (1C10) for 20 min. Cells were measured on a Cytek Aurora flow cytometer.

### 2.2.12 In vitro cDC differentiation and purification of CD172a$^-$ and CD172a$^+$ cDCs from sorted MDPs and CDPs

For the differentiation of MDPs and CDPs into cDCs, FACS-sorted lin$^-$CD135$^+$CD117$^+$ MDPs or lin$^-$CD135$^+$CD117$^-$ CDPs were cultured in a 96-well flat-bottom plate (Sarstedt) in complete Iscove's modified Dulbecco's medium (IMDM) in the presence of murine Flt3L (100 ng/ml) and GM-CSF (20 ng/ml; Peprotech) to stimulate their proliferation and differentiation into cDCs, in particular CD172a$^-$ and CD172a$^+$ cDCs. The medium was supplemented with 10% FCS (Capricorn), glutamic oxaloacetic transaminase (>50 mU/ml) and lactate dehydrogenase (>700 mU/ml), supporting the development of DC [502]. Cells were cultured for 8 days with half of the medium replaced every 3 days including Flt3L and GM-CSF (Peprotech). After 8 days of differentiation in complete IMDM medium, MHC-II$^{hi}$CD11c$^{hi}$B220$^-$CD11b$^+$CD172a$^-$ cDCs and MHC-II$^{hi}$CD11c$^{hi}$B220$^-$CD11b$^+$CD172a$^+$ cDCs were sorted for functional analysis using a BD FACSAria III (BD Biosciences) (**Fig. 2.6**).

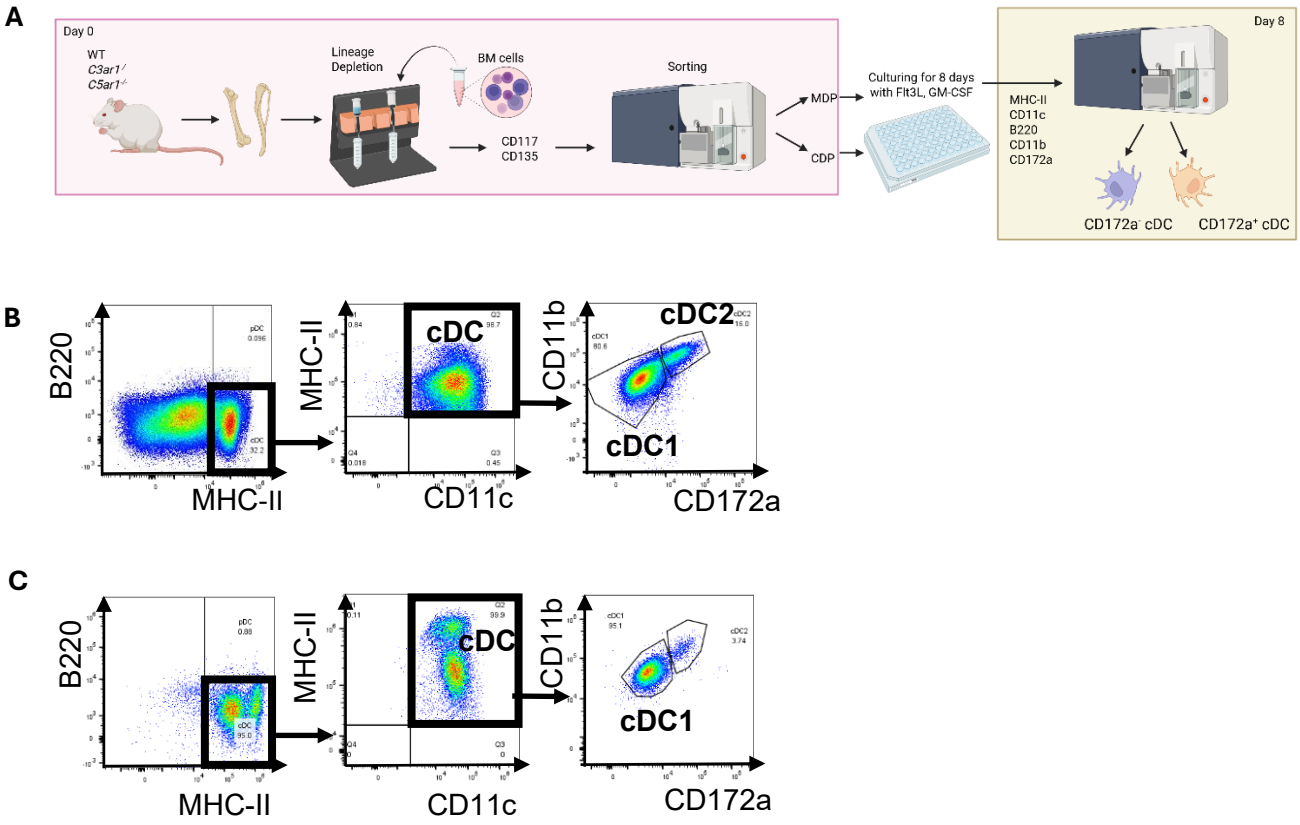


**FIGURE 2.6 Experimental setup and gating strategy to define CD172a$^-$ and CD172a$^+$ cDCs.** **A.** Experimental setup (created with *Biorender.com*). **B-C**. Gating strategy to define the CD172a$^-$ and CD172a$^+$ cDC subsets derived from MDPs (**B**) or CDPs (**C**) after 8-day differentiation. The CD172a$^-$ cDCs were identified as MHC-II$^{hi}$CD11c$^{hi}$B220$^-$CD11b$^+$CD172a$^-$ cells; CD172a$^+$ cDCs were identified as MHC-II$^{hi}$CD11c$^{hi}$B220$^-$CD11b$^+$CD172a$^+$ cells.

### 2.2.13 Isolation and CFSE-labeling of OVA-specific T cell receptor transgenic CD4$^+$ T cells

The spleen was harvested from the OVA-specific T cell receptor (TCR) transgenic (tg) DO11.10*Rag2*$^{-/-}$ mouse strain and placed into ice-cold DPBS. A single-cell suspension was prepared by mechanical disruption of the spleen on a 40 µm cell strainer, with the help of a 5 ml syringe stamp and an additional 10 ml of DPBS. The spleen cells were then centrifuged for 5 min at 350xg at RT. The negative isolation of untouched CD4$^+$ T cells was done using the CD4$^+$ T cell isolation kit from Miltenyi Biotec according to the manufacturer's instructions. The cell pellet was resuspended in 400 µl of MACS buffer and then incubated with 100 µl of biotin-antibody cocktail for 5 min at 4 °C. The biotin antibody cocktail consisted of biotin-conjugated antibodies against CD8a, CD11b, CD11c, CD19, CD45R (B220), CD49b (DX5), CD105, MHC-class II, Ter-119 and TCRγ/δ lineage markers as primary labeling reagent. The cell suspension was then washed with 300 µl of MACS buffer and incubated with 200 µl anti-biotin MicroBeads for 10 min at 4 °C. The cells were then washed with 10 ml MACS buffer and centrifuged for 5 min at 350xg at RT. The pellet was resuspended in 500 µl MACS buffer, followed by magnetic cell separation using the MACS cell separation device. The cells were counted as described in section 2.2.3.4.

The procedure for the spleen harvest from the OT-II OVA TCR tg mouse strain was similar. The spleen was harvested into ice-cold DPBS, and a single-cell suspension was prepared by mashing between frosted slides and then passing through a 70 µm cell strainer. The spleen cells were centrifuged for 5 min at 350xg at RT. After RBC lysis, naïve CD4$^+$ T cells (CD62L$^{hi}$ CD44$^{lo}$) were isolated according to the MojoSort Kit Protocol. A biotin-antibody cocktail was added to the sample and mixed well, followed by 15-minute incubation on ice. Afterwards, streptavidin nanobeads were used and mixed well, followed by 15-minute incubation on ice. Then, staining buffer was added, and the tube was placed in the magnet for 5 min. The sample was poured out, and the liquid containing the cells of interest was collected.

For the 6-Carboxyfluoresceine-succinimidylester (CFSE) labeling of the CD4$^+$ T cells, the CellTrace CFSE cell proliferation kit was used and the labeling was done following the manufacturer's instructions. Briefly, after magnetic separation, T cells were stained with 2 µM CFSE according to the CellTrace CFSE cell proliferation Kit protocol to determine cell proliferation by flow cytometry. At the beginning, cells were centrifuged for 5 min at 350xg at RT and the cell pellet was resuspended and incubated in 500 µl of the CFSE labeling buffer for 10 min at 37 °C in the dark. The reaction was stopped by adding 1 ml ice-cold DPBS and incubating the cells for one minute on ice. The cells were then centrifuged and washed again in 1 ml ice-cold PBS. After centrifugation, the pellet was resuspended in complete IMDM medium (CD4$^+$ T cells from DO11.10*Rag2*$^{-/-}$ mouse) or GM-CSF DC medium (CD4$^+$ T cells from OT-II mouse). Isolated CFSE-labeled CD4$^+$T cells were stained with an anti-CD4 antibody coupled to PE-Cy5 to check for the purity of the isolated cell population by flow cytometry. The purity of CFSE-labeled CD4$^+$ T cells was >99% as determined by flow cytometry. After successful CFSE labeling of CD4$^+$ T cells isolated from DO11.10*Rag2*$^{-/-}$ mouse, the CD4$^+$ T cells were added to a 96-well flat-bottom plate (Sarstedt) in which the FACS-sorted and CD172a$^-$ or CD172a$^+$ cDC were plated the day before. CD4$^+$ T cells isolated from OT-II mice were seeded into a 96-well U-bottom plate (Corning) together with FACS-sorted cDC1 or cDC2 the same day.

### 2.2.14 Co-culture of sorted MDP-derived CD172a$^-$ and CD172a$^+$ cDCs with naïve CD4$^+$ OVA-T cell receptor transgenic T cells

FACS-sorted MDP-derived CD172a$^-$ and CD172a$^+$ cDCs from BALB/c WT, *C3ar1*$^{-/-}$ or *C5ar1*$^{-/-}$ mice were seeded into a 96-well flat-bottom plate (Sarstedt), cultured in complete IMDM medium and pulsed overnight with 10 µM OVA (Sigma). The next day, purified CFSE-labelled OVA-TCR tg CD4$^+$ T cells from DO11.10*Rag2*$^{-/-}$ mice were added at a ratio of 1:5 (CD172a$^-$ or CD172a$^+$ cDC : CD4$^+$ T cell). After 4 days, the supernatant was collected to determine cytokine production. The cells were harvested and T cell proliferation as well T cell differentiation TEFF and TEM cells was determined. Naïve T cells were identified as CD62L$^{hi}$CD44$^-$, TEM as CD62L$^+$CD44$^+$ and TEFF as CD62L$^-$CD44$^+$ cells.

### 2.2.15 Co-culture of sorted splenic cDC1 or cDC2 with naïve CD4$^+$ OVA-T cell receptor transgenic T cells

FACS-sorted splenic cDC1 and cDC2 from C57BL/6 WT or *C5ar1*$^{-/-}$ mice were plated together with naïve CFSE-labelled OVA-TCR tg CD4$^+$ T cells from OT-II mice at a ratio of 1:5 (cDC1 or cDC2 : CD4$^+$ T cell) into a 96-well U-bottom plate (Corning) and

cultured in GM-CSF DC medium. To evaluate their capacity to prime and polarize antigen-specific T cell responses, the cultures were pulsed overnight with 3 or 10 µg/ml LPS-free EndoFit OVA protein (Invivogen), either alone or in combination with the TLR ligands LPS or PAM3CSK4 (**Tab. 2.16**). These stimuli were administered to mimic infection- or inflammation conditions and to assess, how PAMPs modulate DC-mediated antigen presentation and subsequent T cell activation. After 3 days of co-culture, the supernatant was collected to determine cytokine production. The cells were harvested and T cell proliferation as well T cell differentiation into TEFF and TEM was investigated.

**TABLE 2.16 Different in vitro conditions used for the co-culture of splenic cDC1 or cDC2 and CD4⁺ T cells**

| Stimulus | Concentration | Number of stimulations | | | | | |
|---|---|---|---|---|---|---|---|
| | | 1 | 2 | 3 | 4 | 5 | 6 |
| OVA | 3 µg/ml | ■ | | ■ | ■ | | |
| | 10 µg/ml | | ■ | | | ■ | ■ |
| LPS | 100 ng/ml | | | ■ | | ■ | |
| PAM3CSK4 | 100 ng/ml | | | | ■ | | ■ |

## 2.2.16 Determination of effector memory and effector T cell responses in OVA-specific TCR transgenic CD4⁺ T cells

After co-culture with OVA-pulsed CD172a⁻ or CD172a⁺ cDCs, CFSE-labeled CD4⁺ T cells were harvested, and T cell differentiation into TEFF and TEM cells was determined. For this purpose, T cells were harvested, blocked with anti-mouse CD16/32 (eBioscience) for 15min, stained with LIVE/DEAD® fixable viability dye, PE-Cy5-conjugated antibody to CD4 (H129.19, BD), BV785-conjugated antibody to CD44 (IM7), and PE-conjugated antibody to CD62L (MEL14). TEM were defined as CD4⁺CD62L⁺CD44⁺ and TEFF as CD4⁺CD62L⁻CD44⁺ (**Fig. 2.7A**). Additionally, CFSE labeling was used to calculate the cell divisions in TEM and TEFF and the percentage of undivided cells (**Fig. 2.7B**). As a measure of cell proliferation, I calculated the proliferation index by dividing the total number of divisions by the cells that went into division.

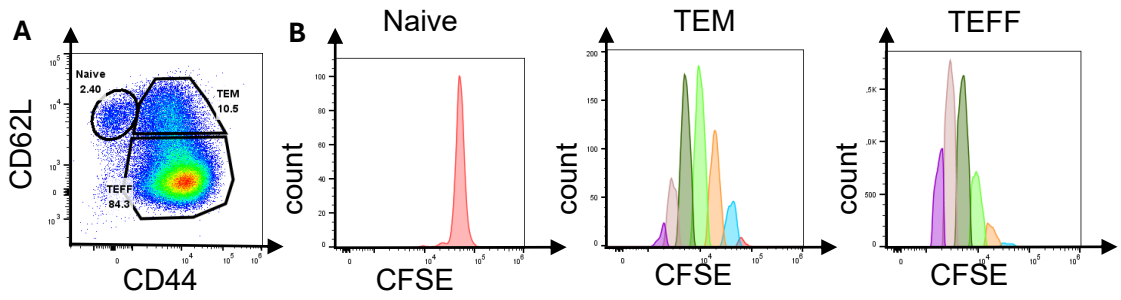


**FIGURE 2.7 Gating strategy to define T cell subsets after 4-day co-culture with OVA-pulsed CD172a⁻ or CD172a⁺ cDCs and cDC-induced proliferation of naïve, TEM and TEFF**

**cells.** **A**. Gating strategy to define naïve CD62L$^{hi}$CD44$^{-}$ T cells, CD62L$^{+}$CD44$^{+}$ TEM and CD62L$^{-}$CD44$^{+}$ TEFF. **B.** Histograms showing the proliferation of CFSE-labelled näive, TEM and TEFF (from left to right) OVA-TCR tg CD4$^{+}$ T cells from DO11.10*Rag2*$^{-/-}$ mice in response to 4-day co-culture with OVA-pulsed CD172a$^{-}$ cDCs from WT mice.

### 2.2.17 Cytokine production of OVA TCR transgenic CD4$^{+}$ T cells in response to co-culture with OVA- pulsed CD172a$^{-}$ and CD172a$^{+}$ cDCs

IL-17A and IFN-γ secretion was determined after 4-day co-culture of CD172a$^{-}$ or CD172a$^{+}$ cDCs and CD4$^{+}$ T cells from OVA TCR tg DO11.10*Rag2*$^{-/-}$ mice using DuoSet ELISA kits (R&D Systems) following the manufacturer's protocol. The detection limit was 15,6 pg/ml for IL-17A and 31,2 pg/ml for IFN-γ. The cytokine concentrations were determined following the manufacturer´s instructions using half of the recommended volume (50 µl instead of 100 µl). Briefly, the ELISA plate (Corning) was coated with 50 µl of the specific capture antibody overnight at RT. Then the capture antibody was decanted, and the plate was washed 3 times with washing buffer. Afterwards, the plate was blocked with 150 µl blocking buffer for 1h at RT and washed again 3 times with washing buffer. Then the standards and samples (50 µl) were added in duplicates to the plate and incubated for 2h at RT. The plate was washed again 3 times with washing buffer and 50 µl of the respective biotinylated detection antibody were added for another 2h at RT. After another wash, 50 µl of streptavidin-horse-radish-peroxidase (HRP) were added and incubated for 20 min at RT in the dark. After washing, 50 µl of tetramethylbenzidine (TMB) substrate was added for 20 min at RT in the dark. The reaction was stopped with 25 µl of 1 M $H_2SO_4$, and the ELISA-plate was analyzed using a FluoStar Omega 0415 reader (BMG Labtech).

### 2.2.18 Cytokine production of OVA TCR transgenic CD4$^{+}$ T cells in response to co-culture with OVA-pulsed splenic cDC1s and cDC2s

IL-17A and IFN-γ secretion was determined 3 days after co-culture of splenic cDC1 or cDC2 and CD4$^{+}$ T cells from OT-II mice using the ELISA MAX™ Standard Set Mouse IL-17A and IFN-γ (BioLegend) following the manufacturer's protocol. The sensitivities were 15,6 pg/ml for IL-17A and IFN-γ. Capture antibodies for IL-17A and IFN-γ were used to coat 96-well flat-bottom plates (Greiner) overnight at 4 °C. Plates were blocked with blocking buffer for 2h at RT. Samples were diluted in blocking buffer and loaded in duplicate and then incubated overnight at 4 °C. The next day, the plate was washed 3 times with washing buffer. Detection antibodies for IL-17A and IFN-γ were added for another 2h at RT. After another wash, 50 µl of streptavidin-HRP was added and incubated for 30 min at RT in the dark. After 4 times of washing, 100 µl of substrate solution was added until most standard wells turned yellow. The reaction was stopped with 50 µl of 1 M $H_2SO_4$, and the ELISA plate was analyzed on a Synergy LX Multi-Mode Plate Reader. The protein concentration was quantified using OPD colorimetric assay using a standard curve of known concentrations for IL-17A and IFN-γ.

### 2.2.19 Immunoassay LEGENDplex

To determine IL-23, IL-1α, IL-1β, TNF-α, MCP-1/CCL2, IL-12p70, IL-17A, IL-6, IL-10, IL-27, IFN-γ, IFN-β, and GM-CSF from supernatants of FACS-sorted MDP-derived CD172a$^{-}$ and CD172a$^{+}$ cDC, which were pulsed with OVA (Sigma) for 24h, the bead-

based multiplex LEGENDplex Mouse Inflammation Panel (13-plex) assay (BioLegend) was used. For IL-12p40 and TGF-β1 (Free Active) production, the LEGENDplex Mouse Macrophage/Microglia Panel Mix and Match Subpanel (BioLegend) was used. These assays use the basic principles of sandwich immunoassays, where the soluble analyte is captured between two antibodies. The different bead sets were conjugated with specific antibodies and can be distinguished by their size and internal fluorescence intensities. First, the sample containing target analytes is incubated with beads, whereby analytes bind to their specific capture bead. Then, a biotinylated detection antibody cocktail is added. Each detection antibody in the cocktail will bind to its specific analyte bound on the capture beads, thus forming capture bead-analyte-detection antibody sandwiches. Biotin serves as an attachment site for streptavidin, which is added afterwards and is conjugated to PE. Samples were measured at a flow cytometer where the internal dye is detected using the APC channel and the fluorescence intensity providing information about the amount of analyte, which is detected in the PE channel. To determine the antibody concentration, standard dilutions of known concentrations were measured for every run[503].

The LEGENDplex was performed according to the manufacturer's instructions, with the alterations of using only a quarter of the volumes suggested by the manufacturer. The V-bottom plate (BioLegend) was wrapped in aluminium foil for all incubation steps. Briefly, 7 µl of assay buffer were loaded into all wells of a V-bottom plate for LEGENDplex™ assay. The standard was prepared by performing a 1:4 serial dilution 5 times with the undiluted standard sample. Then, the first two columns were loaded with 7 µl of prepared standards, and the rest of the wells with 7 µl of the sample. For complete resuspension, the beads were vigorously mixed on a vortexer for 30 s, and 7 µl of mixed beads were added to all wells. During bead addition, a bottle with mixed beads was shaken intermittently to avoid bead settling. Then, the plate was incubated overnight at 4 °C on a plate shaker. The next day, the plate was centrifuged at 250xg for 5 min and the supernatant immediately dumped. Wells were washed with 200 µl wash buffer (WB), incubating for one minute each. Then, the centrifugation step was repeated, and 7 µl of detection antibody was added to each well. The plate was incubated on a plate shaker for 1h. Seven µl streptavidin-PE was added and the plate was incubated for an additional 30 min. The wells were centrifuged and washed with WB buffer as indicated above. Subsequently, 100 µl WB were added and the beads resuspended by pipetting. Analysis was performed on the Cytek Aurora flow cytometer with supported from the CAnaCore. Data were analyzed via LEGENDplex Data Analysis Software (BioLegend in agreement with Qognit, CA, USA) and specified as pg/ml. The detection limits for the individual cytokines are shown in table 2.17.

**TABLE 2.17 Detection limit of cytokines determined by LEGENDplex Mouse Inflammation Panel (13-plex) assay and LEGENDplex Mouse Macrophage/Microglia (2-plex: IL 12p40, TGF-β1) assay**

| Cytokine | pg/ml |
|---|---|
| IL-23 | 47,69 |
| IL-1α | 20,92 |
| IL-1β | 0,24 |

| | |
|---|---|
| TNF-α | 1,20 |
| MCP-1/CCL2 | 3,72 |
| IL-12p70 | 16,13 |
| IL-17A | 6,65 |
| IL-6 | 7,65 |
| IL-10 | 0,45 |
| IL-27 | 7,67 |
| IFN-γ | 26,60 |
| IFN-β | 1,81 |
| GM-CSF | 3,24 |
| IL-12p40 | 0,65 |
| TGF-β1 | 1,08 |

### 2.2.20 Statistical Analysis

Statistical differences between groups were determined using the GraphPad Prism 10 software. When groups were normally distributed, statistical differences between two groups were analyzed by an unpaired t test. If more than two groups were evaluated, the groups were first analyzed by an analysis of variance (one-way ANOVA) followed by a Tukey or Dunnett posthoc multiple-comparison test or a two-way ANOVA followed by a Šidák or Holm-Šidák posthoc multiple-comparison test. If data were not normally distributed, groups were analyzed by Kruskal Wallis test followed by Dunn's posthoc multiple-comparison test. Data are presented as the mean ± standard error of the mean (SEM). *p < 0,05, **p < 0,01, ***p < 0,001, ****p < 0,0001, ns, not significant, as indicated in figure legends.

# 3. Results

## 3.1 Impact of C3aR and C5aR1 on myeloid bone marrow progenitor cells in BALB/c mice

### 3.1.1 The C5a/C5aR1 axis controls the differentiation of Lin- myeloid progenitor cells in the bone marrow

First, I determined the number of BM cells in WT, *C3ar1*$^{-/-}$ and *C5ar1*$^{-/-}$ mice before and after lineage depletion. While I found no differences between the three strains before lineage depletion (**Fig. 3.1A**), the number of Lin$^-$ cells was significantly lower in BM cells isolated from *C5ar1*$^{-/-}$ as compared with WT or *C3ar1*$^{-/-}$ mice suggesting that C5aR1 regulates the differentiation of Lin$^-$ myeloid progenitor cells (**Fig. 3.1B**).

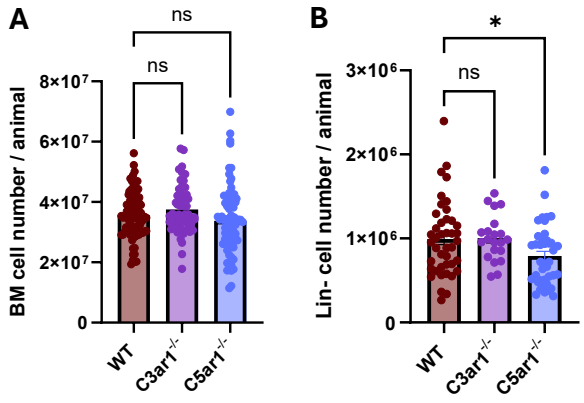


**FIGURE 3.1 Number of total BM (A) and Lin$^-$ (B) cells from WT, *C3ar1*$^{-/-}$ and *C5ar1*$^{-/-}$ mice.** The number of BM cells was calculated by CASY; Lin$^-$ cell numbers determined by the FACSDiva software after sorting, as a population of single, living and PE-Cy5$^-$ cells. Data shown are the mean ± SEM. Differences between groups were determined by Kruskal-Wallis with Dunn's (A) and One-way ANOVA with Dunnett (B) posthoc multiple-comparisons test; ns: not significant, *p<0,05.

### 3.1.2 The C5a/C5aR1 axis controls the differentiation of MDPs and CDPs from Lin$^-$ myeloid progenitor cells

After sorting Lin$^-$CD135$^+$CD117$^+$ MDPs and Lin$^-$CD135$^+$CD117$^-$ CDPs (**Fig. 2.3**), I observed that the number of MDPs was significantly higher than that of CDPs in all mouse strains (**Fig. 3.2A**). Intriguingly, the number of MDPs and CDPs in BMs from *C5ar1*$^{-/-}$ mice was significantly lower as compared with that of WT mice. Also, the number of CDPs from *C3ar1*$^{-/-}$ mice was somewhat lower than that in WT mice, although it did not reach the level of statistical significance (**Fig. 3.2B**). This finding suggests that C5aR1 drives the differentiation of MDPs and CDPs from HSCs and that C3aR may add to this effect (**Fig. 3.3**).

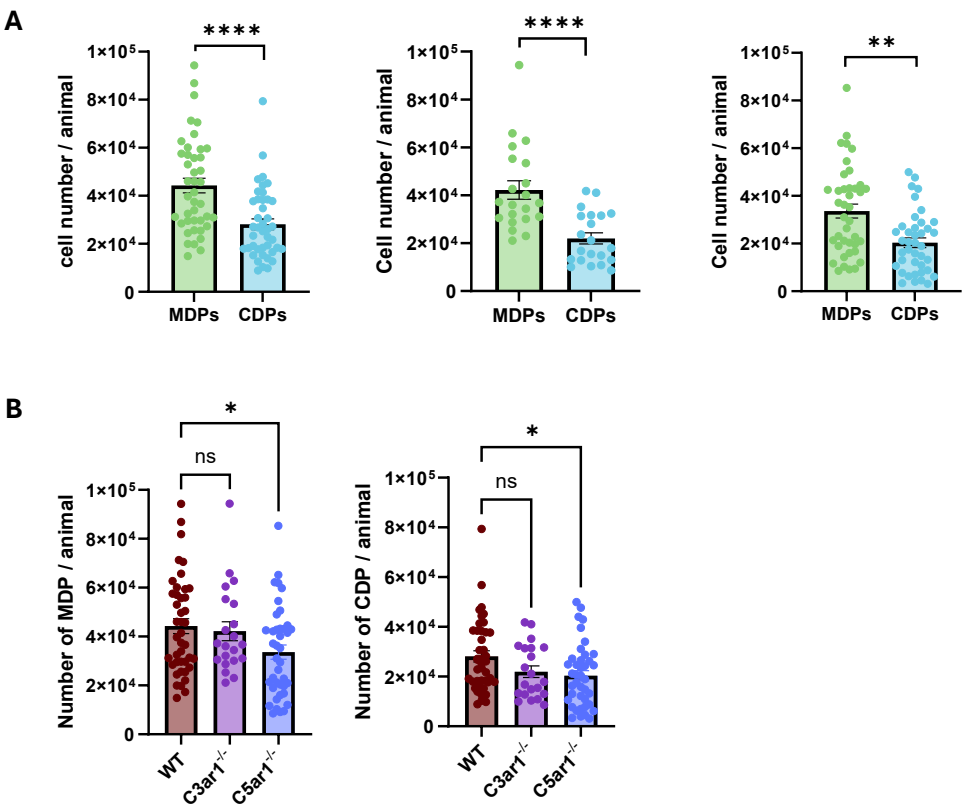


**FIGURE 3.2 Impact of C3aR and C5aR1 on MDP and CDP numbers in the BM. A.** Numbers of BM-derived MDPs and CDPs from WT, *C3ar1*$^{-/-}$ and *C5ar1*$^{-/-}$ (from left to right) mice. **B**. Comparison of MDP (left panel) and CDP (right panel) numbers in BMs from WT, *C3ar1*$^{-/-}$ and *C5ar1*$^{-/-}$ mice. Data shown are the mean ± SEM. Differences between groups in A were determined by Mann-Whitney test. Differences between groups in B were analysed by Kruskal-Wallis test with Dunn's (left panel) or One-way ANOVA with Dunnett (right panel) posthoc multiple-comparisons tests; ns: not significant, *p<0.05, **p<0.01, ****p<0.0001.

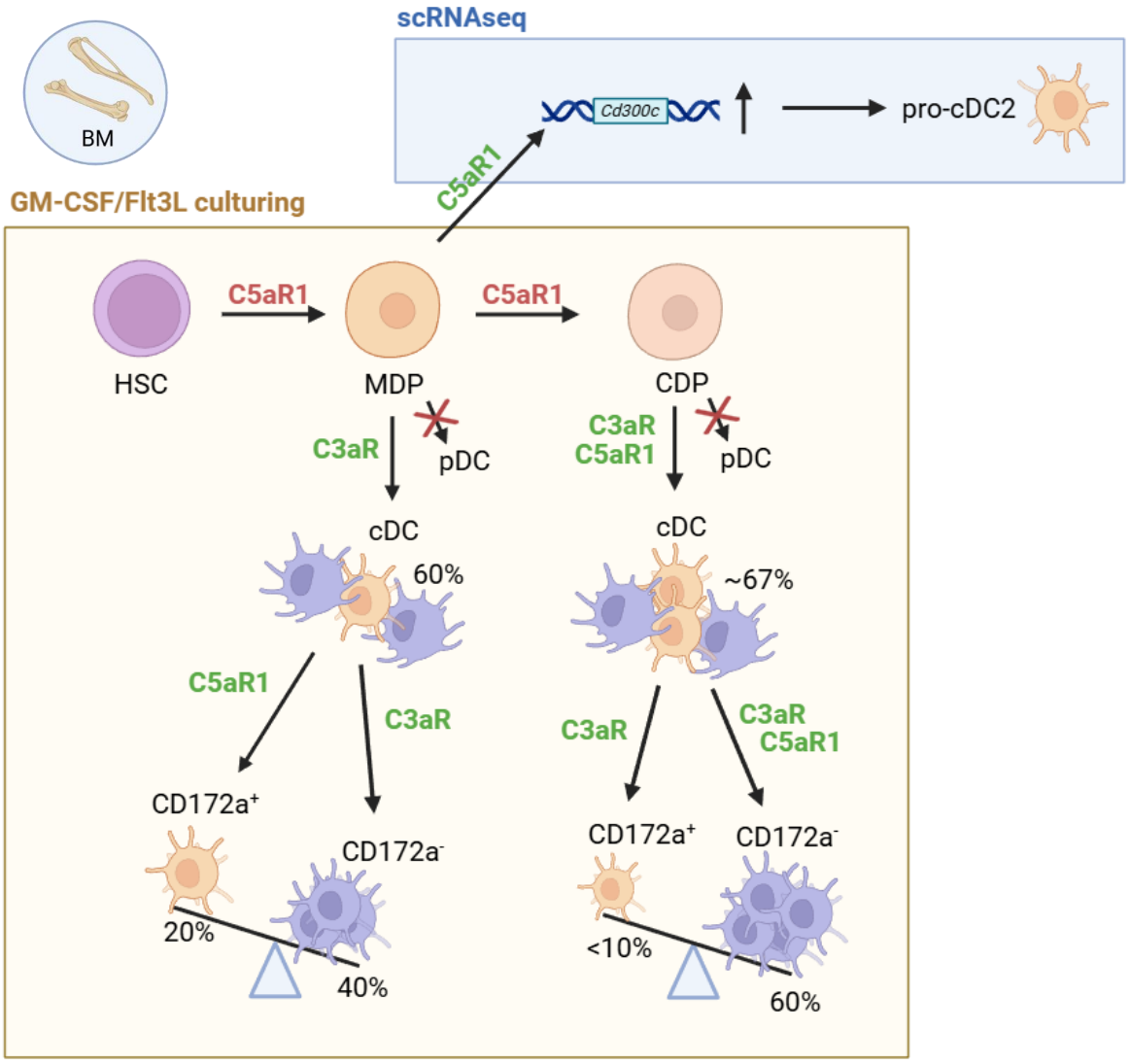


**FIGURE 3.3 Schematic overview of MDP and CDP differentiation from HSCs.** Shown is the CD172a$^-$ and CD172a$^+$ differentiation from MDP and CDP cells with their respective frequencies on day 8 of differentiation. Frequencies were determined from all living cells at the end of GM-CSF/Flt3L culturing on day 8 and represent WT mice (created with *Biorender.com*). The effect of C3aR and C5aR1 is indicated next to the arrow.

### 3.1.3 Expression of C3/C3a, C5/C5a and the anaphylatoxin receptors C3aR and C5aR1 in MDPs or CDPs

In search for mechanisms, underlying the role of C5aR1 as driver of MDP and CDP differentiation, I first assessed the expression of the complement factors C3 and C5, their cleavage fragments C3a and C5a, as well as C3aR and C5aR1. MDPs and CDPs stained negative for C3, C5, the anaphylatoxins and their receptors, suggesting an indirect effect of C5aR1 on MDP and CDP differentiation (**Fig. 3.4**).

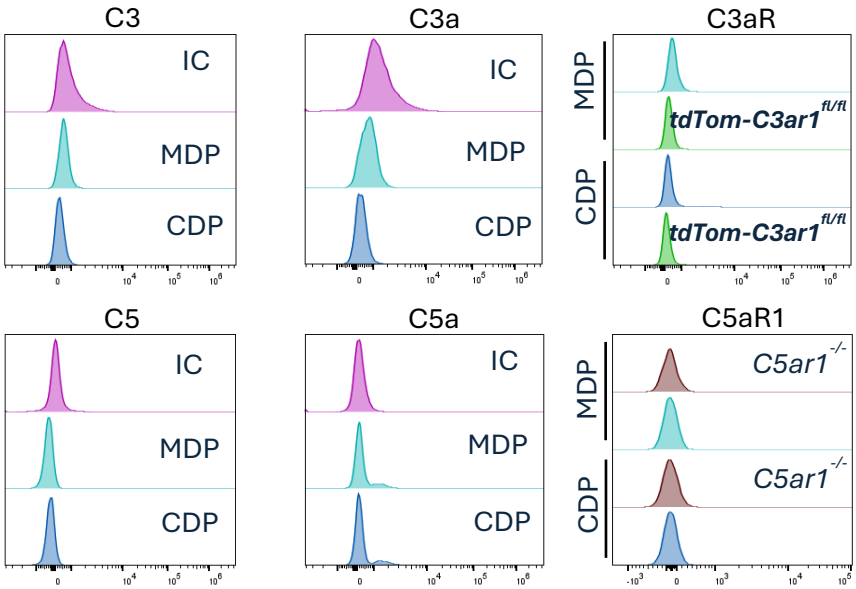


**FIGURE 3.4 Histograms showing the expression of C3, C3a, the tdTomato-C3aR reporter protein, C5, C5a and C5aR1 in MDPs and CDPs from WT mice directly after FACS sorting**. IC: isotype control

### 3.1.4 MDPs from wildtype and *C5ar1*$^{-/-}$ mice differ in their transcriptional profile

To gain additional insights into potential differences of MDP from WT and C5aR1-deficient mice, I determined the transcriptional profiles of MDPs from four WT and four *C5ar1*$^{-/-}$ mice (two males and two females each) by scRNA-seq. After quality control, I found on average 9727 cells per strain, with an average of 3,046 genes expressed per cell. Initial analysis revealed eight clusters with distinct gene expression profiles (**Fig. 3.5**).

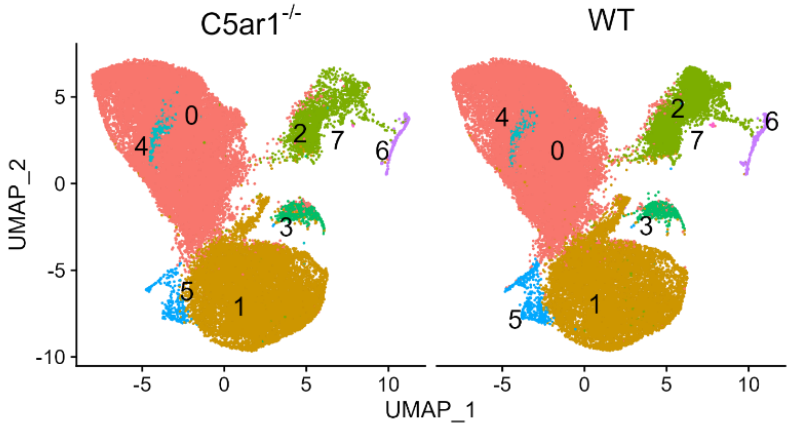


**FIGURE 3.5 UMAP plots showing eight distinct clusters within FACS-sorted MDPs from BM of *C5ar1*$^{-/-}$ (left panel) or WT (right panel) mice**.

At the beginning, trajectory analysis was performed to understand, how cells change and evolve between clusters. Here, I found that cells from clusters 1, 4 and 5 were

evolving from cluster 0. Cluster 3 partially evolved from cluster 1, however cluster 2 has its own origin (**Fig. 3.6**).

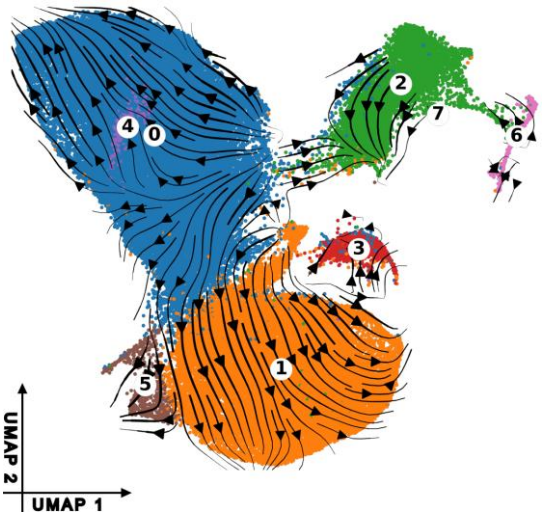


**FIGURE 3.6 UMAP plots showing cluster evolution within BM derived FACS-sorted MDPs.**

Cluster 7 was excluded due to low cell counts. Next, I determined mutually and differentially expressed genes (DEG) in clusters 0-6. I found two groups of clusters, which differed in their pattern of exclusively expressed genes. Clusters 0, 1 and 4 expressed a low number (222-509) as compared with clusters 2, 3, 5 and 6, which expressed a much higher number of such genes (766-1461), suggesting that the latter clusters comprise more differentiated cells (**Fig. 3.7**).

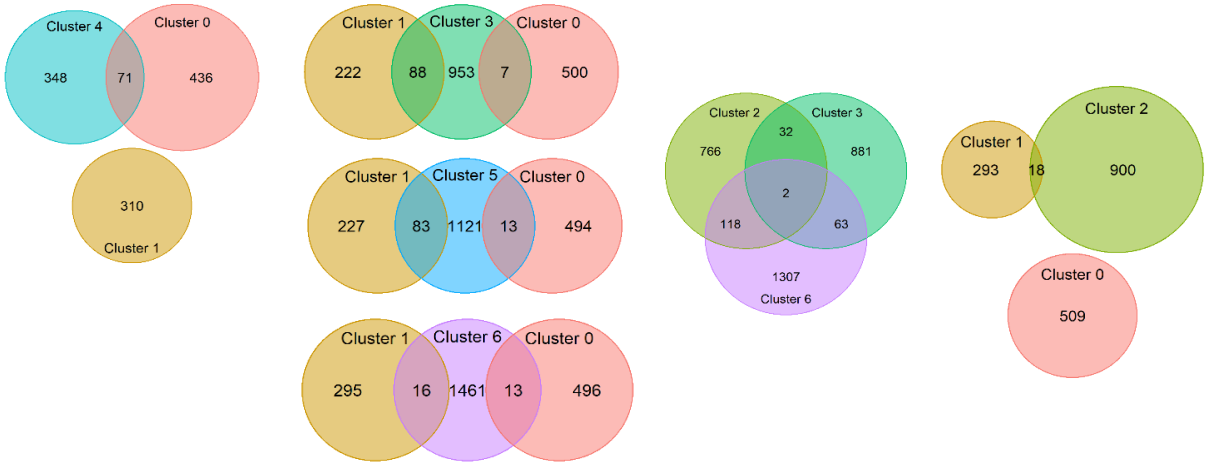


**FIGURE 3.7 Gene expression profiling in MDPs from *C5ar1*$^{-/-}$ and WT mice**. Venn diagrams depicting common and differentially expressed genes (DEG) in clusters 0-6. Venn diagrams were prepared after regressing out the gender and batch cofactors and represent genes with FC>1 and p<0.05.

Next, I compared the top ten DEGs across the seven MDP clusters (**Fig. 3.8**). The biggest cluster, cluster 0, included genes involved in immune regulation, such as *Il7r* and *Cmah*, previously linked to early progenitor stages and hematopoietic stem cell differentiation[504-510]. These genes were also expressed in cluster 4. Further, some genes that regulate hematopoietic stem cell maintenance, differentiation, and lineage

commitment were exclusively expressed in cluster 4[511]. The second biggest cluster, cluster 1, expressed genes involved in cell cycle regulation, chromatin dynamics, and mitosis, all of which play important roles in the proliferation and differentiation of MDPs into DC subsets, macrophages, or moDC. High expression of these genes suggests an undifferentiated and proliferative stage of MDPs. Chromatin-related genes reflect transcriptional reprogramming needed for further development and lineage specification[512,513]. These genes were also expressed within clusters 3, 5, and 6. DEGs from cluster 3 were also expressed widely among the cells from clusters 1, 5, and 6. Such genes are important in mitotic regulation or cell cycle control. They ensure that progenitor cells divide correctly and maintain a balance between proliferation and differentiation[514]. Cells within cluster 5 strongly expressed *Nfil3*, *Id2*, *Rhoa* and *Batf3*, essential for pre-cDC and cDC1 differentiation[515-520]. One of the highly expressed genes in cluster 6 were *Gata1*, which is an important transcriptional regulator of DC differentiation required for the survival of DC precursors[521] and forms a complex with *Zfpm1/FOG1*, another gene highly expressed in cluster 6. In fact, many regulatory functions of *Gata1*-require Zfpm1/FOG1[522]. Finally, genes expressed in cluster 2 represent mitochondrial- and nuclear-encoded genes that are essential for cellular energy production[523,524].

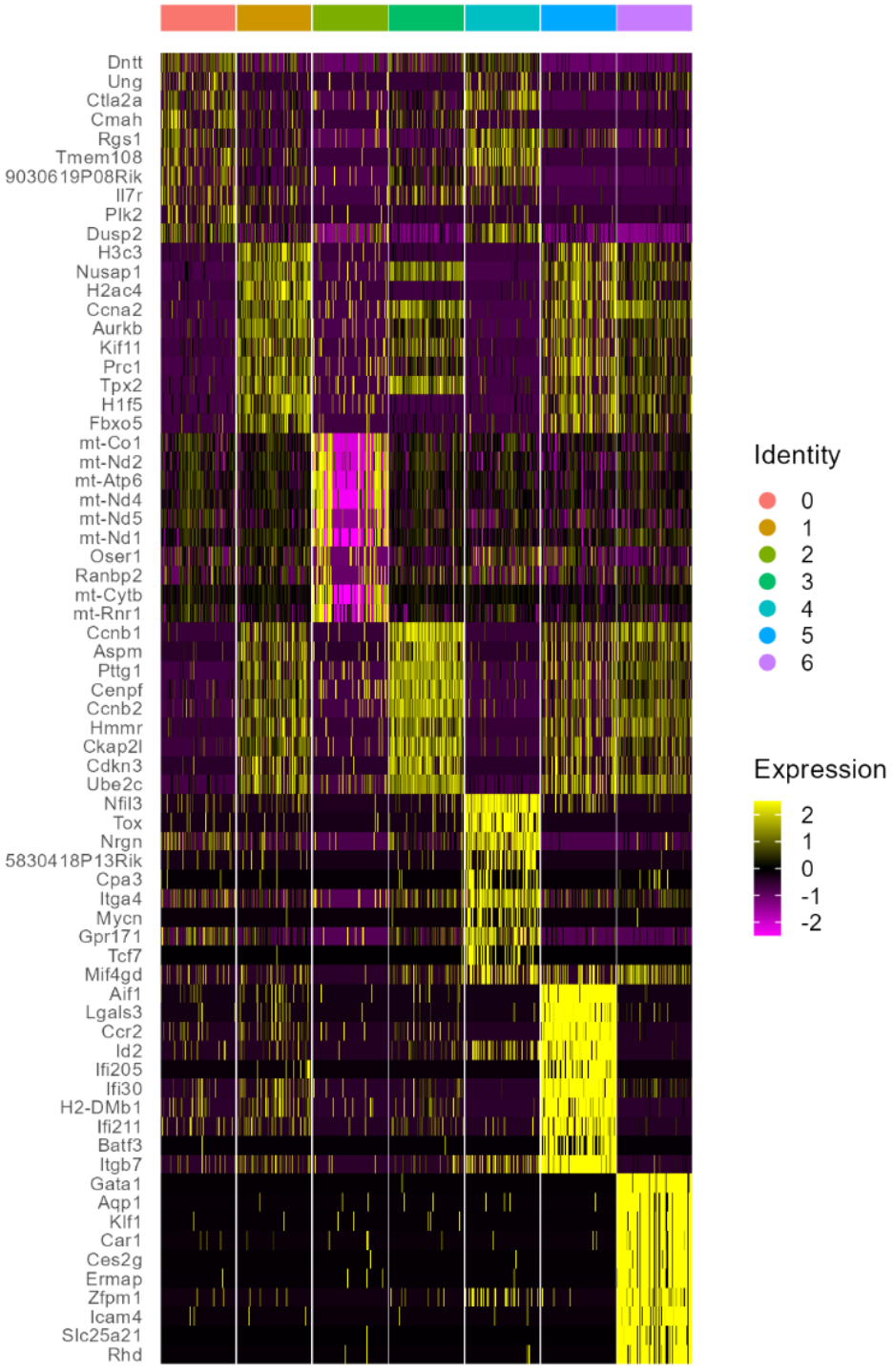


**FIGURE 3.8 Heatmap of the top ten differentially expressed genes (DEGs) across the seven MDP clusters.** The heatmap was prepared after regressing out the gender and batch cofactors and represents up to 100 cells per cluster.

Subsequently, I analyzed the expression levels of signature genes from different myeloid progenitors such as MDPs, CDPs and cMoPs as well as early and late stage pre-cDC1, pre-cDC2 and pre-pDC cells in the different clusters (**Fig. 3.9**).

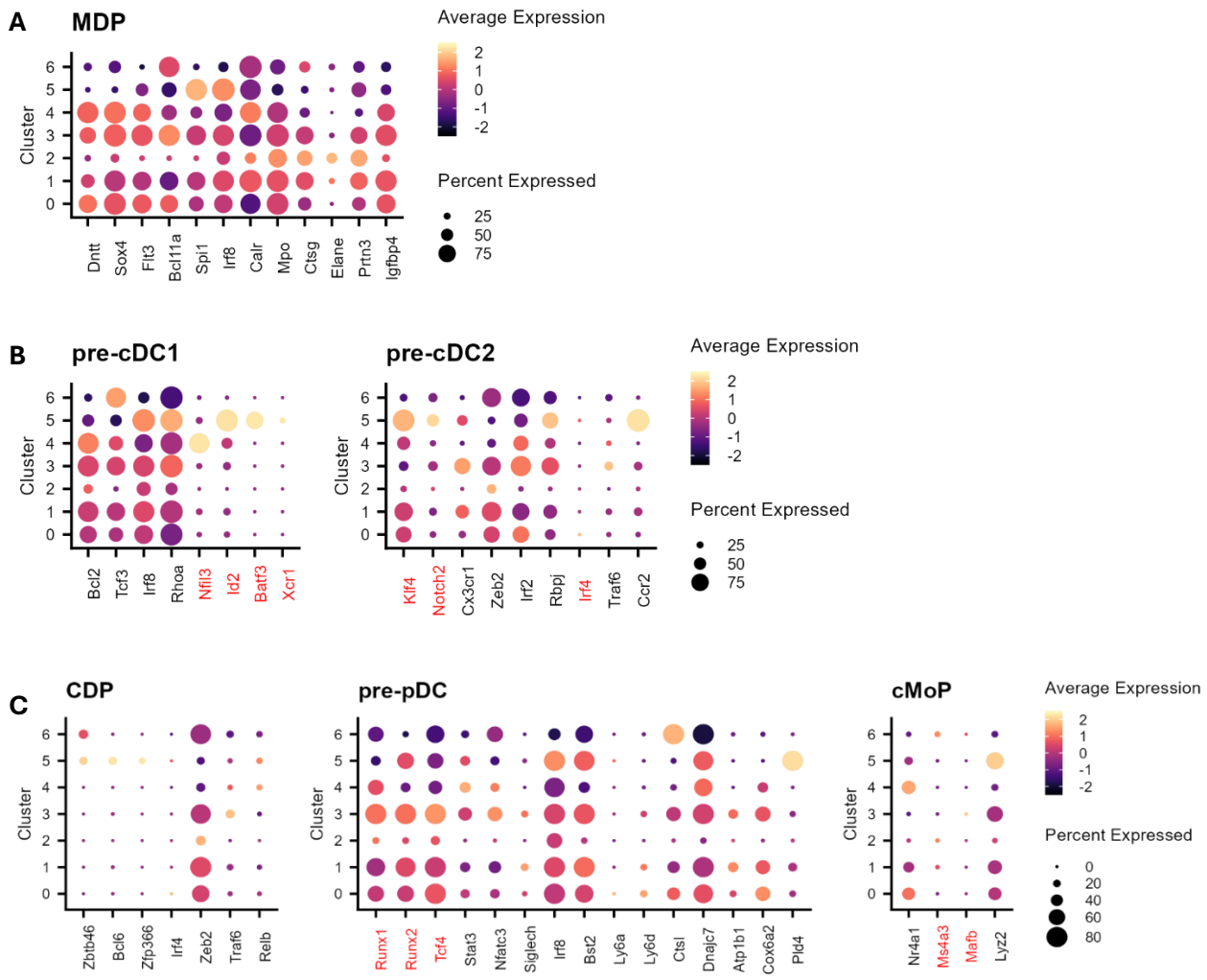


**FIGURE 3.9 Dot plots showing the expression of signature genes of different myeloid lineage progenitors and pre-cDCs or pre-pDCs in clusters 0-6. A, B**: MDP (**A**), pre-cDC1 (**B** left) and pre-cDC2 (**B** right panel) signature genes. **C**. Dot plots depicting the expression levels of selected signature genes from CDPs, pre-pDCs and cMoPs (from left to right). Signature genes marked in red are preferentially expressed in the indicated cell populations.

Previous studies reported overlapping expression of several signature genes in myeloid progenitor and pre-cDC1 or pre-pDC cells. However, they also identified some signature genes almost exclusively expressed in MDPs, CDPs, cMoPs, pre-pDCs, pre-cDC1 or pre-cDC2 (**Fig.3.9**). The majority of MDP signature genes, such as *Dntt, Sox4, Flt3, Bcl11a, Spi1, Irf8, Mpo* were highly expressed in 50-75% of cells from clusters 0, 1, 3, and 4 and some of such genes were also expressed in clusters 2, 5 and 6 (**Fig. 3.9A**). As expected, signature genes of CDPs, such as *Bcl6*, and *Zfp366* were at best marginally expressed in a small set of the different clusters. Of note, I observed a medium *Zeb2* gene expression, which regulates the development of cDC1 or pDCs[140], in 60-80% of cells from clusters 0, 1, 3 and 6 (**Fig. 3.9C, left panel**). Thus, the majority of the sorted $CD117^{+}CD135^{+}$ MDP expressed the expected MDP signature genes. Also, signature genes of pre-pDCs such as *Runx1*, *Runx2* and *Tcf4*, among others, were expressed in 60-80% of cells from clusters 0, 1 and 3 at medium levels (**Fig. 3.9C, middle panel**), indicating that some of the MDPs were differentiating toward the pDC lineage. Interestingly, in 75% of cells from clusters 4 or 5, I found strong

expression levels of signature genes for pre-cDC1 at an early (*Nfil3*) or late (*Id2, Batf3*) stage of development (**Fig. 3.9B**). Further, I also observed a high expression of early stage pre-cDC1 genes *Irf8, Tcf3* or *Rhoa* genes in clusters 5 and 6 (**Fig. 3.9B, left panel**). From the signature genes of pre-cDC2 such as *Klf4, Notch2* or *Irf4,* only *Klf4* was widely expressed at medium to high levels in clusters 0, 1 and 5. Further, I found expression of *Zeb2*, *Irtf2* and *Rbpj* in clusters 0, 1, 3, 4, 5 and 6 in 25-75% of cells with low to medium expression levels (**Fig. 3.9B, right panel**). These data suggest that cells in clusters 4, 5 and 6 already started transcriptional programs to differentiate into cDC1 or cDC2. Of note, I found almost no expression of the cMoP signature genes *Ms4a3*, *Mafb* and only some expression of *Nr4a1*, in 20-40% of cells in clusters 0, 1 and 4 (**Fig. 3.9C, right panel**) suggesting that only a low number of cells in these clusters differentiated toward monocytes.

I also determined the mRNA expression of complement proteins by scRNA-seq analysis. For most complement proteins and receptors, I found no expression except for properdin (*Cfp*), *Cd55*, *Cd59* and C1q binding protein (*C1qbp*) (**Fig. 3.10**). Of note. *C1qbp* was expressed in all clusters, whereas *Cfp* was mainly expressed in clusters 0, 1 and 5 and the two cell-bound complement regulator proteins *Cd55*/DAF and *Cd59* in clusters 0, 1 and 6.

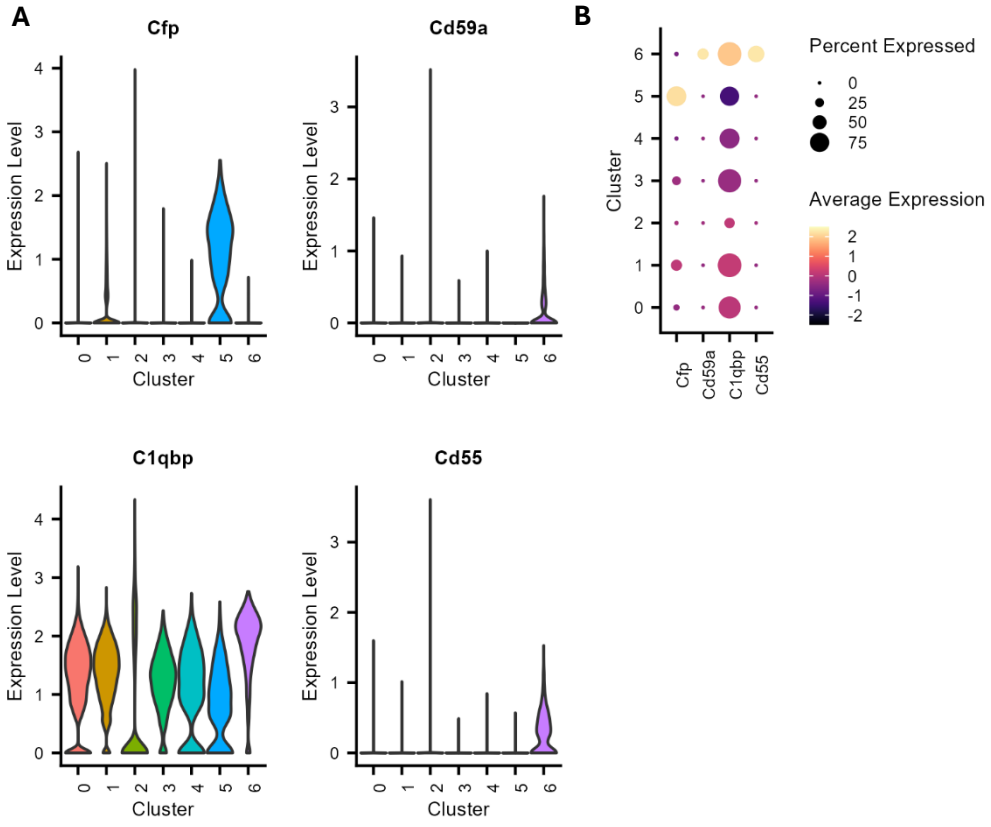


**FIGURE 3.10 Gene expression of *Cfp, Cd59a, C1qbp, Cd55* in clusters 0-6 of MDPs from WT and *C5ar1*$^{-/-}$ mice.** (**A, B**) Violin (A) and (B) dot-plots showing the percent and average expression of the different complement genes.

In a final step, I compared the gene expression levels of MDPs from WT with that of *C5ar1*$^{-/-}$ mice. This analysis identified 5742 genes that were differentially expressed between these two genotypes. In MDPs from WT mice, genes encoding for the

neutrophil serine protease (NSP) cathepsin G (*Ctsg),* neutrophil elastase *(Elane)* proteinase 3 *(Prtn3)* and the sodium-dependent neutral amino acid transporter B(0) solute carrier family 1 member 5 (*Slc1a5*) were higher expressed than in MDPs from *C5ar1*$^{-/-}$ mice (**Fig. 3.11A**).

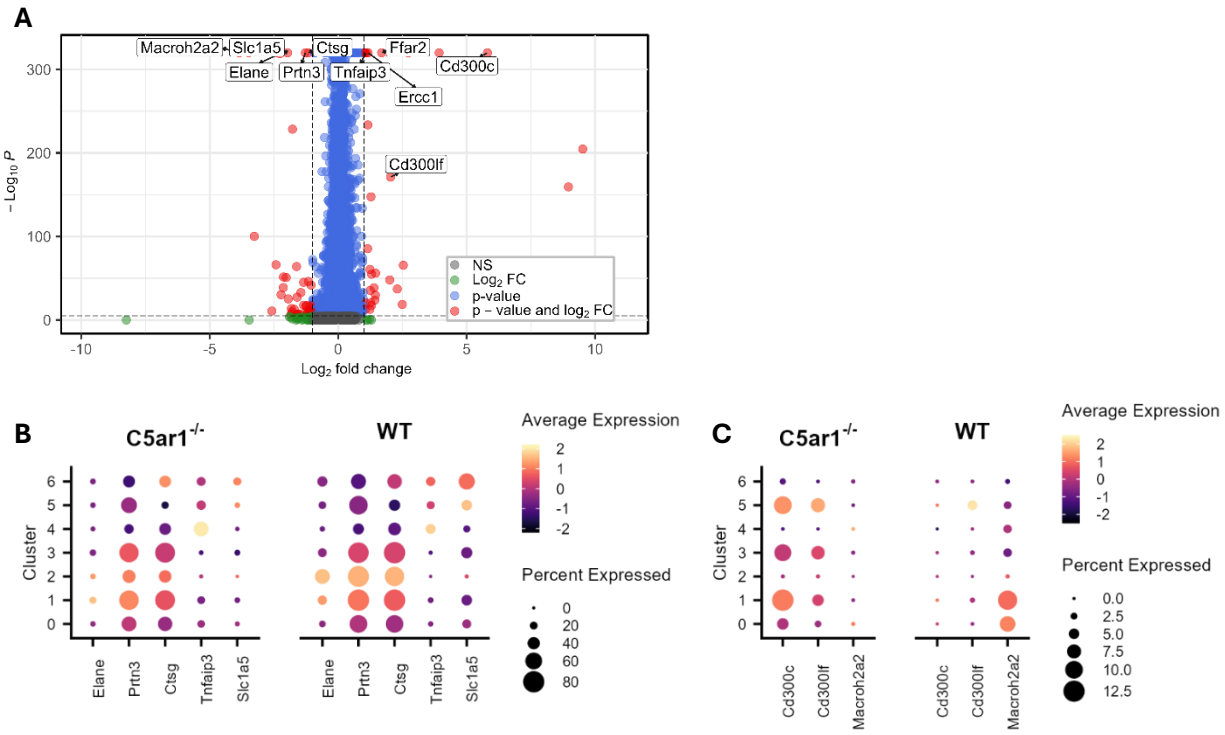


**FIGURE 3.11 Volcano plot depicting differentially expressed genes across all clusters of MDPs from WT and *C5ar1*$^{-/-}$ mice and dot plots showing differentially expressed genes in *C5ar1*$^{-/-}$ vs. WT MDPs**. (**A**) Volcano plot of differentially expressed genes across all clusters from *C5ar1*$^{-/-}$ vs. WT MDPs. The volcano plot was prepared after regressing out the gender and batch cofactors. Red dots on the right part of the x axis represent genes expressed higher in MDPs from *C5ar1*$^{-/-}$ mice; red dots on the left part of the x axis depict genes with higher expression levels in WT MDPs. Y-axis denotes $-\log_{10}$ P values, while X-axis shows $\log_2$-fold change values. (**B,C**). Dot plot depicting the average expression levels of differentially expressed genes in up to 80% (B) or 12.5% (C) of MDP clusters from WT or *C5ar1*$^{-/-}$ mice.

Importantly, the repression of such genes, which jointly catalyze histone H3 amino terminal proteolytic cleavage (H3DN), is critical for monocyte to macrophage differentiation and might be necessary to skew MDP differentiation toward cDC[525]. The difference in NSP expression between WT and *C5ar1*$^{-/-}$ MDPs mainly applies to cluster 2, while the other clusters show as similar expression pattern (**Fig. 3.11B, left panel**). Further, the gene encoding for the histone variant macroH2A2 (*Macroh2a2*), was stronger expressed in 10% of cells from cluster 0 and 12.5% of cells from cluster 1 of WT MDP (**Fig. 3.11A, B right panel**). *Macroh2a2* has been associated with the differentiation potency of pluripotent stem cells[526]. *Slc1a5,* which is frequently found in clusters 0, 1, 2, 3, 5 and 6, is a sodium-dependent transporter located on the cell surface that mediates the uptake of neutral amino acids, such as glutamine, which is important for cell metabolisms, protein biosynthesis and energy production[527,528] (**Fig. 3.12**).

In contrast, *Tnfalp3, Cd300c, Cd300lf, Ffar2* and *Ercc1* were much higher expressed in some clusters of MDPs from *C5ar1*$^{-/-}$ compared to WT mice (**Fig. 3.11**). *Ercc1,* which is frequently found in clusters 1, 3 and 6 plays an important role in proliferating early hematopoietic progenitors[529] while *Tnfalp3,* mainly expressed in cluster 4, is one of the crucial negative regulators of NF-κB activation in myeloid cells and DCs, and was shown to control DC activation[530]. The gene encoding the free fatty acid receptor 2 (FFAR2) is preferentially expressed in clusters 3 and 5. It determines several immune functions of cDCs[531] (**Fig. 3.12**).

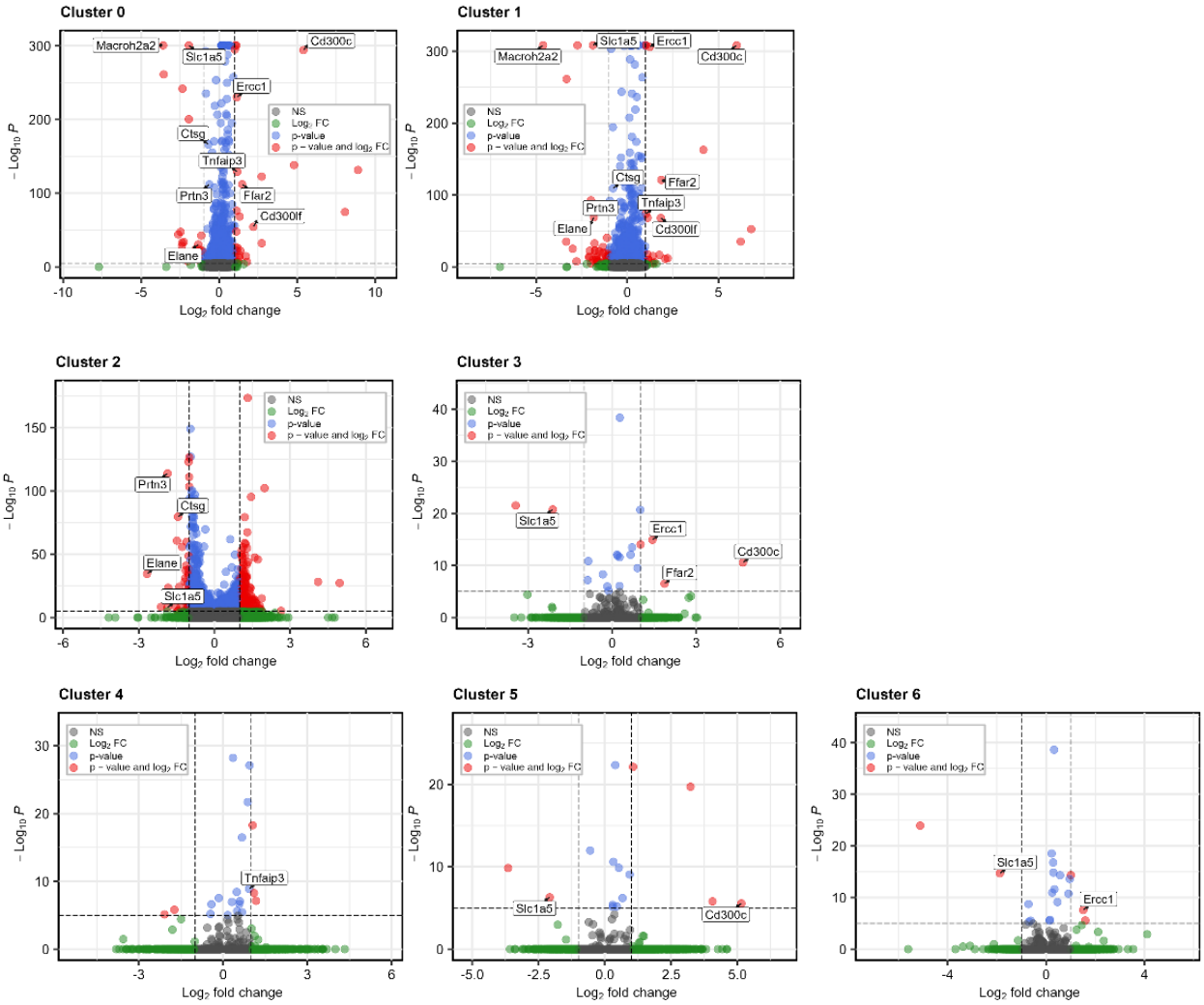


**FIGURE 3.12 Volcano plots depicting differentially expressed genes in clusters 0-6 from MDPs of WT and *C5ar1*$^{-/-}$ mice.** Volcano plots were prepared after regressing out the gender and batch cofactors. Red dots on the right part of the x axis represent genes expressed at higher levels in MDP from *C5ar1*$^{-/-}$ mice while red dots on the left part of the x axis represent genes with higher expression levels in MDP from WT mice. Y-axis denotes $-\log_{10} P$ values while X-axis shows $\log_2$-fold change values.

*Cd300c* was expressed in clusters 0, 1, 3 and 5 (**Fig. 3.11C, right panel, Fig. 3.12**) of MDPs from *C5ar1*$^{-/-}$ but not from WT mice. Importantly, a CD300c fate mapper mouse recently identified a cDC2 progenitor, comprising lymphoid-derived pDC-like and myeloid-derived pre-cDC2, which converge into transcriptionally uniform cDC2 that are critical for humoral antigen responses[58] (**Fig. 3.3**).

## 3.2 Identification and characterization of CDP- and MDP-derived CD172a$^-$ as well as CD172a$^+$ cDCs from BALB/c mice

### 3.2.1 Combined stimulation with GM-CSF and Flt3L drives preferential generation of CD172a$^-$ cDCs from MDPs and CDPs

In the next set of experiments, I determined the potency of sorted MDPs and CDPs from WT, *C5ar1*$^{-/-}$ and *C3ar1*$^{-/-}$ mice to differentiate into CD172a$^-$ or CD172a$^+$ cDCs. For this purpose, I cultured FACS-sorted CD135$^+$CD117$^+$ MDPs or CD135$^+$CD117$^-$ CDPs in the presence of Flt3L and GM-CSF, as receptors for both growth factors are expressed in the two progenitor populations and are required for cDC differentiation[532]. The CD172a$^-$ and CD172a$^+$ cDC subsets were phenotyped on days 1, 3, 6 and 8 as outlined in **Fig. 3.13**.

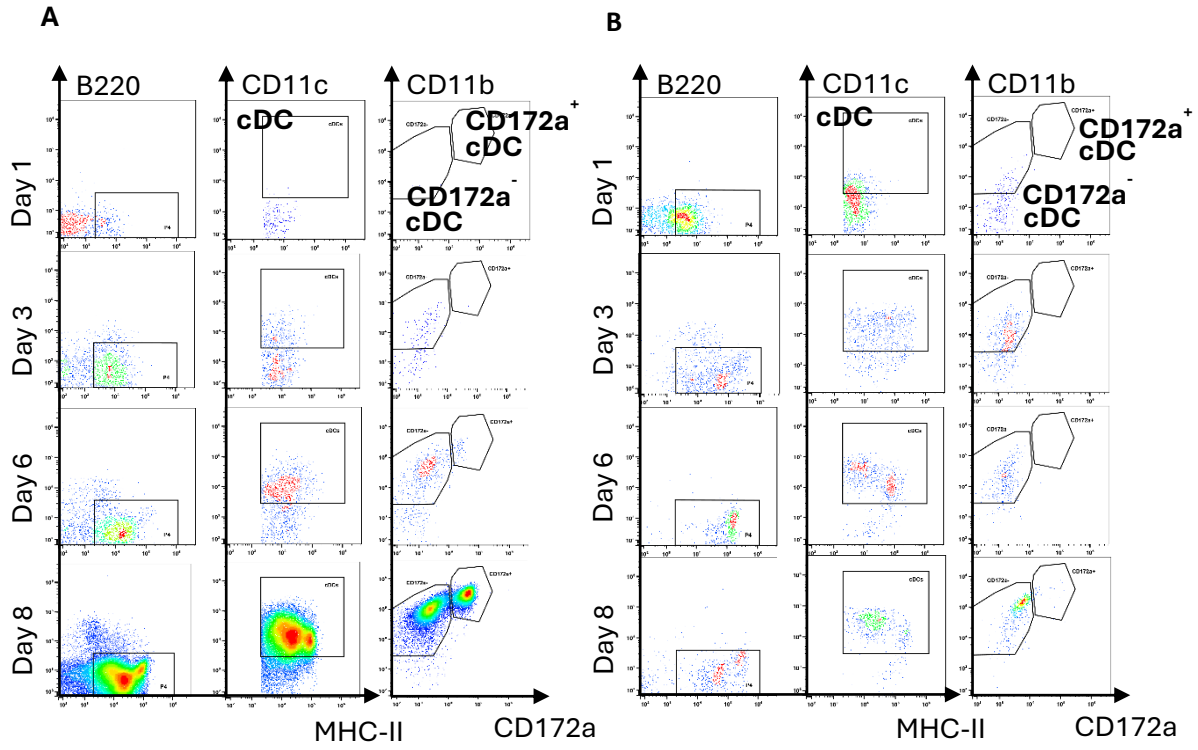


**FIGURE 3.13 Differentiation of MDPs and CDPs into CD172a$^-$ and CD172a$^+$ cDCs in response to GM-CSF and Flt3L stimulation.** (**A, B**) Gating strategy to define CD172a$^-$ and CD172a$^+$ cDCs during differentiation from FACS-sorted MDPs (A) or CDPs (B) at days 1, 3, 6, 8. The CD172a$^-$ cDCs were identified as MHC-II$^{hi}$CD11c$^{hi}$B220$^-$CD11b$^+$CD172a$^-$ cells; CD172a$^+$ cDCs cells were identified as MHC-II$^{hi}$CD11c$^{hi}$B220$^-$CD11b$^+$CD172a$^+$ cells.

GM-CSF/Flt3L stimulation of FACS-sorted MDPs or CDPs from WT, *C3ar1*$^{-/-}$ or *C5ar1*$^{-/-}$ mice resulted in preferential differentiation of MHC-II$^+$CD11c$^+$B220$^-$CD11b$^+$CD172a$^-$ cDCs on day 8 (**Fig. 3.14A**). However, whereas 40% of MDPs differentiated into CD172a$^-$ cDCs and 20% into CD172a$^+$ cDCs, almost 60% of CDPs differentiated into CD172a$^-$ cDCs and less than 10% were CD172a$^-$ cDCs (**Fig. 3.14B, Fig. 3.3**). Also, I

noticed that CDPs differentiated earlier into cDCs than MDPs. Already at day 1, the majority of cells expressed MHC-II and some cells were also CD11c$^+$. In contrast, such MHC-II$^+$CD11c$^+$ cDCs differentiated from MDPs only at day 3 of differentiation (**Fig. 3.13**).

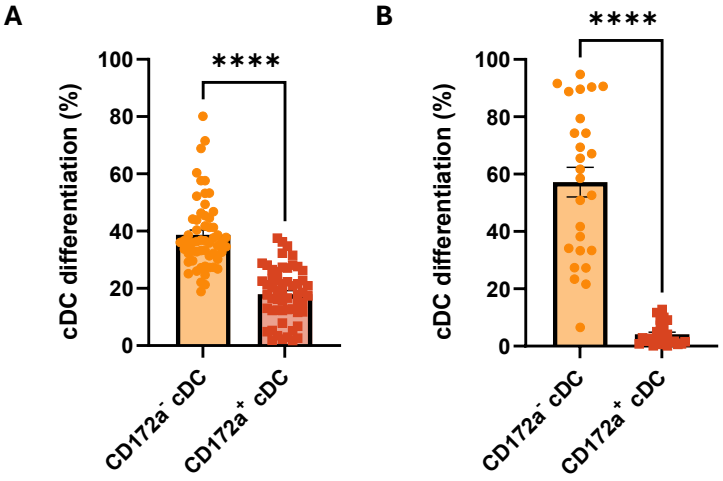


**FIGURE 3.14 CD172a$^-$ and CD172a$^+$ cDC differentiation from MDPs and CDPs after culturing with GM-CSF and Flt3L.** (**A, B**) Frequencies of CD172a$^-$ and CD172a$^+$ cDC differentiated from MDPs (A) or CDPs (B) of WT mice. Frequencies of CD172a$^-$ and CD172a$^+$ cDC refer to all living cells. Data shown are the mean ± SEM, Differences between groups were determined by Mann-Whitney test; ****p<0.0001.

### 3.2.2 Characterization of CD172a$^-$ and CD172a$^+$ cDCs from MDPs after 8 days culture with GM-CSF and Flt3L

To get more insights into the nature of the CD172a$^+$ and CD172a$^-$ cDC subsets, I determined the mRNA expression levels of signature cDC1- and cDC2- and DC3-associated genes (**Fig. 1.5**) by qPCR. Expression of *Id2, Nfil3* and *Klf4* genes were significantly higher in CD172a$^-$ as compared to CD172a$^+$ cDCs. Conversely, *Irf8* and *Irf4* were significantly elevated in CD172a$^+$ compared to CD172a$^-$ cDCs (**Fig. 3.15**). In addition, *Notch2* expression was significantly higher in CD172a$^+$ cDCs from *C5ar1*$^{-/-}$ (**Fig. 3.15B**), but this difference was not observed in CD172a$^+$ cDCs from *tdTomato-C3ar1*$^{fl/fl}$ mice (**Fig. 3.15A**).

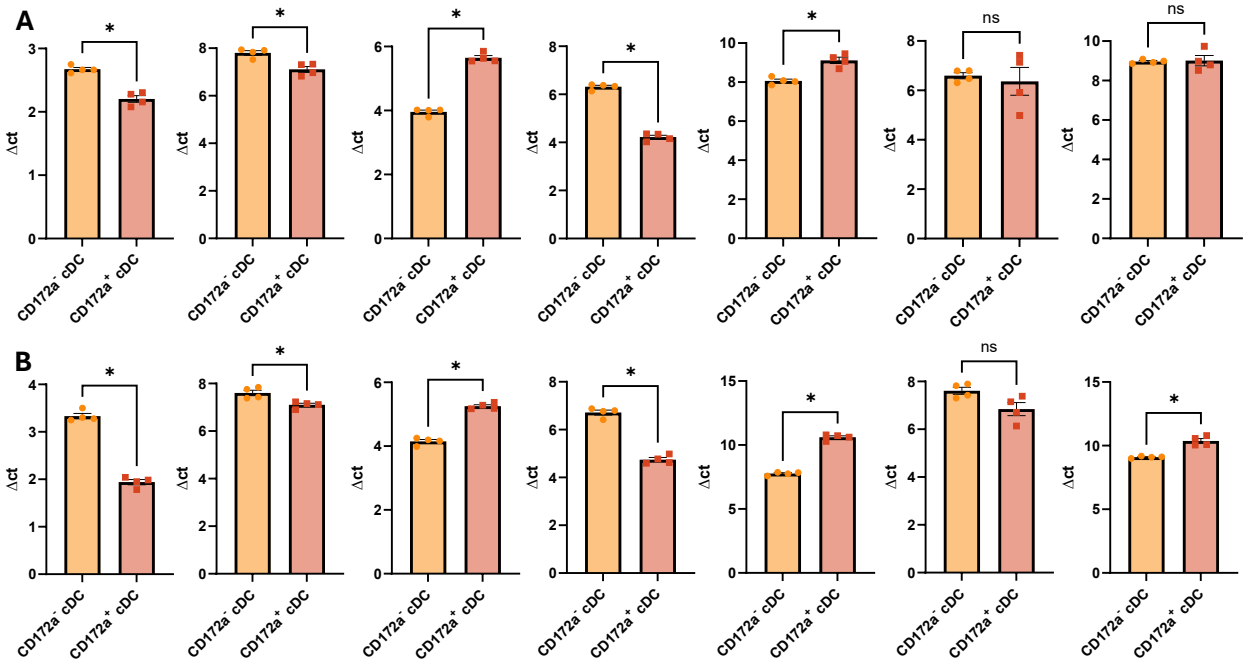


**FIGURE 3.15 Comparison of mRNA expression levels of cDC1, cDC2 and DC3 signature genes in CD172a⁻ and CD172a⁺ cDCs from WT and *C5ar1*$^{-/-}$ mice.** (**A, B**) Expression levels of *Id2, Nfil3, Irf8, Klf4, Irf4, Batf3* and *Notch2* (from left to right) genes in *tdTomato-C3ar1*$^{fl/fl}$ WT (A) and *C5ar1*$^{-/-}$ (B) MDPs after culturing with GM-CSF and Flt3L as assessed by qPCR. The ΔCt value was calculated as the difference between the Ct value of a target gene and the Ct value of a housekeeping gene (*Actb*). Data shown are the mean ± SEM, Differences between groups were determined by Mann-Whitney test; ns: not significant: *p<0.05.

### 3.2.3 The C5a/C5aR1 axis regulates the differentiation of CD172a⁻ or CD172a⁺ cDCs from MDPs and CDPs

In the next set of experiments, I determined the impact of C3aR- or C5aR1-deficiency of sorted MDPs and CDPs to differentiate into CD172a⁻ or CD172a⁺ cDCs. The frequency of MDP-derived cDCs was analyzed starting from day 3, when these cells first began to appear (**Figure 3.13**). The frequency of MDP-derived cDCs steadily increased from 10-20% at day 3 to 60% at day 8, independent of C3aR or C5aR1 expression except a significantly higher frequency of cDCs from MDPs of *C3ar1*$^{-/-}$ mice at day 8 (**Fig. 3.16A**, **Fig. 3.17A**), suggesting that C3aR activation suppressed differentiation from WT MDPs at this time point.

In contrast, already after one day of culture, 30% of WT, 50% of *C3ar1*$^{-/-}$ and 20% of *C5ar1*$^{-/-}$CDPs differentiated into cDCs. This number increased to 70% cDCs from CDPs of WT and *C3ar1*$^{-/-}$ mice and 50% of *C5ar1*$^{-/-}$ mice at day 3 (**Fig. 3.16B, Fig. 3.17B**). At day 6, the frequency of CDP-derived cDCs from WT and *C3ar1*$^{-/-}$mice slightly decreased, whereas it increased to almost 80% with CDPs from *C5ar1*$^{-/-}$ mice. At day 8, the frequency of cDCs differentiated from *C3ar1*$^{-/-}$ or *C5ar1*$^{-/-}$ CDPs reached 80% whereas the frequency of cDCs differentiated from WT CDPs was only at 60% (**Fig. 3.16B**), suggesting that C3aR and C5aR1 activation suppressed CDP-mediated cDC differentiation late in the differentiation process (**Fig. 3.3**). Also, I observed a significantly higher frequency of cDCs that differentiated from CDPs as compared to

MDP in all mouse strains at days 3 and 6. However, at day 8, the frequency of cDCs differentiated from WT MDPs or CDPs were similar, whereas a significantly higher frequency of cDCs differentiated from CDPs as compared with MDPs of *C3ar1*$^{-/-}$ and *C5ar1*$^{-/-}$ mice (**Fig. 3.16C**).

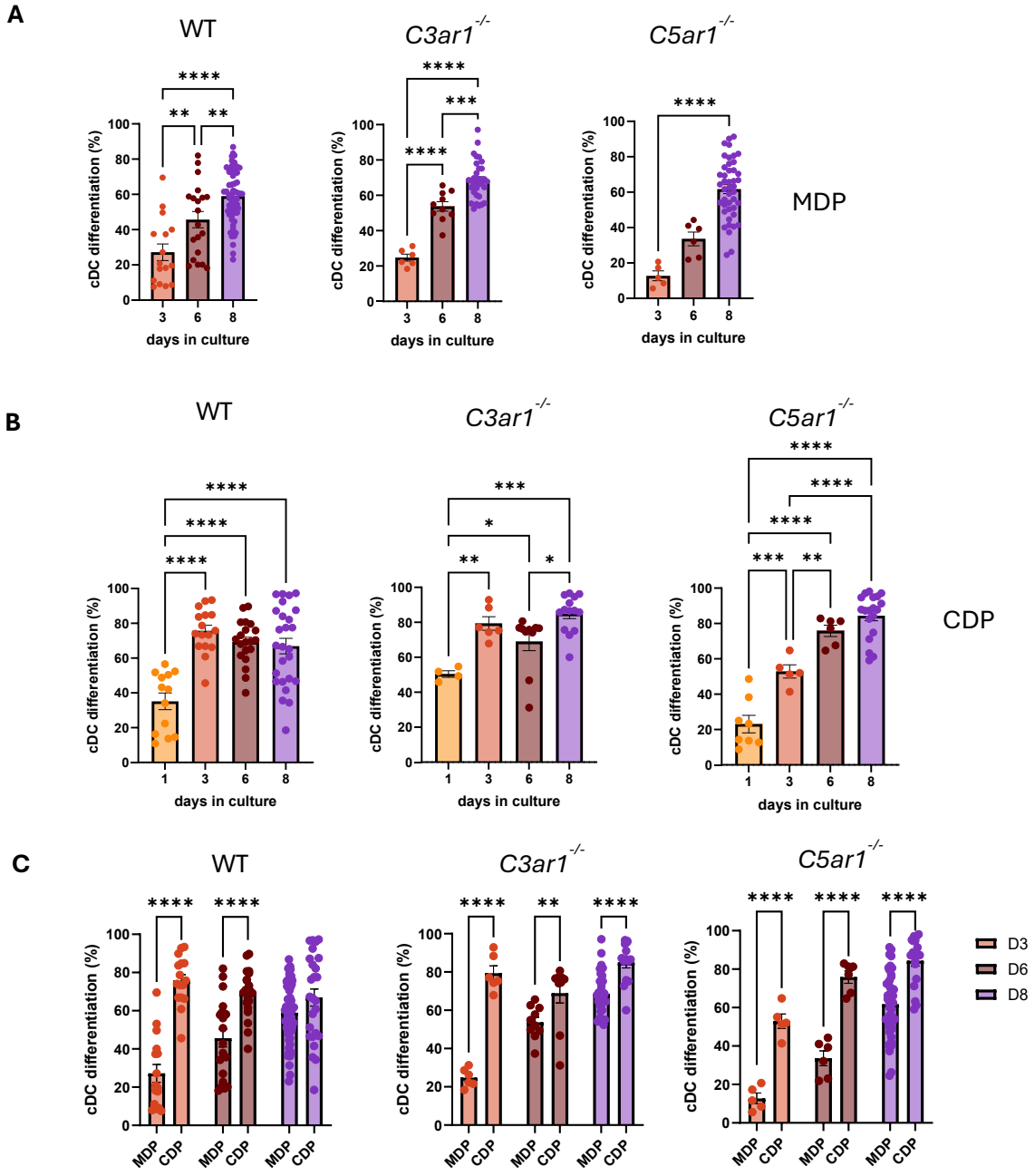


**FIGURE 3.16 Kinetics of cDC differentiation from MDPs and CDPs of WT, *C3ar1*$^{-/-}$ and *C5ar1*$^{-/-}$ mice.** (**A, B**) Frequencies of differentiated cDCs from sorted MDPs (A) and CDPs (B) of WT, *C3ar1*$^{-/-}$, or *C5ar1*$^{-/-}$ (from left to right) mice at days 1, 3, 6 and 8 of differentiation. **C.** Comparison of cDC frequencies from MDPs or CDPs of WT, *C3ar1*$^{-/-}$, or *C5ar1*$^{-/-}$ (from left to right) mice at days 3, 6 and 8 of differentiation. The cDCs were identified as MHC-II$^{hi}$CD11c$^{hi}$B220$^{-}$ cells. Data shown are the mean ± SEM. Differences between groups were determined by One-Way ANOVA with Dunnet (A, B) or Two-Way ANOVA with Šidák (C) posthoc multiple-comparisons test; *p<0.05, **p<0.01, ***p<0.001, ****p<0.0001.

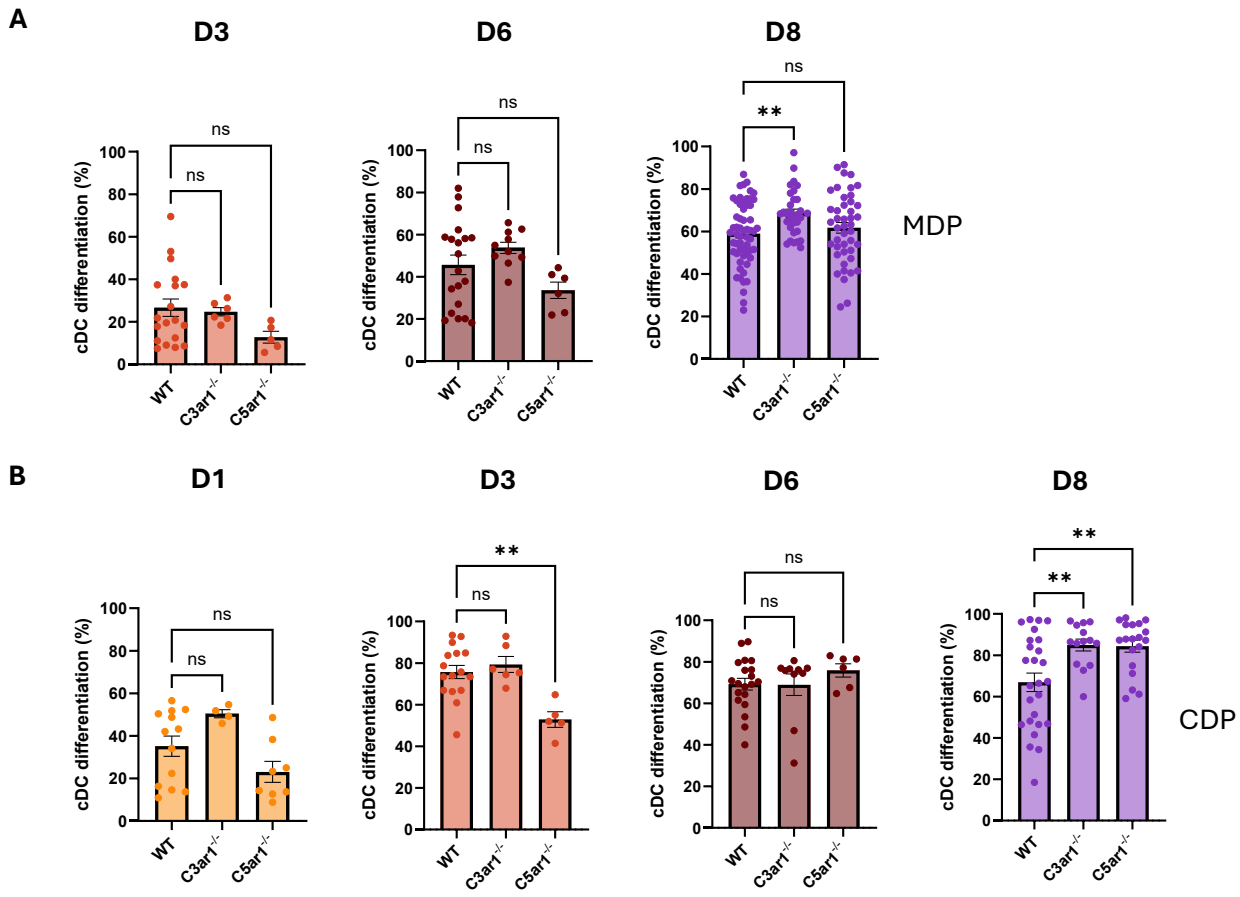


**FIGURE 3.17 Comparison of cDC differentiation from MDPs and CDPs of WT, with that of *C3ar1*$^{-/-}$ and *C5ar1*$^{-/-}$ mice.** (**A, B**) Comparison of cDC frequencies after 1-, 3-, 6- and 8-day differentiation from sorted WT, *C3ar1*$^{-/-}$, and *C5ar1*$^{-/-}$ MDPs (A) or CDPs (B). The cDCs were identified as MHC-II$^{hi}$CD11c$^{hi}$B220$^{-}$ cells. Frequencies of cDC refer to all living cells. Data shown are the mean ± SEM. Differences between groups were determined by One-Way ANOVA with Dunnet posthoc multiple-comparisons test; n.s.: not significant *p<0.05, **p<0.01; D: day.

In the next step I determined the frequencies of MDP-derived CD172a$^{-}$ cDCs from day 3, when these cells first began to appear. The frequency of MDP-derived CD172a$^{-}$ cDCs steadily increased from 5% (*C5ar1*$^{-/-}$) or 15% (WT and *C3ar1*$^{-/-}$) at day 3 to 20% (*C5ar1*$^{-/-}$) or 30-35% (WT or *C3ar1*$^{-/-}$) at day 6 and 40% (WT and *C5ar1*$^{-/-}$) or 45% (*C3ar1*$^{-/-}$) at day 8 (**Fig. 3.18A**). These data point toward a delay in the differentiation of CD172a$^{-}$ cDCs from *C5ar1*$^{-/-}$ MPDs in the differentiation process at days 3 and 6, suggesting that C5aR1 signaling contributes to the early differentiation process of CD172a$^{-}$ cDCs from MDPs. In contrast, the frequency of CD172a$^{-}$ cDCs differentiated from MDPs of *C3ar1*$^{-/-}$ mice at day 8 was significantly higher than that differentiated from WT MDPs, suggesting that C3aR signaling inhibits the differentiation of CD172a$^{-}$ cDCs later in the differentiation process (**Fig. 3.18A, Fig. 3.19A, Fig. 3.3**).

In contrast to the differentiation of CD172a$^{-}$ cDCs from MPDs already after one day of culture, 10% of CDPs from WT and *C3ar1*$^{-/-}$ mice or 7% of CDPs from *C5ar1*$^{-/-}$ mice differentiated to CD172a$^{-}$ cDCs. This number increased to 45% or 38% CD172a$^{-}$ cDCs from CDPs of WT or *C3ar1*$^{-/-}$ mice and 20% of *C5ar1*$^{-/-}$ mice at day 3 (**Fig. 3.18B, Fig.**

**3.19B**). Thus, like the delay of CD172a$^-$ cDC differentiation from *C5ar1*$^{-/-}$ MDPs, I observed a delay in the differentiation of this cDC subsets with CDPs from *C5ar1*$^{-/-}$ mice. At day 6, the frequency of CDP-derived CD172a$^-$ cDC from WT mice remained at the 40% level whereas it increased to 50% CD172a$^-$ cDCs with CDPs from *C3ar1*$^{-/-}$ *and C5ar1*$^{-/-}$ mice. The frequency of CD172a$^-$ cDCs differentiated from WT CDPs slightly increased to 58% on day 8. Of note, the frequency of CD172a$^-$ cDCs differentiated from CDPs of *C3ar1*$^{-/-}$ and *C5ar1*$^{-/-}$mice increased to 80% on day 8 (**Fig. 3.18B**), suggesting that C3aR and C5aR1 activation suppressed CDP-mediated CD172a$^-$ cDC differentiation late in the differentiation process.

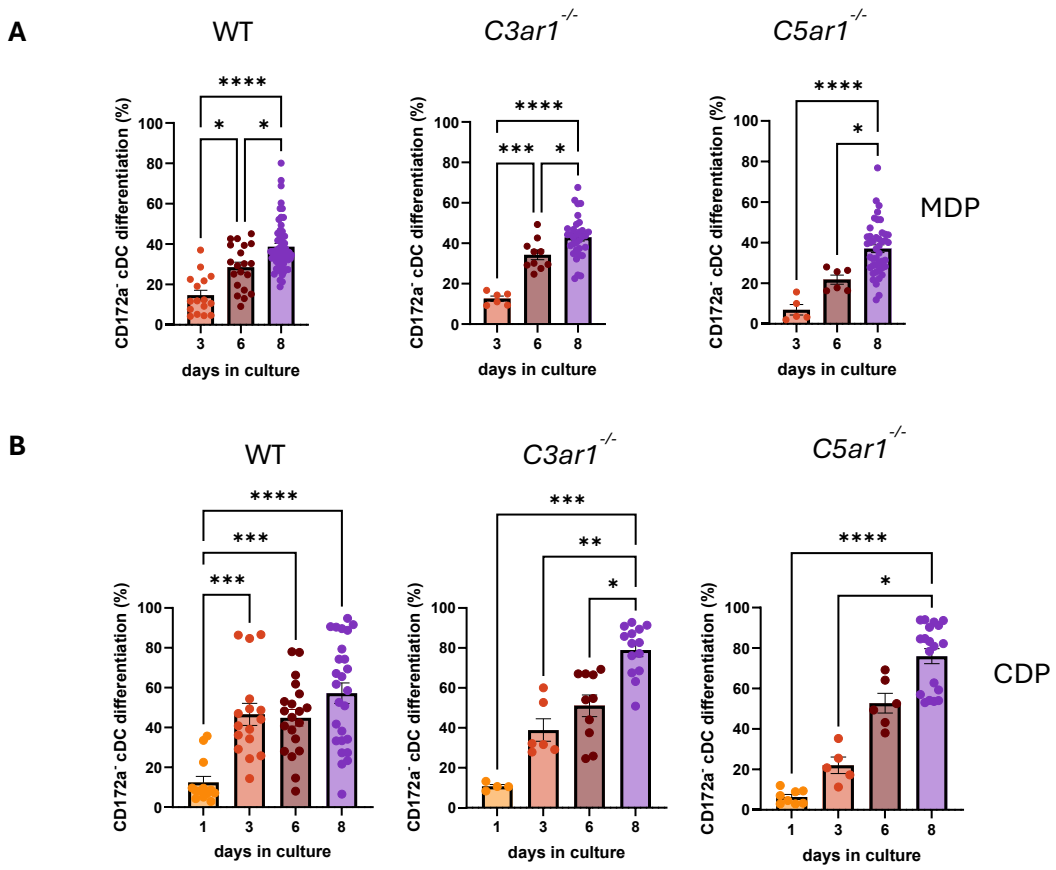


**FIGURE 3.18 Kinetics of CD172a$^-$ cDC differentiation from MDPs and CDPs of WT, *C3ar1*$^{-/-}$ and *C5ar1*$^{-/-}$ mice.** (**A, B**) Frequencies of CD172a$^-$ cDCs from sorted MDPs (A) and CDPs (B) of WT, *C3ar1*$^{-/-}$, or *C5ar1*$^{-/-}$ (from left to right) mice at days 1, 3, 6 and 8 of differentiation. CD172a$^-$ cDC were identified as MHC-II$^{hi}$CD11c$^{hi}$B220$^-$CD11b$^+$CD172a$^-$ cells. Data shown are the mean ± SEM. Differences between groups were determined by Kruskal-Wallis test with Dunn's (A: WT; B: *C3ar1*$^{-/-}$, *C5ar1*$^{-/-}$) or One-Way ANOVA with Dunnet (A: *C3ar1*$^{-/-}$, *C5ar1*$^{-/-}$; B: WT) posthoc multiple-comparison tests.; ns: not significant: *p<0.05, **p<0.01, ***p<0.001, ****p<0.0001.

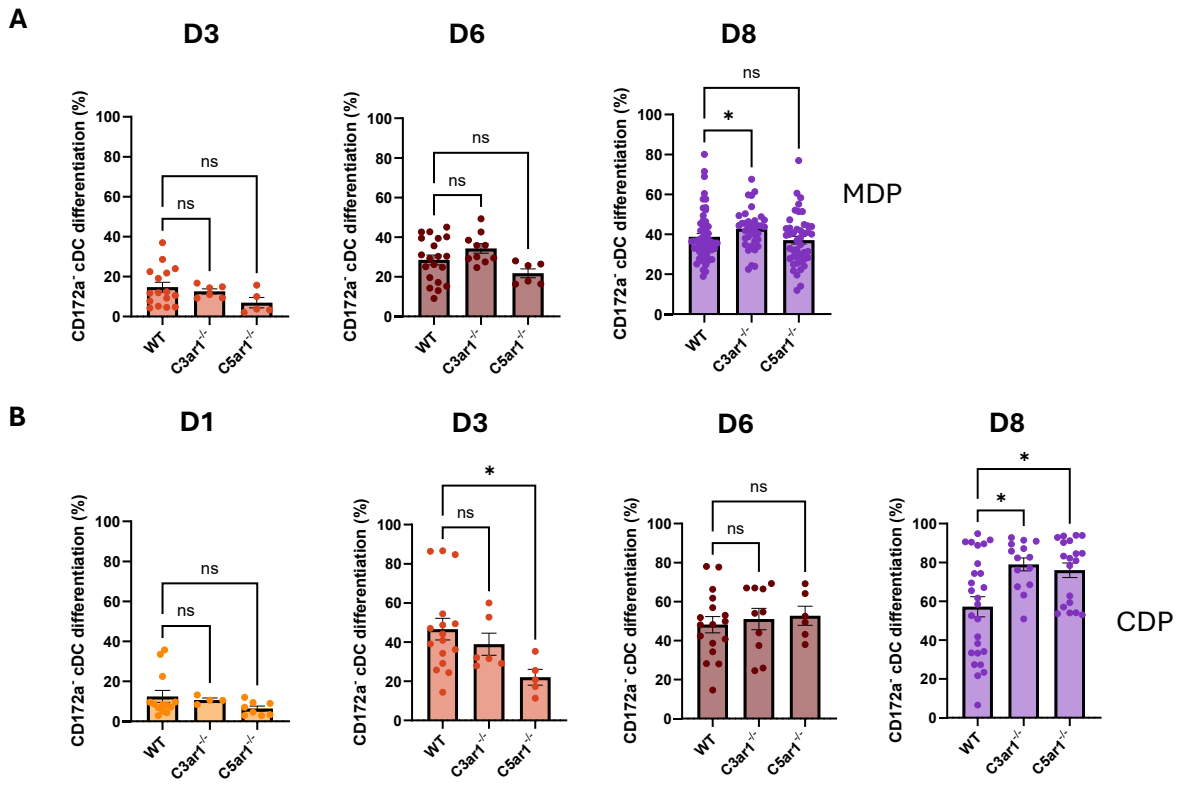


**FIGURE 3.19 Comparison of CD172a⁻ cDC differentiation from MDPs and CDPs of WT, with that of *C3ar1*$^{-/-}$ and *C5ar1*$^{-/-}$ mice.** (**A, B**) Comparison of CD172a⁻ cDC frequencies after 1-, 3-, 6- and 8-day differentiation from sorted WT, *C3ar1*$^{-/-}$, and *C5ar1*$^{-/-}$ MDPs (A) or CDPs (B). CD172a⁻ cDCs were identified as MHC-II$^{hi}$CD11c$^{hi}$B220$^{-}$CD11b$^{+}$CD172a$^{-}$ cells. Frequencies of CD172a⁻ cDCs refer to all living cells. Data shown are the mean ± SEM. Differences between groups were determined by Kruskal-Wallis test with Dunn's (A: D8; B: D1-3, D8) or One-way ANOVA with Dunnett (A: D3-6; B: D6) posthoc multiple-comparisons test; n.s.: not significant *p<0.05; D: day.

Finally, I assessed the impact of C3aR or C5aR1-deficiency on the differentiation of the CD172a⁺ cDC subset from MDPs or CDPs. MDP-derived CD172a⁺ cDCs started to appear at day 3 at a very low frequency and steadily increased to 17% until day 8. Of note, the frequency of *C5ar1*$^{-/-}$ MDP-differentiated CD172a⁺ cDCs at days 3 and 6 was much lower than that differentiated from WT MDPs (5% vs. 1% at day 3 and 14% vs. 7% at day 6) (**Fig. 3.20A, Fig. 3.21A**), suggesting a role for C5aR1 signaling in MDPs during the early differentiation toward CD172a⁺ cDCs. In contrast, the frequency of *C5ar1*$^{-/-}$ MDP-differentiated CD172a⁺ cDCs at day 8 was even significantly higher than that of WT or *C3ar1*$^{-/-}$ MPD-differentiated CD172a⁺ cDCs pointing toward a dual effect of C5aR1 during the differentiation process, i.e. as a driver in the early but an inhibitor at the late phase at day 8 (**Fig.3.3**).

The differentiation of CD172a⁺ cDCs from CDPs of either WT or anaphylatoxin receptor-deficient mice was minor and reached a maximum frequency of 4-5% at day 8, independent of the genetic background of the CDPs. Of note, one and three days after differentiation, I observed higher frequencies of CD172a⁺ cDCs from CDP of *C3ar1*$^{-/-}$ as compared to WT mice, suggesting that C3aR signaling suppresses CDP-derived CD172a⁺ cDC differentiation early in the differentiation process (**Fig. 3.20B, 3.21B, Fig. 3.3**).

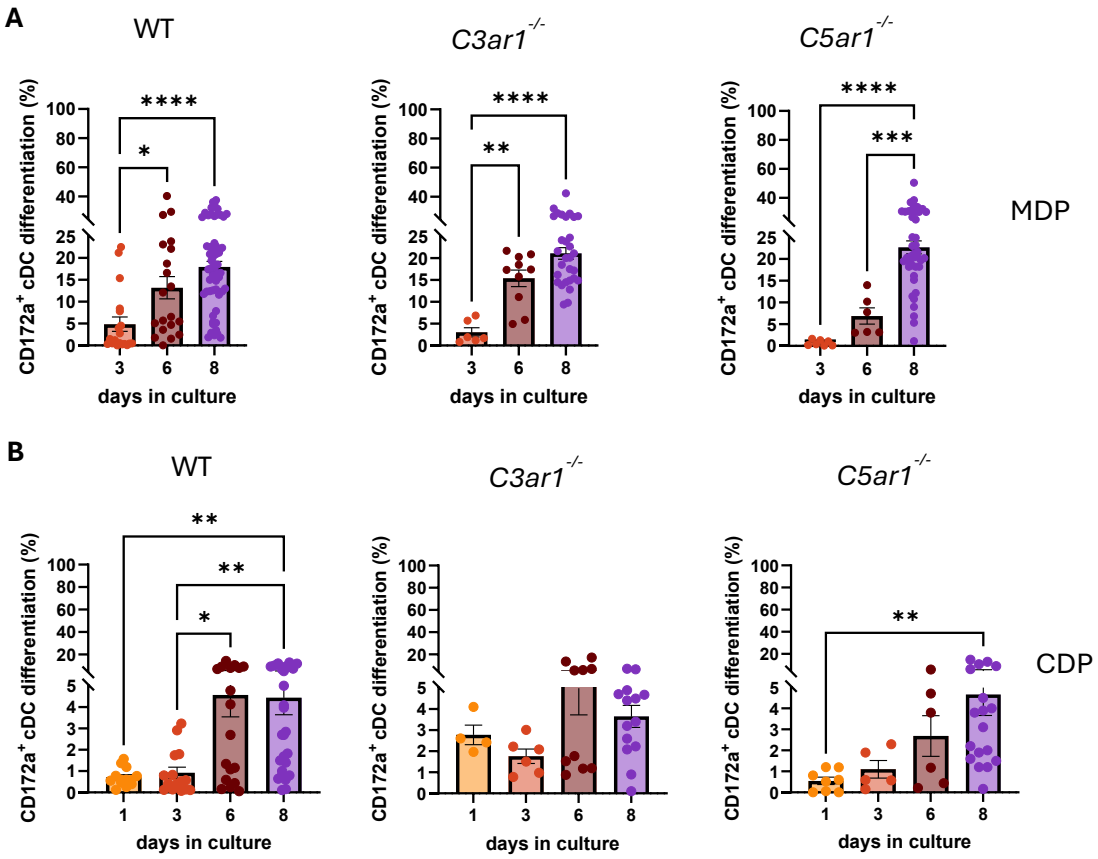


**FIGURE 3.20 Kinetics of CD172a$^+$ cDC differentiation from MDPs and CDPs of WT, *C3ar1*$^{-/-}$ and *C5ar1*$^{-/-}$ mice.** (**A, B**) Frequencies of CD172a$^+$ cDCs from sorted MDPs (A) and CDPs (B) of WT, *C3ar1*$^{-/-}$, or *C5ar1*$^{-/-}$ (from left to right) mice at days 1, 3, 6 and 8 of differentiation. CD172a$^+$ cDC were identified as MHC-II$^{hi}$CD11c$^{hi}$B220$^-$CD11b$^+$CD172a$^+$ cells. Data shown are the mean ± SEM. Differences between group were determined by Kruskal-Wallis test with Dunn's (A: WT; B) or One-Way ANOVA with Dunnet (A: *C3ar1*$^{-/-}$, *C5ar1*$^{-/-}$) posthoc multiple-comparison tests.; ns: not significant: *p<0.05, **p<0.01, ***p<0.001, ****p<0.0001.

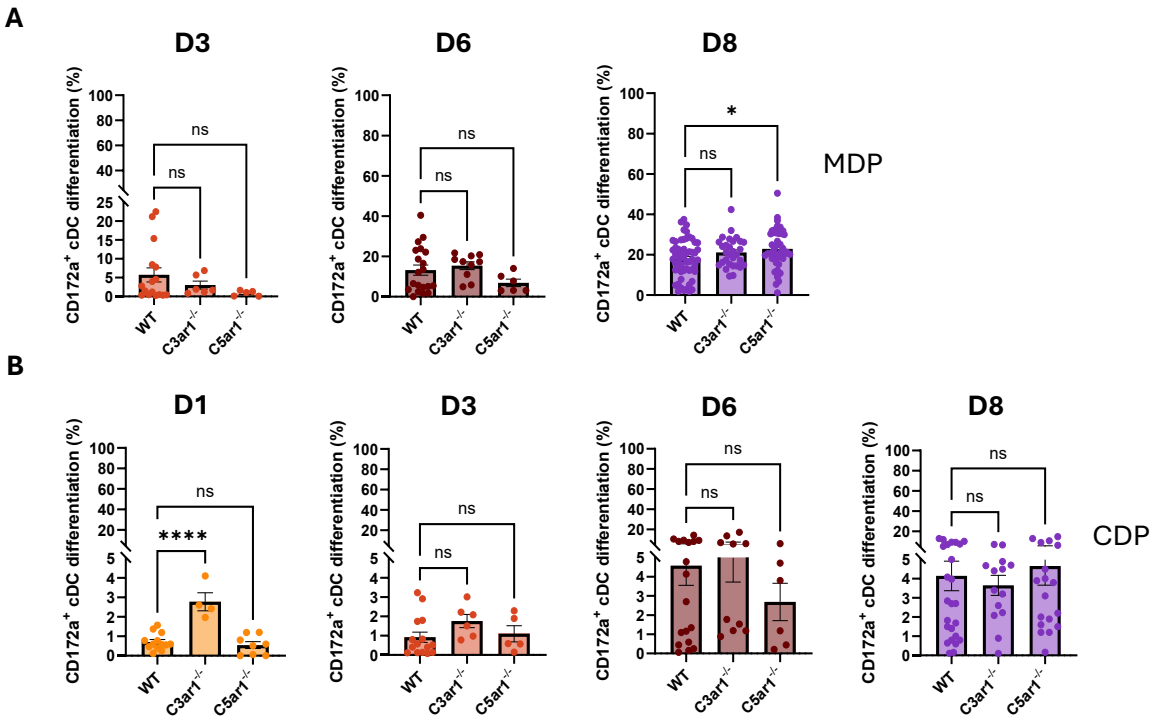


**Figure 3.21 Comparison of CD172a⁺ cDC differentiation from MDPs and CDPs of WT, with that of *C3ar1*$^{-/-}$ and *C5ar1*$^{-/-}$ mice.** (**A, B**) Frequencies of CD172a⁺ cDCs from sorted MDPs (C) and CDPs (D) of WT, *C3ar1*$^{-/-}$, or *C5ar1*$^{-/-}$ (from left to right) mice at days 1, 3, 6 and 8 of differentiation. CD172a⁺ cDCs were identified as MHC-II$^{hi}$CD11c$^{hi}$B220$^{-}$CD11b$^{+}$CD172a$^{+}$ cells. The frequencies of CD172a⁺ cDCs refer to all living cells. Data shown are the mean ± SEM. Differences between groups were determined by Kruskal-Wallis test with Dunn's (A: D3-6; B: D3-8) or One-way ANOVA with Dunnett (A: D8; B: D1) posthoc multiple-comparisons test; *p<0.05, ****p<0.0001, n.s.: not significant; D: day.

Taken together, my findings demonstrate that MDPs and CDPs differentiate preferentially toward the CD172a⁻ cDC subset. CD172a⁻ cDCs differentiate quicker from CDPs than from MDPs (**Fig. 3.22A**), whereas CD172a⁺ cDCs differentiate quicker from MDPs than from CDPs (**Fig. 3.22B**). Further, the potency of MDPs to differentiate into the CD172a⁺ cDC subset is much higher than that of CDPs (**Fig. 3.22B**), whereas the potency of CDPs to differentiate into CD172a⁻ cDCs is much higher than that of MDPs (**Fig. 3.22A**). Of note, *C5ar1*$^{-/-}$ MDPs show only a higher potency to differentiate into CD172a⁺ cDCs at the late day 8 time point (**Fig. 3.3**).

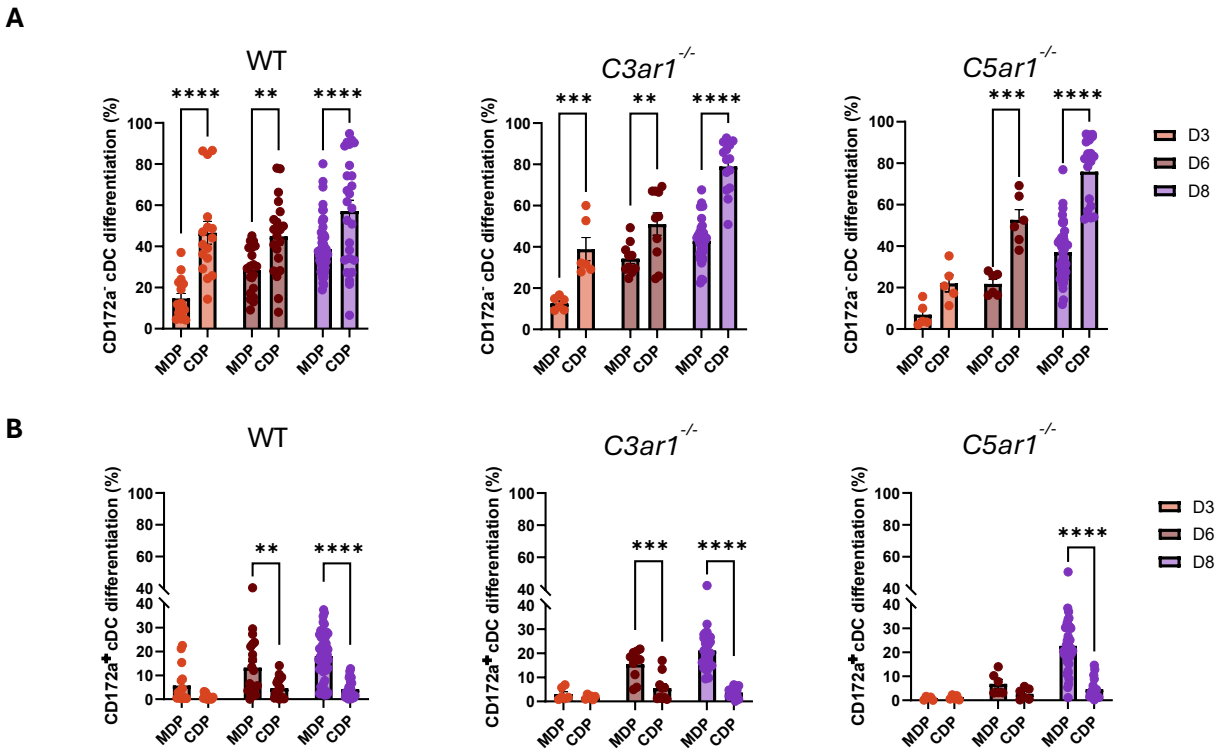


**FIGURE 3.22 Kinetics of CD172a⁻ and CD172a⁺ cDC differentiation from MDPs and CDPs of WT, *C3ar1*$^{-/-}$ and *C5ar1*$^{-/-}$ mice.** (**A, B**) Comparison of CD172a⁻ cDCs (A) or CD172a⁺ cDCs (B) frequencies differentiated from MDPs or CDPs of WT, *C3ar1*$^{-/-}$, or *C5ar1*$^{-/-}$ (from left to right) mice at days 1, 3, 6 and 8 of differentiation. Data shown are the mean ± SEM. Differences between groups were determined by Two-Way ANOVA with Šidák posthoc multiple-comparison test; ns: not significant, **p<0.01, ***p<0.001, ****p<0.0001.

### 3.2.4 Expression of complement factors, anaphylatoxins and anaphylatoxin receptors in CDP- and MDP-differentiated CD172a⁻ or CD172a⁺ cDC subsets

The impact of C3aR- or C5aR1-deficiency on the differentiation of the two CD172a positive and negative cDC subsets from MDPs or CDPs, as outlined above, suggests the induction of an autocrine complement loop activating C3aR and/or C5aR1 during cDC differentiation. First, I determined the expression of C3, C3a and the C3aR as well as C5, C5a and C5aR1 during CD172a⁻ cDC differentiation from CDPs. The majority of CDP-derived CD172a⁻ cDCs (~70%) expressed low levels of C3 but not C3a at day one of differentiation (**Fig. 3.23**). At day 3, the frequency of C3⁺ CD172a⁻ cDC cells decreased to <8% and remained at that low level until day 8, associated with low C3 expression levels (**Fig. 3.23**). In contrast, the frequency of C3a⁺ CD172a⁻ cDCs steadily increased to ~35 % at day 8, which was associated with an increased expression level of C3a until day 6, followed by a sharp decline on day 8. Of note, CD172a⁻ cDCs exclusively expressed C3aR intracellularly. However, the frequency of C3aR⁺ CD172a⁻ cDCs was very low and reached at best ~10% (**Fig. 3.23, 3.25A**). Thus, CD172a⁻ cDCs express C3 during the early phase of differentiation and cleave it into C3a during the differentiation process until day 8. The increasing intracellular expression of C3aR points toward activation of the receptor during the differentiation process (**Fig. 3.23, 3.25A**).

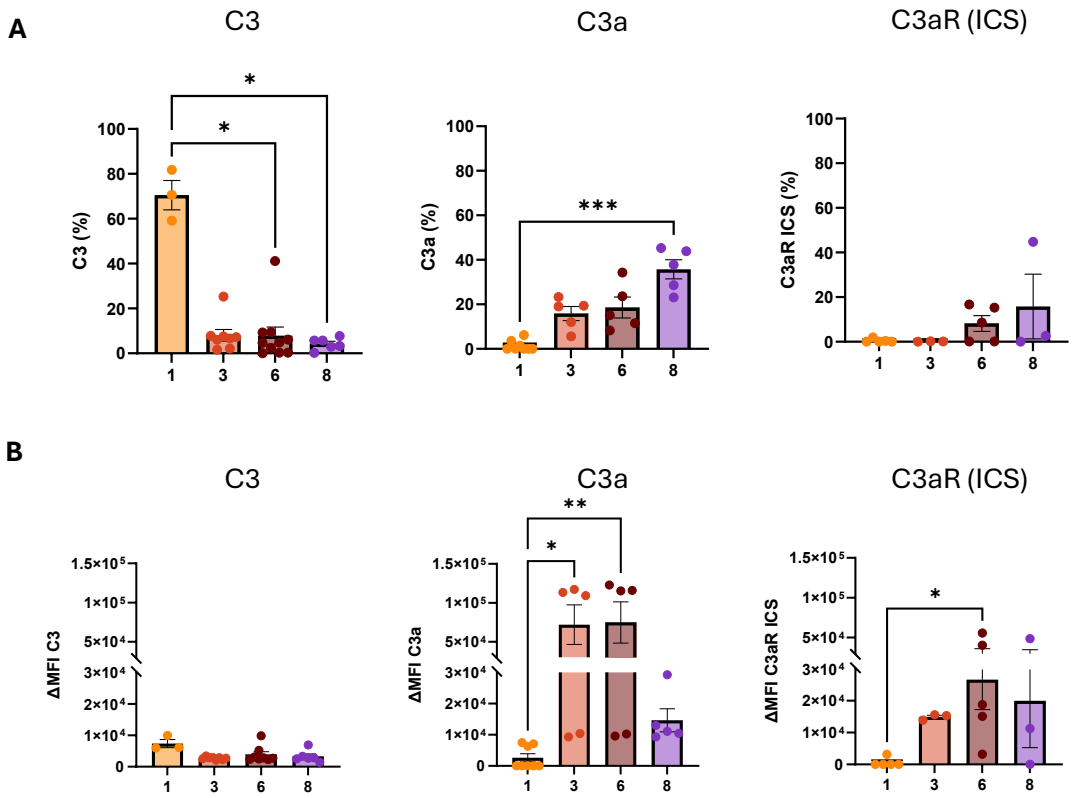


**FIGURE 3.23 Frequencies and expression levels of C3, C3a and C3aR in CD172a⁻ cDCs during 8-day differentiation from CDPs.** (**A, B**) Frequencies (A) and expression levels (B) of C3, C3a or intracellular (ICS) C3aR (from left to right) in CD172a⁻ cDCs at days 1, 3, 6 and 8 of differentiation. The expression levels were determined as MFI normalized to the MFI of the FMO control (ΔMFI). Data shown are the mean ± SEM. Differences between groups were determined by Kruskal-Wallis test with Dunn's posthoc multiple-comparisons test; *p<0.05, **p<0.01, ****p<0.0001.

In sharp contrast, almost all CDP-derived CD172a⁻ cDCs cells already expressed C5 and C5a at day one of differentiation. A high frequency of C5- and C5a-expressing CD172a⁻ cDCs cells was evident during the entire differentiation period until day 8, although it was somewhat lower at day 8. Further, I observed a high frequency of 95-97% CD172a⁻ cDCs cells expressing C5aR1 exclusively intracellularly. The expression levels of C5, C5a and C5aR1 did not change during the differentiation period (**Fig. 3.24, Fig. 3.25**). These data demonstrate CD172a⁻ cDC-autonomous C5 production and C5a generation, which may activate intracellular C5aR1 to control CD172a⁻ cDC differentiation from CDP.

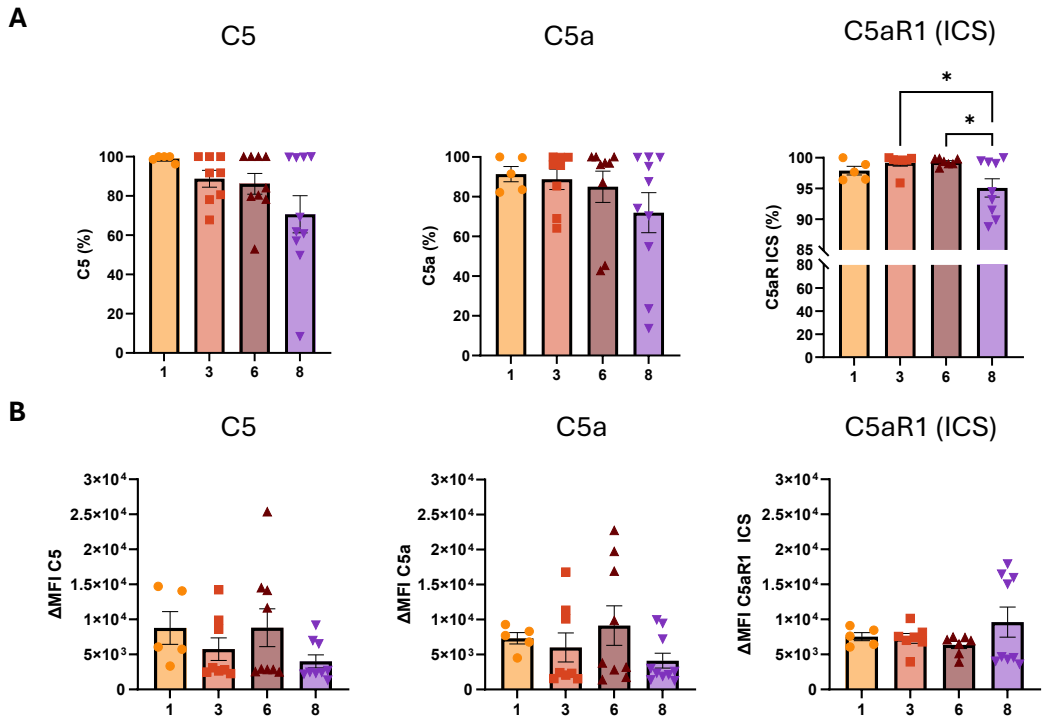


**FIGURE 3.24 Frequencies and expression levels of C5, C5a and C5aR1 in CDP-derived CD172a⁻ cDC during 8-day differentiation.** (**A, B**) Frequencies (A) and expression levels (B) of CD172a⁻ cDC expressing C5, C5a and intracellular (ICS) C5aR1 (from left to right) at days 1, 3, 6 and 8 of differentiation. The expression levels were determined as MFI normalized to the MFI of the FMO control (ΔMFI). Data shown are the mean ± SEM. Differences between groups were determined by Kruskal-Wallis test with Dunn's (A: C5a, B) or One-way ANOVA with Tukey (A: C5, C5aR1) posthoc multiple-comparisons test; *p<0.05.

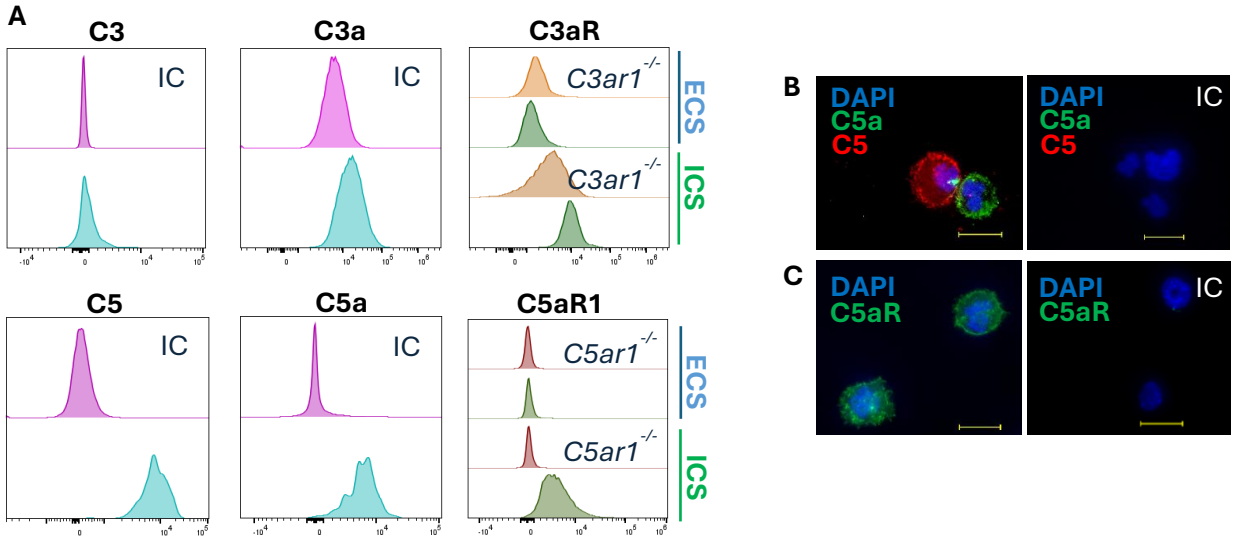


**FIGURE 3.25 Expression of C3, C5, C3a, C5a and their corresponding anaphylatoxin receptors (C3aR and C5aR1) in CDP-derived CD172a⁻ cDCs after 8-day differentiation.** **A**. Histograms showing the expression of C3, C3a, C3aR, C5, C5a and C5aR1 in CDP-derived CD172a⁻ cDCs from WT mice. Cells from *C3ar1*$^{-/-}$ or *C5ar1*$^{-/-}$ mice were used as controls for C3aR and C5aR1 staining; IC: isotype control. (**B, C**). Immunofluorescence staining of C5 and C5a (B) and C5aR1 (C) expression in CD172a⁻ cDCs. IC: isotype control; Scale bars = 20 µm.

As outlined above, I found no CD172a$^-$ cDC differentiated from MDPs at day one of differentiation (**Fig. 3.13**). Ater 3 days of differentiation, I observed that almost 20% of CD172a$^-$ cDCs expressed C3. During the next 3-5 days, the frequency of C3-expressing CD172a$^-$ cDCs increased to 25-30% (**Fig. 3.26A; Fig. 3.28A, B**). The expression level of C3 did not change during the differentiation process (**Fig. 3.26C**). Only a very low fraction (2%) of CD172a$^-$ cDCs expressed C3a at day 3, which increased to almost 10% at day 8 with a similar expression level. As for CDP-differentiated CD172a$^-$ cDC, I found C3aR expression in MDP-differentiated CD172a$^-$ cDC exclusively intracellularly in a very small fraction of cells at a low expression level (**Fig. 3.26A, C; 3.28A, B**).

A different picture emerged regarding C5, C5a and C5aR1 expression. At day 3 of differentiation, 90% of CD172a$^-$ cDC expressed C5. The frequency of C5$^+$ CD172a$^-$ cDC decreased to 70 % on days 6 and increased again to 80% at day 8. I observed a similar pattern for C5a. Also, most MDP-differentiated CD172a$^-$ cDC expressed C5aR1 intracellularly during the 8 days observation period. However, in contrast to C3aR, around 20% CD172a$^-$ cDC expressed C5aR1 on the cell surface at day 3 and around 38% at day 6 (**Fig. 3.26B, 3.28A, C, D**). While the expression levels of C5 and C5a did not change during the differentiation process, the intracellular C5aR1 expression increased significantly at the end of the CD172a- cDC subset differentiation (**Fig. 3.26D**).

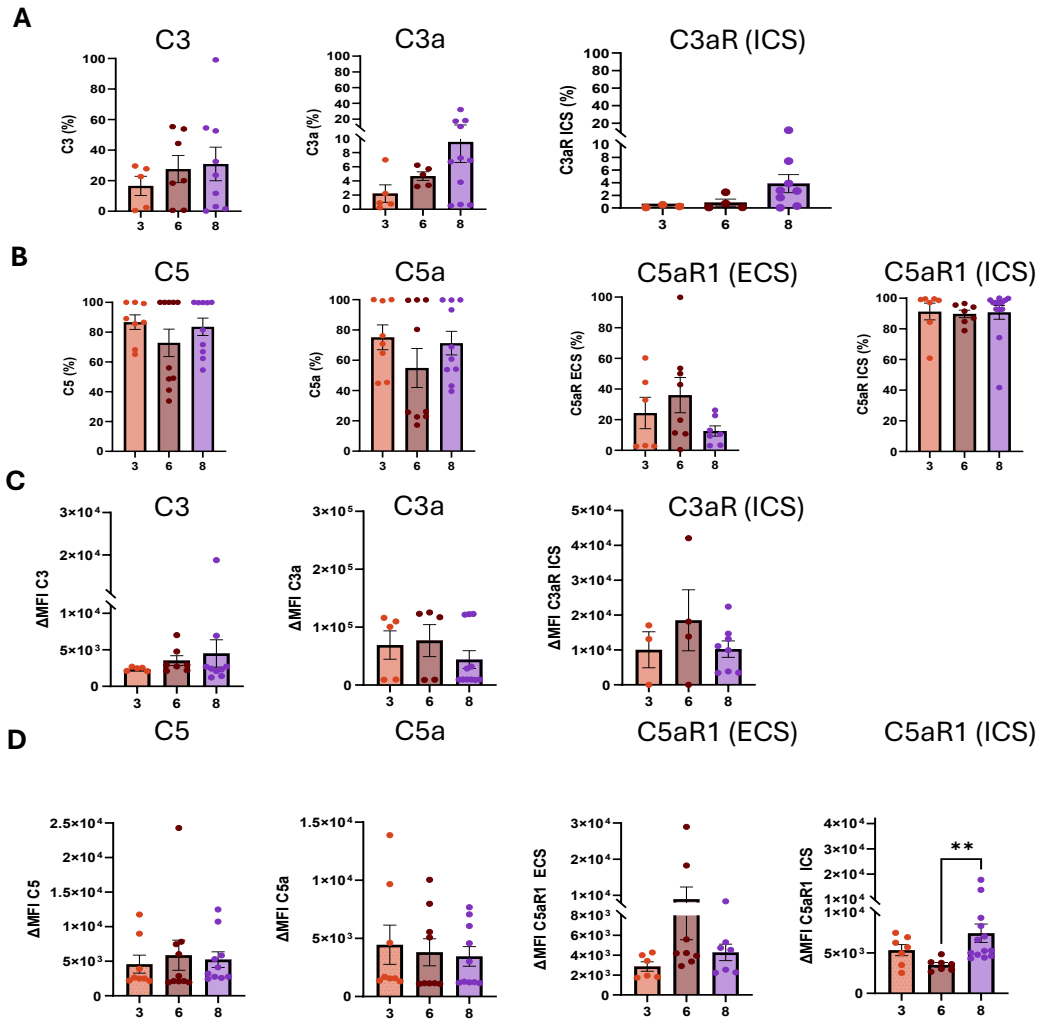

**FIGURE 3.26 Frequencies and expression levels of C3, C3a, C5, C5a and their corresponding receptors in CD172a$^-$ cDCs during 8-day differentiation from MDPs.** (**A, B**) Frequencies of CD172a$^-$ cDCs expressing (A) C3, C3a, intracellular (ICS) C3aR (from left to right) or (B) C5, C5a, extracellular (ECS) and intracellular (ICS) C5aR1 (from left to right) at days 1, 3, 6 and 8 of differentiation. (**C, D**) Expression levels of (C) C3, C3a and intracellular (ICS) C3aR (from left to right) or (D) C5, C5a, extracellular (ECS) and intracellular (ICS) C5aR1 (from left to right) in CD172a$^-$ cDCs at days 1, 3, 6 and 8 of differentiation. The expression levels were determined as MFI normalized to the MFI of the FMO control (ΔMFI). Data shown are the mean ± SEM. Differences between groups were determined by Kruskal-Wallis test with Dunn's (A: C3a, C3aR; B: C5, C5a, C5aR1 (ICS), C-D) or One-way ANOVA with Dunnet (A: C3; B:C5aR1 (ECS)) posthoc multiple-comparisons test; **p<0.01.

Finally, I determined C3/C3a, C5/C5a, C3aR as well as C5aR1 expression in CD172a$^+$ cDCs during differentiation from MDPs. At days 3-8, 20-30% of CD172a$^+$ cDCs expressed C3, whereas only a minor fraction of 4-6% expressed C3a. Only a minor fraction of CD172a$^+$ cDCs expressed intracellular C3aR during the 8-day differentiation (**Fig. 3.26A, 3.28A, E, F**). Of note, the expression levels of C3 was consistently higher in CD172a$^+$ cDC than in CD172a$^-$ cDCss during the differentiation process (**Fig. 3.26C, 3.27C, 3.29A**). From day 6 to 8, the frequency of C5$^+$ CD172a$^+$ cDCs was increasing from 80% to 100% associated with a slight increase in the C5 expression level. Also, the frequency of C5a$^+$ CD172a$^+$ cDCs and the expression level of C5a increased at this time of differentiation (**Fig. 3.27B, D, 3.28A, G, H, 3.29B**). Whereas C5aR1 expression in CD172a$^-$ cDCs was predominantly intracellular, I observed a high frequency (50-70%) of CD172a$^+$ cDCs during days 3-8 of differentiation that strongly expressed C5aR1 on the cell surface (**Fig. 3.27B, D, 3.28A, D, H, 3.29B**). Further, the frequency of CD172a$^+$ cDCs that expressed C5aR1 intracellularly, strongly increased between day 6 and 8 of differentiation and was associated with a strong increase of the C5aR1 expression level (**Fig. 3.27B, D**).

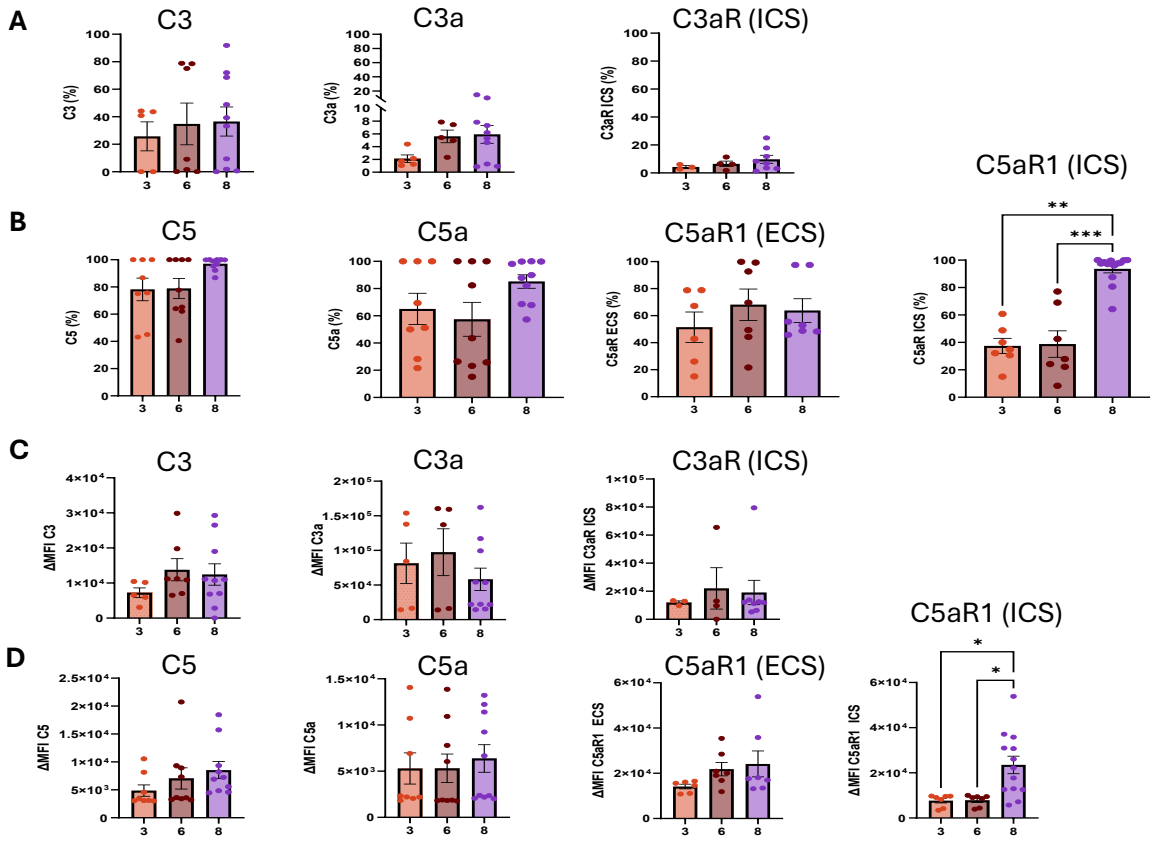


**FIGURE 3.27 Frequencies and expression levels of C3, C3a, C5, C5a and their corresponding receptors in CD172a⁺ cDC after 8-day differentiation from MDPs. (A, B)** Frequencies of CD172a⁺ cDCs expressing (A) C3, C3a, intracellular (ICS) C3aR (from left to right) or (B) C5, C5a, extracellular (ECS) and intracellular (ICS) C5aR1 (from left to right) at days 1, 3, 6 and 8 of differentiation. (**C, D**) Expression levels of (C) C3, C3a and intracellular (ICS) C3aR (from left to right) or (D) C5, C5a, extracellular (ECS) and intracellular (ICS) C5aR1 (from left to right) in CD172a⁺ cDCs at days 1, 3, 6 and 8 of differentiation. The expression levels were determined as MFI normalized to the MFI of the FMO control (ΔMFI). Data shown in are the mean ± SEM. Differences between groups were determined by Kruskal-Wallis test with Dunn's posthoc multiple-comparisons test; *p<0.05, **p<0.01, ***p<0.001.

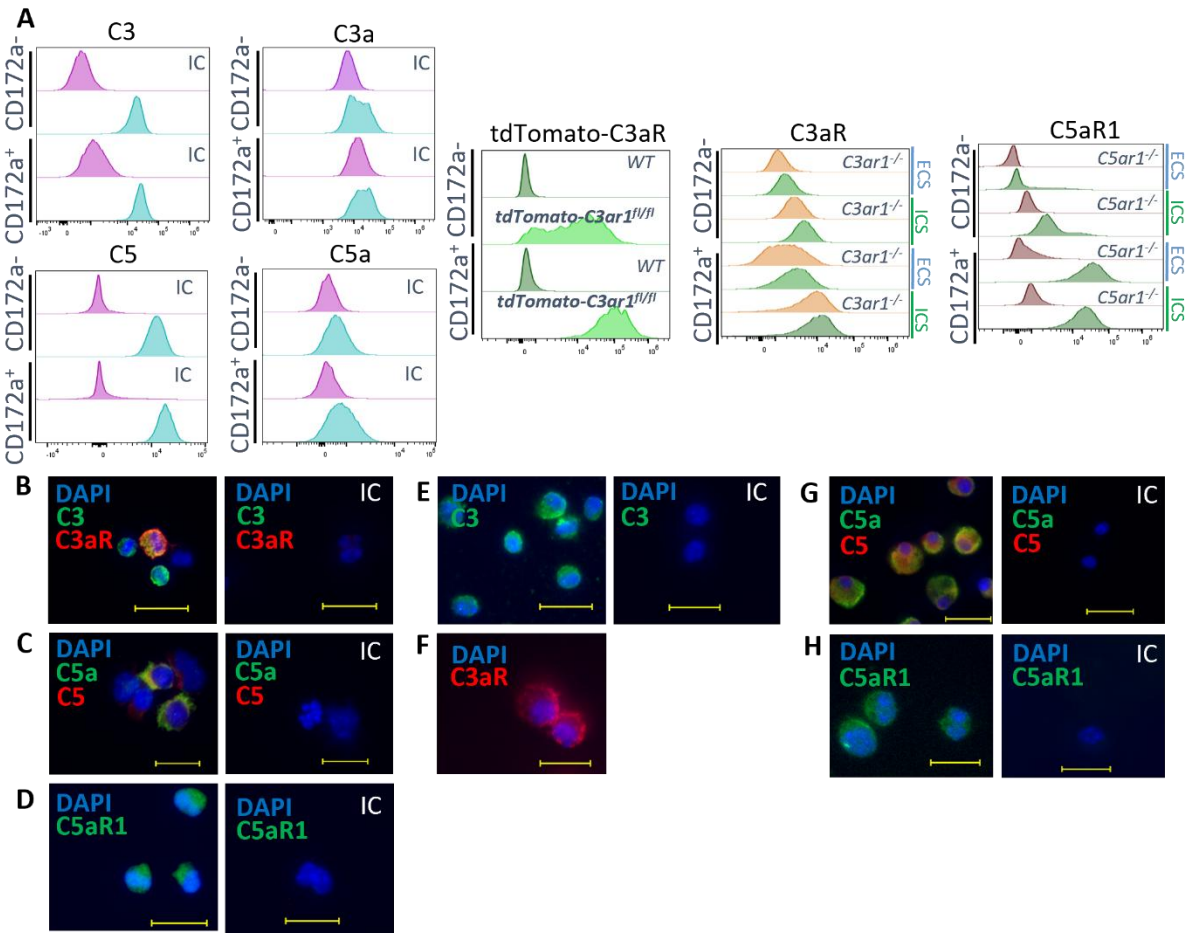


**FIGURE 3.28 Expression of C3, C3a, C5, C5a and their corresponding receptors in CD172a⁻ and CD172a⁺ cDCs after 8-day differentiation from MDPs**. **A**. Histograms showing the expression of C3, C3a, C5, C5a, the tdTomato-C3aR reporter protein, C3aR, and C5aR1 in CD172a⁻ and CD172a⁺ cDCs from WT mice. Extracellular (ECS) and intracellular (ICS) expression of C3aR and C5aR1 was determined. Cells from *C3ar1*$^{-/-}$ or *C5ar1*$^{-/-}$ mice were used as controls for C3aR and C5aR1 staining; IC: isotype control. (**B-H**). Immunofluorescence staining of C3 and C3aR expression (B), C5 and C5a expression (C) as well as C5aR1 expression (D) in CD172a⁻ cDCs; C3 (E), C3aR (F), C5 and C5a (G) as well as C5aR1 expression (H) in CD172a⁺ cDCs. Scale bars = 20 µm. IC: isotype control.

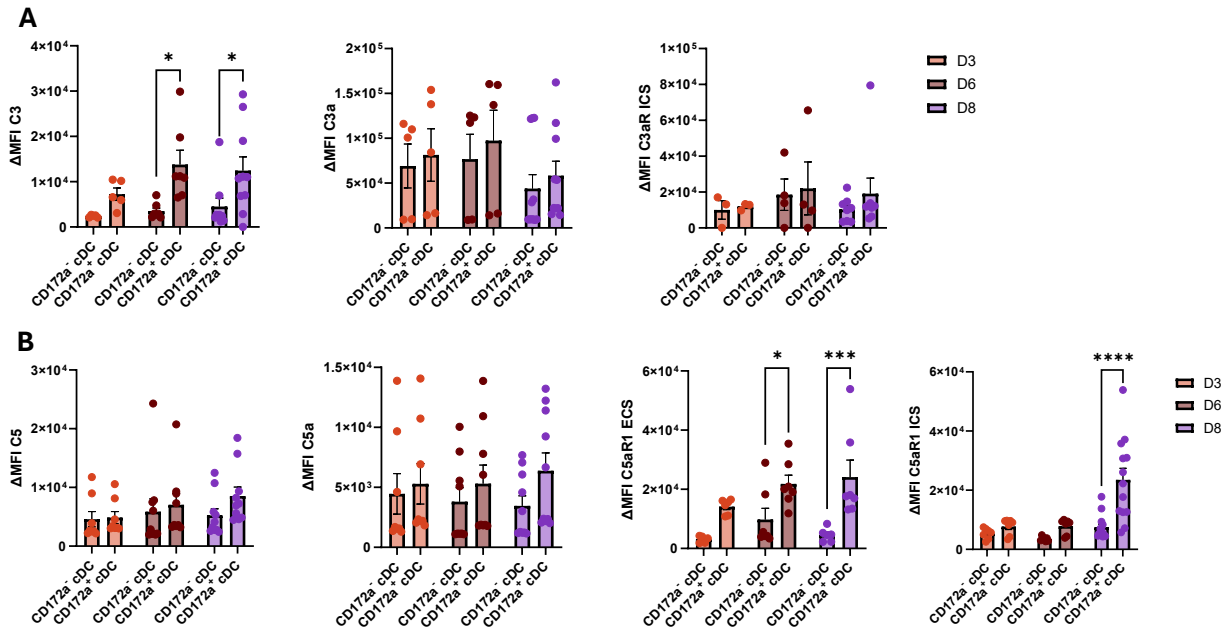


**FIGURE 3.29 Comparison of the expression levels of C3, C5, C3a, C5a and their corresponding receptors in CD172a⁻ and CD172a⁺ cDCs after 8-day differentiation from MDPs**. (**A, B**) Comparison of expression levels of (A) C3, C3a or intracellular (ICS) C3aR (from left to right) and (B) C5, C5a (upper panel, from left to right), extracellular (ECS) or intracellular (ICS) C5aR1 (lower panel, from left to right) between CD172a⁻ and CD172a⁺ cDCs at days 1, 3, 6 and 8 of differentiation. The expression levels were determined as MFI normalized to the MFI of the FMO control (ΔMFI). Data shown are the mean ± SEM. Differences between groups were analyzed by Two-Way ANOVA with Šidák (A: C3, C3a; B: C5, C5a, C5aR1 (ICS)) or Holm-Šidák (A: C3aR (ICS); B: C5aR1 (ECS)) posthoc multiple-comparison test;ns: not significant; *p<0.05, ***p<0.001, ****p<0.0001.

Taken together, I identified autocrine production of C3 and C5 and generation of the respective anaphylatoxins C3a and C5a in CD172a⁻ and CD172a⁺ cDCs during the differentiation from MDPs or CDPs. The frequency of cDC producing C5/C5a was consistently higher than that of C3/C3a. Further, the extracellular C5aR1 expression was consistently higher in CD172a⁺ than in CD172a⁻ cDCs, whereas intracellular C5aR1 expression was higher in CD172a⁺ than in CD172a⁻ cDCs at the end of the differentiation process (**Fig.3.29B**). Thus, the anaphylatoxins may bind to their cognate C3aR and C5aR1 during the differentiation from MDPs or CDPs, which were expressed within CD172a⁻ and CD172a⁺ cDC subsets. During the differentiation process from MDPs, C5a may also bind to extracellular C5aR1 expressed on both cDC subsets.

## 3.3 Functional characterization of MDP-derived CD172a$^-$ and CD172a$^+$ cDCs

### 3.3.1 Impact of ovalbumin stimulation on costimulatory molecule expression in MDP-derived CD172a$^-$ or CD172a$^+$ cDC subsets

The costimulatory molecules CD40, CD80 and CD86 play critical roles in cDC-mediated activation of naïve T cells. Thus, I determined the expression pattern of these costimulatory molecules and of MHC-II in 8 day-differentiated CD172a$^-$ and CD172a$^+$ cDCs from MDPs of WT, *C3ar1*$^{-/-}$ and *C5ar1*$^{-/-}$ mice in response to 24h OVA stimulation. I found that almost all CD172a$^-$ and CD172a$^+$ cDCs from WT mice strongly expressed CD80 (**Fig. 3.30A left panel, 3.30B left panel**).

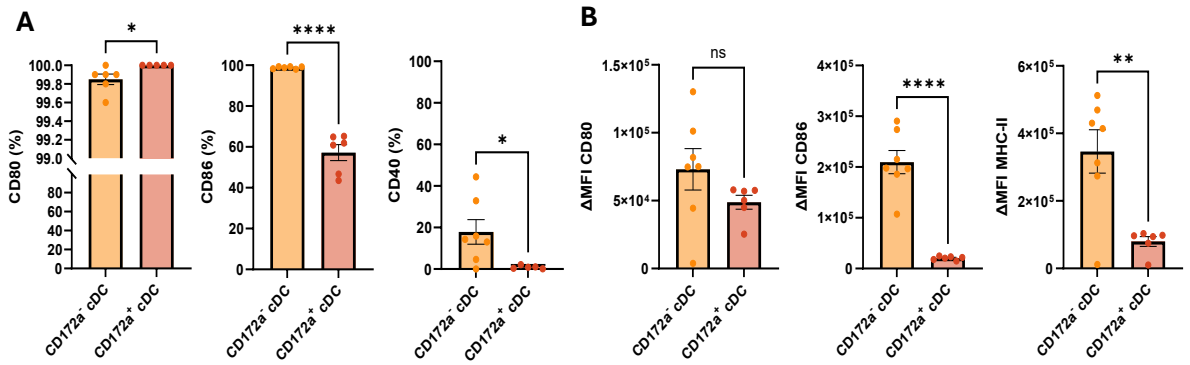


**FIGURE 3.30 Frequencies and expression levels of co-stimulatory molecules and MHC-II in MDP-derived CD172a$^-$ and CD172a$^+$ cDCs from WT mice in response to 24h OVA stimulation**. (**A, B**) Frequencies (A) and expression levels (B) of CD80- (left panel), CD86- (middle panel), CD40- (A, right panel) or MHC-II (B, right panel) in CD172a$^-$ and CD172a$^+$ cDCs differentiated from MDPs of WT mice. Data shown are the mean ± SEM. Differences between groups were determined by unpaired t test; *p<0.05, **p<0.01, ****p<0.0001.

In contrast, I identified a considerably lower frequency of CD86$^+$ CD172a$^+$ cDCs as compared to CD86$^+$CD172a$^-$ cDCs (**Fig. 3.30A, middle panel**), which was associated with much lower CD86 expression levels in CD172a$^+$ cDCs as compared to CD172a$^-$ cDCs (**Fig. 3.30B, middle panel**). In contrast to CD80 and CD86, I found CD40 expression in only ~20% of CD172a$^-$ cDCs and at best in a minor fraction of CD172a$^+$ cDCs (**Fig. 3.30A, right panel**). Based on the gating strategy (**Fig. 2.6**), all CD172a$^-$ and CD172a$^+$ cDCs cells expressed MHC-II, however, the expression level was significantly higher in CD172a$^-$ as compared to CD172a$^+$ cDCs (**Fig. 3.30 B, right panel, Fig. 3.35**).

Similar to what I observed in CD172a$^-$ and CD172a$^+$ cDCs from WT mice, I found a high frequency of CD80$^+$ CD172a$^-$ and CD172a$^+$ cDC in *C3ar1*$^{-/-}$ (**Fig. 3.31A**) and *C5ar1*$^{-/-}$ (**Fig. 3.31B**) mice, with a slightly lower frequency of CD80$^+$ CD172a$^+$ than CD80$^+$ CD172a$^-$ cDCs in *C3ar1*$^{-/-}$ mice.

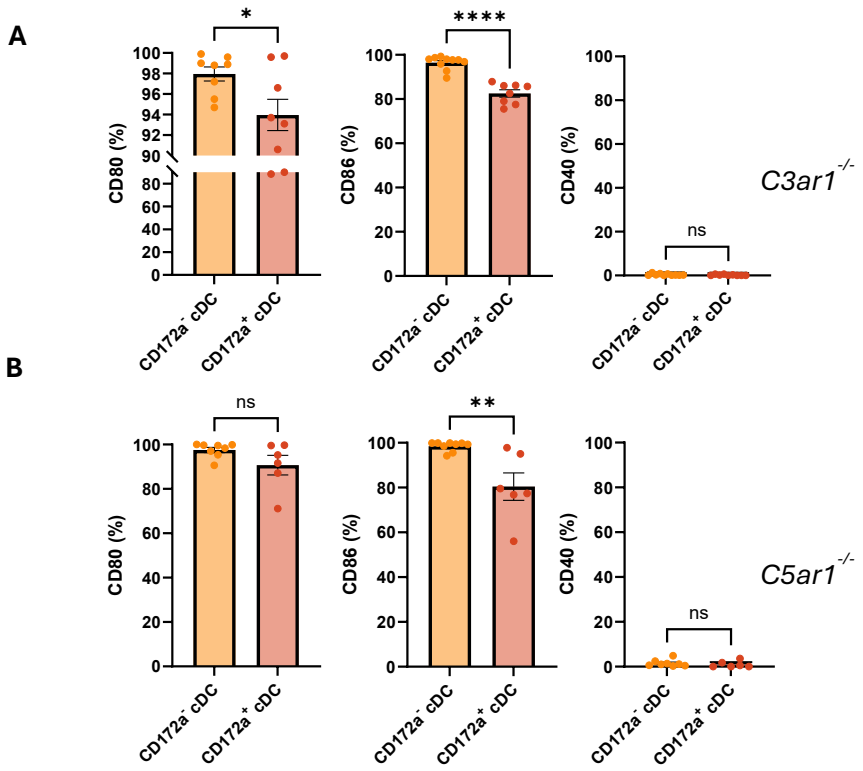


**FIGURE 3.31 Frequencies of MDP-derived CD172a⁻ and CD172a⁺ cDCs from *C3ar1*$^{-/-}$ and *C5ar1*$^{-/-}$ mice expressing CD80, CD86 and CD40 after 24h stimulation with OVA antigen.** (**A, B**) Frequencies of CD80 (left panel), CD86 (middle left panel), and CD40 (right panel) in MDP-derived CD172a⁻ and CD172a⁺ cDCs from (A) *C3ar1*$^{-/-}$ and (B) *C5ar1*$^{-/-}$ mice. The expression levels were determined as MFI normalized to the MFI of the FMO control (ΔMFI). Data shown are the mean ± SEM. Differences between groups were determined by unpaired t test; ns: not significant, *p<0.05, **p<0.01, ****p<0.0001.

Like WT CD172a⁻ cDC, almost all CD172a⁻ cDCs from *C3ar1*$^{-/-}$ or *C5ar1*$^{-/-}$ mice expressed CD86, and the frequency of CD86⁺ CD172a⁺ cDCs was significantly lower (**Fig. 3.31A, B; both middle panels**). In contrast to WT mice, I could hardly detect any CD172a⁻ or CD172a⁺ cDCs from *C3ar1*$^{-/-}$ or *C5ar1*$^{-/-}$ mice expressing CD40 (**Fig. 3.31A, B, both right panels**). The expression levels of CD80 were similar in *C3ar1*$^{-/-}$ and *C5ar1*$^{-/-}$ CD172a⁻ and CD172a⁺ cDCs (**Fig. 3.32A**), whereas the expression levels of CD86 and MHC-II in *C3ar1*$^{-/-}$ and *C5ar1*$^{-/-}$ CD172a⁻ cDCs were significantly higher than in CD172a⁺ cDC **(Fig. 3.32B, C, Fig. 3.35)**.

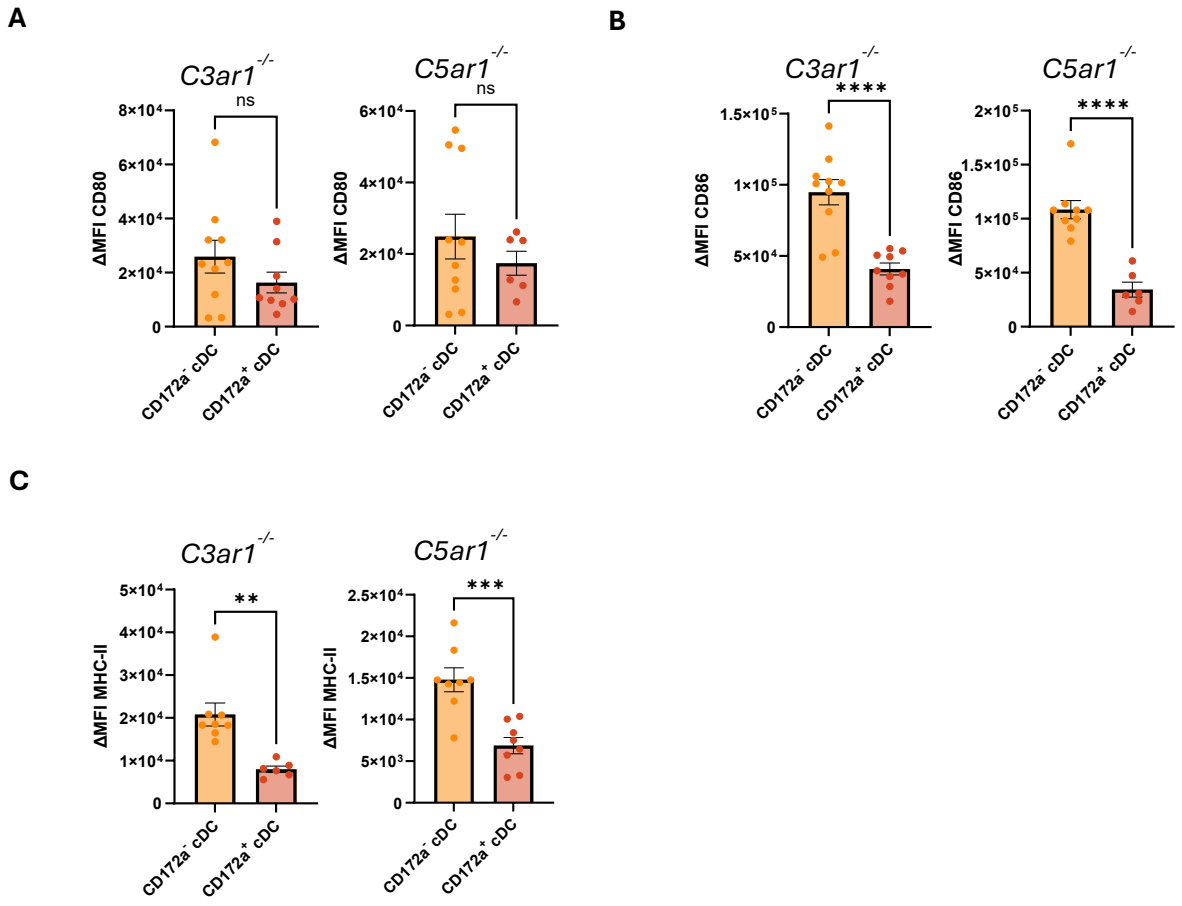


**FIGURE 3.32 Expression levels of costimulatory molecules and MHC-II in MDP-derived CD172a⁻ and CD172a⁺ cDCs from *C3ar1*$^{-/-}$ and *C5ar1*$^{-/-}$ mice after 24h OVA stimulation.** **(A-C)** Comparison of the expression levels of (A) CD80, (B) CD86, and (C) MHC-II in MDP-derived CD172a⁻ cDCs with those of CD172a⁺ cDCs from *C3ar1*$^{-/-}$ (left panel) or *C5ar1*$^{-/-}$ mice (right panel). The expression levels were determined as MFI normalized to the MFI of the FMO control (ΔMFI). Data shown are the mean ± SEM. Differences between groups were determined by unpaired t test; ns: not significant, **p<0.01, ***p<0.001, ****p<0.0001.

In the next step, I compared the frequencies of CD80⁺, CD86⁺ or CD40⁺ CD172a⁻ cDC cells and their expression levels side-by-side in WT, *C3ar1*$^{-/-}$ and *C5ar1*$^{-/-}$ mice. I found a slight reduction in the frequency of CD80⁺ but not of CD86⁺ cells from *C3ar1*$^{-/-}$ and *C5ar1*$^{-/-}$ mice associated with a significant reduction in the expression levels of both molecules when compared with CD172a⁻ cDCs from WT mice (**Fig. 3.33A, B left and middle panels**). The frequency of CD40⁺ CD172a⁻ cDCs from *C3ar1*$^{-/-}$ and *C5ar1*$^{-/-}$ mice was much lower than that from WT mice (**Fig. 3.33A, right panel**). Finally, the MHC-II expression levels in CD172a⁻ cDCs from *C3ar1*$^{-/-}$ and *C5ar1*$^{-/-}$ mice were much lower than those found in WT mice (**Fig. 3.33B, right panel, Fig. 3.35**).

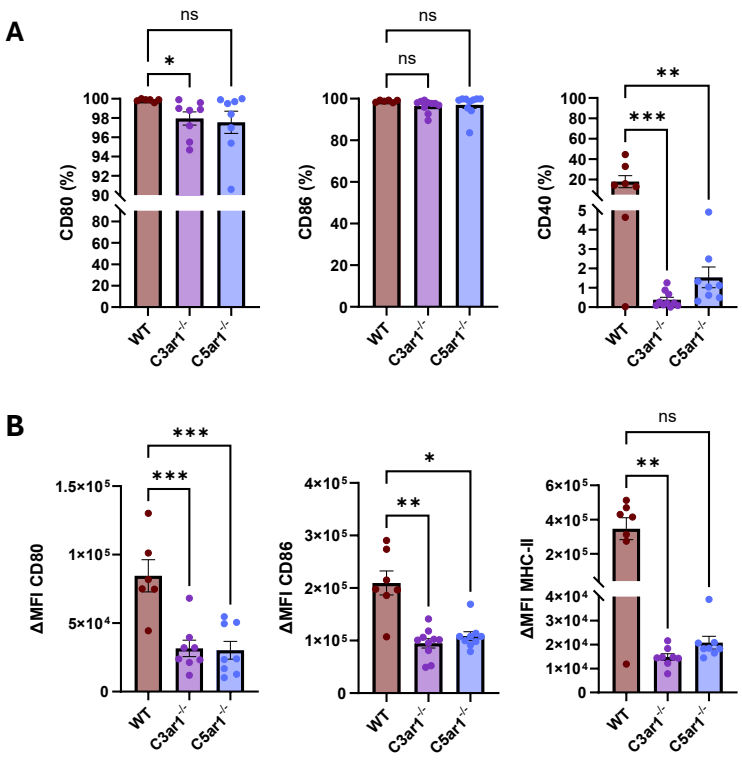


**FIGURE 3.33 Frequencies and expression levels of co-stimulatory molecules and MHC-II in MDP-derived CD172a⁻ cDC from WT, *C3ar1*$^{-/-}$ and *C5ar1*$^{-/-}$ mice in response to 24h OVA stimulation.** (**A, B**) Comparison of the frequencies (A) and expression levels (B) of CD80- (left panel), CD86- (middle panel), CD40- (A, right panel) or MHC-II (B, right panel) in CD172a⁻ cDC derived from MDP of WT, *C3ar1*$^{-/-}$ or *C5ar1*$^{-/-}$ mice. The expression levels were determined as MFI normalized to the MFI of the FMO control (ΔMFI). Data shown are the mean ± SEM. Differences between groups were determined by Kruskal-Wallis test with Dunn's (A: CD80, CD86; B:CD86, CD40) or One-Way ANOVA with Dunnett (A: CD40; B: CD80) posthoc multiple-comparisons test; ns: not significant, *p<0.05, **p<0.01, ***p<0.001.

Like the slight reduction of CD80⁺ CD172a⁻ cDCs, the frequencies of CD80⁺ CD172a⁺ cDCs from *C3ar1*$^{-/-}$ and *C5ar1*$^{-/-}$ mice and their expression levels were reduced in comparison to those from WT mice (**Fig. 3.34A, B; left panel**). In contrast to CD172a⁻ cDCs, I observed higher frequencies and expression levels of CD86⁺ in CD172a⁺ cDCs from *C3ar1*$^{-/-}$ and *C5ar1*$^{-/-}$ mice as compared to those from WT mice (**Fig. 3.34A, B; middle panel**). The frequencies of CD40⁺ CD172a⁺ cDCs were very low in all mouse strains (**Fig. 3.34A; right panel**). As in CD172a⁻ cDCs, the MHC-II expression levels in CD172a⁺ cDCs from WT mice were much higher than in those from *C3ar1*$^{-/-}$ or *C5ar1*$^{-/-}$ mice (**Fig. 3.34B, right panel, Fig. 3.35**).

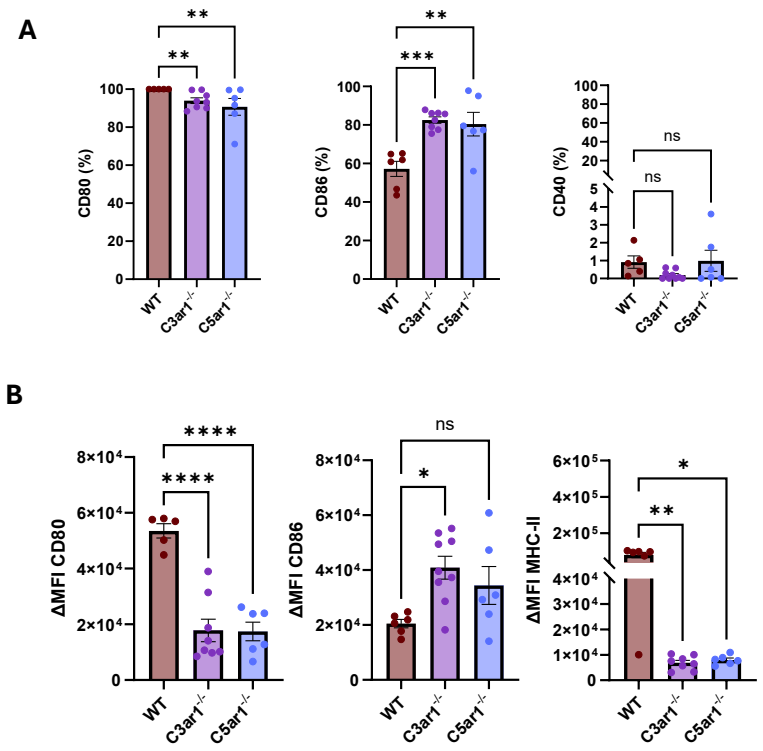


**FIGURE 3.34 Frequencies and expression levels of co-stimulatory molecules and MHC-II in MDP-derived CD172a$^+$ cDCs from WT, *C3ar1*$^{-/-}$ and *C5ar1*$^{-/-}$ mice in response to 24h OVA stimulation.** (**A, B**) Comparison of the frequencies (A) and expression levels (B) of CD80- (left panel), CD86- (middle panel), CD40- (A, right panel) or MHC-II (B, right panel) in CD172a$^+$ cDC cells derived from MDPs of WT, *C3ar1*$^{-/-}$ or *C5ar1*$^{-/-}$ mice. The expression levels were determined as MFI normalized to the MFI of the FMO control (ΔMFI). Data shown are the mean ± SEM. Differences between groups were determined by Kruskal-Wallis test with Dunn's (A: CD80, CD40; B: CD40) or One-Way ANOVA with Dunnett (A: CD86; B: CD80, CD86) posthoc multiple-comparisons test; ns: not significant, *p<0.05, **p<0.01, ***p<0.001, ****p<0.0001.

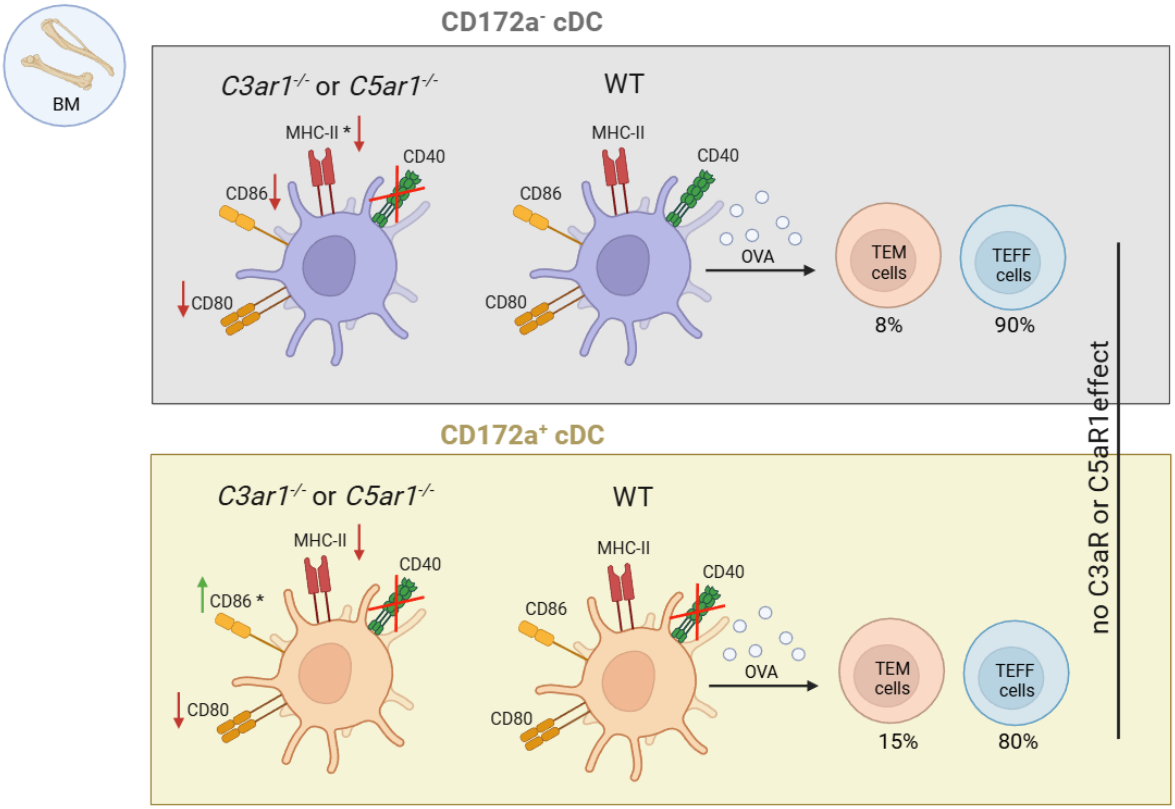


**FIGURE 3.35 Graphic summary of co-stimulatory molecule and MHC-II expression in MDP-derived CD172a$^-$ and CD172a$^+$ cDCs and the resulting cDC-driven TEFF and TEM CD4$^+$ T cell responses.** Arrows indicate the expression levels, i.e. up-upregulation or down-downregulation of the indicated costimulatory molecules or MHC-II; * denotes effects specific to *C3ar1*$^{-/-}$. The figure also shows the potency of CD172a$^-$ and CD172a$^+$ cDCs from WT mice to drive the proliferation of CD4$^+$ TEFF and TEM cells. Frequencies for cDC-driven TEFF and TEM cells were determined using WT mice. Blue circles represent OVA (created with *Biorender.com*).

### 3.3.2 Impact of C3aR and C5aR1 on CD172a$^-$ and CD172a$^+$ cDC-driven effector and effector memory T cell responses

Given the impact of C3aR and C5aR1-deficiency on co-stimulatory molecule and MHC-II expression, I sought to determine the impact of both receptors on CD172a$^-$ and CD172a$^+$ cDC-driven T cell proliferation and differentiation. Co-culture of CD172a$^-$ or CD172a$^+$ cDCs with T cells from OVA TCR tg DO11.10*Rag2*$^{-/-}$ in the presence of OVA for 4 days resulted in the proliferation and differentiation of CD44$^+$CD62L$^-$ TEFF and CD44$^+$CD62$^+$ TEM cells (**Fig. 2.7**). Co-culture of CD172a$^-$ or CD172a$^+$ cDC from WT, *C3ar1*$^{-/-}$ or *C5ar1*$^{-/-}$ mice with OVA TCR tg T cells resulted in vigorous T cell proliferation resulting in ~90% (CD172a$^-$ cDCs) or 75-80% (CD172a$^+$ cDC) of TEFF and ~5-7% (CD172a$^-$ cDC) or 14-18% (CD172a$^+$ cDCs) TEM (**Fig. 3.36A, B, Fig. 3.35**).

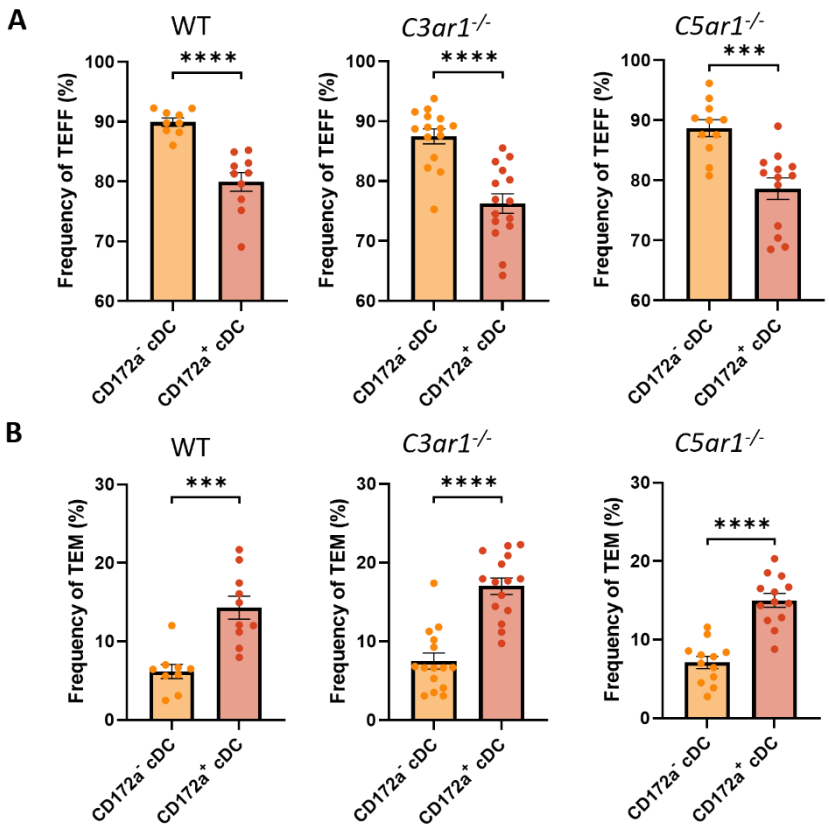


**FIGURE 3.36 Potency of MDP-derived CD172a⁻ and CD172a⁺ cDCs from WT, *C3ar1*$^{-/-}$ or *C5ar1*$^{-/-}$ mice to drive the proliferation of CD4⁺ TEFF and TEM cells**. (**A, B**) Frequencies of proliferated OVA-TCR tg (**A**) TEFF or (**B**) TEM cells in response to co-culture with OVA-pulsed CD172a⁻ or CD172a⁺ cDCs from WT, *C3ar1*$^{-/-}$ or *C5ar1*$^{-/-}$ (from left to right). Data shown are the mean ± SEM. Differences between groups were determined by unpaired t test; outliers were identified; ***p<0.001, ****p<0.0001.

These data demonstrate a higher potency of CD172a⁻ cDCs to drive TEFF cell differentiation from naïve T cells than that of CD172a⁺ cDCs. In contrast, CD172a⁺ cDCs are more potent inducers of TEM cells than CD172a⁻ cDCs. Both, induction of TEFF and TEM cells by CD172a⁻ and CD172a⁺ cDC were independent of C3aR or C5aR1 expression on the two cDC subsets (**Fig. 3.37, Fig. 3.35**).

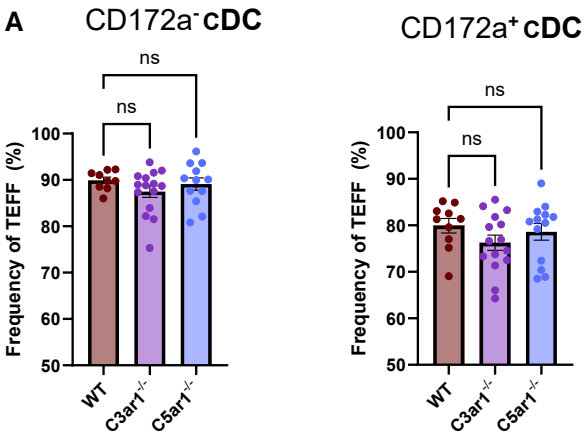

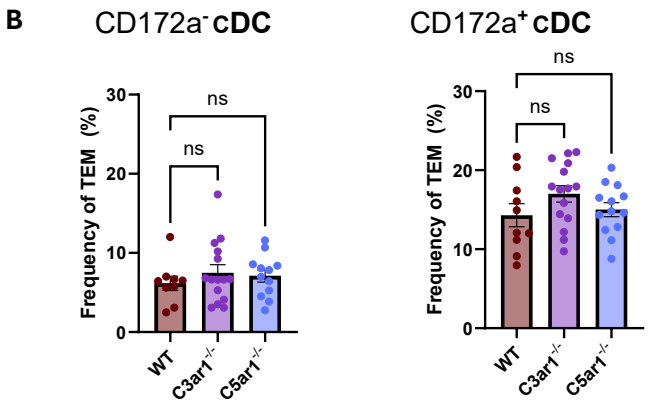


**FIGURE 3.37 Potency of MDP-derived CD172a⁻ and CD172a⁺ cDCs from WT, *C3ar1*$^{-/-}$ and *C5ar1*$^{-/-}$ mice to drive the proliferation of CD4⁺ TEFF or TEM cells in response to OVA stimulation**. (**A, B**) Frequencies of proliferated TEFF (A) or TEM (B) cells in response to OVA-pulsed CD172a⁻ cDCs (left panel) or CD172a⁺ cDCs (right panel) from WT, *C3ar1*$^{-/-}$ or *C5ar1*$^{-/-}$ mice. Data shown are the mean ± SEM. Differences between groups were analyzed by Kruskal-Wallis test with Dunn's (A: CD172a⁻ cDC; B: CD172a⁻ cDC) or One-Way ANOVA with Dunnett (A: CD172a⁺ cDC; B: CD172a⁺ cDC) posthoc multiple-comparisons test; ns: not significant.

A more detailed analysis showed a significantly higher proliferation index of TEM cells induced by CD172a⁺ cDCs from *C3ar1*$^{-/-}$, but not from *C5ar1*$^{-/-}$ mice (**Fig. 3.38A**). Indeed, I found a higher frequency of TEM with 3-5 divisions, when the T cells were activated with C3aR1-deficient CD172a⁺ cDCs. In contrast, WT cDCs induced a higher frequency of TEM cells that divided one or two times. For C5aR1-deficient CD172a⁺ cDCs, I found only a higher frequency of TEM cells that divided three times (**Fig. 3.38B**). The TEFF cell proliferation indices induced by CD172a⁻ or CD172a⁺ cDC from WT, *C3ar1*$^{-/-}$ or *C5ar1*$^{-/-}$ mice were similar (**Fig. 3.38C**).

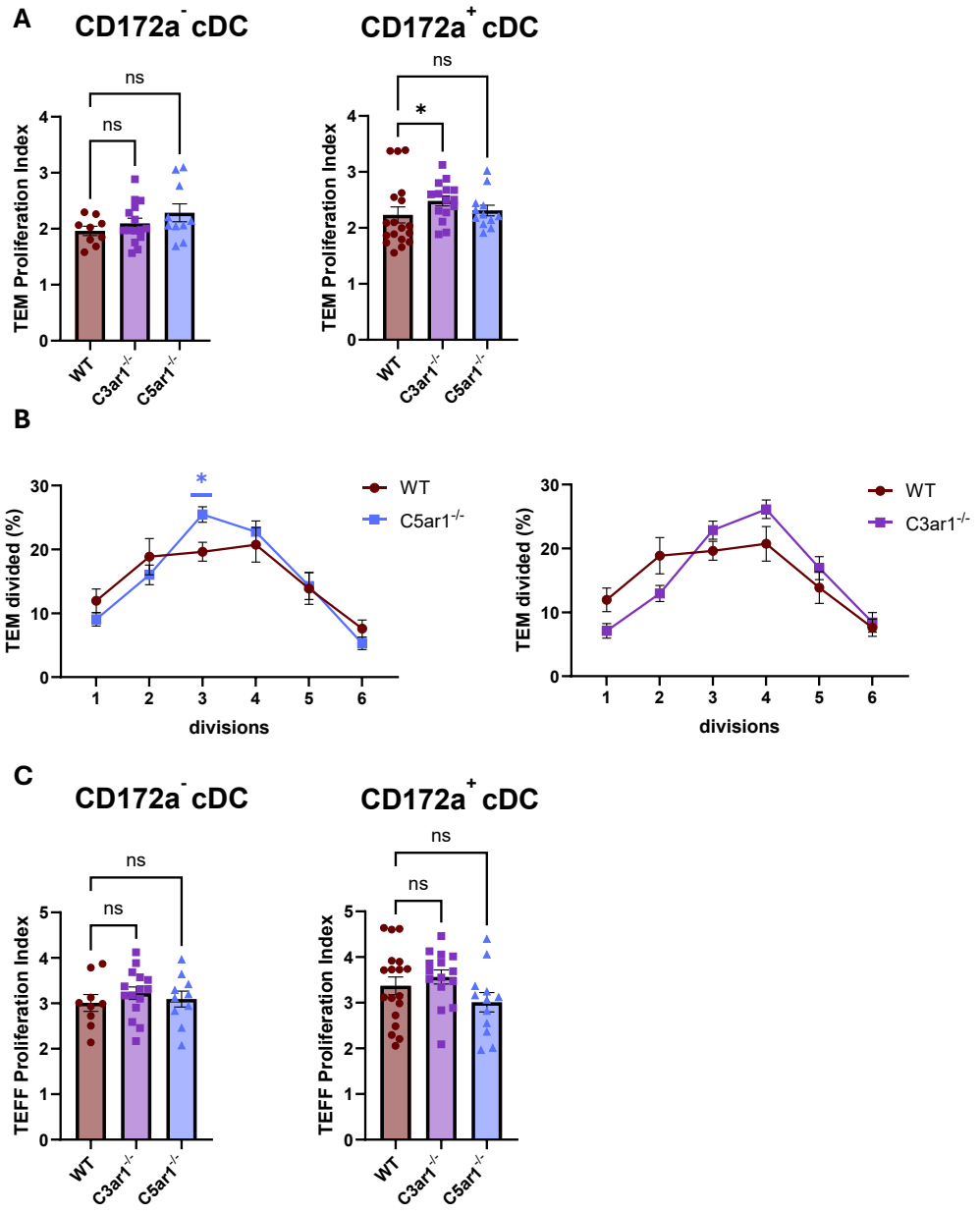


**FIGURE 3.38 Detailed analysis of the potency of MDP-derived CD172a⁻ and CD172a⁺ cDCs from WT, *C3ar1*$^{-/-}$ and *C5ar1*$^{-/-}$ mice to drive CD4⁺ TEM or TEFF cell proliferation in response to OVA stimulation.** **A**. Proliferation index of TEM cells in response to OVA-pulsed CD172a⁻ cDCs (left panel) or CD172a⁺ cDCs (right panel). **B**. Frequencies of OVA-TCR tg TEM cells that have undergone 1-6 divisions in response to co-culture with OVA-pulsed CD172a⁺ cDCs from WT and *C5ar1*$^{-/-}$ (left panel) or WT and *C3ar1*$^{-/-}$ mice (right panel). **C**. Proliferation index of TEFF cells in response to OVA-pulsed CD172a⁻ cDCs (left panel) or CD172a⁺ cDCs (right panel). The proliferation index was calculated by dividing the total number of divisions by the number of cells that went into division. Data shown are the mean ± SEM. Differences between groups were analyzed by One-Way ANOVA with Dunnett post hoc multiple-comparisons test; *p<0.05, ns: not significant.

### 3.3.3 The C3a/C3aR and the C5a/C5aR1 axis control antigen-induced pro-inflammatory cytokine production from CD172a$^-$ and CD172a$^+$ cDCs differentiated from MDPs

In the next set of experiments, I compared the potency of CD172a$^-$ and CD172a$^+$ cDCs to produce pro-inflammatory and T cell-differentiating cytokines in response to antigen stimulation. First, I found that the potency of CD172a$^+$ cDCs from WT, *C3ar1*$^{-/-}$ or *C5ar1*$^{-/-}$ was much higher than that of CD172a$^-$ cDCs to induce the production of IL-1α, IL-1β, IL-6 or TNF-α. In contrast, both cDC subsets showed a similar but low potency to induce the production of IL-12p40 and TGF-β. Of note, CD172a$^+$ cDCs from C3aR1-deficient mice induced slightly more TGF-β than their CD172a$^-$ cDC counterparts (**Fig. 3.39A-C**, **Fig. 3.44**).

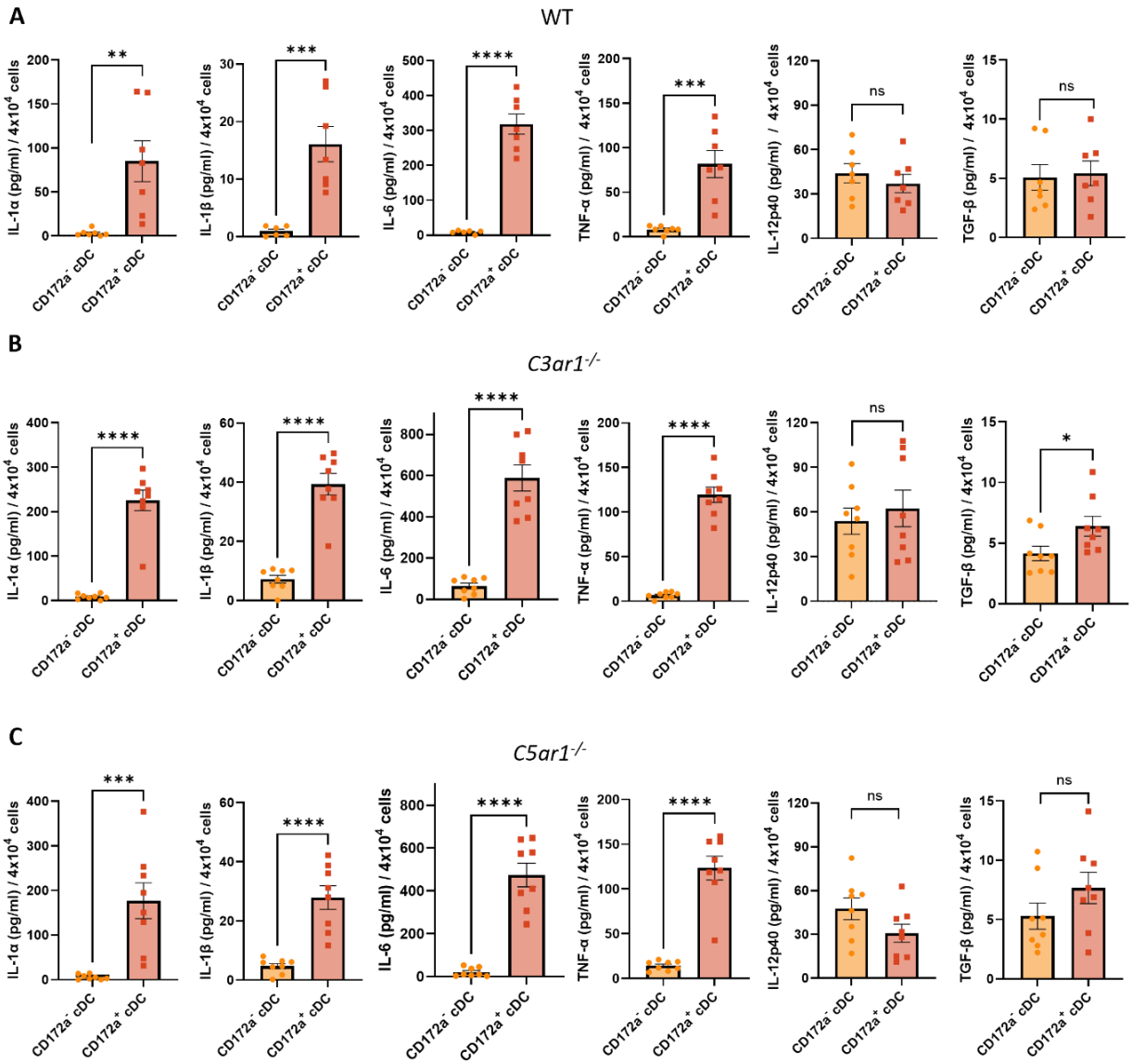


**FIGURE 3.39 Cytokine production from MDP-derived CD172a$^-$ and CD172a$^+$ cDCs in response to 24h OVA stimulation.** (**A-C**) IL-1α, IL-1β, IL-6, TNF-α, IL-12p40 and TGF-β (from left to right) production from MDP-derived CD172a$^-$ or CD172a$^+$ cDCs of WT (A), *C3ar1*$^{-/-}$ (B) or *C5ar1*$^{-/-}$ (C) mice. The determined concentrations were normalized to 4 x 10$^4$ cDCs, which was the lowest yield of cDCs after FACS sorting. Data shown are the mean ± SEM. Differences

between groups were determined by unpaired t test; ns: not significant, *p<0.05, **p<0.01, ***p<0.001, ****p<0.0001.

Side-by-side comparison of WT, *C3ar1*$^{-/-}$ and *C5ar1*$^{-/-}$ CD172a$^{-}$ cDC- or CD172a$^{+}$ cDC-induced cytokine production revealed a higher potency of CD172a$^{-}$ or CD172a$^{+}$ cDCs from *C3ar1*$^{-/-}$ mice to drive the production of most of the evaluated cytokines except TNF-α. CD172a$^{-}$ cDCs but not CD172a$^{+}$ cDCs from *C5ar1*$^{-/-}$ mice showed a higher potency to promote IL-1β and TNF-α production than CD172a$^{-}$ cDCs from WT mice (**Fig. 3.40A, B, Fig 3.44**).

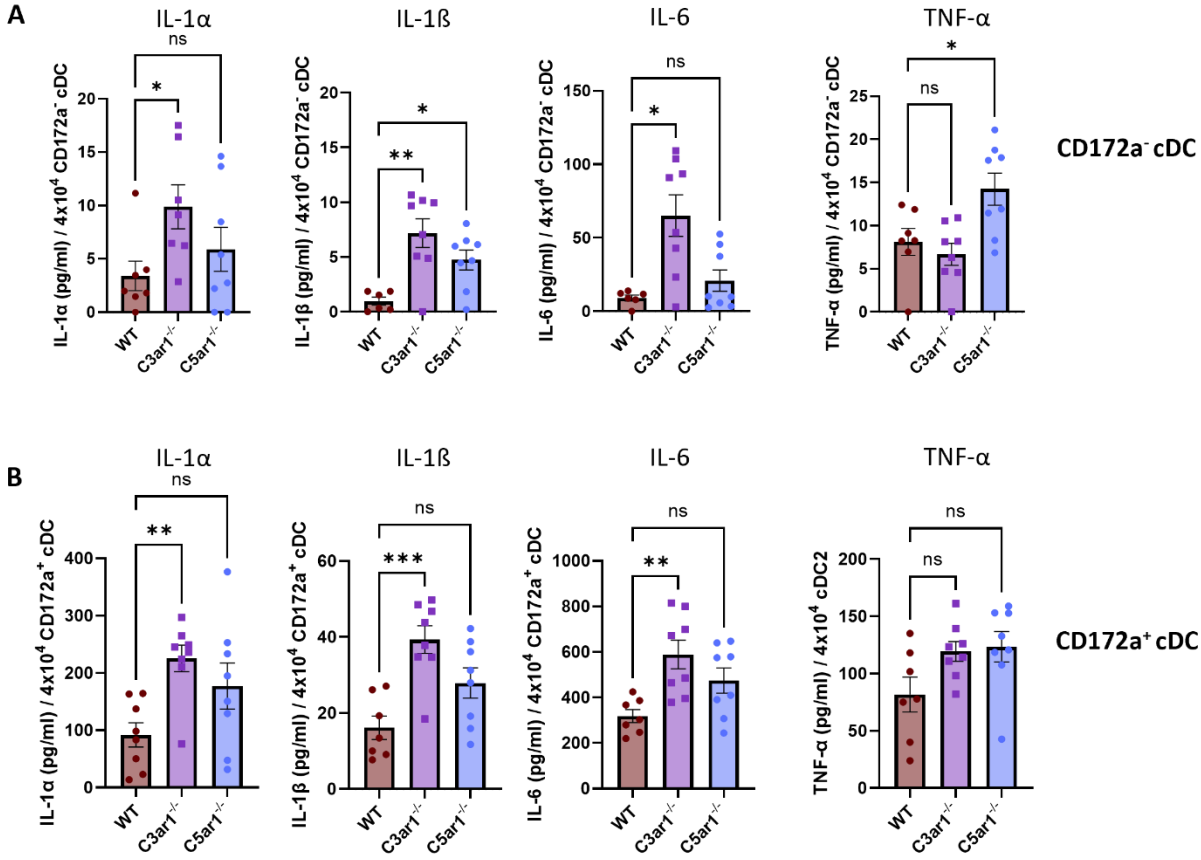


**FIGURE 3.40 Cytokine production from MDP-derived CD172a$^{-}$ and CD172a$^{+}$ cDCs of WT, *C3ar1*$^{-/-}$ or *C5ar1*$^{-/-}$ mice in response to 24h OVA stimulation.** (**A, B**) Comparison of IL-1α, IL-1β, IL-6 and TNF-α production from MDP-derived CD172a$^{-}$ (A) or CD172a$^{+}$ cDCs (B) of WT, *C3ar1*$^{-/-}$ and *C5ar1*$^{-/-}$ mice. The determined concentrations were normalized to 4 x $10^4$ cDCs, which was the lowest yield of cDCs after FACS sorting. Data shown are the mean ± SEM. Differences between groups were determined by Kruskal-Wallis test with Dunn's (A: IL-1α, IL-6; B: IL-1α;) or One-Way ANOVA with Dunnett (A: IL-1β, TNF-α; B: IL-1β, IL-6, TNF-α) posthoc multiple-comparisons test; outliers were identified; ns – not significant, *p<0.05, **p<0.01, ***p<0.001.

I found no differences between genotypes in IL-12p40 and TGF-β production from CD172a$^{-}$ or CD172a$^{+}$ cDCs (**Fig. 3.41**). Further, I found no production of IL-10, IL-12p70, IL-23, IL-27, IFN-β, IFN-γ, IL-17A or CCL2 from the two cDC subsets (data not shown). GM-CSF was excluded from the cytokine analysis, as it was used in the cell culture conditions.

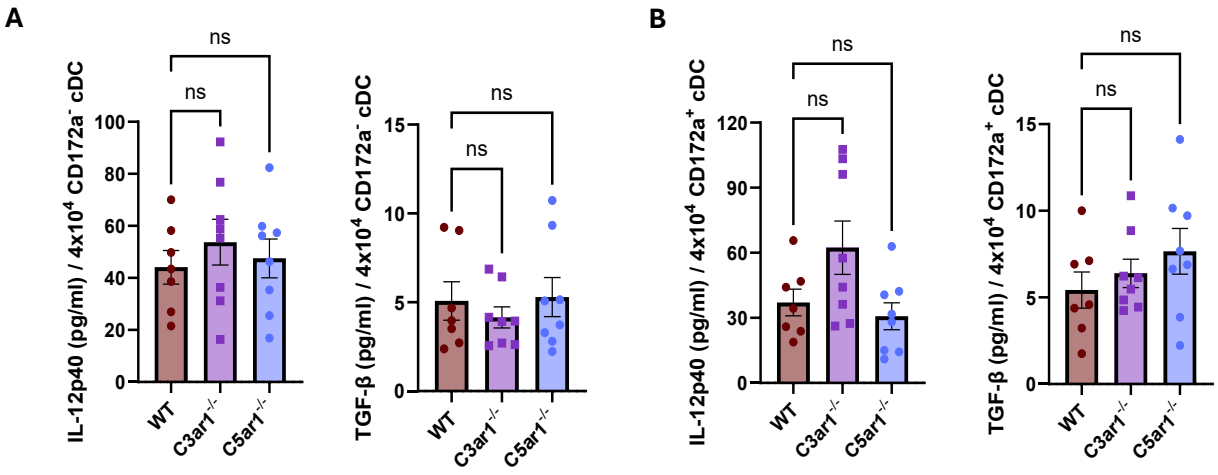


**FIGURE 3.41 IL12p40 and TGF-β production from MDP-derived CD172a$^-$ and CD172a$^+$ cDCs of WT, *C3ar1*$^{-/-}$ or *C5ar1*$^{-/-}$ mice in response to 24h OVA stimulation**. (**A, B**) Comparison of IL-12p40 and TGF-β production from MDP-derived CD172a$^-$ (A) or CD172a$^+$ cDCs (B) of WT, *C3ar1*$^{-/-}$ and *C5ar1*$^{-/-}$ mice. The determined concentrations were normalized to 4 x $10^4$ cDCs, which was the lowest yield of cDCs after FACS sorting. Data shown are the mean ± SEM. Differences between groups were determined by One-Way ANOVA with Dunnett posthoc multiple-comparisons test; ns: not significant.

### 3.3.4 Differential impact of the C3a/C3aR and C5a/C5aR1 axes on ovalbumin-induced IL-17A and IFN-γ production from T cells in response to CD172a$^-$ or CD172a$^+$ cDC activation

In the final set of experiments, I assessed the potency of CD172a$^-$ and CD172a$^+$ cDCs from WT, *C3ar1*$^{-/-}$ and *C5ar1*$^{-/-}$ mice to differentiate OVA TCR tg T cells into IFN-γ producing Th1 and/or IL-17A-producing Th17 cells. First, I found that CD172a$^+$ cDCs from either strain had a much higher potency to differentiate naïve T cells into IL-17A-producing Th17 cells than CD172a$^-$ cDCs (**Fig. 3.42A**). However, I found no strain-specific differences. In contrast, CD172a$^-$ and CD172a$^+$ cDCs from WT mice differentiated naïve Th cells with an equal potency to IFN-γ-producing Th1 cells, whereas CD172a$^+$ cDC cells from *C3ar1*$^{-/-}$ or *C5ar1*$^{-/-}$ mice were more potent drivers of Th1 lineage commitment than their CD172a$^-$ cDC counterparts (**Fig. 3.42B**).

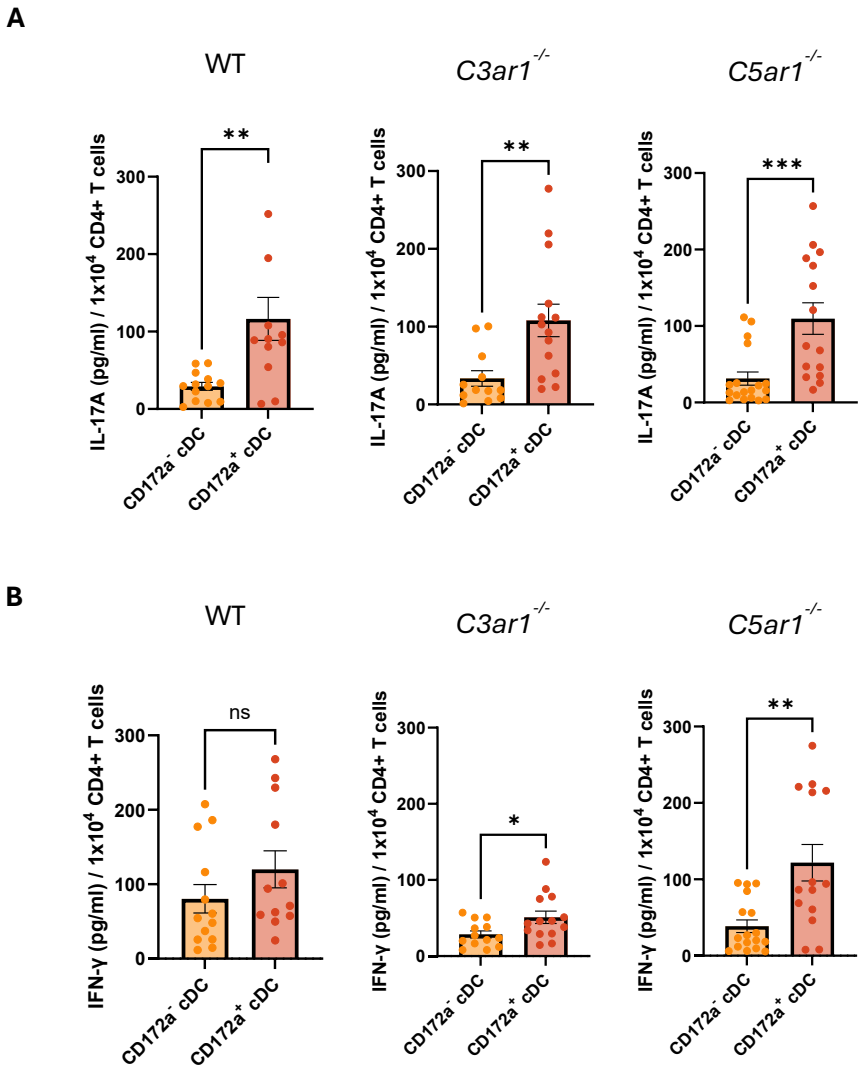


**FIGURE 3.42 IL-17A and IFN-γ production from CD4⁺ T cells in response to stimulation with OVA-pulsed MDP-derived CD172a⁻ and CD172a⁺ cDCs from WT, *C3ar1*$^{-/-}$ or *C5ar1*$^{-/-}$ mice.** (**A, B**) IL-17A (A) or IFN-γ (B) production from OVA-TCR tg T cells co-cultured with MDP-derived CD172a⁻ or CD172a⁺ cDCs from WT, *C3ar1*$^{-/-}$ or *C5ar1*$^{-/-}$ mice (from left to right). The determined concentrations were normalized to 1 x $10^4$ T cells. Data shown are the mean ± SEM. Differences between groups were determined by unpaired t test; ns – not significant, *p<0.05, **p<0.01, ***p<0.001.

Finally, I compared the potency of CD172a⁻ cDCs from WT, *C3ar1*$^{-/-}$ or *C5ar1*$^{-/-}$ mice to drive the differentiation of naïve Th cells toward IL-17A or IFN-γ-producing Th1 cells side-by-side. While I observed no difference in the potency of the CD172a⁻ cDCs from either strain to promote Th17 commitment, I found a significantly higher potency of WT as compared to C3aR- or C5aR1-deficient cells to induce IFN-γ production from the OVA-TCR tg T cells (**Fig. 3.43A**). Regarding CD172a⁺ cDCs, I found a similar potency from WT and *C5ar1*$^{-/-}$ mice to induce Th1 lineage commitment, which was significantly higher than that of CD172a⁺ cDC from *C3ar1*$^{-/-}$ mice. As for CD172a⁻ cDCs, IL-17A production was not affected by C3aR or C5aR1-deficiency (**Fig. 3.43B, Fig. 3.44**).

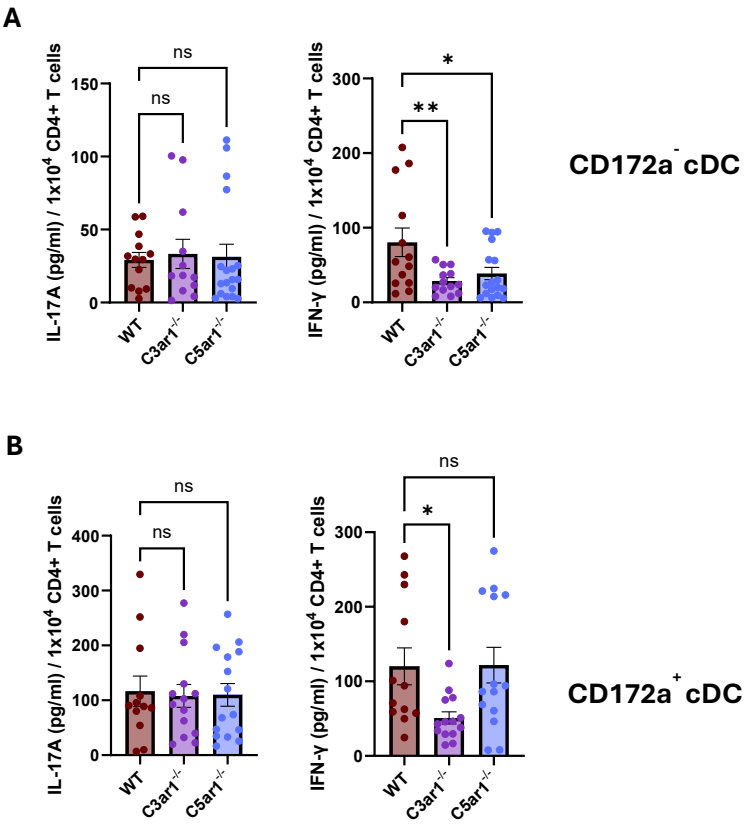


**FIGURE 3.43 Comparison of IL-17A and IFN-γ production from CD4⁺ T cells in response to stimulation with OVA-pulsed MDP-derived CD172a⁻ and CD172a⁺ cDCs of WT, with that of *C3ar1*$^{-/-}$ and *C5ar1*$^{-/-}$ mice.** (**A, B**) Comparison of IL-17A and IFN-γ production from OVA-TCR tg T cells co-cultured with MDP-derived CD172a⁻ (A) or CD172a⁺ cDCs (B) from WT, *C3ar1*$^{-/-}$ or *C5ar1*$^{-/-}$ mice. The determined concentrations were normalized to 1 x $10^4$ T cells. Data shown are the mean ± SEM. Differences between groups were determined by Kruskal-Wallis test with Dunn's (A: CD172a⁻ cDCs; B: CD172a⁺ cDCs) or One-Way ANOVA with Dunnett (A: CD172a⁺ cDCs; B: CD172a⁻ cDCs) posthoc multiple-comparisons test; outliers were identified; ns – not significant, *p<0.05, **p<0.01.

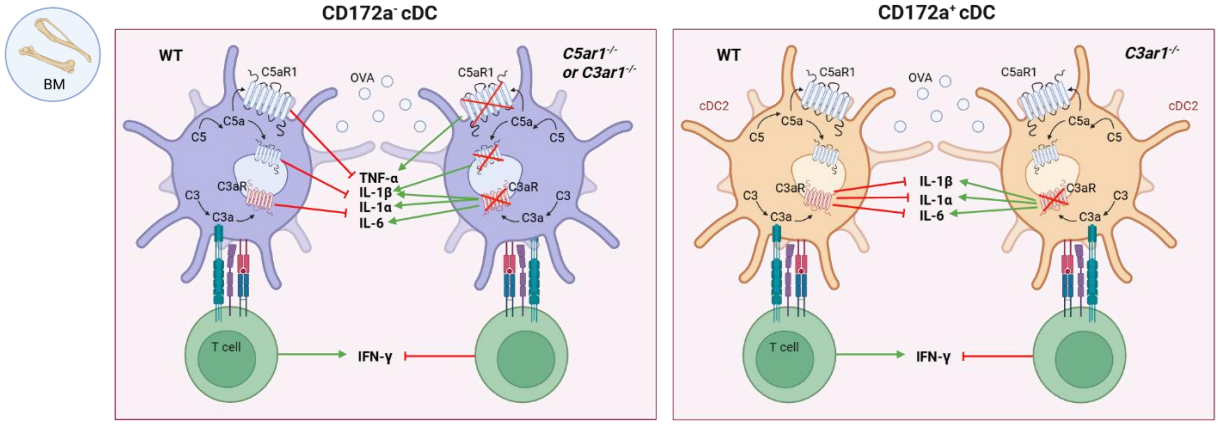


**FIGURE 3.44 Graphic summary of cytokine production in response to OVA stimulation and Th cell differentiation.** In the upper part, the figure shows the expression of the complement components/cleavage fragments C3/C3a, C5/C5a, and their receptors C3aR and C5aR1 in CD172a⁻ (left) and CD172a⁺ (right) cDCs from MDPs after 8-day differentiation and their impact on cDC-driven TNF-a, IL-1a, IL-1β and IL-6 production. At the bottom, the impact of C3aR- or C5aR1-signaling in CD172a⁻ or CD172a⁺ cDCs on IFN-γ prodcution from OVA

TCR tg CD4$^+$ Th cells from DO11.10*Rag2*$^{-/-}$ mice is shown. Blue circles represent OVA (created with *Biorender.com*).

## 3.4 The impact of C5aR1 on splenic DC mobilization and function

As a doctoral researcher in the IRTG 1911 program, I had the opportunity to conduct part of my PhD research in Prof. Pasare's laboratory at Cincinnati Children's Hospital Medical Center. The aim of this collaboration was to complement the in vitro work outlined above and assess the contribution of the C5a/C5aR1 axis on the mobilization and function of cDC in vivo.

### 3.4.1 B16-Flt3L injections increase the frequency of DCs in the lung

First, I took advantage of the B16-Flt3L injection model, which was well established in the Pasare lab[533,534] to mobilize cDCs from the BM. Analysis of lung samples confirmed that the injection of B16-Flt3L melanoma cells into both WT and *C5ar1*$^{-/-}$ mice resulted in significantly elevated frequencies of cDCs as compared to non-injected mice (**Fig. 3.45**). This finding is in line with observations previously reported by the Karsunky group[485].

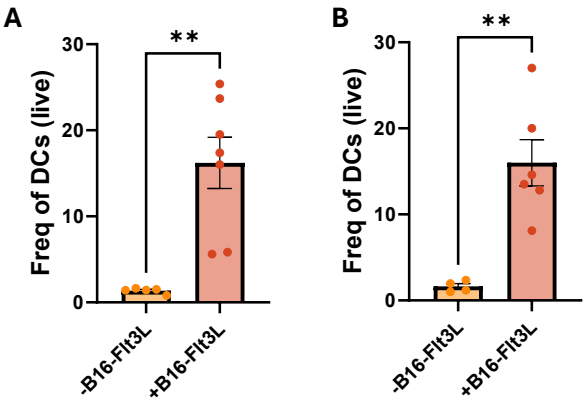


**FIGURE 3.45 Impact of B16-Flt3L melanoma cell injections on DC mobilization into the lung.** (**A, B**) Frequencies of pulmonary Lin$^-$SiglecF$^-$CD11c$^+$CD11b$^+$ DCs in the presence or absence of B16-Flt3L injection into WT (A) or *C5ar1*$^{-/-}$ mice (B). – B16-Flt3L – not injected with B16-Flt3L cells; + B16-Flt3L – injected with B16-Flt3L cells. Data shown are the mean ± SEM. Differences between groups were determined by unpaired t test; **p<0,01.

### 3.4.2 C5aR1 deficiency results in an increased frequency of splenic CD11c$^+$ DCs after B16-Flt3L injection

In the next step, I determined the proportion of splenic CD11c$^+$ DCs among single cells after B16-Flt3L injections into WT and *C5ar1*$^{-/-}$ mice. I found a significantly higher frequency of splenic CD11c$^+$ cDCs in *C5ar1*$^{-/-}$ than in WT mice (70% vs. 60%) (**Fig. 3.46**). This finding suggests a role for C5aR1 in CD11c$^+$ DC differentiation, mobilization or survival.

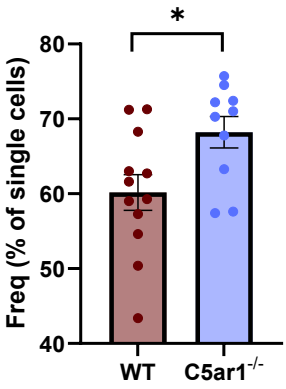


**FIGURE 3.46 Impact of C5aR1 on the frequency of splenic CD11c⁺ DCs after injection of B16-Flt3L cells.** Shown is the frequency of splenic CD11c⁺ cDCs from single cells after B16-Flt3L injection of WT and *C5ar1*$^{-/-}$ mice. Data shown are the mean ± SEM. Differences between groups were determined by unpaired t test; *p<0,05.

### 3.4.3 C5aR1 reduces the frequency of pDCs but not of cDCs in the spleen after B16-Flt3L injection

Next, I performed a side-by-side comparison of splenic cDC and pDC frequencies in B16-Flt3L-injected WT and *C5ar1*$^{-/-}$ mice (**Fig. 3.47**), based on the gating strategy outlined in **Fig. 2.2**. The results showed a high and similar cDC frequency in the spleen of WT and *C5ar1*$^{-/-}$ mice in response to B16-Flt3L injection (**Fig. 3.47A**). In contrast, the frequency of pDCs was significantly higher in *C5ar1*$^{-/-}$ mice as compared to WT mice (**Fig. 3.47B**), suggesting a role for C5aR1 in pDC differentiation, mobilization or survival. Furthermore, approximately half of all single cells were identified as cDCs in both WT and *C5ar1*$^{-/-}$ mice following B16-Flt3L melanoma cell injection (**Fig. 3.47A**).

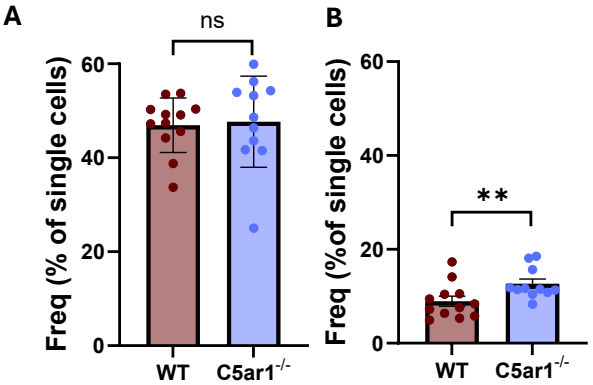


**FIGURE 3.47 Impact of C5aR1 on the frequencies of cDCs and pDCs in the spleen in response to injection of B16-Flt3L cells**. (**A, B**) Potency of B16-Flt3L injection to increase splenic cDC (A) and pDC (B) frequencies in *C5ar1*$^{-/-}$ as compared to WT mice. Data shown are the mean ± SEM. Differences between groups were determined by Mann-Whitney test; ns – not significant, **p<0.01.

### 3.4.4 Flt3L-mediated mobilization of cDC1s and cDC2s into the spleen is independent of C5aR1 expression

In the next step, I investigated whether B16-Flt3L injection influences the frequencies of cDC1 and cDC2 subsets in the spleen and if C5aR1 contributes to this process (**Fig. 3.48**). No preferential differentiation toward either DC subset was observed. Analysis of cDC1 and cDC2 frequencies among all single cells revealed that B16-Flt3L melanoma injections resulted in approximately 20% cDC1 and 20% cDC2 in both WT and *C5ar1*$^{-/-}$ mice (**Fig. 3.48A, B**).

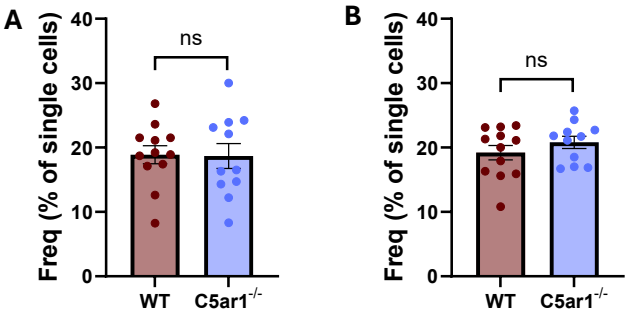


**FIGURE 3.48 Impact of B16-Flt3L cell injection on cDC1 and cDC2 frequencies in the spleen of WT and *C5ar1*$^{-/-}$ mice.** (**A, B**) Similar frequencies of cDC1s (A) and cDC2s (B) in the spleen of WT and *C5ar1*$^{-/-}$ mice after B16-Flt3L injection. Data shown are the mean ± SEM. Differences between groups were determined by unpaired t test; ns – not significant.

### 3.4.5 cDC1s fail to induce antigen-specific T cell differentiation into TEFF and TEM cells in the absence of TLR ligands

Next, I sorted XCR1$^{+}$CD172a$^{-}$ cDC1s from total CD11c$^{+}$ DCs and incubated them with LPS-free OVA (3 or 10 µg/ml) for 72h in the absence of TLR ligands with OVA-specific TCR tg CFSE-labelled OT-II CD4$^{+}$ T cells. Subsequently, I assessed the generation of TEM and TEFF populations. When pulsed with antigen alone, without TLR ligand stimulation, cDC1 derived from B16-Flt3L-injected WT and *C5ar1*$^{-/-}$ mice failed to induce TEM or TEFF responses (**Fig. 3.49A, B, Fig. 3.54**).

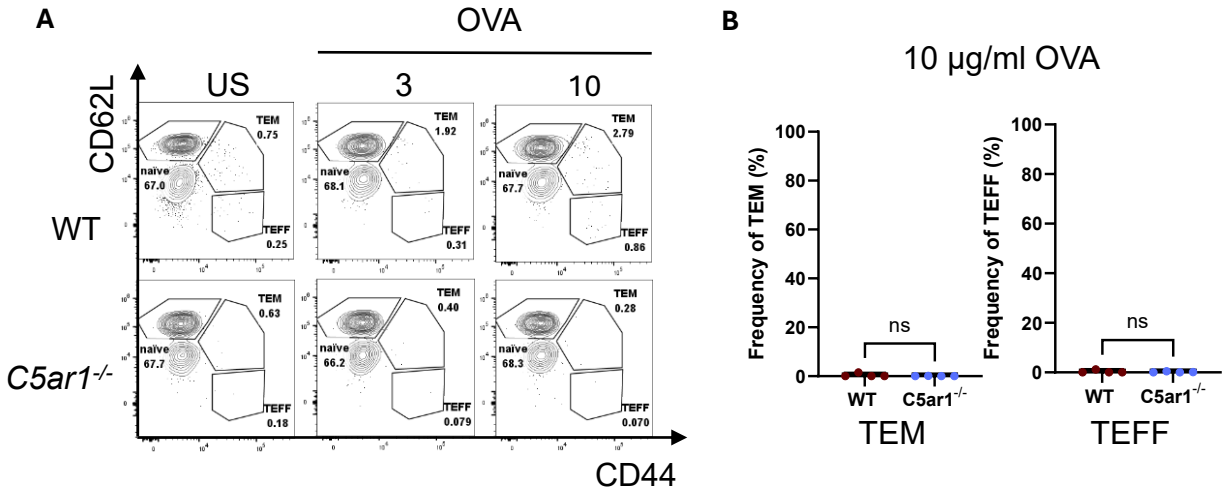


**FIGURE 3.49 Ability of splenic cDC1 from B16-Flt3L–injected WT and *C5ar1*$^{-/-}$ mice to promote TEM or TEFF differentiation in response to LPS-free OVA. A**. Contour plots

showing naïve T cells, TEM and TEFF cells in response to stimulation with 3 or 10 µg/ml OVA-pulsed splenic cDC1 from WT and *C5ar1*$^{-/-}$ mice injected with B16-Flt3L cells. **B**. Frequency of TEM and TEFF in response to stimulation with 10 µg/ml OVA-pulsed splenic cDC1 from WT and *C5ar1*$^{-/-}$ mice injected with B16-Flt3L. TEM were identified as CD4$^{+}$CD62L$^{+}$CD44$^{+}$cells, TEFF were identified as CD4$^{+}$CD62L$^{-}$CD44$^{+}$ cells. Data shown are the mean ± SEM. Differences between groups were determined by unpaired t test; ns – not significant.

### 3.4.6 TLR4 activation promotes antigen-induced TEM and TEFF cell generation by cDC1s

Next, sorted cDC1 were incubated with LPS-free OVA (3 or 10 µg/ml) for 72h in the presence of LPS with OVA-specific TCR tg CFSE-labelled OT-II CD4$^{+}$ T cells. Activation of TLR4 by LPS enhanced cDC1-driven TEM and TEFF cell generation in response to antigen stimulation (**Fig. 3.50A**). No significant statistical differences between WT and *C5ar1*$^{-/-}$ mice were detected (**Fig. 3.50B, Fig. 3.54**).

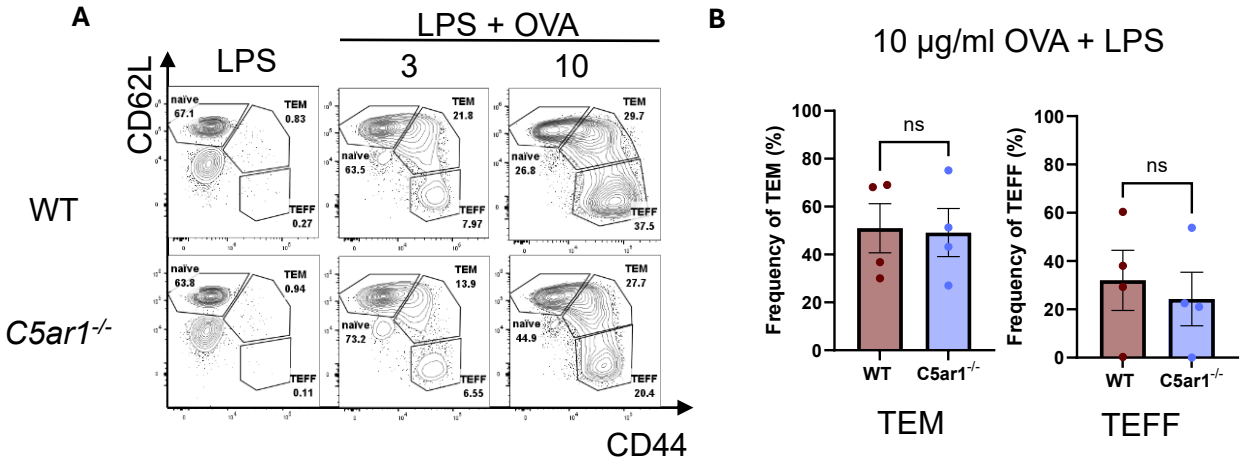


**FIGURE 3.50 TLR4 activation promotes antigen-induced TEM and TEFF cell generation by cDC1s.** **A**. Contour plots depicting naïve T cells, TEM and TEFF cells in response to LPS stimulation combined with 3 or 10 µg/ml OVA-pulsed splenic cDC1 from WT and *C5ar1*$^{-/-}$ mice injected with B16-Flt3L. **B**. Frequency of TEM and TEFF cells in response to LPS stimulation combined with 10 µg/ml OVA-pulsed splenic cDC1s from WT and *C5ar1*$^{-/-}$ mice injected with B16-Flt3L. TEM were identified as CD4$^{+}$CD62L$^{+}$CD44$^{+}$cells, TEFF were identified as CD4$^{+}$CD62L$^{-}$CD44$^{+}$ cells. Data shown are the mean ± SEM. Differences between groups were determined by unpaired t test; ns – not significant.

### 3.4.7 Impact of C5aR1 on cDC2-induced TEFF and TEM differentiation in response to LPS-free OVA

Next, I incubated sorted XCR1$^{-}$CD172a$^{+}$ cDC2s with LPS-free OVA (3 or 10 µg/ml) in the absence of TLR ligands and co-cultured them for 72h with OVA-specific TCR tg CFSE-labelled OT-II CD4$^{+}$ T cells. In contrast to cDC1s (**Fig. 3.49**), I found that cDC2s induced TEM and TEFF cell differentiation in the absence of PRR activation (**Fig. 3.51A**). Importantly, C5aR1-deficient cDC2s induced a somewhat higher frequency of TEM than WT cDC2s, whereas TEFF were virtually absent, when *C5ar1*$^{-/-}$ cDC2s were used for T cell stimulation (**Fig. 3.51B**), suggesting that C5aR1 in cDC2s is critical for TEFF differentiation in response to low dose antigen stimulation in the absence of PRR priming (**Fig. 3.54**).

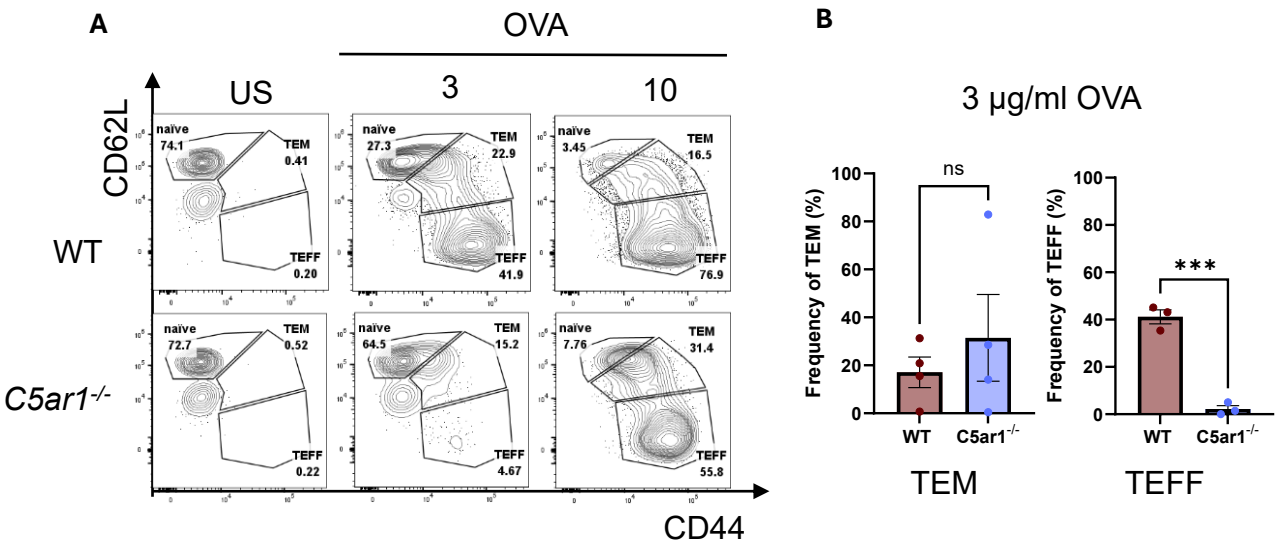


**FIGURE 3.51 Impact of C5aR1-dficiency on the ability of cDC2s to promote TEM or TEFF differentiation in response to LPS-free OVA after injection of B16-Flt3L into WT and *C5ar1*$^{-/-}$ mice.** **A**. Contour plots showing naïve, TEM and TEFF differentiation in response to stimulation with 3 or 10 µg/ml OVA-pulsed splenic cDC2 from WT and *C5ar1*$^{-/-}$ mice injected with B16-Flt3L. **B**. Frequency of TEM and TEFF in response to stimulation with 3 µg/ml OVA-pulsed splenic cDC2s from WT and *C5ar1*$^{-/-}$ mice injected with B16-Flt3L. TEM were identified as CD4$^{+}$CD62L$^{+}$CD44$^{+}$cells, TEFF were identified as CD4$^{+}$CD62L$^{-}$CD44$^{+}$ cells. Data shown are the mean ± SEM. Differences between groups were determined by unpaired t test; ns – not significant, ***p<0.001.

### 3.4.8 TLR4 stimulation drives strong and dominant TEFF and a lower TEM cell generation by cDC2s with no effect of C5aR1

In the next set of experiments, I determined the impact of cDC2s on TEFF and TEM proliferation from naïve OVA-specific TCR tg CFSE-labelled OT-II CD4$^{+}$ T cells in response to combined OVA and TLR4 stimulation by LPS (3 and 10 µg/ml). As expected, this approach resulted in vigorous proliferation of TEFF and less proliferation of TEM cells (**Fig. 3.52 and Fig 3.53**). C5aR1 deficiency had no impact on TEFF or TEM differentiation (**Fig. 3.53, Fig. 3.54**).

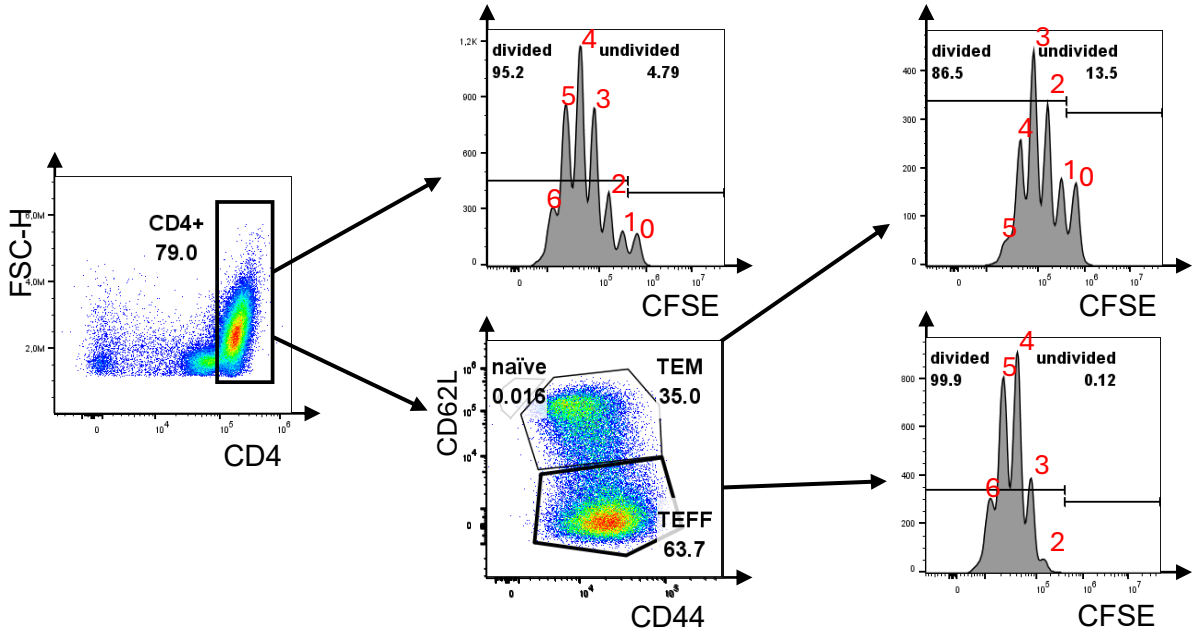


**FIGURE 3.52 Gating strategy to define TEM and TEFF cells after 3-day co-culture with LPS and OVA-pulsed (3 µg/ml) cDC2s and their proliferation.** Shown is the gating strategy to define $CD4^+CD62L^+CD44^+$ TEM and $CD4^+CD62L^-CD44^+$ TEFF (left panel). Histograms show the proliferation of CFSE-labelled total $CD4^+$ (middle upper panel) TEM (upper right panel) and TEFF (lower right panel) OVA-TCR tg T cells from OT-II mice.

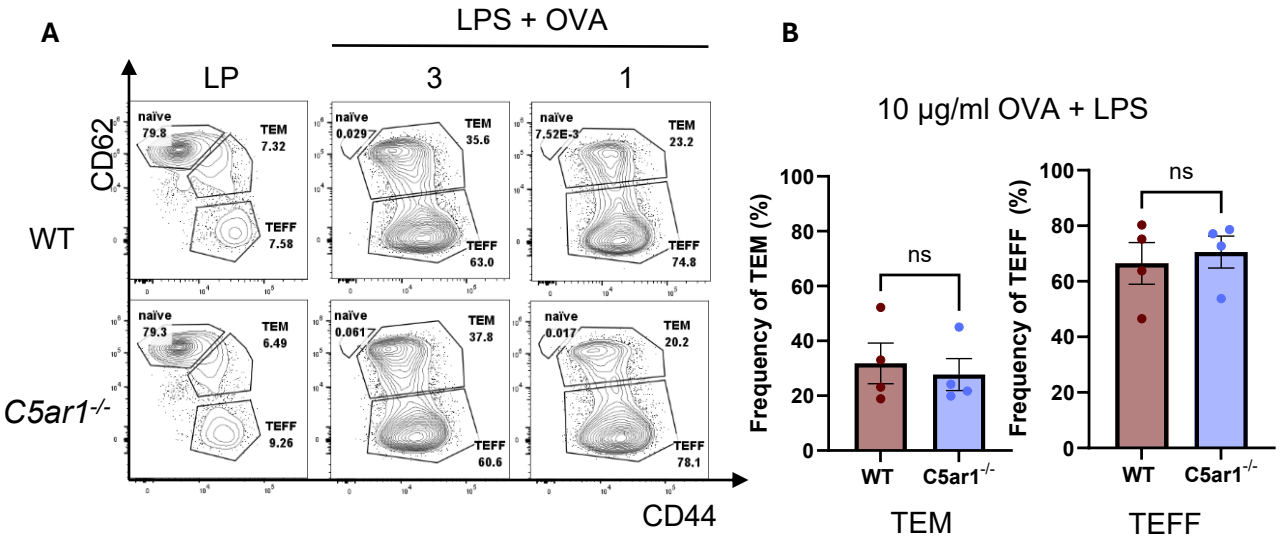


**FIGURE 3.53 Impact of C5aR1 and TLR4 stimulation on TEFF and TEM cell differentiation by antigen-pulsed cDC2s.** **A**. Contour plots showing naïve T cells, TEM and TEFF in response to LPS stimulation combined with 3 or 10 µg/ml OVA-pulsed splenic cDC2s from WT and *C5ar1*$^{-/-}$ mice injected with B16-Flt3L cells. **B.** Frequency of TEM and TEFF in response to LPS stimulation combined with 10 µg/ml OVA-pulsed splenic cDC2s from WT and *C5ar1*$^{-/-}$ mice injected with B16-Flt3L cells. TEM were identified as $CD4^+CD62L^+CD44^+$ cells, TEFF were identified as $CD4^+CD62L^-CD44^+$ cells. Data shown are the mean ± SEM. Differences between groups were determined by unpaired t test; ns – not significant.

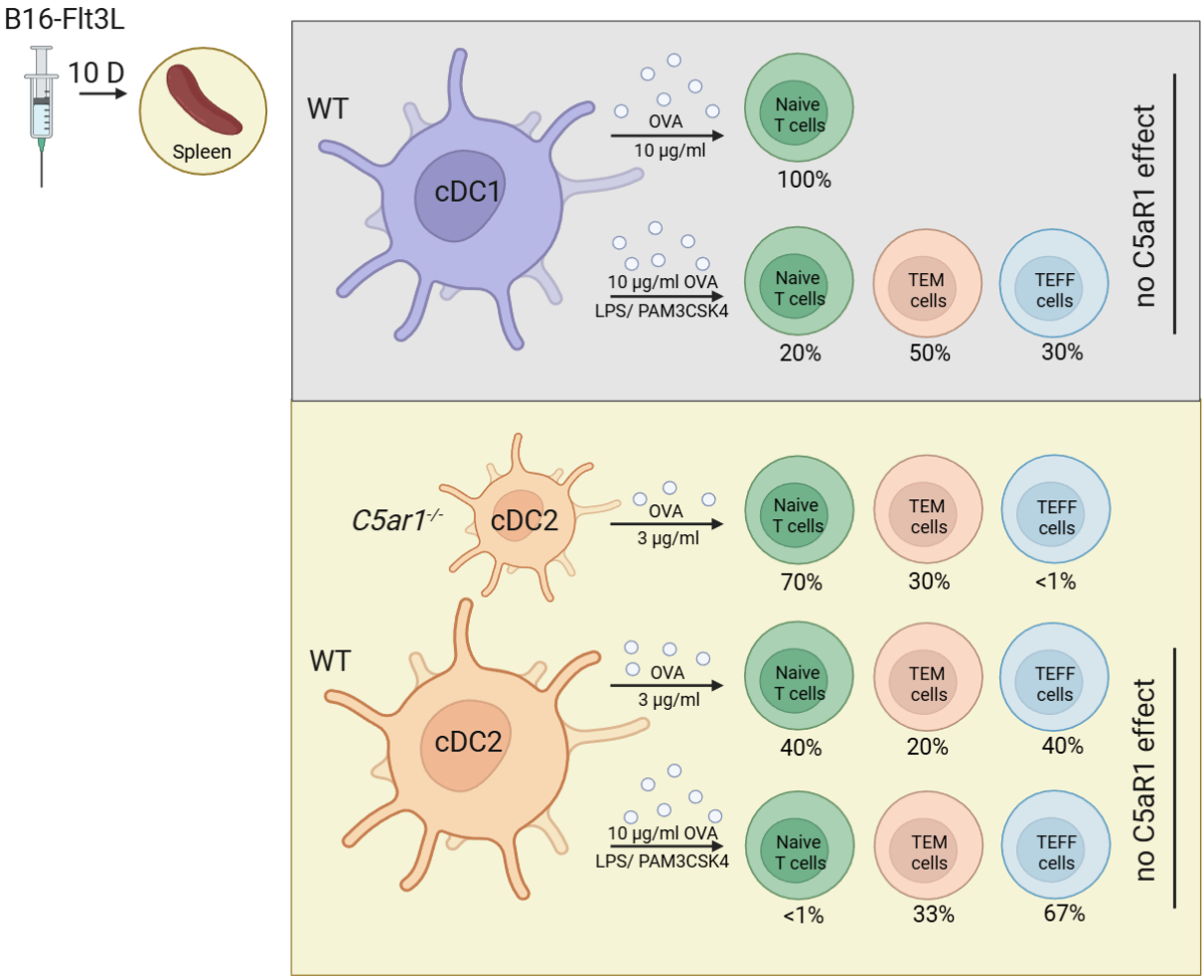


**FIGURE 3.54 Graphic summary showing the potency of splenic cDC1 and cDC2 subsets from B16-Flt3L–injected WT and *C5ar1*$^{-/-}$ mice to promote TEM or TEFF differentiation from naïve T cells in response to stimulation with LPS-free OVA ± LPS or PAM3CSK4.** Blue circles represent OVA (created with *Biorender.com*).

### 3.4.9 Th1 priming by splenic cDC2 is compromised in the absence of C5aR1

In the final set of experiments, I assessed the potency of cDC1s and cDC2s from WT and *C5ar1*$^{-/-}$ mice to differentiate OVA TCR tg OT-II T cells into IFN-γ producing Th1 and/or IL-17A-producing Th17 cells. Strikingly, I found a strong and dominant IFN-γ production upon WT cDC2 cell stimulation with OVA in the presence of LPS or PAM3CSK4, two TLR4 or TLR2 ligands, and OT-II cell co-culture, which was significantly reduced using *C5ar1*$^{-/-}$ cDC2 cells (**Fig. 3.55, Fig. 3.56**). I did not observe any IL-17A producing Th17 cells (data not shown).

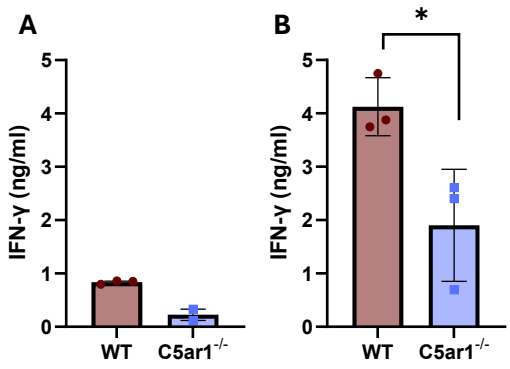


**FIGURE 3.55 Impact of C5aR1 on cDC2-induced differentiation of IFN-γ producing Th1 cells in response to OVA and different TLR ligands.** (**A, B**) Shown is the IFN-γ production in response to cDC2 stimulation with OVA (3 µg/ml) and either LPS (A) or PAM3CSK4 (B). The determined concentrations were normalized to 1 x $10^5$ T cells. Data shown are the mean ± SEM. Differences between groups were determined by unpaired t test; *p<0,05.

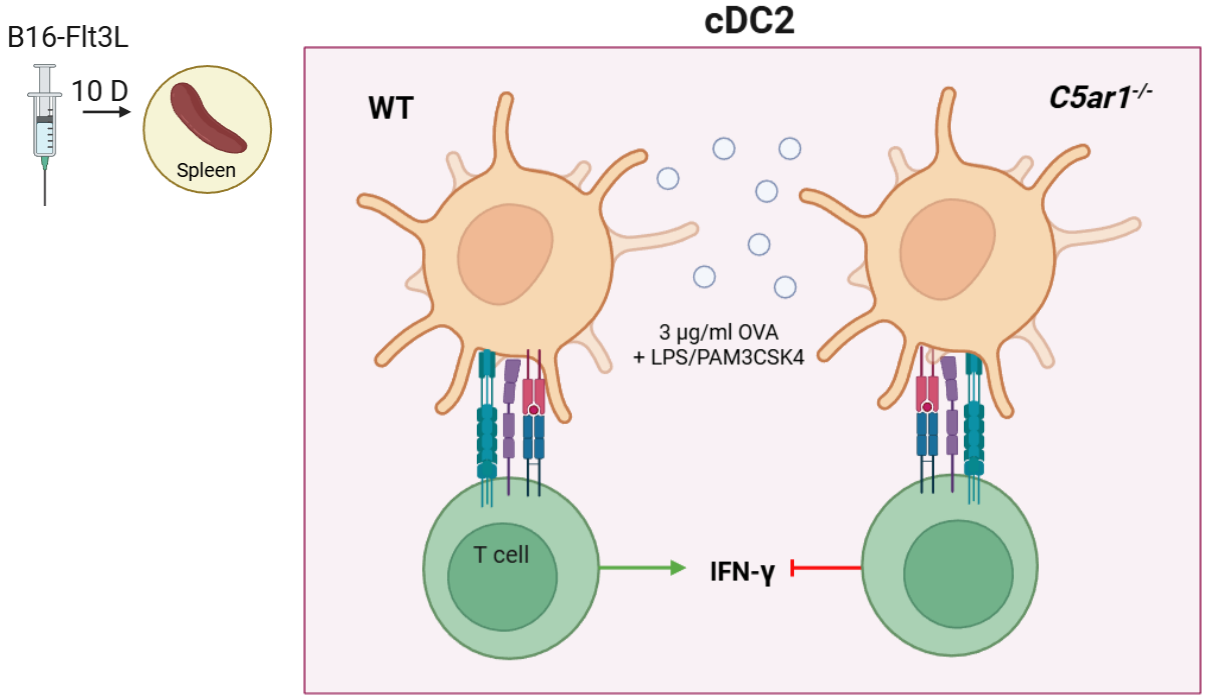


**FIGURE 3.56 Graphic summary illustrating the impact of C5aR1 on cDC2-induced differentiation of IFN-γ-producing Th1 cells in response to OVA stimulation with or without TLR ligand activation by LPS or PAM3CSK4.** Blue circles represent OVA (created with *Biorender.com*).

# 4. Discussion

## 4.1 Impact of complement receptor deficiency on BM progenitor numbers and expression of complement system proteins in BM- resident MDPs and CDPs

DCs arise from the BM-derived HSPCs, progressing through progenitor stages such as MDPs and CDPs[49-52]. While numerous studies have examined the many facets of DC biology, the majority have focused predominantly on their immunological functions rather than the mechanisms underlying their differentiation, in particular regarding the role of complement[535,536]. To help closing this gap, I first determined the potential impact of the two anaphylatoxin receptors C3aR and C5aR1 on the number of MDPs and CDPs in the BM of BALB/c mice. I observed significantly fewer $lin^-$ cells in *C5ar1*$^{-/-}$ BM, along with reduced MDP and CDP numbers, indicating that C5aR1 promotes MDP and CDP differentiation from HSPCs. This finding is in line with a recent report showing reduced numbers of Sca-$1^+$c-$kit^+lin^-$ (SKL) in BM from *C5*- and *C5ar1*-deficient mice[481]. However, in contrast to SKL cells, which expressed C3, C3aR, C5 and C5aR1 at the mRNA level[481], MDPs and CDPs lacked expression of C3/C3a, C5/C5a and their anaphylatoxin receptors, suggesting an indirect role for C5aR1.

Of note, the scRNA-seq data (see below 4.2) demonstrated that MDPs express some complement proteins such as the soluble complement regulator protein, Cfp and C1qbp, and the cell-bound regulators CD55 and CD59. Cfp is well established as a stabilizer of the AP C3 convertase by binding to and extending the half-life of the C3bBb complex, thereby promoting complement activation[322,323]. In addition to its role as a regulator of the AP, Cfp serves as a ligand for NKp46 on NKp46-expressing cells, including NK cells and ILC1s[537]. Further, several studies have demonstrated that Cfp can function as a PRR, binding to microorganisms[538], cells[539-546] and a variety of biological substrates such as LPS, myeloperoxidase, heparan sulfate proteoglycans, FH-related protein 5, acetylated LDL, and zymosan[321,547-552], thereby promoting activation of the AP. As Cfp is mainly expressed in the more differentiated cluster five, it may suggest a PRR-like function as MDPs differentiate toward DCs, consistent with previous reports of Cfp expression in murine[553,554] and human[555-557] DCs.

Another complement regulator protein that was strongly expressed throughout most MDP clusters is C1qbp, a multifunctional and multicompartmental protein[558,559], that has been detected at the plasma membrane as well as in the nucleus, cytoplasm[560-563] and mitochondria[562-565]. These findings of C1qbp being distributed in different compartments is consistent with the strong expression of C1qbp I observe across all MDP clusters from both *C5ar1*$^{-/-}$ and WT mice. Taken together, my findings are consistent with the literature, which supports a differentiation-dependent regulation of complement expression, with several complement genes being induced only upon maturation or under inflammatory conditions[566].

## 4.2 Gene expression profiling in MDPs from *C5ar1*$^{-/-}$ and WT mice

To determine a potential impact of C5aR1 on MDP function, i.e. the differentiation of MDPs toward the DC lineage, I compared single-cell transcriptomic analysis of MDPs from *C5ar1*$^{-/-}$ with that of WT mice. The available literature does not provide a single, dedicated scRNA-seq dataset on isolated murine MDPs that would allow a direct, one-to-one comparison with my MDP scRNA-seq acquired data. Reviews on DC ontogeny explicitly note that most single-cell studies have focused on downstream DC progenitors (CDP, pre-cDC) or peripheral DC subsets, and that MDPs are usually inferred or embedded within broader myeloid progenitor clusters rather than analyzed as a purified population[109,567].

Some work has combined fate mapping, bulk or limited scRNA-seq, and in vitro differentiation to study MDP-derived monocytes and DCs (e.g. Yáñez et al. on MDP vs GMP monocyte output[568]; Liu et al. on Ly6C$^{+}$ MDP-derived DC3[61]), but these approaches either focused on monocyte-committed progenitors and their progeny, or mixed DC/monocyte compartments, and not on highly purified MDPs as performed in my thesis. Thus, a side-by-side comparison of scRNA-seq data from sorted MDP population with an existing public MDP-only dataset is currently not feasible.

The closest possible comparison of the scRNA-seq data from the sorted CD135$^{+}$CD117$^{+}$ MDPs is with the data from Liu et al.[61], who performed scRNA-seq analysis of BM progenitors defined as CD16/32$^{lo}$CD135$^{+}$CD115$^{-}$ and CD16/32$^{lo}$ CD135$^{+/-}$CD115$^{+}$ from *Ms4a2*$^{Cre}$-*Rosa*$^{TdT}$ mice to dissect early DC lineage commitment. Their analysis identified three transcriptionally distinct DC lineages in murine BM, and clustering of the scRNA-seq data resolved 11 clusters that together captured the heterogeneity of these DC-committed and MDP populations. In contrast, my scRNA-seq analysis of MDPs, defined as lin$^{-}$CD135$^{+}$CD117$^{+}$ and thus distinct from the progenitor populations examined by Liu et al.[61], revealed eight distinct clusters, each characterized by unique DEGs. Notably, I observed transitional cell populations, whose differentiation stage led to the formation of additional separate clusters with their own distinct set of DEGs, reflecting dynamic cellular evolution within the MDPs. An interesting observation, consistent with the findings of Liu et al.[61], is that although the FACS-sorted populations were not identical but highly similar, my analysis likewise resolved eight clusters that correspond well to the clusters described in their study. My data confirmed that FACS-sorted MDPs maintain a transcriptional profile enriched for canonical MDP signature genes, while the expression of CDP-associated markers was minor. Intriguingly, a subset of MDPs exhibited early signs of lineage priming toward the pro-cDC1 and -cDC2 lineage, as demonstrated by Liu et al.[61]. In contrast, I found almost no expression of the cMoP signature genes associated with moDCs or macrophages, also confirmed by Liu et al.[61]. Importantly, I found a couple of genes that were differentially expressed in MDPs from WT and C5aR1-deficient mice. Genes upregulated in *C5ar1*$^{-/-}$ MDPs such as *Ercc1, Tnfalp3* and *Ffar2* are involved in progenitor proliferation[529], DC activation[530] and regulation, and determining several immune DC functions[531]. *Ercc1* encodes a key DNA repair factor required for interstrand crosslink and nucleotide excision repair. Increased *Ercc1* expression in MDPs would therefore be predicted to enhance genome maintenance during repeated

cell divisions, support progenitor survival under stress, and preserve the MDP pool during high turnover conditions[529,569]. *Tnfaip3*/A20 is a ubiquitin-editing enzyme and a crucial negative regulator of NF-κB signaling. Elevated Tnfaip3 in MDPs would be expected to dampen NF-κB-driven inflammatory signaling, restrain premature activation or differentiation toward hyperinflammatory DCs, and promote controlled response to TLR or cytokine stimuli[570,571]. FFAR2 senses short-chain fatty acids and modulates several myeloid functions, including macrophage cytokine production and DC-mediated IgA responses and barrier maintenance. Higher FFAR2 expression in MDPs could render them more responsive to microbiota-derived metabolites, biasing their differentiation toward DCs with altered cytokine profiles[531]. Interestingly, one of the differentially expressed genes, *Cd300c,* identified by Rodrigues et al., supports cDC2 and pDC lineage commitment[58]. These findings suggest that C5aR1 plays a role in MDP differentiation into cDCs, in particular cDC2.

Interestingly, I found upregulation of genes in WT MDPs such as *Elane*, *Ctsg*, *Mpo* and *Prtn3,* but not *Igfbp4*, which had previously been reported by Liu et al.[61]. Elevated *Ctsg* in MDPs suggests partial engagement of a granulocytic transcriptional program[572,573], which could bias MDPs toward granulocyte/monocyte lineages rather than sole DC fates, or increase proteolytic potential once cells differentiate, affecting processing of cytokines, chemokines, or extracellular matrix[572,574]. Higher *Macroh2a2* expression in MDPs would be expected to reduce transcriptional plasticity and self-renewal capacity or promote commitment and make reprogramming toward alternative fates more difficult, pushing MDPs toward a more locked-in differentiated trajectory[575-577]. Increased *Elane* in MDPs implies engagement of early granulocytic programming and granule biogenesis, predisposing cells toward neutrophil-like differentiation[572,578], or potential ER stress or unfolded protein response if elastase load is high, which in congenital neutropenia models impairs myeloid maturation; in MDPs this might alter survival or skew differentiation under stress[579,580]. *Slc1a5*, sodium-dependent glutamine transporter, supports glutamine uptake required for biosynthesis, energy production, and activation of growth pathways such as mTOR and ERK in proliferating cells. Upregulated *Slc1a5* in MDPs would be expected to increase glutamine influx, thereby promoting anabolic metabolism, proliferation, and potentially faster or more robust differentiation into downstream myeloid and DC subsets, especially under glutamine-replete conditions[581-584]. Recent work shows that *Prtn3* negatively regulates STAT3-dependent myeloid differentiation and that its depletion enhances granulocytic and monocytic differentiation from progenitors[572,585]. Thus, higher *Prtn3* in MDPs could restrain STAT3-driven differentiation programs and maintain MDPs in a more immature or aberrantly biased state or modulate apoptosis and inflammatory signaling once cells commit, as PR3 also affects caspase-3-dependent neutrophil death[572,586].

Interestingly, strong *Klf4* and *Irf8* expression in MDP cluster 5 fits well with current models of DC3 ontogeny and supports the idea that DC3 can arise directly from MDPs[61]. *Klf4* and *Irf8* are among the key transcription factors that shape DC2/DC3 development[61,112,137], together with *Irf4*[587] and *Zeb2*[588], which collectively define lineage identity and functional specialization within the cDC2 compartment.

In particular, Klf4 has been identified as a key transcription factor for a subset of cDC2, particularly ESAM$^-$ cDC2b-like cells, and is required for Th2-skewing functions of Irf4$^+$ cDC2 in vivo[112]. Recent work on DC3 shows that *Klf4*, together with *Irf8*, is part of the

transcriptional program that defines this subset and distinguishes it from classical cDC2, both in mice and humans. Thus, high *Klf4* levels in cluster 5 suggest that this fraction of MDPs is already transcriptionally biased toward a DC3/cDC2b-like fate[61,62,79,112,589-591].

*Irf8* is a central regulator of DC development, with dosage-dependent roles: high *Irf8* favors cDC1 and pDC trajectories, while lower or intermediate levels contribute to cDC2 and DC3 development. Human data using *Irf8* allelic series indicate that DC3 arise from an IRF8$^{lo}$ myeloid pathway that is distinct from the Irf8$^{hi}$ route generating pDCs, cDC1, and cDC2, reinforcing the view that DC3 share ontogeny with monocytes and MDP-derived lineages. In mice, DC3 have been shown to originate from Ly6C$^{+}$ MDPs via defined intermediate stages, and their development depends on both *Klf4* and *Irf8*[61,62,592,593]. Taken together, the strong co-expression of Klf4 and Irf8 in cluster 5 of MDP is consistent with a DC3-primed progenitor state and provides a mechanistic link between MDP transcriptional programming and the emergence of a DC3-like CD172a$^{+}$ subset[61,79].

## 4.3 Impact of C3aR or C5aR1-deficiency on differentiation of cDCs from BM precursors in response to Flt3L and GM-CSF

In the next step, I did set up an in vitro system to determine the impact of C3aR and C5aR1 activation on cDC differentiation from MDPs or CDPs. After lineage depletion, I noticed that MDPs were significantly more abundant than CDPs in cultures from all mouse strains, reflecting their dominant presence in the early differentiation stages. Several studies support that MDPs are more abundant than CDPs, both in vivo and in culture. In steady state, Flt3/Flt3L signaling controls the size of the MDP pool in BM[70,532], and Flt3L treatment increases MDP numbers roughly tenfold, indicating a relatively large and cytokine-sensitive progenitor population upstream of CDPs[70,594]. In contrast, CDPs are consistently described as a more rare and more DC-committed subset. In Flt3L-driven in vitro systems, CDPs rather than MDPs have been reported as the main expanding progenitors at early culture time points, implying that MDPs start more numerous but CDPs become the dominant proliferating fraction under these specific conditions. Human data mirror this hierarchy, with MDPs representing a larger fraction of CD34$^{+}$ cells than CDPs in cord blood[594-598].

In my thesis project, I initially cultured the different precursors cells with Flt3L alone, as previously demonstrated by another research group[599]. However, I observed limited precursor survival under those conditions. Differences in culture duration, cytokine concentration, or cell density may account for this discrepancy and might have been suboptimal to support efficient cDC differentiation. Flt3 encodes a class III receptor tyrosine kinase that is closely related to Kit and M-CSFR or Fms[600]. Some studies show that Flt3L alone is sufficient to generate BM CD11c$^{+}$ DCs[597] and cDC1, cDC2, and pDC populations[599,601]. The cDC1s generated under this condition resemble their in vivo counterparts in several key aspects, including their dependence on Irf8[599] and Batf3[53] for development, and production of IL-12 by *Toxoplasma gondii* soluble tachyzoite

antigen[602]. Nevertheless, Flt3L-driven BM cultures typically generate relatively few cDC1s compared with the much larger numbers of moDCs obtained in GM-CSF–supplemented cultures[603,604], what makes investigating cDC1 on a large-scale challenging.

GM-CSF has the capacity to drive DC differentiation from precursor cells and to promote DC activation both in vitro and in vivo[603,605-618]. Consequently, much of the current understanding of DC biology is based on studies using HSPCs cultured with defined growth factors[51,603,604,619,620]. In particular, GM-CSF-BM culture has been used to generate $CD11c^{+}MHCII^{+}$ BMDCs [603,621]. However, during the past few years it became increasingly clear that $CD11c^{+}MHCII^{+}$ BMDCs represent a heterogeneous population composed of bona fide cDCs and monocyte-derived macrophages, which both undergo maturation upon LPS stimulation but respond in distinct ways and can still be distinguished phenotypically and functionally[603,621,622]. Brasel et al.[597] have shown that GM-CSF is not strictly required for DC generation in vitro, in line with earlier work demonstrating that neutralization of GM-CSF does not block DC development from murine thymic precursors cultured in a cytokine cocktail containing TNF-α, IL-1β, IL-7, SCF, and IL-3[623]. Moreover, lymphoid tissues from $GM\text{-}CSF^{-/-}$ mice have normal DC numbers[75], yet these mice display impaired antigen-specific T- and B-cell activation due to defective APC function, which could be rescued by administration of exogenous GM-CSF with the immunogen[624].

Other studies combined GM-CSF and IL-4 to induce DC differentiation from progenitor cells or peripheral monocytes[604,625]. However, this culture systems results in highly heterogeneous cell populations, which include not only DCs but also significant proportions of monocytic cells and macrophages[622]. Inaba et al.[603] demonstrated that murine BM cells cultured with GM-CSF for 6-8 days generate large numbers of mature DCs, which can be further activated and enriched by adding IL-4[604,626]. These GM-CSF/IL-4 derived DCs express classical surface markers such as DEC205, MHC-II, CD80, and CD86, and exhibit robust allo-stimulatory capacity[626]. The myeloid origin of these cells is supported by their expression of CD11b, 33D1, and F4/80 and the absence of CD8α expression. Alternatively, lymphoid-related DCs can be generated from thymus-derived $CD4^{low}$ precursors cultured with a cocktail of cytokines including SCF, IL-1, TNF-α, IL-3, and IL-7, but without GM-CSF[623]. These DCs express varying levels of CD11b, high MHC-II, CD80 and CD86, but lack CD8α, found on a subset of DCs from mice lymphoid tissues[627].

In light of these studies, I finally decided to add GM-CSF to the Flt3L culture. When using only Flt3L, the differentiation typically favors pDC differentiation; however, the addition of GM-CSF shifted the differentiation toward cDCs. As a result, the culture conditions used in this thesis promoted the generation of cDCs rather than pDCs.

During the 8-day culture in the presence of GM-CSF and Flt3L, which has previously been demonstrated to be critical for the physiologic differentiation of cDCs from BM precursors[532], I observed that CDP-derived cDCs begin to appear already after one day of culture. In contrast, MDP-derived cDCs differentiated more slowly, and were detectable only at day 3 and at a lower frequency as compared to CDP-derived cDCs on day one. This observation is consistent with the existing literature. MDPs are upstream, less-committed progenitors that give rise to both monocytes and CDPs

whereas CDPs are a downstream of MDPs and are expected to produce differentiated cDCs more rapidly when placed in differentiation-permissive culture conditions[598,628]. In vitro and in vivo studies indicate that more differentiated progenitors (such as CDPs or pre-cDCs) downregulate stem/progenitor markers and enter terminal differentiation faster than upstream progenitors, which must first progress through intermediate transcriptional and proliferative stages before acquiring a mature DC phenotype[629,630]. Additionally, fate-mapping and kinetic analyses show that MDPs require additional division and lineage-commitment steps to generate DCs (and monocytes) and are therefore often detected later in differentiation assays (e.g., as in my research, around day 3), whereas CDP-derived cDCs appear earlier (day 1) and at higher initial frequency because CDPs are already poised toward the DC fate[76,598]. An additional factor are the culture conditions (cytokine mix, cell density, Flt3L vs GM-CSF, and duration), which strongly influence the relative expansion and apparent kinetics of progenitor-derived DCs; Flt3L favors expansion of DC-committed progenitors and pre-cDCs, accelerating CDP-derived cDC appearance, while MDP-derived DCs and monocyte-derived populations emerge with delayed kinetics[597,631].

Notably, *C3ar1*$^{-/-}$ MDPs differentiated in higher frequencies toward cDCs than WT or *C5ar1*$^{-/-}$ MDPs at day 8. In comparison, *C5ar1*$^{-/-}$ MDPs and CDPs differentiated in lower frequencies toward cDCs than WT or *C3ar1*$^{-/-}$ CDPs at days one and three. Together, these findings point toward an important role of C5aR1 during the early differentiation process of cDCs from MDPs and CDPs. In contrast, during the differentiation process of cDCs from CDPs between days 6 and 8, C3aR and C5aR1 suppressed the cDC differentiation as evidenced by higher cDC frequencies as compared to those induced by WT CDPs.

To the best of my knowledge, this is the first report demonstrating a role for C3aR and C5aR1 in cDC differentiation from BM precursors. Studies available from Ratajczak group demonstrate a clear role for complement components in HSPC trafficking, mobilization and engraftment, but none of the published work directly investigated MDP or CDP differentiation into DC subsets. Ratajczak et al. showed that intracellular and extracellular complement components (C3, C5 and signaling via C5aR1) regulate HSPC mobilization and homing, and that C3- and C5-deficient animals differ in mobilization efficiency and engraftment after transplantation[481,632]. Mechanistically, their work links complosome activity to mitochondrial ROS production, NLRP3 inflammasome activation and altered HSPC trafficking, and shows that C5-deficiency or C5aR1 loss produces a “poor-mobilizer” phenotype and impaired homing/engraftment compared with C3 deficiency[633]. Importantly, analyses were focused on HSPC frequency, mobilization kinetics, homing, engraftment and metabolic/trafficking pathways, rather than on downstream lineage differentiation of specific DC progenitors[481,634]. No experimental data were reported that characterize the differentiation of MDPs or CDPs into cDC1/cDC2/DC3 subsets in C3aR- or C5aR1-deficient mice.

I observed that all cDCs that differentiated from MDPs or CDPs at day 8 strongly expressed CD11c and MHC-II as well as CD11b, suggesting their differentiation into cDC2s. In support of this view, I could identify one population that expressed CD172a, also known as signal regulatory protein alpha (SIRPα), in particular after differentiation from MDPs. CD172a is an important immunoregulatory receptor that serves both as a

lineage marker and as a functional modulator in DC biology. Its expression is tightly linked to the developmental and functional diversification of cDC subsets. In mice, CD172a expression distinguishes cDC2 and DC3 from cDC1, as cDC1 are typically CD172a$^{-}$, while BM pre-DC2 are CD172a$^{low}$ and DC3 are CD172a$^{+}$[61]. Liu et al. showed that both subsets, BM pre-DC2 and DC3 express similar levels of CD11c. This finding is in line with my observation that CD172a$^{-}$ cDCs may represent CD172a$^{low}$ pre-cDC2, while CD172a$^{+}$ cDCs align well with DC3, which I will discuss further below (see 4.4).

During DC differentiation from CDPs, commitment toward the cDC1 lineage is driven by transcription factors such as IRF8, ID2, and BATF3, which are associated with the loss of CD172a expression. Conversely, cDC2 differentiation depends on IRF4, Notch2, and KLF4, transcriptional programs that coincide with the acquisition of CD172a. The DC3 subset, which arises from CD115$^{+}$CD135$^{+}$Ly6C$^{+}$ progenitors, also expresses CD172a, together with IRF8 and KLF4, reflecting features that partially overlap with both cDC2 and monocytes[61,63].

Functionally, CD172a interacts with its ligand CD47, a self-signal that negatively regulates phagocytosis and modulates antigen uptake, migration, and cytokine production. This signalling axis is particularly relevant for cDC2 and DC3, which are specialized in antigen presentation to CD4$^{+}$ T cells and the induction of Th1, Th2 and Th17 responses, whereas cDC1, lacking CD172a, are more efficient in cross-presentation to CD8$^{+}$ T cells[635,636].

Taken together, CD172a not only marks distinct developmental trajectories of DC subsets but also contributes to their functional specialization. Its selective expression reflects the transcriptional programming and immunoregulatory functions that define cDC2 and DC3 identity, emphasizing that the presence or absence of CD172a is both a phenotypic and functional hallmark of DC heterogeneity.

In addition to CD172a$^{+}$ cDCs, I found a population of CD172a$^{-}$ cDCs. This population emerged from MDPs at day 3, whereas CDPs gave rise to CD172a$^{-}$ cDCs as early as day 1 of culture. In fact, my data demonstrate that MDPs and CDPs preferentially differentiated into CD172a$^{-}$ cDCs, with CDPs doing so more rapidly and with a higher potency. This is compatible with current concepts, although the exact CD172a-based bias that I found has not been explicitly described before. As already mentioned above, MDPs differentiate upstream of CDPs and retain broader monocyte/DC potential, so they need more cell cycles and intermediate stages before acquiring a fully cDC phenotype, which fits with slower and less efficient cDC generation from MDPs than from the more DC-restricted CDPs. CDPs are committed to the cDC1/cDC2 lineages and give rise to pre-cDCs that rapidly differentiate into mature cDCs in vitro and in vivo, so faster and more potent cDC output from CDPs compared with MDPs is well in line with DC ontogeny models[567,637]. Regarding CD172a, the literature shows that both MDPs and CDPs can generate CD172a$^{+}$ cDC2 and CD172a$^{-}$ cDC1-like cells under Flt3L-driven conditions, but previous reports did not demonstrate a preferential skewing of both progenitors toward CD172a$^{-}$ cDCs. Most work focused on cDC1 vs. cDC2 frequencies or transcription factor dependence rather than discrimination of two DC subsets by CD172a. My finding that MDPs and CDPs preferentially differentiate into CD172a$^{-}$ cDCs and that such differentiation occurs earlier and more efficiently with CDPs, is mechanistically in line with the hierarchy, i.e. more committed progenitors

differentiate faster to cDCs, and represents a more detailed, CD172a-focused observation that extends existing data on cDC differentiation from BM precursors[77,107,567,638,639].

Notably, *C5ar1*$^{-/-}$ CDPs differentiated in lower frequencies toward CD172a$^{-}$ cDCs than WT or *C3ar1*$^{-/-}$ CDPs early in the differentiation process, suggesting that C5aR1 signaling contributes to early differentiation of CD172a$^{-}$ cDCs. In contrast, C3aR seems to suppress CD172a$^{+}$ cDC differentiation during early differentiation pointing toward a complex, opposing action of C5aR1 and C3aR during early cDC differentiation. A different picture emerged in the late differentiation process. Here, C3aR and C5aR1 seem to act in concert and suppress CD172a$^{-}$ but not CD172a$^{+}$ cDC differentiation from CDPs[58].

Interesting in this context is the study on cDC2 ontogeny by Rodrigues et al., who showed that mature CD11c$^{+}$MHCII$^{+}$XCR1$^{-}$CD11b$^{+}$ cDC2 arise from at least two progenitor streams[58]. One is a CD300c pro-cDC2 that derives from DC-committed progenitors (including CDP-derived pre-cDC2) and exclusively generates cDC2 in vitro and in vivo. The second one is an MDP-derived DC3 lineage (Ms4a3-Cre-traced) that bypasses CDPs and converges transcriptionally to a cDC2-like phenotype but is ontogenetically distinct. In this context, I expected that CDP-derived cells in my thesis project should give rise to classical cDC2, matching the phenotype used in the report by Rodrigues et al. In contrast, the MDP-derived cDCs characterized by the CD11b$^{+}$CD172a$^{+}$ phenotype should be more closely related to the DC3-like, monocyte-linked branch, which was traced by *Ms4a3* and ontogenetically separated from Cd300c-traced pro-cDC2.

## 4.4 Potential DC3 origin of MDP-derived CD172a$^{-}$ and CD172a$^{+}$ DCs

To determine the developmental origin of CD172a$^{+}$ and CD172a$^{-}$ cDCs from MDPs I ran a qPCR analysis on such cDCs differentiated from MDPs from *C5ar1*$^{-/-}$ and *tdTomato-C3ar1*$^{fl/fl}$ mice after 8-day culture in the presence of Flt3L and GM-CSF. I focused on signature genes of cDC1, cDC2 and DC3 subsets[57-59,61,76-80]. My qPCR analysis revealed that *Id2* was the most highly expressed gene in both *C5ar1*$^{-/-}$ and *tdTomato-C3ar1*$^{fl/fl}$ mice. This finding is notable because *Id2* has been reported to be predominantly expressed during cDC1 differentiation, suggesting a potential cDC1-like identity for these cells[58,61,77-80]. Furthermore, both cDC cell populations showed markedly higher expression of *Irf8* compared to *Irf4*, which further supports a cDC1-associated transcriptional profile.

The relatively high expression of *Klf4* may point to an alternative explanation. It has been shown that DC3 arise from Flt3 (CD135$^{+}$) cells that are CD117$^{-}$ but express CSFR1 (CD115$^{+}$)[61]. Such CD135$^{+}$CD115$^{+}$ cells are mainly Ly6c$^{+}$ and can be further discriminated by their CD11c and CD172 expression into two subsets, i.e. CD172$^{-}$ CD11c$^{-}$ pro-DC3 and CD11c$^{+}$CD172$^{-}$ pre-cDC2. Thus, the CD135$^{+}$CD117$^{-}$ MDPs comprise the CD115$^{+}$ cells that could give rise to the DC3[61]. Consistent with this interpretation, *Klf4* and *Irf8* are both known to be required for DC3 development[57-

[59,61,76-80], and their relatively high expression in these populations supports a potential DC3 identity rather than canonical cDC1 or cDC2 lineages.

Additionally, scRNA-seq data discussed above (see 4.2) with strong *Klf4* and *Irf8* expression support that MDP can give rise to DC3 during their differentiation process. The findings by Rodrigues et al.[58] (see 4.3), further show that cDC2s are not a homogenous lineage but a mixture of ontogenetically distinct streams of a dedicated pro-cDC2 alongside an MDP/DC3-derived pathway. Also, the authors compared CD300c-traced cDC2s to Ms4a3-Cre-traced DC3, a monocyte-derived subset that bypasses the CDP stage and also acquired a cDC2-like XCR1$^{-}$CD11b$^{+}$ surface phenotype. Cd300c-traced cDC2 and Ms4a3-traced DC3 differ in their transcriptome, surface phenotype and tissue distribution, despite both falling into the XCR1$^{-}$CD11b$^{+}$ cDC2 gate. This finding supports the view that the MDP-derived CD172a$^{+}$ DCs are DC3s.

## 4.5 Expression of C3, C5, C3a, C5a and their corresponding anaphylatoxin receptors (C3aR and C5aR1) in MDP- and CDP-derived CD172a$^{-}$ and CD172a$^{+}$ DC after 8 days differentiation

The existing literature primarily reports on the presence of C3aR and C5aR1 on fully differentiated BMDCs[426]. However, no studies have systematically monitored the expression dynamics of these complement receptors throughout the DC differentiation process. To gain deeper insights into the role of C3aR and C5aR1 in cDC subset differentiation, I determined the expression of complement factors C3, C5 their small cleavage fragments C3a and C5a and their cognate C3aR and C5aR1. While I found none of the complement proteins at baseline I detected C3/C3a, C5/C5a and their receptors during the cDCs differentiation process. I observed early C3 production in differentiating CD172a$^{-}$ DC, which was converted to C3a during differentiation and increasing intracellular C3aR expression. Further, CDP-derived CD172a$^{-}$ expressed C5, generated C5a, and showed strong intracellular C5aR1 expression during the entire CD172a$^{-}$ differentiation process. These findings are in line with the emerging concept of autocrine intracellular complement activation, i.e. the complosome, regulating important functions of innate and adaptive immune cells such as survival, autophagy, differentiation and activation[640]. My results demonstrate autocrine intracellular C3 and C5 production during physiologic CD172a$^{-}$ DC differentiation, associated with generation of C3a and C5a, which can bind to intracellularly expressed C3aR and C5aR1. In line with the impact of C3aR and C5aR1 deficiency on cDC differentiation, my findings suggest that intracellular complement activation functions as a novel regulator of CD172a$^{-}$ DC differentiation from CDPs and, to a lesser extent, from MDPs. There is also a minor effect of C5aR1 on early CD172a$^{-}$ cDC differentiation from MDPs on day 3, although this effect does not reach the level of statistical significance.

Previous studies from the Köhl laboratory and from others showed expression of C3/C3a, C5/C5a, and their corresponding C3aR and C5aR1 on BMDCs. Antoniou et

al. found in the OVA/HDM asthma model that pulmonary cDC2s express C5aR1 at steady state, and allergen sensitization induced C5 and cleavage into C5a[641]. Other studies showed that GM-CSF or Flt3L-induced BMDCs express complement receptors, including C5aR1[642], and respond to locally produced C5a/C3a[354]. Interestingly, Antoniou et al. found that pharmacological targeting C5aR1 signaling of sensitized cDC2s controls DC-mediated T cell proliferation suggesting that C5aR1 signaling on pulmonary DCs controls allergen sensitization[641]. Another study showed that C5aR1 engagement on BMDCs enhances antigen presentation, co-stimulatory molecule expression and cytokine production, thereby influencing T cell activation and polarization in vitro and in vivo[354,642]. Strainic et al.[353,354] showed that BMDCs produce C3 (around 1000-fold higher mRNA than T cells) and upregulate C5, C5aR, and C3aR transcripts during antigen presentation to T cells, enabling autocrine/paracrine complement signaling that enhances DC-T cell interactions. Laumonnier et al.[457] reported that C3aR and C5aR1 are required on HDM-pulsed BMDCs for IL-23 production and Th17 differentiation, with double knockout DCs showing impaired allergic responses upon transfer.

Putting my data in the context of the previous findings, C5a generated in CD172a$^+$ cDCs could signal through C5aR1 either as an intracellular/autocrine loop followed by secretion, or via extracellular generation from secreted C5 cleaved by locally active proteases. Both routes are possible and not mutually exclusive. At this point it is unknown, if cDCs secrete intact C5 or if C5 is cleaved intracellularly and C5a is subsequently secreted. Importantly, my findings are in line with several studies[379,457,458,643,644] that position cell-derived complement, including C3 and C5, as a local autocrine/paracrine system in DCs and T cells, where complement fragments generated intracellularly can be secreted and engage C3aR/C5aR1 on the same cell or neighboring cells. With regard to CD172a$^+$ cDCs, it is conceivable that C5 is synthesized and at least partly cleaved to C5a in an intracellular compartment and that C5a is then secreted to bind to the C5aR1 on the cell membrane thereby regulating maturation or tolerogenic programs, depending on the environmental context. Such a mechanism would result in a tightly coupled positive or negative feedback loop in the same cell that is already known to shape DC activation states and cytokine output.

As an alternative view CD172a$^+$ cDCs may predominantly secrete intact C5, which is then cleaved extracellularly either by canonical C5 convertases assembled from complement components in the local milieu or by non-canonical proteases known to generate C5a independently of the classical convertase complexes. In vitro and tissue studies show that non-hepatic cells can release C5 that is subsequently cleaved in the pericellular space to C5a, providing a diffuse cloud of ligand that can act in a paracrine manner on C5aR1-expressing DCs and other myeloid cells[333]. Following this concept, CD172$^+$ cDCs would produce C5, which is converted into C5a in the cDC microenvironment and then engages C5aR1 on both, CD172a$^+$ and CD172a$^-$ cDCs, potentially amplifying intercellular crosstalk.

My observation of stronger C5aR1 expression in CD172a$^+$ relative to CD172a$^-$ cDCs fits well with an autocrine loop model, in which the C5a/C5aR1 axis preferentially imprints this subset with a distinct activation or tolerogenic phenotype, as described for C5aR1-high DC populations in inflammatory and tumor settings. However, evidence

that DC- and T cell–derived complement frequently operates in a combined autocrine/paracrine fashion suggests that extracellular generation from secreted C5 is likely to contribute as soon as there is sufficient C5, protease activity, and limited surface DAF/CD55 to restrain local C5a formation. Discriminating between these mechanisms experimentally would require comparing intracellular vs. secreted C5/C5a, testing protease or convertase inhibition in the in vitro culture system, and assessing whether blocking C5aR1 signaling (mixed cultures of C5aR1$^+$ and C5aR1$^-$ DCs) alters the phenotype of neighboring cells, which would specifically support an extracellular/paracrine component.

## 4.6 Expression of co-stimulatory molecules and MHC-II in MDP-derived CD172a$^-$ and CD172a$^+$ DC from WT, *C3ar1*$^{-/-}$ and *C5ar1*$^{-/-}$ mice in response to OVA stimulation

In addition to the role of the anaphylatoxins and their receptors in DC differentiation, I also explored, if they had an impact on the function of CD172a$^-$ and CD172a$^+$ cDCs. For this purpose, I focused on MDP-derived cDCs, as the yield of CD172a$^-$ and, in particular of CD172a$^-$ cDCs from CDPs, was too low to perform functional assays in sufficient numbers for statistical evaluation. I first examined the frequency and expression levels of different costimulatory molecules on the surface of CD172a$^-$ and CD172a$^+$ cDCs in response to 24h OVA stimulation. I found that both cDC subsets differed in their expression of costimulatory molecules. While the majority of CD172a$^-$ or CD172a$^+$ cDCs expressed high levels of CD80, frequencies and expression levels of CD86 and CD40 were much lower in CD172a$^+$ than in CD172a$^-$ DCs. This was also true for expression levels of MHC-II in CD172a$^+$ DCs.

MHC-II is a vital molecule on DCs that binds antigen-derived peptides and presents them to CD4$^+$ TCRs on Th cells. This is essential for Th cell activation, proliferation, and differentiation into effector subsets. The density of MHC-II complexes directly influences T cell potency[645,646]. Antoniou et al.[641] demonstrated a direct correlation between MHC-II density and T cell activation efficiency. Indeed, lower MHC-II expression limits the number of available peptide-loaded MHC-II molecules, thereby reducing TCR engagement avidity and serial triggering needed for full T cell responses. Similar effects have been reported by other groups[647,648]. My data align with this paradigm: the substantially lower MHC-II expression on CD172a$^+$ cDCs compared to CD172a$^-$ cDCs suggests a reduced potency for antigen-peptide presentation to CD4$^+$ Th cells, likely yielding weaker T cell proliferation and effector priming. This subset specific difference may reflect functional specialization, where CD172a$^+$ cDCs prioritize other roles like cytokine production over high-avidity CD4$^+$ T cell stimulation.

Importantly, CD80, CD86 and MHC-II expression were markedly reduced in CD172a$^-$ DCs from *C3ar1*$^{-/-}$ and *C5ar1*$^{-/-}$ mice. Also, only a very minor fraction of CD172a$^-$ cDCs from *C3ar1*$^{-/-}$ and *C5ar1*$^{-/-}$ mice expressed CD40. The same picture emerged in case of CD172a$^+$ DCs except for CD86, which was expressed on more cells at a higher levels in the absence of C3aR or C5aR1.

CD80, CD86, and CD40 are key costimulatory molecules on cDCs that deliver signals to $CD4^+$ T cells via CD28/CTLA-4 and CD40L interactions, promoting T cell proliferation, survival, cytokine production and their differentiation. Upon DC activation, these molecules are upregulated to license full T cell responses, with CD86 often induced earlier and more robustly than CD80, while CD40 engagement amplifies both and sustains DC function[649-652]. Data on costimulatory molecule expression specifically in BM cDC2 and DC3 from BALB/c or C57BL/6 mice are limited, and most studies instead characterize total BMDCs or bulk cDC2-like populations generated in vitro [596,653]. Nevertheless, available work on BMDC cultures and cDC2-biased systems provide a reasonable framework for interpreting CD80, CD86, and CD40 expression in the $CD172a^-$ and $CD172a^+$ cDC subsets. Protocols that used Flt3L (often with leukemia inhibitory factor and IL-10) generate cDC2-like cells from murine BM that uniformly express high levels of MHC-II, CD11c, CD11b, and costimulatory molecules CD40, CD80, and CD86 after maturation, independent of the genetic background of the mouse strain. In these cultures, TLR stimulation (e.g., TLR3, TLR4, TLR9 ligands) consistently upregulates CD80, CD86, and CD40 and confers strong potency to drive OT-II $CD4^+$ T cell proliferation and IFN-γ production, indicating that BM-derived cDC2 can exert a strongly immunogenic costimulatory phenotype[596]. GM-CSF-driven BMDCs from BALB/c and C57BL/6 show low CD80/CD86/CD40 at early time points and high expression upon full maturation, supporting efficient T cell stimulation but without clear subset resolution into cDC1/cDC2/DC3. Studies manipulating CD80/CD86 in murine BMDCs demonstrate that reducing these molecules markedly impairs Th cell activation and skews cytokine production, underlining their central role in $CD4^+$ T cell priming in this context[651,654-656].

However, there is minor knowledge about BM cDC2 and DC3. Rather, most analyses have been performed with cDC2/DC3 from blood or tissues such as spleen, tumors, or inflamed organs, where cDC2 typically show strong CD86/CD40 upregulation and DC3 display a somewhat more monocyte-like, context-dependent pattern of CD80/CD86/CD40[233,657,658]. Direct side-by-side profiling of BM cDC2 and DC3 in BALB/c or C57BL/6 is lacking. Extrapolation from in vitro BM cultures and peripheral cDC2/DC3 implies that, once matured, both subsets can express substantial CD80, CD86, and CD40, with cDC2 likely achieving the more classically high-costimulatory profile for robust $CD4^+$ T cell activation. This is in line with my findings, which show a stronger potency of $CD172a^-$ cDCs as compared to $CD172a^+$ cDCs to present antigen peptides via MHC-II to $CD4^+$ Th cells and drive their proliferation. Such proliferation also requires CD80/CD86-mediated engagement of CD28 on the T cell side. The reduced MHC-II and CD80/CD86 expression in $CD172a^-$ cDCs in the absence of the two anaphylatoxin receptors points toward a lower potency to promote T cell proliferation. The higher CD86 expression in *C3ar1*$^{-/-}$ or *C5ar1*$^{-/-}$ $CD172a^+$ cDCs may suggest a compensation mechanism to account for the reduced expression of CD86.

In summary, my findings suggest that intracellular C3/C3a and C3aR activation as well as intra and/or extracellular C5/C5a/C5aR1 activation not only affects the differentiation of the two cDC subsets but also controls the distribution and the expression levels of costimulatory molecules and of MHC-II after differentiation, which are critical for cDC-mediated activation of $CD4^+$ Th cells.

## 4.7 Potency of MDP-derived CD172a$^-$ and CD172a$^+$ cDCs from WT, *C3ar1*$^{-/-}$ or *C5ar1*$^{-/-}$ mice to drive CD4$^+$ T cell proliferation

In the next step, I determined the consequences of the observed differences between MHC-II and costimulatory molecule expression in CD172a$^-$ and CD172a$^+$ cDCs and the impact of C3aR or C5aR1-deficiency on the proliferation of CD4$^+$ Th cells. In line with the lower expression of MHC-II, CD86 and CD40 in CD172a$^-$ as compared to CD172a$^+$ cDCs, I found that CD172a$^-$ cDCs were more potent inducers of TEFF than CD172a$^+$ cDCs. In contrast, CD172a$^+$ cDCs induced TEM cells at a higher frequency than CD172a$^-$ cDCs. Despite lower MHC-II and CD40 expression, both cDC subsets from *C3ar1*$^{-/-}$ or *C5ar1*$^{-/-}$ mice were as potent as WT cDCs to drive TEFF cell proliferation from OVA-TCR transgenic DO.11.10 T cells. This is most likely due to the high 10 mM OVA concentration used to pulse the cDC subsets. Future studies with lower concentrations of OVA may help to assess the impact of lower MHC-II and costimulatory molecule expression in *C3ar1*$^{-/-}$ and *C5ar1*$^{-/-}$ CD172a$^{+/-}$ cDC subsets under conditions of limited antigen availability. Of note, the proliferation index of TEM cells was higher with CD172a$^+$ cDCs from *C3ar1*$^{-/-}$ as compared to WT mice. The higher frequency CD80 and CD86 expressing CD172a$^+$ cDCs and the higher expression levels of such molecules in *C3ar1*$^{-/-}$ as compared to WT CD172a$^+$ cDCs may account for this effect.

## 4.8 Cytokine production from OVA-pulsed MDP-derived CD172a$^-$ and CD172a$^+$ cDCs from WT, *C3ar1*$^{-/-}$ or *C5ar1*$^{-/-}$ mice

Cytokine production in response to antigen stimulation and PRR-induced priming serves as a critical signal from cDCs to differentiate CD4$^+$ Th cell into different Th subsets. Thus, I determined the production of such cytokines from the two cDC subsets in response to T cell-dependent antigen stimulation. In contrast to the higher expression of costimulatory molecules and MHC-II in CD172a$^-$ as compared to CD172a$^+$ cDCs, associated with a higher potency to drive TEFF cell proliferation after OVA stimulation, I observed a much higher potency of CD172a$^+$ cDCs than that of CD172a$^-$ cDCs to produce the cytokines IL-1α, IL-1β, IL-6 and TNF-α in response to OVA stimulation. In contrast, both cDC subsets showed a similar potency to induce the production of IL-12p40 and TGF-β. Furthermore, CD172a$^+$ cDCs from C3aR-deficient mice produced more TGF-β than CD172a$^-$ cDCs. Importantly, cytokine production from CD172a$^-$ and CD172a$^+$ cDCs differentiated from MDPs of *C3ar1*$^{-/-}$ mice, and to some extent of *C5ar1*$^{-/-}$ mice, was higher than that of WT mice. Side-by-side comparison of WT, *C3ar1*$^{-/-}$ and *C5ar1*$^{-/-}$ CD172a$^-$ - or CD172a$^+$ cDC-induced cytokine production revealed a higher potency of CD172a$^-$ or CD172a$^+$ cDCs from *C3ar1*$^{-/-}$ mice to drive the production of most of the evaluated cytokines except TNF-α. In addition, CD172a$^-$ but not CD172a$^+$ cDCs from *C5ar1*$^{-/-}$ mice showed a higher potency to promote IL-1β and TNF-α production than CD172a$^-$ cDCs from WT mice. The production of the evaluated cytokines, such as IL-6 and IL-1β is important to promote Th17 polarization (especially with TGF-β), while IL-12p40 is critical for Th1 polarization.

The cDC2 and DC3 subsets are key in shaping the cytokine profile of antigen-specific $CD4^+$ T cells, but they do so with distinct qualities rather than simple differences in strength of activation, and their output is tightly shaped by concomitant PRR signals such as LPS, which is present in most OVA preparations. LPS-mediated TLR4 priming results in cDC maturation, boosting costimulatory molecule expression and polarizing their cytokine production, which then imprints either Th1/Th2/Th17 fates in OVA-specific T cells[108,659-661]. In lung and intestinal OVA models, cDC2 presenting OVA drive IL-4, IL-5 and IL-13**,** and, depending on subset and adjuvant, substantial IL-17A and IL-22[662]. When cDC2 encounter OVA together with LPS, TLR4 signaling enhances their maturation (CD80/CD86/CD40, MHC-II) and induces IL-6, IL-1β, IL-12 and IL-23, conditions that strengthen Th17 polarization while still permitting Th1/Th2 cytokine production depending on the tissue and additional cues[663]. This goes together with my findings showing higher expression of the pro-inflammatory cytokines IL-6 and IL-1β from $CD172a^+$ than from $CD172a^-$ cDCs. Similarly, LPS-primed DC3 presenting antigen tend to drive inflammatory Th1/Th17 responses via IL-1β/IL-23 rather than tolerogenic or purely Th2 outcomes. This is in line with my finding that the LPS-containing OVA preparation that I used for this part of my thesis project resulted in strong, cytokine-rich effector responses rather than regulatory or hyporesponsive T cells[233,664-666] at least for $CD172a^+$ cDC2s.

## 4.9 IL-17A and IFN-γ production from $CD4^+$ T cells in response to stimulation with OVA-pulsed MDP-derived $CD172a^-$ and $CD172a^+$ cDCs from WT, *C3ar1*$^{-/-}$ or *C5ar1*$^{-/-}$ mice

In the final set of my in vitro experiments, I assessed the potency of the two cDC subsets to drive the differentiation of $CD4^+$ T cells. Interestingly, I found that $CD172a^+$ cDCs from either strain had a higher potency in differentiating naïve T cells into IL-17A-producing Th17 cells than $CD172a^-$ cDCs. This finding aligns with the prevailing view that cDC2s are Th17-prone although this has yet to be conclusively demonstrated for BM-derived CD172a-defined cDC subsets[667,668]. Notably, however, $CD172a^-$ and $CD172a^+$ cDCs from WT mice differentiated naïve Th cells with an equal potency to IFN-γ-producing Th1 cells, indicating that under conditions of intact C3aR or C5aR1 signaling in cDCs, the Th1 axis is not subset segregated in the GM-CSF/Flt3L BMDC differentiation system. In contrast, $CD172a^+$ cDCs from *C3ar1*$^{-/-}$ or *C5ar1*$^{-/-}$ mice were more effective drivers of Th1 lineage commitment than their $CD172a^-$ cDC counterparts. In line with spleen DC data, where C5aR1 deficiency biased toward Treg/Th17 rather than enhancing Th1[379], I found that $CD172a^-$ cDCs from *C3ar1*$^{-/-}$ or *C5ar1*$^{-/-}$ mice were less potent drivers of IFN-γ-producing Th1 cells than their WT counterparts. This also applies to $CD172a^+$ cDCs in case of C3aR-deficient mice. My data also show that there is a higher potency of $CD172a^+$ cDCs (DC3-like) as compared with $CD172a^-$ cDCs within the C3aR- or C5aR1-deficient background to drive IFN-γ production from Th cells.

The cDC2s are well established as the main $CD4^+$ T cell-priming cDC subset and are especially efficient at inducing Th2 and Th17 responses, while still supporting Th1 immunity depending on stimuli and tissue context. DC3 (and related

inflammatory/moDCs) have been shown to drive robust Th17 and mixed Th1/Th17 differentiation by producing IL-1 family cytokines and IL-23 in response to inflammatory cues. In BM systems, GM-CSF/Flt3L-derived DCs can be programmed toward Th17 vs. Th1 by skewing the IL-23/IL-12 balance (e.g., via prostaglandin $E_2$), and DCs enriched for IL-23 promote Th17 at the expense of Th1/Th2 both in vitro and in vivo. Against this background, my finding that CD172a$^+$ cDCs are superior Th17 inducers compared with CD172a$^-$ cDCs is fully in line with cDC2/DC3 biology, but it demonstrates this bias explicitly in a defined CD172a$^+$ vs. CD172a$^-$ BM-cDC system[667-671].

Several studies have shown that C3aR/C5aR on DCs shape Th1, Th17, and Treg differentiation by modulating the DC cytokine milieu. Spleen-derived DCs from *C5ar1*$^{-/-}$ mice drive fewer Th1 cells but more Tregs and Th17, associated with reduced IL-12p70 and increased TGF-β and IL-6/IL-23 signals; C5aR1 signaling therefore sets the threshold between Th1, Treg, and Th17 fates during priming. Conversely, C3aR/C5aR signaling in APCs and T cells promotes pathogenic Th1/Th17 and suppresses Tregs in graft-versus-host disease (GVHD) and pulmonary models, showing that anaphylatoxins can either enhance or restrain Th17 depending on cellular context and compartment. Most of this work used splenic or moDCs and did not differentiate CD172a$^+$ vs. CD172a$^-$ cDCs, nor did it focus on BM-resident cDC2/DC3[379,672-674].

The current literature shows that anaphylatoxin receptors on DCs regulate the Th1/Th17/Treg balance, but this mainly applies to spleen or moDCs. My findings demonstrate that within the BM-derived cDC subsets, CD172a$^+$ cDCs are clearly superior Th17 inducers as compared with CD172a$^-$ cDCs, directly linking Th17 potency to this BM-DC3-like cells. Further, the data show that deletion of C3aR1 or C5aR1 selectively increases the Th1-driving capacity of CD172a$^+$ cDCs relative to CD172a$^-$ cDCs, revealing subset specific complement control of Th1 vs. Th17 differentiation that was not clear from previous DC studies[379,672,674]. Thus, the findings of this thesis contribute to a better understanding of the complement-DC-Th axis by C3aR and C5aR1, showing that anaphylatoxin receptors in BM-cDC2/DC3 do not simply push toward or away from Th17 in a uniform manner but instead calibrate Th1 vs. Th17 output differentially across CD172a-defined cDC subsets.

## 4.10 C5aR1 controls splenic CD11c$^+$ DC mobilization through an impact on pDCs but not cDCs in response to B16-Flt3L cell injection

My in vitro experiments clearly demonstrated that C3aR and C5aR1 contribute to cDC differentiation and function. During my research stay at the laboratory of Prof. Pasare I extended the scope of my experimental approach and examined the differentiation of DCs from BM in response to Flt3L in vivo using B16-Flt3L melanoma cell injection. As expected from previous experiments in the Pasare laboratory[533,534] and in others[484,486], I found a markedly increased frequency of DCs compared to non-injected mice. Previous studies had shown that B16-Flt3L tumor injections results in expansion of pDC and cDC populations, with B16-Flt3L acting as a classic benchmark for in vivo

DC expansion[675]. In tumor-bearing mice, B16-Flt3L sites contain increased fractions of DCs (including CD11b$^{-/lo}$ cDC1-like cells) and pDCs, and Flt3L-dependent DCs help to recruit NK cells and Tregs and modulate anti-tumor immunity[676]. Flt3L signaling through Flt3 on DC progenitors engages PI3K–mTOR pathways, which are required for optimal development, particularly of pDCs and CD8$^+$/CD103$^+$ cDCs[675]. Previously, the Pasare lab[533,534] observed robust expansion of both pDCs and cDCs in response to B16-Flt3L cells, which enabled detailed functional studies on these populations.

Interestingly, C5aR1 deficiency further enhanced the frequency of splenic CD11c$^+$ DCs following B16-Flt3L cell treatment. Surprisingly, this effect appeared to be specific to pDCs, as C5aR1 deficiency led to an increased frequency of splenic pDCs but not cDCs and Flt3L-driven expansion of cDC1 and cDC2 populations into the spleen occurred independent of C5aR1 expression.

In these systems, sustained Flt3L production by the tumor increases total CD11c$^+$MHC-II$^+$ cDCs and CD11c$^{int}$PDCA1$^+$ pDCs in spleen, lymph nodes, and within the tumor bed, and the expanded DCs are functionally competent to respond to TLR ligands and stimulate T cell proliferation[675,677]. No direct studies link complement activation (e.g., C5a/C3a signaling) to pDC or cDC differentiation/mobilization specifically in the B16-Flt3L model. Complement receptors on DCs modulate their maturation, cytokine output, and survival via pathways like mTORC1 and mitophagy suppression, but these effects have been characterized in contexts like GVHD[672] or inflammation rather than Flt3L-driven expansion[437,556].

In the B16-Flt3L system, Flt3L itself dominates DC expansion through Flt3-STAT3/PI3K-mTOR signaling, with tumors inducing transient cDC and sustained pDC/Treg increases independently of complement. Inflammatory cues like type I IFN enhance pDC development alongside Flt3L[119], while mTOR and STAT5 tune cDC subset balance during tumor-driven Flt3L surges[675,676,678-680]. Guermonprez et al. found that in infection models (e.g., *Plasmodium*) innate sensing (TLRs, IL-1R) triggers inflammatory Flt3L release from non-hematopoietic cells, mobilizing DC precursors from BM via CXCR4 downregulation, paralleling potential tumor effects in B16-Flt3L but without complement involvement[200].

## 4.11 C5aR1 controls antigen and TLR-driven T cell proliferation and differentiation by splenic cDC2s

Regarding the potency of cDC2s and cDC1s to induce antigen-specific T cell proliferation, my findings demonstrate that only cDC2s but not cDC1s drive T cell proliferation in the absence of PRR priming by TLR ligands such as LPS. Moreover, C5aR1 activation appears to be crucial for the antigen-driven T cell proliferation at low antigen concentrations. These data identify C5aR1 signaling as a critical maturation pathway for cDC2s in the absence of PRRs such as TLRs. This is remarkable, as previous findings suggested that TLR activation is critical for antigen presentation by cDCs to T cells[681,682]. Also, while antigen-challenge of cDC1s in the presence of LPS preferentially induced TEM proliferation, such stimulation of cDC2 resulted in strong and preferential TEFF cell proliferation. The literature supports the idea that, under

strong PRR priming, cDC1 and cDC2 do not simply differ in magnitude of priming but imprint qualitatively different effector programs on $CD4^+$ T cells, i.e. cDC1 favoring more memory-like Th1 responses and cDC2 favoring abundant, cytokine-rich effector responses[518,667].

The cDC1 preferentially drive type 1 immunity, cross-presentation, and long-lived anti-tumor or anti-viral protection. In vaccination and tumor models, cDC1-based vaccines are repeatedly superior at generating durable $CD4^+$ and $CD8^+$ memory responses compared with cDC2, indicating that cDC1 priming favors the formation and maintenance of memory-biased effector pools rather than maximal short-lived effector bursts. Under TLR agonist conditioning, cDC1 still induce strong effector function (e.g. Th1 cytokines), but their hallmark is efficient seeding of memory-competent T cells with robust recall capacity[284,518,683,684].

The cDC2 subset excels at priming $CD4^+$ T cells against soluble or extracellular antigens and are major drivers of Th2 and Th17 effector responses. Multiple antigen-targeting studies show that cDC2 induce broad, cytokine-rich $CD4^+$ effector responses (IL-4, IL-5, IL-13, IL-17, IL-21), often generating large effector pools on a per-cell basis, whereas cDC1 responses are more focused and memory-oriented. With strong TLR stimulation (including LPS), cDC2 upregulate costimulatory molecules and inflammatory cytokines efficiently, which aligns with preferential expansion of short-lived, highly functional effector T cells[518,661,667,685,686].

These behaviours of cells are conceptually expected under uniform TLR4 priming. However, most published studies focus on Th1/Th2/Th17/Tfh polarization and overall magnitude, not on explicit TEM vs. TEFF partitioning of the $CD4^+$ compartment[108,667,685], so the observed TEM bias for cDC1 and TEFF bias for cDC2 that adds a novel layer of complexity to cDC function rather than being directly predicted in detail by existing data.

Importantly, C5aR1 signaling did not affect TEFF or TEM cell differentiation induced by cDC1 or cDC2 in response to OVA with TLR ligands, suggesting that under conditions of strong PRR activation, C5aR1 signaling does not add to the maturation process of cDCs.

There are numerous studies[458,687,688] that demonstrate extensive crosstalk between C5aR1 (and to lesser extents C3aR or C5aR2) and TLRs that bidirectionally regulates cDC maturation, with outcomes ranging from synergistic proinflammatory activation to anti-inflammatory modulation.

TLR3/4/9 ligands induce DCs to produce C3/C5 and C5a locally, which then engages autocrine C3aR/C5aR1 signaling to amplify maturation, marked by upregulated CD80/CD86/CD40/MHC-II, enhanced IL-12/IL-6 production, and superior T cell priming, as shown in murine BMDCs and in vivo models of transplant rejection[354,458,689,690]. This pathway requires *C3ar1/C5ar1* for full TLR-driven gene expression changes and TEFF expansion, positioning complement as an essential intracellular intermediary in TLR responses[458]. Conversely, C5aR1 activation inhibits TLR-induced proinflammatory cytokines (TNF-α, IL-6, IL-12) in human moDCs and slanDCs via accelerated ERK/p38/CREB phosphorylation, which boosts IL-10 and dampens Th1/CD8 responses while preserving DC maturation markers[687]. C5aR1

signaling on tumor-associated cDC2/moDCs promotes a tolerogenic phenotype (low maturation markers, poor T cell stimulation), and its absence enhances TLR-driven activation. C3aR/C5aR2 show similar regulatory synergy with TLRs in asthma/allergy models, restraining excessive Th2/Th17 via DC cytokine tuning[642,691].

The net effect depends on timing and dose of C5a, as well as the DC subset. Low C5a synergizes with TLRs to promote proinflammatory DC function, while high and sustained C5aR1 engagement induces tolerance via CREB/IL-10, as observed across moDCs, slanDCs, and cDCs. This duality underscores the role of the anaphylatoxins in fine-tuning TLR-initiated cDC maturation for balanced immunity.

Direct evidence for C5aR2-TLR crosstalk specifically regulating cDC maturation remains sparse compared to C5aR1, with most studies focusing on its roles as a modulator of C5aR1 signaling or in non-DC cells like macrophages and epithelial cells. TLR activation (e.g., LPS/TLR4) enhances C5a-induced proinflammatory responses in human PBMCs and moDCs by reducing C5aR2 expression and activity, thereby relieving its negative regulation of C5aR1 and amplifying IL-8/HMGB1 release, though this primarily tunes C5a hypersensitivity rather than directly maturing cDCs via C5aR2. No studies explicitly show C5aR2 mediating TLR-driven upregulation of DC maturation markers (CD80/CD86/CD40/MHC-II) or cytokine production in bona fide cDCs[692-694].

These findings are consistent with my data from MDP-derived cDC subsets, which demonstrated that the absence of C5aR1 did not affect the proliferation of TEFF cell induction by either CD172a$^-$ or CD172a$^+$ cDCs. Finally, I observed that C5aR1 contributes to the dominant induction of IFN-γ producing Th1 cells by spleen-derived cDC2s, which is accordance with my finding that C5aR1 controls antigen-driven IFN-γ production from OVA-tg T cells in response to stimulation with CD172a$^-$ cDCs. Collectively, these results uncover a novel role of C5aR1 in antigen-driven TEFF differentiation by splenic cDC2 cells and their differentiation into Th1 cells upon PRR activation.

## 4.12 The mouse as a model organism to study spleen- and BM-derived cDC differentiation and functions

As already discussed in detail, DCs represent a highly heterogeneous population present in humans and mice, including cDC1, cDC2, and DC3 subsets. Although these subsets share conserved transcriptional programs and functional roles across species, important phenotypic and molecular differences have been reported between murine and human DCs[64,65,81]. Therefore, while murine models are indispensable for mechanistic studies of DC differentiation and function, translating these findings to humans requires careful consideration of interspecies differences.

The use of inbred strains ensures high experimental reproducibility, while the availability of genetically modified lines, such as knockout and reporter knock-in mice, provides powerful tools for studying the functions of specific genes and molecular pathways.

My findings on DCs need to be considered in the context of strain-specific differences in DC differentiation and function. Several studies have highlighted that BMDCs generated from BALB/c mice exhibit a distinct phenotype compared with those derived from other mouse strains. In particular, BALB/c BMDCs often display reduced functional maturation, reflected in lower surface expression of co-stimulatory molecules and weakened production of IL-12 upon stimulation[695-697].

On the other hand, splenic DCs from C57BL/6 mice have been reported to express higher levels of certain TLRs, including TLR9, and respond with robust IL-12 secretion and Th1-polarizing activity when compared with their BALB/c counterparts[696]. More recent comparative work confirms these differences. C57BL/6 DCs, whether BM–derived or splenic, tend to upregulate MHC-II and co-stimulatory molecules more strongly and produce higher levels of pro-inflammatory cytokines such as IL-12p40 and IFN-γ in response to identical stimuli[696,697]. Such findings reinforce the established paradigm that C57BL/6 mice are generally Th1-, whereas BALB/c mice are Th2-biased, with these biases are already imprinted at the level of DC differentiation and function[698].

Taken together, these data underscore an important point: while both BALB/c and C57BL/6 mice serve as valuable model systems for studying DC biology, their baseline immune biases and DC subset characteristics are not directly interchangeable. Functional differences between BMDCs and splenic DCs from these strains may reflect intrinsic transcriptional programming, differential responsiveness to growth factors such as GM-CSF or Flt3L, and broader Th1/Th2 systemic predispositions. Therefore, direct one-to-one comparisons between strains must be interpreted with caution.

# Conclusions and future prospective

My thesis project revealed that C5aR1 functions as a critical regulator of BM progenitor cell homeostasis, specifically impacting MDPs and CDPs. Single-cell transcriptomics of MDPs from C5aR1-deficient mice uncovered increased CD300c expression, a marker identifying a pro-cDC2 progenitor population that is essential for humoral immunity. I also found autonomous complement factor production , particularly of C3, C5, and their cleavage into the active fragments C3a and C5a during cDC differentiation. Additionally, I noted the expression of C3aR and C5aR1 suggesting an autocrine regulatory loop that guides the differentiation of cDC subsets from CDPs and MDPs during different phases of cDC differentiation. This is further corroborated by altered kinetics of $CD172a^-$ and $CD172a^+$ cDC differentiation in the absence of C3aR or C5aR1. My findings further suggest that this autocrine loop not only regulates cDC subset differentiation but functional properties as evidenced by altered MHC-II and costimulatory molecule expression and the potency of MDP-derived cDC subsets to differentiate $CD4^+$ T cell into IFN-γ-producing Th1 cells in response to antigen challenge. Importantly, my experiments with in vivo expanded splenic cDC2s corroborated these results suggesting that the impact of C5aR1 on Th1 differentiation also applies to cDCs after homing into secondary lymphoid organs such as the spleen. My B16-Flt3L injection experiments further showed that C5aR1 also regulates the expansion splenic DCs and revealed that cDC2 subsets are more effective than cDC1 in driving antigen-specific proliferation of naïve $CD4^+$ T cells in the absence microbial

cues and that C5aR1 serves as an important cDC2 maturation signal under these conditions. Together, these findings establish a novel autocrine complement axis that influences cDC development and T cell immunity.

Future directions should include the precise classification of CD172a$^-$ and CD172a$^+$ cDCs in the DC nomenclature, particularly given the upregulation of CD300c, a marker associated with pro-cDC2 progenitors, in several clusters based on the transcriptomic profiling data. Confirming CD172a$^+$ cDCs as DC3 by qPCR would be invaluable, especially considering the limited understanding of DC3 functions in murine models. Further, adoptive transfer of sorted CD172a$^-$ and CD172a$^+$ DCs into cDC-deficient mice would help to clarify their in vivo behavior and functional roles. To explore synergistic or redundant roles of C3aR and C5aR1 on cDC differentiation and function, mice with combined deficiency of C3aR and C5aR1 would be instrumental. In line, using C5aR2-deficient mice would further add to the picture of how C5a controls DC biology. Pharmacologic interventions using specific C5aR1 antagonists such as PMX53[699,700] could be tested to assess the impact of C5aR1 on cDC differentiation and function to validate the findings from genetic knockouts. Transcriptomic profiling of sorted CD172a$^-$ and CD172a$^+$ cDCs at baseline and post-OVA stimulation would provide insights into transcriptional programs driving differentiation and activation. Further, dose-response studies employing different OVA concentrations could determine, if antigen-load influences TEM and TEFF generation, revealing potential thresholds for anaphylatoxin-mediated effects. Intracellular staining for IL-17A and IFN-γ would complement the existing data to confirm Th17 and Th1 cell subset induction. Additionally, mechanistic studies to dissect the synergy between C5aR1 and TLR4 signaling pathways, alongside assessment of IL-12 production by splenic C5aR1-deficient DC following TLR activation, are warranted. Finally, analysis of T-bet and other lineage-defining transcription factors in T cells primed with WT or C5aR1-deficient DC, as well as single-cell transcriptomics of splenic cDC1 and cDC2 subsets across genotypes, will deepen our understanding of how anaphylatoxin receptors influence DC-mediated T cell programming.

Understanding DC biology is essential because DCs serve as the principal APCs that bridge innate and adaptive immunity, orchestrating immune responses by activating naïve T cells and maintaining immune tolerance. They play critical roles in detecting pathogens, presenting antigens, and directing the differentiation of various T cell subsets, thus influencing both protective immunity and immune regulation. Moreover, DCs are pivotal in controlling inflammation, shaping immune homeostasis, and are implicated in autoimmune diseases, infections, cancer, and transplantation responses, making them vital targets for therapeutic interventions and vaccine development. Understanding their dynamic functionalities provides insights vital for designing effective immunotherapies and advancing clinical applications.

# References


1. Littman RJ. The plague of Athens: epidemiology and paleopathology. *Mt Sinai J Med*. 2009;76(5):456-467.
2. Smith KA. Louis pasteur, the father of immunology? *Front Immunol*. 2012;3:68.
3. Matzinger P. The danger model: a renewed sense of self. *Science*. 2002;296(5566):301-305.
4. Tomar N, De RK. A brief outline of the immune system. *Methods Mol Biol*. 2014;1184:3-12.
5. Kohl J. The role of complement in danger sensing and transmission. *Immunol Res*. 2006;34(2):157-176.
6. Murphy K, Weaver C, Berg L, Barton G. Janeway's immunobiology (ed 10th edition.). New York, NY: W.W. Norton and Company; 2022.
7. Bonilla FA, Oettgen HC. Adaptive immunity. *J Allergy Clin Immunol*. 2010;125(2 Suppl 2):S33-40.
8. Kaur BP, Secord E. Innate Immunity. *Immunol Allergy Clin North Am*. 2021;41(4):535-541.
9. Dainichi T, Kitoh A, Otsuka A, et al. The epithelial immune microenvironment (EIME) in atopic dermatitis and psoriasis. *Nat Immunol*. 2018;19(12):1286-1298.
10. Turvey SE, Broide DH. Innate immunity. *J Allergy Clin Immunol*. 2010;125(2 Suppl 2):S24-32.
11. Rimer J, Cohen IR, Friedman N. Do all creatures possess an acquired immune system of some sort? *Bioessays*. 2014;36(3):273-281.
12. Wendeln AC, Degenhardt K, Kaurani L, et al. Innate immune memory in the brain shapes neurological disease hallmarks. *Nature*. 2018;556(7701):332-338.
13. Khodadadi L, Cheng Q, Radbruch A, Hiepe F. The Maintenance of Memory Plasma Cells. *Front Immunol*. 2019;10:721.
14. Pancer Z, Cooper MD. The evolution of adaptive immunity. *Annu Rev Immunol*. 2006;24:497-518.
15. Modlin RL. Innate immunity: ignored for decades, but not forgotten. *J Invest Dermatol*. 2012;132(3 Pt 2):882-886.
16. Kaufmann SH. Immunology's foundation: the 100-year anniversary of the Nobel Prize to Paul Ehrlich and Elie Metchnikoff. *Nat Immunol*. 2008;9(7):705-712.
17. Lokaj J, John C. [Ilya Ilich Metchnikov and Paul Ehrlich: 1908 Nobel Prize winners for their research on immunity]. *Epidemiol Mikrobiol Imunol*. 2008;57(4):119-124.
18. Carpenter S, O'Neill LAJ. From periphery to center stage: 50 years of advancements in innate immunity. *Cell*. 2024;187(23):6780-6782.
19. Buchmann K. Evolution of Innate Immunity: Clues from Invertebrates via Fish to Mammals. *Front Immunol*. 2014;5:459.
20. Riera Romo M, Perez-Martinez D, Castillo Ferrer C. Innate immunity in vertebrates: an overview. *Immunology*. 2016;148(2):125-139.
21. Janeway CA, Jr. Approaching the asymptote? Evolution and revolution in immunology. *Cold Spring Harb Symp Quant Biol*. 1989;54 Pt 1:1-13.
22. Beutler B. Innate immunity: an overview. *Mol Immunol*. 2004;40(12):845-859.
23. Iwasaki A, Medzhitov R. Control of adaptive immunity by the innate immune system. *Nat Immunol*. 2015;16(4):343-353.
24. Medzhitov R, Janeway CA, Jr. Decoding the patterns of self and nonself by the innate immune system. *Science*. 2002;296(5566):298-300.
25. Foo SS, Reading PC, Jaillon S, Mantovani A, Mahalingam S. Pentraxins and Collectins: Friend or Foe during Pathogen Invasion? *Trends Microbiol*. 2015;23(12):799-811.
26. Takeuchi O, Akira S. Pattern recognition receptors and inflammation. *Cell*. 2010;140(6):805-820.
27. Cooper D, Eleftherianos I. Memory and Specificity in the Insect Immune System: Current Perspectives and Future Challenges. *Front Immunol*. 2017;8:539.

28. Goic B, Vodovar N, Mondotte JA, et al. RNA-mediated interference and reverse transcription control the persistence of RNA viruses in the insect model Drosophila. *Nat Immunol*. 2013;14(4):396-403.
29. West C, Silverman N. Drosophilosophical: Re-thinking Adaptive Immunity in the Fly. *Cell*. 2017;169(2):188-190.
30. Flemming A. Insect Immunity: Mechanism of adaptive immunity found in the fruitfly. *Nat Rev Immunol*. 2017;17(5):278-279.
31. Kasamatsu J. Evolution of innate and adaptive immune systems in jawless vertebrates. *Microbiol Immunol*. 2013;57(1):1-12.
32. Basha S, Surendran N, Pichichero M. Immune responses in neonates. *Expert Rev Clin Immunol*. 2014;10(9):1171-1184.
33. Boehm T, Swann JB. Origin and evolution of adaptive immunity. *Annu Rev Anim Biosci*. 2014;2:259-283.
34. LeBien TW, Tedder TF. B lymphocytes: how they develop and function. *Blood*. 2008;112(5):1570-1580.
35. Kondo M. Lymphoid and myeloid lineage commitment in multipotent hematopoietic progenitors. *Immunol Rev*. 2010;238(1):37-46.
36. Cooper MD. The early history of B cells. *Nat Rev Immunol*. 2015;15(3):191-197.
37. Sallusto F, Lanzavecchia A. The instructive role of dendritic cells on T-cell responses. *Arthritis Res*. 2002;4 Suppl 3(Suppl 3):S127-132.
38. Rothoeft T, Balkow S, Krummen M, et al. Structure and duration of contact between dendritic cells and T cells are controlled by T cell activation state. *Eur J Immunol*. 2006;36(12):3105-3117.
39. Walchli S, Kumari S, Fallang LE, et al. Invariant chain as a vehicle to load antigenic peptides on human MHC class I for cytotoxic T-cell activation. *Eur J Immunol*. 2014;44(3):774-784.
40. Mellman I, Steinman RM. Dendritic cells: specialized and regulated antigen processing machines. *Cell*. 2001;106(3):255-258.
41. Wilson NS, Villadangos JA. Regulation of antigen presentation and cross-presentation in the dendritic cell network: facts, hypothesis, and immunological implications. *Adv Immunol*. 2005;86:241-305.
42. Steinman RM, Cohn ZA. Identification of a novel cell type in peripheral lymphoid organs of mice. I. Morphology, quantitation, tissue distribution. *J Exp Med*. 1973;137(5):1142-1162.
43. Li Z, Yang Y, Zong J, et al. Dendritic cells immunotargeted therapy for atherosclerosis. *Acta Pharm Sin B*. 2025;15(2):792-808.
44. Collin M, Ginhoux F. Human dendritic cells. *Semin Cell Dev Biol*. 2019;86:1-2.
45. Vandenabeele S, Wu L. Dendritic cell origins: puzzles and paradoxes. *Immunol Cell Biol*. 1999;77(5):411-419.
46. Wu L, Liu YJ. Development of dendritic-cell lineages. *Immunity*. 2007;26(6):741-750.
47. Merad M, Sathe P, Helft J, Miller J, Mortha A. The dendritic cell lineage: ontogeny and function of dendritic cells and their subsets in the steady state and the inflamed setting. *Annu Rev Immunol*. 2013;31:563-604.
48. Doulatov S, Notta F, Eppert K, Nguyen LT, Ohashi PS, Dick JE. Revised map of the human progenitor hierarchy shows the origin of macrophages and dendritic cells in early lymphoid development. *Nat Immunol*. 2010;11(7):585-593.
49. Lee J, Zhou YJ, Ma W, et al. Lineage specification of human dendritic cells is marked by IRF8 expression in hematopoietic stem cells and multipotent progenitors. *Nat Immunol*. 2017;18(8):877-888.
50. Fogg DK, Sibon C, Miled C, et al. A clonogenic bone marrow progenitor specific for macrophages and dendritic cells. *Science*. 2006;311(5757):83-87.

51. Naik SH, Sathe P, Park HY, et al. Development of plasmacytoid and conventional dendritic cell subtypes from single precursor cells derived in vitro and in vivo. *Nat Immunol*. 2007;8(11):1217-1226.
52. Onai N, Obata-Onai A, Schmid MA, Ohteki T, Jarrossay D, Manz MG. Identification of clonogenic common Flt3+M-CSFR+ plasmacytoid and conventional dendritic cell progenitors in mouse bone marrow. *Nat Immunol*. 2007;8(11):1207-1216.
53. Grajales-Reyes GE, Iwata A, Albring J, et al. Batf3 maintains autoactivation of Irf8 for commitment of a CD8alpha(+) conventional DC clonogenic progenitor. *Nat Immunol*. 2015;16(7):708-717.
54. Schlitzer A, Sivakamasundari V, Chen J, et al. Identification of cDC1- and cDC2-committed DC progenitors reveals early lineage priming at the common DC progenitor stage in the bone marrow. *Nat Immunol*. 2015;16(7):718-728.
55. Liu K, Victora GD, Schwickert TA, et al. In vivo analysis of dendritic cell development and homeostasis. *Science*. 2009;324(5925):392-397.
56. See P, Dutertre CA, Chen J, et al. Mapping the human DC lineage through the integration of high-dimensional techniques. *Science*. 2017;356(6342).
57. Minutti CM, Piot C, Pereira da Costa M, et al. Distinct ontogenetic lineages dictate cDC2 heterogeneity. *Nat Immunol*. 2024;25(3):448-461.
58. Rodrigues PF, Trsan T, Cvijetic G, et al. Progenitors of distinct lineages shape the diversity of mature type 2 conventional dendritic cells. *Immunity*. 2024;57(7):1567-1585 e1565.
59. Brown CC, Gudjonson H, Pritykin Y, et al. Transcriptional Basis of Mouse and Human Dendritic Cell Heterogeneity. *Cell*. 2019;179(4):846-863 e824.
60. Amon L, Seichter A, Vurnek D, et al. Clec12A, CD301b, and FcgammaRIIB/III define the heterogeneity of murine DC2s and DC3s. *Cell Rep*. 2024;43(3):113949.
61. Liu Z, Wang H, Li Z, et al. Dendritic cell type 3 arises from Ly6C(+) monocyte-dendritic cell progenitors. *Immunity*. 2023;56(8):1761-1777 e1766.
62. Cytlak U, Resteu A, Pagan S, et al. Differential IRF8 Transcription Factor Requirement Defines Two Pathways of Dendritic Cell Development in Humans. *Immunity*. 2020;53(2):353-370 e358.
63. Dutertre CA, Becht E, Irac SE, et al. Single-Cell Analysis of Human Mononuclear Phagocytes Reveals Subset-Defining Markers and Identifies Circulating Inflammatory Dendritic Cells. *Immunity*. 2019;51(3):573-589 e578.
64. Villani AC, Satija R, Reynolds G, et al. Single-cell RNA-seq reveals new types of human blood dendritic cells, monocytes, and progenitors. *Science*. 2017;356(6335).
65. Bourdely P, Anselmi G, Vaivode K, et al. Transcriptional and Functional Analysis of CD1c(+) Human Dendritic Cells Identifies a CD163(+) Subset Priming CD8(+)CD103(+) T Cells. *Immunity*. 2020;53(2):335-352 e338.
66. Rodrigues PF, Alberti-Servera L, Eremin A, Grajales-Reyes GE, Ivanek R, Tussiwand R. Distinct progenitor lineages contribute to the heterogeneity of plasmacytoid dendritic cells. *Nat Immunol*. 2018;19(7):711-722.
67. Feng J, Pucella JN, Jang G, et al. Clonal lineage tracing reveals shared origin of conventional and plasmacytoid dendritic cells. *Immunity*. 2022;55(3):405-422 e411.
68. Segura E. Human dendritic cell subsets: An updated view of their ontogeny and functional specialization. *Eur J Immunol*. 2022;52(11):1759-1767.
69. McKenna HJ, Stocking KL, Miller RE, et al. Mice lacking flt3 ligand have deficient hematopoiesis affecting hematopoietic progenitor cells, dendritic cells, and natural killer cells. *Blood*. 2000;95(11):3489-3497.
70. Waskow C, Liu K, Darrasse-Jeze G, et al. The receptor tyrosine kinase Flt3 is required for dendritic cell development in peripheral lymphoid tissues. *Nat Immunol*. 2008;9(6):676-683.
71. Maraskovsky E, Brasel K, Teepe M, et al. Dramatic increase in the numbers of functionally mature dendritic cells in Flt3 ligand-treated mice: multiple dendritic cell subpopulations identified. *J Exp Med*. 1996;184(5):1953-1962.

72. Anandasabapathy N, Breton G, Hurley A, et al. Efficacy and safety of CDX-301, recombinant human Flt3L, at expanding dendritic cells and hematopoietic stem cells in healthy human volunteers. *Bone Marrow Transplant*. 2015;50(7):924-930.
73. Pulendran B, Banchereau J, Burkeholder S, et al. Flt3-ligand and granulocyte colony-stimulating factor mobilize distinct human dendritic cell subsets in vivo. *J Immunol*. 2000;165(1):566-572.
74. Ding Y, Wilkinson A, Idris A, et al. FLT3-ligand treatment of humanized mice results in the generation of large numbers of CD141+ and CD1c+ dendritic cells in vivo. *J Immunol*. 2014;192(4):1982-1989.
75. Vremec D, Lieschke GJ, Dunn AR, Robb L, Metcalf D, Shortman K. The influence of granulocyte/macrophage colony-stimulating factor on dendritic cell levels in mouse lymphoid organs. *Eur J Immunol*. 1997;27(1):40-44.
76. Liu Z, Gu Y, Chakarov S, et al. Fate Mapping via Ms4a3-Expression History Traces Monocyte-Derived Cells. *Cell*. 2019;178(6):1509-1525 e1519.
77. Anderson DA, 3rd, Dutertre CA, Ginhoux F, Murphy KM. Genetic models of human and mouse dendritic cell development and function. *Nat Rev Immunol*. 2021;21(2):101-115.
78. Backer RA, Probst HC, Clausen BE. Classical DC2 subsets and monocyte-derived DC: Delineating the developmental and functional relationship. *Eur J Immunol*. 2023;53(3):e2149548.
79. Zhang S, Audiger C, Chopin M, Nutt SL. Transcriptional regulation of dendritic cell development and function. *Front Immunol*. 2023;14:1182553.
80. Ascic E, Pereira CF. Transcription factor-mediated reprogramming to antigen-presenting cells. *Curr Opin Genet Dev*. 2025;90:102300.
81. Guilliams M, Ginhoux F, Jakubzick C, et al. Dendritic cells, monocytes and macrophages: a unified nomenclature based on ontogeny. *Nat Rev Immunol*. 2014;14(8):571-578.
82. Guermonprez P, Gerber-Ferder Y, Vaivode K, Bourdely P, Helft J. Origin and development of classical dendritic cells. *Int Rev Cell Mol Biol*. 2019;349:1-54.
83. Shortman K, Heath WR. The CD8+ dendritic cell subset. *Immunol Rev*. 2010;234(1):18-31.
84. Bedoui S, Whitney PG, Waithman J, et al. Cross-presentation of viral and self antigens by skin-derived CD103+ dendritic cells. *Nat Immunol*. 2009;10(5):488-495.
85. Edelson BT, Kc W, Juang R, et al. Peripheral CD103+ dendritic cells form a unified subset developmentally related to CD8alpha+ conventional dendritic cells. *J Exp Med*. 2010;207(4):823-836.
86. Ginhoux F, Liu K, Helft J, et al. The origin and development of nonlymphoid tissue CD103+ DCs. *J Exp Med*. 2009;206(13):3115-3130.
87. Sung SS, Fu SM, Rose CE, Jr., Gaskin F, Ju ST, Beaty SR. A major lung CD103 (alphaE)-beta7 integrin-positive epithelial dendritic cell population expressing Langerin and tight junction proteins. *J Immunol*. 2006;176(4):2161-2172.
88. del Rio ML, Rodriguez-Barbosa JI, Kremmer E, Forster R. CD103- and CD103+ bronchial lymph node dendritic cells are specialized in presenting and cross-presenting innocuous antigen to CD4+ and CD8+ T cells. *J Immunol*. 2007;178(11):6861-6866.
89. Crozat K, Guiton R, Guilliams M, et al. Comparative genomics as a tool to reveal functional equivalences between human and mouse dendritic cell subsets. *Immunol Rev*. 2010;234(1):177-198.
90. Schraml BU, van Blijswijk J, Zelenay S, et al. Genetic tracing via DNGR-1 expression history defines dendritic cells as a hematopoietic lineage. *Cell*. 2013;154(4):843-858.
91. Guilliams M, Dutertre CA, Scott CL, et al. Unsupervised High-Dimensional Analysis Aligns Dendritic Cells across Tissues and Species. *Immunity*. 2016;45(3):669-684.
92. Chandra J, Kuo PT, Hahn AM, Belz GT, Frazer IH. Batf3 selectively determines acquisition of CD8(+) dendritic cell phenotype and function. *Immunol Cell Biol*. 2017;95(2):215-223.
93. Chopin M, Lun AT, Zhan Y, et al. Transcription Factor PU.1 Promotes Conventional Dendritic Cell Identity and Function via Induction of Transcriptional Regulator DC-SCRIPT. *Immunity*. 2019;50(1):77-90 e75.

94. Rosa FF, Pires CF, Kurochkin I, et al. Direct reprogramming of fibroblasts into antigen-presenting dendritic cells. *Sci Immunol*. 2018;3(30).
95. Carotta S, Dakic A, D'Amico A, et al. The transcription factor PU.1 controls dendritic cell development and Flt3 cytokine receptor expression in a dose-dependent manner. *Immunity*. 2010;32(5):628-641.
96. Meredith MM, Liu K, Darrasse-Jeze G, et al. Expression of the zinc finger transcription factor zDC (Zbtb46, Btbd4) defines the classical dendritic cell lineage. *J Exp Med*. 2012;209(6):1153-1165.
97. Lewis KL, Caton ML, Bogunovic M, et al. Notch2 receptor signaling controls functional differentiation of dendritic cells in the spleen and intestine. *Immunity*. 2011;35(5):780-791.
98. Hemont C, Neel A, Heslan M, Braudeau C, Josien R. Human blood mDC subsets exhibit distinct TLR repertoire and responsiveness. *J Leukoc Biol*. 2013;93(4):599-609.
99. Hatscher L, Amon L, Heger L, Dudziak D. Inflammasomes in dendritic cells: Friend or foe? *Immunol Lett*. 2021;234:16-32.
100. Molla MD, Akalu Y, Geto Z, Dagnew B, Ayelign B, Shibabaw T. Role of Caspase-1 in the Pathogenesis of Inflammatory-Associated Chronic Noncommunicable Diseases. *J Inflamm Res*. 2020;13:749-764.
101. Lauterbach H, Bathke B, Gilles S, et al. Mouse CD8alpha+ DCs and human BDCA3+ DCs are major producers of IFN-lambda in response to poly IC. *J Exp Med*. 2010;207(12):2703-2717.
102. Flores-Langarica A, Cook C, Muller Luda K, et al. Intestinal CD103(+)CD11b(+) cDC2 Conventional Dendritic Cells Are Required for Primary CD4(+) T and B Cell Responses to Soluble Flagellin. *Front Immunol*. 2018;9:2409.
103. Gribonika I, Stromberg A, Chandode RK, et al. Migratory CD103(+)CD11b(+) cDC2s in Peyer's patches are critical for gut IgA responses following oral immunization. *Mucosal Immunol*. 2024;17(4):509-523.
104. Luciani C, Hager FT, Cerovic V, Lelouard H. Dendritic cell functions in the inductive and effector sites of intestinal immunity. *Mucosal Immunol*. 2022;15(1):40-50.
105. Rivera CA, Randrian V, Richer W, et al. Epithelial colonization by gut dendritic cells promotes their functional diversification. *Immunity*. 2022;55(1):129-144 e128.
106. Russler-Germain EV, Yi J, Young S, et al. Gut Helicobacter presentation by multiple dendritic cell subsets enables context-specific regulatory T cell generation. *Elife*. 2021;10.
107. Shin JY, Wang CY, Lin CC, Chu CL. A recently described type 2 conventional dendritic cell (cDC2) subset mediates inflammation. *Cell Mol Immunol*. 2020;17(12):1215-1217.
108. Papaioannou NE, Salei N, Rambichler S, et al. Environmental signals rather than layered ontogeny imprint the function of type 2 conventional dendritic cells in young and adult mice. *Nat Commun*. 2021;12(1):464.
109. Chen B, Zhu L, Yang S, Su W. Unraveling the Heterogeneity and Ontogeny of Dendritic Cells Using Single-Cell RNA Sequencing. *Front Immunol*. 2021;12:711329.
110. Yin X, Yu H, Jin X, et al. Human Blood CD1c+ Dendritic Cells Encompass CD5high and CD5low Subsets That Differ Significantly in Phenotype, Gene Expression, and Functions. *J Immunol*. 2017;198(4):1553-1564.
111. Korenfeld D, Gorvel L, Munk A, et al. A type of human skin dendritic cell marked by CD5 is associated with the development of inflammatory skin disease. *JCI Insight*. 2017;2(18).
112. Tussiwand R, Everts B, Grajales-Reyes GE, et al. Klf4 expression in conventional dendritic cells is required for T helper 2 cell responses. *Immunity*. 2015;42(5):916-928.
113. Satpathy AT, Briseno CG, Lee JS, et al. Notch2-dependent classical dendritic cells orchestrate intestinal immunity to attaching-and-effacing bacterial pathogens. *Nat Immunol*. 2013;14(9):937-948.
114. Li S, Dislich B, Brakebusch CH, Lichtenthaler SF, Brocker T. Control of Homeostasis and Dendritic Cell Survival by the GTPase RhoA. *J Immunol*. 2015;195(9):4244-4256.
115. Klebanoff CA, Spencer SP, Torabi-Parizi P, et al. Retinoic acid controls the homeostasis of pre-cDC-derived splenic and intestinal dendritic cells. *J Exp Med*. 2013;210(10):1961-1976.

116. Heidkamp GF, Sander J, Lehmann CHK, et al. Human lymphoid organ dendritic cell identity is predominantly dictated by ontogeny, not tissue microenvironment. *Sci Immunol*. 2016;1(6).
117. Macri C, Pang ES, Patton T, O'Keeffe M. Dendritic cell subsets. *Semin Cell Dev Biol*. 2018;84:11-21.
118. Schlitzer A, McGovern N, Ginhoux F. Dendritic cells and monocyte-derived cells: Two complementary and integrated functional systems. *Semin Cell Dev Biol*. 2015;41:9-22.
119. Swiecki M, Colonna M. The multifaceted biology of plasmacytoid dendritic cells. *Nat Rev Immunol*. 2015;15(8):471-485.
120. Reizis B. Plasmacytoid Dendritic Cells: Development, Regulation, and Function. *Immunity*. 2019;50(1):37-50.
121. Bar-On L, Birnberg T, Lewis KL, et al. CX3CR1+ CD8alpha+ dendritic cells are a steady-state population related to plasmacytoid dendritic cells. *Proc Natl Acad Sci U S A*. 2010;107(33):14745-14750.
122. Lau CM, Nish SA, Yogev N, Waisman A, Reiner SL, Reizis B. Leukemia-associated activating mutation of Flt3 expands dendritic cells and alters T cell responses. *J Exp Med*. 2016;213(3):415-431.
123. Araujo AM, Dekker JD, Garrison K, et al. Lymphoid origin of intrinsically activated plasmacytoid dendritic cells in mice. *Elife*. 2024;13.
124. Schmid ET, Pang IK, Carrera Silva EA, et al. AXL receptor tyrosine kinase is required for T cell priming and antiviral immunity. *Elife*. 2016;5.
125. Zhang D, Zhao Y, Wang L, et al. Axl Mediates Resistance to Respiratory Syncytial Virus Infection Independent of Cell Attachment. *Am J Respir Cell Mol Biol*. 2022;67(2):227-240.
126. O'Keeffe M, Hochrein H, Vremec D, et al. Mouse plasmacytoid cells: long-lived cells, heterogeneous in surface phenotype and function, that differentiate into CD8(+) dendritic cells only after microbial stimulus. *J Exp Med*. 2002;196(10):1307-1319.
127. Sawai CM, Sisirak V, Ghosh HS, et al. Transcription factor Runx2 controls the development and migration of plasmacytoid dendritic cells. *J Exp Med*. 2013;210(11):2151-2159.
128. Gilliet M, Cao W, Liu YJ. Plasmacytoid dendritic cells: sensing nucleic acids in viral infection and autoimmune diseases. *Nat Rev Immunol*. 2008;8(8):594-606.
129. Kawai T, Akira S. Toll-like receptors and their crosstalk with other innate receptors in infection and immunity. *Immunity*. 2011;34(5):637-650.
130. Honda K, Yanai H, Negishi H, et al. IRF-7 is the master regulator of type-I interferon-dependent immune responses. *Nature*. 2005;434(7034):772-777.
131. Schmid MA, Kingston D, Boddupalli S, Manz MG. Instructive cytokine signals in dendritic cell lineage commitment. *Immunol Rev*. 2010;234(1):32-44.
132. Chen YL, Chen TT, Pai LM, Wesoly J, Bluyssen HA, Lee CK. A type I IFN-Flt3 ligand axis augments plasmacytoid dendritic cell development from common lymphoid progenitors. *J Exp Med*. 2013;210(12):2515-2522.
133. Grajkowska LT, Ceribelli M, Lau CM, et al. Isoform-Specific Expression and Feedback Regulation of E Protein TCF4 Control Dendritic Cell Lineage Specification. *Immunity*. 2017;46(1):65-77.
134. Ghosh HS, Ceribelli M, Matos I, et al. ETO family protein Mtg16 regulates the balance of dendritic cell subsets by repressing Id2. *J Exp Med*. 2014;211(8):1623-1635.
135. Bigley V, Maisuria S, Cytlak U, et al. Biallelic interferon regulatory factor 8 mutation: A complex immunodeficiency syndrome with dendritic cell deficiency, monocytopenia, and immune dysregulation. *J Allergy Clin Immunol*. 2018;141(6):2234-2248.
136. Hambleton S, Salem S, Bustamante J, et al. IRF8 mutations and human dendritic-cell immunodeficiency. *N Engl J Med*. 2011;365(2):127-138.
137. Sichien D, Scott CL, Martens L, et al. IRF8 Transcription Factor Controls Survival and Function of Terminally Differentiated Conventional and Plasmacytoid Dendritic Cells, Respectively. *Immunity*. 2016;45(3):626-640.

138. Tailor P, Tamura T, Morse HC, 3rd, Ozato K. The BXH2 mutation in IRF8 differentially impairs dendritic cell subset development in the mouse. *Blood*. 2008;111(4):1942-1945.
139. Allman D, Dalod M, Asselin-Paturel C, et al. Ikaros is required for plasmacytoid dendritic cell differentiation. *Blood*. 2006;108(13):4025-4034.
140. Wu X, Briseno CG, Grajales-Reyes GE, et al. Transcription factor Zeb2 regulates commitment to plasmacytoid dendritic cell and monocyte fate. *Proc Natl Acad Sci U S A*. 2016;113(51):14775-14780.
141. Chopin M, Preston SP, Lun ATL, et al. RUNX2 Mediates Plasmacytoid Dendritic Cell Egress from the Bone Marrow and Controls Viral Immunity. *Cell Rep*. 2016;15(4):866-878.
142. Modrow S, Falke D, Truyen U, Schätzl H. Molecular virology. Heidelberg: Springer; 2013.
143. Steinman RM. Decisions about dendritic cells: past, present, and future. *Annu Rev Immunol*. 2012;30:1-22.
144. Lohrer MF, Liu Y, Hanna DM, et al. Determination of the Maturation Status of Dendritic Cells by Applying Pattern Recognition to High-Resolution Images. *J Phys Chem B*. 2020;124(39):8540-8548.
145. Landi A, Aligodarzi MT, Khodadadi A, Babiuk LA, van Drunen Littel-van den Hurk S. Defining a standard and weighted mathematical index for maturation of dendritic cells. *Immunology*. 2018;153(4):532-544.
146. Tiberio L, Del Prete A, Schioppa T, Sozio F, Bosisio D, Sozzani S. Chemokine and chemotactic signals in dendritic cell migration. *Cell Mol Immunol*. 2018;15(4):346-352.
147. Zanna MY, Yasmin AR, Omar AR, et al. Review of Dendritic Cells, Their Role in Clinical Immunology, and Distribution in Various Animal Species. *Int J Mol Sci*. 2021;22(15).
148. Sato K, Fujita S. Dendritic cells: nature and classification. *Allergol Int*. 2007;56(3):183-191.
149. Steinman RM, Hawiger D, Nussenzweig MC. Tolerogenic dendritic cells. *Annu Rev Immunol*. 2003;21:685-711.
150. Wu J, Wu H, An J, Ballantyne CM, Cyster JG. Critical role of integrin CD11c in splenic dendritic cell capture of missing-self CD47 cells to induce adaptive immunity. *Proc Natl Acad Sci U S A*. 2018;115(26):6786-6791.
151. Sansom DM. CD28, CTLA-4 and their ligands: who does what and to whom? *Immunology*. 2000;101(2):169-177.
152. Tivol EA, Borriello F, Schweitzer AN, Lynch WP, Bluestone JA, Sharpe AH. Loss of CTLA-4 leads to massive lymphoproliferation and fatal multiorgan tissue destruction, revealing a critical negative regulatory role of CTLA-4. *Immunity*. 1995;3(5):541-547.
153. Waterhouse P, Penninger JM, Timms E, et al. Lymphoproliferative disorders with early lethality in mice deficient in Ctla-4. *Science*. 1995;270(5238):985-988.
154. O'Sullivan B, Thomas R. Recent advances on the role of CD40 and dendritic cells in immunity and tolerance. *Curr Opin Hematol*. 2003;10(4):272-278.
155. Lechmann M, Berchtold S, Hauber J, Steinkasserer A. CD83 on dendritic cells: more than just a marker for maturation. *Trends Immunol*. 2002;23(6):273-275.
156. Fujimoto Y, Tu L, Miller AS, et al. CD83 expression influences CD4+ T cell development in the thymus. *Cell*. 2002;108(6):755-767.
157. Garcia-Martinez LF, Appleby MW, Staehling-Hampton K, et al. A novel mutation in CD83 results in the development of a unique population of CD4+ T cells. *J Immunol*. 2004;173(5):2995-3001.
158. Inaba K, Young JW, Steinman RM. Direct activation of CD8+ cytotoxic T lymphocytes by dendritic cells. *J Exp Med*. 1987;166(1):182-194.
159. Kronin V, Winkel K, Suss G, et al. A subclass of dendritic cells regulates the response of naive CD8 T cells by limiting their IL-2 production. *J Immunol*. 1996;157(9):3819-3827.
160. den Haan JM, Lehar SM, Bevan MJ. CD8(+) but not CD8(-) dendritic cells cross-prime cytotoxic T cells in vivo. *J Exp Med*. 2000;192(12):1685-1696.

161. Bevan MJ. Cross-priming for a secondary cytotoxic response to minor H antigens with H-2 congenic cells which do not cross-react in the cytotoxic assay. *J Exp Med*. 1976;143(5):1283-1288.
162. Pooley JL, Heath WR, Shortman K. Cutting edge: intravenous soluble antigen is presented to CD4 T cells by CD8- dendritic cells, but cross-presented to CD8 T cells by CD8+ dendritic cells. *J Immunol*. 2001;166(9):5327-5330.
163. Hildner K, Edelson BT, Purtha WE, et al. Batf3 deficiency reveals a critical role for CD8alpha+ dendritic cells in cytotoxic T cell immunity. *Science*. 2008;322(5904):1097-1100.
164. Martinez-Lopez M, Iborra S, Conde-Garrosa R, Sancho D. Batf3-dependent CD103+ dendritic cells are major producers of IL-12 that drive local Th1 immunity against Leishmania major infection in mice. *Eur J Immunol*. 2015;45(1):119-129.
165. Sanchez-Paulete AR, Cueto FJ, Martinez-Lopez M, et al. Cancer Immunotherapy with Immunomodulatory Anti-CD137 and Anti-PD-1 Monoclonal Antibodies Requires BATF3-Dependent Dendritic Cells. *Cancer Discov*. 2016;6(1):71-79.
166. Roberts EW, Broz ML, Binnewies M, et al. Critical Role for CD103(+)/CD141(+) Dendritic Cells Bearing CCR7 for Tumor Antigen Trafficking and Priming of T Cell Immunity in Melanoma. *Cancer Cell*. 2016;30(2):324-336.
167. Atif SM, Nelsen MK, Gibbings SL, et al. Cutting Edge: Roles for Batf3-Dependent APCs in the Rejection of Minor Histocompatibility Antigen-Mismatched Grafts. *J Immunol*. 2015;195(1):46-50.
168. Bachem A, Hartung E, Guttler S, et al. Expression of XCR1 Characterizes the Batf3-Dependent Lineage of Dendritic Cells Capable of Antigen Cross-Presentation. *Front Immunol*. 2012;3:214.
169. Becker M, Guttler S, Bachem A, et al. Ontogenic, Phenotypic, and Functional Characterization of XCR1(+) Dendritic Cells Leads to a Consistent Classification of Intestinal Dendritic Cells Based on the Expression of XCR1 and SIRPalpha. *Front Immunol*. 2014;5:326.
170. Spranger S, Dai D, Horton B, Gajewski TF. Tumor-Residing Batf3 Dendritic Cells Are Required for Effector T Cell Trafficking and Adoptive T Cell Therapy. *Cancer Cell*. 2017;31(5):711-723 e714.
171. Seillet C, Jackson JT, Markey KA, et al. CD8alpha+ DCs can be induced in the absence of transcription factors Id2, Nfil3, and Batf3. *Blood*. 2013;121(9):1574-1583.
172. Tussiwand R, Lee WL, Murphy TL, et al. Compensatory dendritic cell development mediated by BATF-IRF interactions. *Nature*. 2012;490(7421):502-507.
173. Durai V, Bagadia P, Granja JM, et al. Cryptic activation of an Irf8 enhancer governs cDC1 fate specification. *Nat Immunol*. 2019;20(9):1161-1173.
174. Schonheit J, Kuhl C, Gebhardt ML, et al. PU.1 level-directed chromatin structure remodeling at the Irf8 gene drives dendritic cell commitment. *Cell Rep*. 2013;3(5):1617-1628.
175. Theisen DJ, Ferris ST, Briseno CG, et al. Batf3-Dependent Genes Control Tumor Rejection Induced by Dendritic Cells Independently of Cross-Presentation. *Cancer Immunol Res*. 2019;7(1):29-39.
176. Miller JC, Brown BD, Shay T, et al. Deciphering the transcriptional network of the dendritic cell lineage. *Nat Immunol*. 2012;13(9):888-899.
177. Mashayekhi M, Sandau MM, Dunay IR, et al. CD8alpha(+) dendritic cells are the critical source of interleukin-12 that controls acute infection by Toxoplasma gondii tachyzoites. *Immunity*. 2011;35(2):249-259.
178. Askenase MH, Han SJ, Byrd AL, et al. Bone-Marrow-Resident NK Cells Prime Monocytes for Regulatory Function during Infection. *Immunity*. 2015;42(6):1130-1142.
179. Diebold SS, Montoya M, Unger H, et al. Viral infection switches non-plasmacytoid dendritic cells into high interferon producers. *Nature*. 2003;424(6946):324-328.
180. Schulz O, Diebold SS, Chen M, et al. Toll-like receptor 3 promotes cross-priming to virus-infected cells. *Nature*. 2005;433(7028):887-892.

181. Bachem A, Guttler S, Hartung E, et al. Superior antigen cross-presentation and XCR1 expression define human CD11c+CD141+ cells as homologues of mouse CD8+ dendritic cells. *J Exp Med*. 2010;207(6):1273-1281.
182. Crozat K, Tamoutounour S, Vu Manh TP, et al. Cutting edge: expression of XCR1 defines mouse lymphoid-tissue resident and migratory dendritic cells of the CD8alpha+ type. *J Immunol*. 2011;187(9):4411-4415.
183. Dorner BG, Dorner MB, Zhou X, et al. Selective expression of the chemokine receptor XCR1 on cross-presenting dendritic cells determines cooperation with CD8+ T cells. *Immunity*. 2009;31(5):823-833.
184. Mattiuz R, Wohn C, Ghilas S, et al. Novel Cre-Expressing Mouse Strains Permitting to Selectively Track and Edit Type 1 Conventional Dendritic Cells Facilitate Disentangling Their Complexity in vivo. *Front Immunol*. 2018;9:2805.
185. Ohta T, Sugiyama M, Hemmi H, et al. Crucial roles of XCR1-expressing dendritic cells and the XCR1-XCL1 chemokine axis in intestinal immune homeostasis. *Sci Rep*. 2016;6:23505.
186. Janela B, Patel AA, Lau MC, et al. A Subset of Type I Conventional Dendritic Cells Controls Cutaneous Bacterial Infections through VEGFalpha-Mediated Recruitment of Neutrophils. *Immunity*. 2019;50(4):1069-1083 e1068.
187. Del Fresno C, Saz-Leal P, Enamorado M, et al. DNGR-1 in dendritic cells limits tissue damage by dampening neutrophil recruitment. *Science*. 2018;362(6412):351-356.
188. Brewitz A, Eickhoff S, Dahling S, et al. CD8(+) T Cells Orchestrate pDC-XCR1(+) Dendritic Cell Spatial and Functional Cooperativity to Optimize Priming. *Immunity*. 2017;46(2):205-219.
189. Bonifaz LC, Bonnyay DP, Charalambous A, et al. In vivo targeting of antigens to maturing dendritic cells via the DEC-205 receptor improves T cell vaccination. *J Exp Med*. 2004;199(6):815-824.
190. Bozzacco L, Trumpfheller C, Siegal FP, et al. DEC-205 receptor on dendritic cells mediates presentation of HIV gag protein to CD8+ T cells in a spectrum of human MHC I haplotypes. *Proc Natl Acad Sci U S A*. 2007;104(4):1289-1294.
191. Caminschi I, Proietto AI, Ahmet F, et al. The dendritic cell subtype-restricted C-type lectin Clec9A is a target for vaccine enhancement. *Blood*. 2008;112(8):3264-3273.
192. Lahoud MH, Ahmet F, Zhang JG, et al. DEC-205 is a cell surface receptor for CpG oligonucleotides. *Proc Natl Acad Sci U S A*. 2012;109(40):16270-16275.
193. Li J, Ahmet F, Sullivan LC, et al. Antibodies targeting Clec9A promote strong humoral immunity without adjuvant in mice and non-human primates. *Eur J Immunol*. 2015;45(3):854-864.
194. Tullett KM, Leal Rojas IM, Minoda Y, et al. Targeting CLEC9A delivers antigen to human CD141(+) DC for CD4(+) and CD8(+)T cell recognition. *JCI Insight*. 2016;1(7):e87102.
195. Fossum E, Grodeland G, Terhorst D, et al. Vaccine molecules targeting Xcr1 on cross-presenting DCs induce protective CD8+ T-cell responses against influenza virus. *Eur J Immunol*. 2015;45(2):624-635.
196. Hartung E, Becker M, Bachem A, et al. Induction of potent CD8 T cell cytotoxicity by specific targeting of antigen to cross-presenting dendritic cells in vivo via murine or human XCR1. *J Immunol*. 2015;194(3):1069-1079.
197. Garris CS, Arlauckas SP, Kohler RH, et al. Successful Anti-PD-1 Cancer Immunotherapy Requires T Cell-Dendritic Cell Crosstalk Involving the Cytokines IFN-gamma and IL-12. *Immunity*. 2018;49(6):1148-1161 e1147.
198. Gubin MM, Zhang X, Schuster H, et al. Checkpoint blockade cancer immunotherapy targets tumour-specific mutant antigens. *Nature*. 2014;515(7528):577-581.
199. Breton G, Lee J, Liu K, Nussenzweig MC. Defining human dendritic cell progenitors by multiparametric flow cytometry. *Nat Protoc*. 2015;10(9):1407-1422.
200. Guermonprez P, Helft J, Claser C, et al. Inflammatory Flt3l is essential to mobilize dendritic cells and for T cell responses during Plasmodium infection. *Nat Med*. 2013;19(6):730-738.

201. Salmon H, Idoyaga J, Rahman A, et al. Expansion and Activation of CD103(+) Dendritic Cell Progenitors at the Tumor Site Enhances Tumor Responses to Therapeutic PD-L1 and BRAF Inhibition. *Immunity*. 2016;44(4):924-938.
202. Sanchez-Paulete AR, Teijeira A, Quetglas JI, et al. Intratumoral Immunotherapy with XCL1 and sFlt3L Encoded in Recombinant Semliki Forest Virus-Derived Vectors Fosters Dendritic Cell-Mediated T-cell Cross-Priming. *Cancer Res*. 2018;78(23):6643-6654.
203. Bottcher JP, Bonavita E, Chakravarty P, et al. NK Cells Stimulate Recruitment of cDC1 into the Tumor Microenvironment Promoting Cancer Immune Control. *Cell*. 2018;172(5):1022-1037 e1014.
204. Theisen D, Murphy K. The role of cDC1s in vivo: CD8 T cell priming through cross-presentation. *F1000Res*. 2017;6:98.
205. Theisen DJ, Davidson JTt, Briseno CG, et al. WDFY4 is required for cross-presentation in response to viral and tumor antigens. *Science*. 2018;362(6415):694-699.
206. Kretzer NM, Theisen DJ, Tussiwand R, et al. RAB43 facilitates cross-presentation of cell-associated antigens by CD8alpha+ dendritic cells. *J Exp Med*. 2016;213(13):2871-2883.
207. De Silva NS, Simonetti G, Heise N, Klein U. The diverse roles of IRF4 in late germinal center B-cell differentiation. *Immunol Rev*. 2012;247(1):73-92.
208. Huber M, Lohoff M. IRF4 at the crossroads of effector T-cell fate decision. *Eur J Immunol*. 2014;44(7):1886-1895.
209. Calabro S, Gallman A, Gowthaman U, et al. Bridging channel dendritic cells induce immunity to transfused red blood cells. *J Exp Med*. 2016;213(6):887-896.
210. Kumamoto Y, Linehan M, Weinstein JS, Laidlaw BJ, Craft JE, Iwasaki A. CD301b(+) dermal dendritic cells drive T helper 2 cell-mediated immunity. *Immunity*. 2013;39(4):733-743.
211. Linehan JL, Dileepan T, Kashem SW, Kaplan DH, Cleary P, Jenkins MK. Generation of Th17 cells in response to intranasal infection requires TGF-beta1 from dendritic cells and IL-6 from CD301b+ dendritic cells. *Proc Natl Acad Sci U S A*. 2015;112(41):12782-12787.
212. Persson EK, Uronen-Hansson H, Semmrich M, et al. IRF4 transcription-factor-dependent CD103(+)CD11b(+) dendritic cells drive mucosal T helper 17 cell differentiation. *Immunity*. 2013;38(5):958-969.
213. Plantinga M, Guilliams M, Vanheerswynghels M, et al. Conventional and monocyte-derived CD11b(+) dendritic cells initiate and maintain T helper 2 cell-mediated immunity to house dust mite allergen. *Immunity*. 2013;38(2):322-335.
214. Reboldi A, Arnon TI, Rodda LB, Atakilit A, Sheppard D, Cyster JG. IgA production requires B cell interaction with subepithelial dendritic cells in Peyer's patches. *Science*. 2016;352(6287):aaf4822.
215. Schlitzer A, McGovern N, Teo P, et al. IRF4 transcription factor-dependent CD11b+ dendritic cells in human and mouse control mucosal IL-17 cytokine responses. *Immunity*. 2013;38(5):970-983.
216. von Moltke J, Ji M, Liang HE, Locksley RM. Tuft-cell-derived IL-25 regulates an intestinal ILC2-epithelial response circuit. *Nature*. 2016;529(7585):221-225.
217. Briseno CG, Satpathy AT, Davidson JTt, et al. Notch2-dependent DC2s mediate splenic germinal center responses. *Proc Natl Acad Sci U S A*. 2018;115(42):10726-10731.
218. Alspach E, Lussier DM, Miceli AP, et al. MHC-II neoantigens shape tumour immunity and response to immunotherapy. *Nature*. 2019;574(7780):696-701.
219. Bennett SR, Carbone FR, Karamalis F, Miller JF, Heath WR. Induction of a CD8+ cytotoxic T lymphocyte response by cross-priming requires cognate CD4+ T cell help. *J Exp Med*. 1997;186(1):65-70.
220. Binnewies M, Mujal AM, Pollack JL, et al. Unleashing Type-2 Dendritic Cells to Drive Protective Antitumor CD4(+) T Cell Immunity. *Cell*. 2019;177(3):556-571 e516.
221. Wculek SK, Cueto FJ, Mujal AM, Melero I, Krummel MF, Sancho D. Dendritic cells in cancer immunology and immunotherapy. *Nat Rev Immunol*. 2020;20(1):7-24.

222. Wimmers F, Subedi N, van Buuringen N, et al. Single-cell analysis reveals that stochasticity and paracrine signaling control interferon-alpha production by plasmacytoid dendritic cells. *Nat Commun*. 2018;9(1):3317.
223. Kumagai Y, Kumar H, Koyama S, Kawai T, Takeuchi O, Akira S. Cutting Edge: TLR-Dependent viral recognition along with type I IFN positive feedback signaling masks the requirement of viral replication for IFN-alpha production in plasmacytoid dendritic cells. *J Immunol*. 2009;182(7):3960-3964.
224. Li XD, Wu J, Gao D, Wang H, Sun L, Chen ZJ. Pivotal roles of cGAS-cGAMP signaling in antiviral defense and immune adjuvant effects. *Science*. 2013;341(6152):1390-1394.
225. Bruni D, Chazal M, Sinigaglia L, et al. Viral entry route determines how human plasmacytoid dendritic cells produce type I interferons. *Sci Signal*. 2015;8(366):ra25.
226. Dasgupta S, Erturk-Hasdemir D, Ochoa-Reparaz J, Reinecker HC, Kasper DL. Plasmacytoid dendritic cells mediate anti-inflammatory responses to a gut commensal molecule via both innate and adaptive mechanisms. *Cell Host Microbe*. 2014;15(4):413-423.
227. Heras-Murillo I, Adan-Barrientos I, Galan M, Wculek SK, Sancho D. Dendritic cells as orchestrators of anticancer immunity and immunotherapy. *Nat Rev Clin Oncol*. 2024;21(4):257-277.
228. Santegoets SJ, Duurland CL, Jordanova EJ, et al. CD163(+) cytokine-producing cDC2 stimulate intratumoral type 1 T cell responses in HPV16-induced oropharyngeal cancer. *J Immunother Cancer*. 2020;8(2).
229. Nakamizo S, Dutertre CA, Khalilnezhad A, et al. Single-cell analysis of human skin identifies CD14+ type 3 dendritic cells co-producing IL1B and IL23A in psoriasis. *J Exp Med*. 2021;218(9).
230. Bakdash G, Buschow SI, Gorris MA, et al. Expansion of a BDCA1+CD14+ Myeloid Cell Population in Melanoma Patients May Attenuate the Efficacy of Dendritic Cell Vaccines. *Cancer Res*. 2016;76(15):4332-4346.
231. Kvedaraite E, Hertwig L, Sinha I, et al. Major alterations in the mononuclear phagocyte landscape associated with COVID-19 severity. *Proc Natl Acad Sci U S A*. 2021;118(6).
232. Winheim E, Rinke L, Lutz K, et al. Impaired function and delayed regeneration of dendritic cells in COVID-19. *PLoS Pathog*. 2021;17(10):e1009742.
233. Girard M, Law JC, Edilova MI, Watts TH. Type I interferons drive the maturation of human DC3s with a distinct costimulatory profile characterized by high GITRL. *Sci Immunol*. 2020;5(53).
234. Curtsinger JM, Schmidt CS, Mondino A, et al. Inflammatory cytokines provide a third signal for activation of naive CD4+ and CD8+ T cells. *J Immunol*. 1999;162(6):3256-3262.
235. Mempel TR, Henrickson SE, Von Andrian UH. T-cell priming by dendritic cells in lymph nodes occurs in three distinct phases. *Nature*. 2004;427(6970):154-159.
236. Sun L, Su Y, Jiao A, Wang X, Zhang B. T cells in health and disease. *Signal Transduct Target Ther*. 2023;8(1):235.
237. Cortez JT, Montauti E, Shifrut E, et al. CRISPR screen in regulatory T cells reveals modulators of Foxp3. *Nature*. 2020;582(7812):416-420.
238. Gao Y, Wang C, Wang Z, et al. Semaphorin 3A contributes to sepsis-induced immunosuppression by impairing CD4(+) T cell anergy. *Mol Med Rep*. 2021;23(4).
239. Ramsdell F, Rudensky AY. Foxp3: a genetic foundation for regulatory T cell differentiation and function. *Nat Immunol*. 2020;21(7):708-709.
240. von Knethen A, Heinicke U, Weigert A, Zacharowski K, Brune B. Histone Deacetylation Inhibitors as Modulators of Regulatory T Cells. *Int J Mol Sci*. 2020;21(7).
241. Panduro M, Benoist C, Mathis D. Tissue Tregs. *Annu Rev Immunol*. 2016;34:609-633.
242. Huehn J, Polansky JK, Hamann A. Epigenetic control of FOXP3 expression: the key to a stable regulatory T-cell lineage? *Nat Rev Immunol*. 2009;9(2):83-89.
243. Giganti G, Atif M, Mohseni Y, et al. Treg cell therapy: How cell heterogeneity can make the difference. *Eur J Immunol*. 2021;51(1):39-55.

244. Hsieh CS, Liang Y, Tyznik AJ, Self SG, Liggitt D, Rudensky AY. Recognition of the peripheral self by naturally arising CD25+ CD4+ T cell receptors. *Immunity*. 2004;21(2):267-277.
245. Sakaguchi S, Miyara M, Costantino CM, Hafler DA. FOXP3+ regulatory T cells in the human immune system. *Nat Rev Immunol*. 2010;10(7):490-500.
246. Zhang X, Zhang X, Qiu C, et al. The imbalance of Th17/Treg via STAT3 activation modulates cognitive impairment in P. gingivalis LPS-induced periodontitis mice. *J Leukoc Biol*. 2021;110(3):511-524.
247. Hoechst B, Gamrekelashvili J, Manns MP, Greten TF, Korangy F. Plasticity of human Th17 cells and iTregs is orchestrated by different subsets of myeloid cells. *Blood*. 2011;117(24):6532-6541.
248. Santamaria JC, Borelli A, Irla M. Regulatory T Cell Heterogeneity in the Thymus: Impact on Their Functional Activities. *Front Immunol*. 2021;12:643153.
249. Bennett CL, Christie J, Ramsdell F, et al. The immune dysregulation, polyendocrinopathy, enteropathy, X-linked syndrome (IPEX) is caused by mutations of FOXP3. *Nat Genet*. 2001;27(1):20-21.
250. Shimizu J, Yamazaki S, Takahashi T, Ishida Y, Sakaguchi S. Stimulation of CD25(+)CD4(+) regulatory T cells through GITR breaks immunological self-tolerance. *Nat Immunol*. 2002;3(2):135-142.
251. Kaech SM, Wherry EJ. Heterogeneity and cell-fate decisions in effector and memory CD8+ T cell differentiation during viral infection. *Immunity*. 2007;27(3):393-405.
252. Chaplin DD. Overview of the immune response. *J Allergy Clin Immunol*. 2010;125(2 Suppl 2):S3-23.
253. Marshall JS, Warrington R, Watson W, Kim HL. An introduction to immunology and immunopathology. *Allergy Asthma Clin Immunol*. 2018;14(Suppl 2):49.
254. Joshi NS, Cui W, Chandele A, et al. Inflammation directs memory precursor and short-lived effector CD8(+) T cell fates via the graded expression of T-bet transcription factor. *Immunity*. 2007;27(2):281-295.
255. Kaech SM, Tan JT, Wherry EJ, Konieczny BT, Surh CD, Ahmed R. Selective expression of the interleukin 7 receptor identifies effector CD8 T cells that give rise to long-lived memory cells. *Nat Immunol*. 2003;4(12):1191-1198.
256. Davis MM, Boniface JJ, Reich Z, et al. Ligand recognition by alpha beta T cell receptors. *Annu Rev Immunol*. 1998;16:523-544.
257. Ruterbusch M, Pruner KB, Shehata L, Pepper M. In Vivo CD4(+) T Cell Differentiation and Function: Revisiting the Th1/Th2 Paradigm. *Annu Rev Immunol*. 2020;38:705-725.
258. Zhu J, Yamane H, Paul WE. Differentiation of effector CD4 T cell populations (*). *Annu Rev Immunol*. 2010;28:445-489.
259. Di Dalmazi G, Ippolito S, Lupi I, Caturegli P. Hypophysitis induced by immune checkpoint inhibitors: a 10-year assessment. *Expert Rev Endocrinol Metab*. 2019;14(6):381-398.
260. Iervasi E, Strangio A, Saverino D. Hypothalamic expression of PD-L1: does it mediate hypothalamitis? *Cell Mol Immunol*. 2019;16(6):625-626.
261. Wei SC, Levine JH, Cogdill AP, et al. Distinct Cellular Mechanisms Underlie Anti-CTLA-4 and Anti-PD-1 Checkpoint Blockade. *Cell*. 2017;170(6):1120-1133 e1117.
262. Cenerenti M, Saillard M, Romero P, Jandus C. The Era of Cytotoxic CD4 T Cells. *Front Immunol*. 2022;13:867189.
263. Geginat J, Paroni M, Maglie S, et al. Plasticity of human CD4 T cell subsets. *Front Immunol*. 2014;5:630.
264. Luckheeram RV, Zhou R, Verma AD, Xia B. CD4(+)T cells: differentiation and functions. *Clin Dev Immunol*. 2012;2012:925135.
265. Hossen MM, Ma Y, Yin Z, et al. Current understanding of CTLA-4: from mechanism to autoimmune diseases. *Front Immunol*. 2023;14:1198365.
266. Scheipers P, Reiser H. Role of the CTLA-4 receptor in T cell activation and immunity. Physiologic function of the CTLA-4 receptor. *Immunol Res*. 1998;18(2):103-115.

267. Di Stasi V, La Sala D, Cozzi R, et al. Immunotherapy-Related Hypophysitis: A Narrative Review. *Cancers (Basel)*. 2025;17(3).
268. Akdis CA, Arkwright PD, Bruggen MC, et al. Type 2 immunity in the skin and lungs. *Allergy*. 2020;75(7):1582-1605.
269. Eyerich S, Zielinski CE. Defining Th-cell subsets in a classical and tissue-specific manner: Examples from the skin. *Eur J Immunol*. 2014;44(12):3475-3483.
270. Mucida D, Cheroutre H. The many face-lifts of CD4 T helper cells. *Adv Immunol*. 2010;107:139-152.
271. Zhu J. T Helper Cell Differentiation, Heterogeneity, and Plasticity. *Cold Spring Harb Perspect Biol*. 2018;10(10).
272. Jiang Z, Zhu H, Wang P, et al. Different subpopulations of regulatory T cells in human autoimmune disease, transplantation, and tumor immunity. *MedComm (2020)*. 2022;3(2):e137.
273. Godfrey DI, Uldrich AP, McCluskey J, Rossjohn J, Moody DB. The burgeoning family of unconventional T cells. *Nat Immunol*. 2015;16(11):1114-1123.
274. Kortekaas Krohn I, Aerts JL, Breckpot K, et al. T-cell subsets in the skin and their role in inflammatory skin disorders. *Allergy*. 2022;77(3):827-842.
275. Chung HK, McDonald B, Kaech SM. The architectural design of CD8+ T cell responses in acute and chronic infection: Parallel structures with divergent fates. *J Exp Med*. 2021;218(4).
276. Sallusto F, Lenig D, Forster R, Lipp M, Lanzavecchia A. Two subsets of memory T lymphocytes with distinct homing potentials and effector functions. *Nature*. 1999;401(6754):708-712.
277. Masopust D, Vezys V, Marzo AL, Lefrancois L. Preferential localization of effector memory cells in nonlymphoid tissue. *Science*. 2001;291(5512):2413-2417.
278. Clark RA, Chong B, Mirchandani N, et al. The vast majority of CLA+ T cells are resident in normal skin. *J Immunol*. 2006;176(7):4431-4439.
279. Sathaliyawala T, Kubota M, Yudanin N, et al. Distribution and compartmentalization of human circulating and tissue-resident memory T cell subsets. *Immunity*. 2013;38(1):187-197.
280. Croft M, Bradley LM, Swain SL. Naive versus memory CD4 T cell response to antigen. Memory cells are less dependent on accessory cell costimulation and can respond to many antigen-presenting cell types including resting B cells. *J Immunol*. 1994;152(6):2675-2685.
281. Strutt TM, McKinstry KK, Dibble JP, et al. Memory CD4+ T cells induce innate responses independently of pathogen. *Nat Med*. 2010;16(5):558-564, 551p following 564.
282. Jain A, Irizarry-Caro RA, McDaniel MM, et al. T cells instruct myeloid cells to produce inflammasome-independent IL-1beta and cause autoimmunity. *Nat Immunol*. 2020;21(1):65-74.
283. McDaniel MM, Chawla AS, Jain A, et al. Effector memory CD4(+) T cells induce damaging innate inflammation and autoimmune pathology by engaging CD40 and TNFR on myeloid cells. *Sci Immunol*. 2022;7(67):eabk0182.
284. Ferris ST, Durai V, Wu R, et al. cDC1 prime and are licensed by CD4(+) T cells to induce anti-tumour immunity. *Nature*. 2020;584(7822):624-629.
285. Jain A, Song R, Wakeland EK, Pasare C. T cell-intrinsic IL-1R signaling licenses effector cytokine production by memory CD4 T cells. *Nat Commun*. 2018;9(1):3185.
286. Goverman J. Autoimmune T cell responses in the central nervous system. *Nat Rev Immunol*. 2009;9(6):393-407.
287. Skapenko A, Leipe J, Lipsky PE, Schulze-Koops H. The role of the T cell in autoimmune inflammation. *Arthritis Res Ther*. 2005;7 Suppl 2(Suppl 2):S4-14.
288. Wu H, Liao W, Li Q, et al. Pathogenic role of tissue-resident memory T cells in autoimmune diseases. *Autoimmun Rev*. 2018;17(9):906-911.
289. Skarnes RC, Watson DW. Antimicrobial factors of normal tissues and fluids. *Bacteriol Rev*. 1957;21(4):273-294.
290. Arbore G, Kemper C, Kolev M. Intracellular complement - the complosome - in immune cell regulation. *Mol Immunol*. 2017;89:2-9.

291. Kolev M, Le Friec G, Kemper C. Complement--tapping into new sites and effector systems. *Nat Rev Immunol*. 2014;14(12):811-820.
292. Nesargikar PN, Spiller B, Chavez R. The complement system: history, pathways, cascade and inhibitors. *Eur J Microbiol Immunol (Bp)*. 2012;2(2):103-111.
293. Noris M, Remuzzi G. Overview of complement activation and regulation. *Semin Nephrol*. 2013;33(6):479-492.
294. Reis ES, Mastellos DC, Hajishengallis G, Lambris JD. New insights into the immune functions of complement. *Nat Rev Immunol*. 2019;19(8):503-516.
295. Koski CL, Ramm LE, Hammer CH, Mayer MM, Shin ML. Cytolysis of nucleated cells by complement: cell death displays multi-hit characteristics. *Proc Natl Acad Sci U S A*. 1983;80(12):3816-3820.
296. Bexborn F, Andersson PO, Chen H, Nilsson B, Ekdahl KN. The tick-over theory revisited: formation and regulation of the soluble alternative complement C3 convertase (C3(H2O)Bb). *Mol Immunol*. 2008;45(8):2370-2379.
297. Harboe M, Mollnes TE. The alternative complement pathway revisited. *J Cell Mol Med*. 2008;12(4):1074-1084.
298. Lu JH, Thiel S, Wiedemann H, Timpl R, Reid KB. Binding of the pentamer/hexamer forms of mannan-binding protein to zymosan activates the proenzyme C1r2C1s2 complex, of the classical pathway of complement, without involvement of C1q. *J Immunol*. 1990;144(6):2287-2294.
299. Morgan BP. Complement membrane attack on nucleated cells: resistance, recovery and non-lethal effects. *Biochem J*. 1989;264(1):1-14.
300. Phillips AE, Toth J, Dodds AW, et al. Analogous interactions in initiating complexes of the classical and lectin pathways of complement. *J Immunol*. 2009;182(12):7708-7717.
301. Rawal N, Rajagopalan R, Salvi VP. Activation of complement component C5: comparison of C5 convertases of the lectin pathway and the classical pathway of complement. *J Biol Chem*. 2008;283(12):7853-7863.
302. Tegla CA, Cudrici C, Patel S, et al. Membrane attack by complement: the assembly and biology of terminal complement complexes. *Immunol Res*. 2011;51(1):45-60.
303. Wallis R, Mitchell DA, Schmid R, Schwaeble WJ, Keeble AH. Paths reunited: Initiation of the classical and lectin pathways of complement activation. *Immunobiology*. 2010;215(1):1-11.
304. Ricklin D, Barratt-Due A, Mollnes TE. Complement in clinical medicine: Clinical trials, case reports and therapy monitoring. *Mol Immunol*. 2017;89:10-21.
305. Ziccardi RJ. The first component of human complement (C1): activation and control. *Springer Semin Immunopathol*. 1983;6(2-3):213-230.
306. Hughes-Jones NC, Gorick BD, Miller NG, Howard JC. IgG pair formation on one antigenic molecule is the main mechanism of synergy between antibodies in complement-mediated lysis. *Eur J Immunol*. 1984;14(11):974-978.
307. Loos M. The complement system: activation and control. *Curr Top Microbiol Immunol*. 1985;121:7-18.
308. Bally I, Rossi V, Lunardi T, Thielens NM, Gaboriaud C, Arlaud GJ. Identification of the C1q-binding Sites of Human C1r and C1s: a refined three-dimensional model of the C1 complex of complement. *J Biol Chem*. 2009;284(29):19340-19348.
309. Gaboriaud C, Thielens NM, Gregory LA, Rossi V, Fontecilla-Camps JC, Arlaud GJ. Structure and activation of the C1 complex of complement: unraveling the puzzle. *Trends Immunol*. 2004;25(7):368-373.
310. Gal P, Dobo J, Zavodszky P, Sim RB. Early complement proteases: C1r, C1s and MASPs. A structural insight into activation and functions. *Mol Immunol*. 2009;46(14):2745-2752.
311. Gregory LA, Thielens NM, Arlaud GJ, Fontecilla-Camps JC, Gaboriaud C. X-ray structure of the Ca2+-binding interaction domain of C1s. Insights into the assembly of the C1 complex of complement. *J Biol Chem*. 2003;278(34):32157-32164.

312. Nordahl EA, Rydengard V, Nyberg P, et al. Activation of the complement system generates antibacterial peptides. *Proc Natl Acad Sci U S A*. 2004;101(48):16879-16884.
313. Nagasawa S, Stroud RM. Cleavage of C2 by C1s into the antigenically distinct fragments C2a and C2b: demonstration of binding of C2b to C4b. *Proc Natl Acad Sci U S A*. 1977;74(7):2998-3001.
314. Nilsson B, Nilsson Ekdahl K. The tick-over theory revisited: is C3 a contact-activated protein? *Immunobiology*. 2012;217(11):1106-1110.
315. Coulthard LG, Woodruff TM. Is the complement activation product C3a a proinflammatory molecule? Re-evaluating the evidence and the myth. *J Immunol*. 2015;194(8):3542-3548.
316. Bajic G, Degn SE, Thiel S, Andersen GR. Complement activation, regulation, and molecular basis for complement-related diseases. *EMBO J*. 2015;34(22):2735-2757.
317. Feinberg H, Uitdehaag JC, Davies JM, Wallis R, Drickamer K, Weis WI. Crystal structure of the CUB1-EGF-CUB2 region of mannose-binding protein associated serine protease-2. *EMBO J*. 2003;22(10):2348-2359.
318. Garred P, Genster N, Pilely K, et al. A journey through the lectin pathway of complement-MBL and beyond. *Immunol Rev*. 2016;274(1):74-97.
319. Gregory LA, Thielens NM, Matsushita M, et al. The X-ray structure of human mannan-binding lectin-associated protein 19 (MAp19) and its interaction site with mannan-binding lectin and L-ficolin. *J Biol Chem*. 2004;279(28):29391-29397.
320. Rosbjerg A, Genster N, Pilely K, Garred P. Evasion Mechanisms Used by Pathogens to Escape the Lectin Complement Pathway. *Front Microbiol*. 2017;8:868.
321. Kimura Y, Miwa T, Zhou L, Song WC. Activator-specific requirement of properdin in the initiation and amplification of the alternative pathway complement. *Blood*. 2008;111(2):732-740.
322. Fearon DT, Austen KF. Properdin: binding to C3b and stabilization of the C3b-dependent C3 convertase. *J Exp Med*. 1975;142(4):856-863.
323. Hourcade DE. The role of properdin in the assembly of the alternative pathway C3 convertases of complement. *J Biol Chem*. 2006;281(4):2128-2132.
324. Alcorlo M, Tortajada A, Rodriguez de Cordoba S, Llorca O. Structural basis for the stabilization of the complement alternative pathway C3 convertase by properdin. *Proc Natl Acad Sci U S A*. 2013;110(33):13504-13509.
325. Spitzer D, Mitchell LM, Atkinson JP, Hourcade DE. Properdin can initiate complement activation by binding specific target surfaces and providing a platform for de novo convertase assembly. *J Immunol*. 2007;179(4):2600-2608.
326. Hajishengallis G, Reis ES, Mastellos DC, Ricklin D, Lambris JD. Novel mechanisms and functions of complement. *Nat Immunol*. 2017;18(12):1288-1298.
327. Aleshin AE, DiScipio RG, Stec B, Liddington RC. Crystal structure of C5b-6 suggests structural basis for priming assembly of the membrane attack complex. *J Biol Chem*. 2012;287(23):19642-19652.
328. Serna M, Giles JL, Morgan BP, Bubeck D. Structural basis of complement membrane attack complex formation. *Nat Commun*. 2016;7:10587.
329. Morgan BP, Dankert JR, Esser AF. Recovery of human neutrophils from complement attack: removal of the membrane attack complex by endocytosis and exocytosis. *J Immunol*. 1987;138(1):246-253.
330. Morgan BP, Gasque P. Extrahepatic complement biosynthesis: where, when and why? *Clin Exp Immunol*. 1997;107(1):1-7.
331. Oikonomopoulou K, DeAngelis RA, Chen H, et al. Induction of complement C3a receptor responses by kallikrein-related peptidase 14. *J Immunol*. 2013;191(7):3858-3866.
332. Huber-Lang M, Sarma JV, Zetoune FS, et al. Generation of C5a in the absence of C3: a new complement activation pathway. *Nat Med*. 2006;12(6):682-687.
333. Huber-Lang M, Younkin EM, Sarma JV, et al. Generation of C5a by phagocytic cells. *Am J Pathol*. 2002;161(5):1849-1859.

334. Donado CA, Theisen E, Zhang F, et al. Granzyme K activates the entire complement cascade. *Nature*. 2025;641(8061):211-221.
335. Lan F, Li J, Miao W, et al. GZMK-expressing CD8(+) T cells promote recurrent airway inflammatory diseases. *Nature*. 2025;638(8050):490-498.
336. Satyam A, Kannan L, Matsumoto N, et al. Intracellular Activation of Complement 3 Is Responsible for Intestinal Tissue Damage during Mesenteric Ischemia. *J Immunol*. 2017;198(2):788-797.
337. Jung HS, Jeong SY, Yang J, et al. Neuroprotective effect of mesenchymal stem cell through complement component 3 downregulation after transient focal cerebral ischemia in mice. *Neurosci Lett*. 2016;633:227-234.
338. Abdul-Aziz M, Tsolaki AG, Kouser L, et al. Complement factor H interferes with Mycobacterium bovis BCG entry into macrophages and modulates the pro-inflammatory cytokine response. *Immunobiology*. 2016;221(9):944-952.
339. Appledorn DM, McBride A, Seregin S, et al. Complex interactions with several arms of the complement system dictate innate and humoral immunity to adenoviral vectors. *Gene Ther*. 2008;15(24):1606-1617.
340. Chen ZL, Su YJ, Zhang HL, Gu PQ, Gao LJ. The role of the globular heads of the C1q receptor in HPV-16 E2-induced human cervical squamous carcinoma cell apoptosis via a mitochondria-dependent pathway. *J Transl Med*. 2014;12:286.
341. Arbore G, West EE, Spolski R, et al. T helper 1 immunity requires complement-driven NLRP3 inflammasome activity in CD4(+) T cells. *Science*. 2016;352(6292):aad1210.
342. Liszewski MK, Kolev M, Le Friec G, et al. Intracellular complement activation sustains T cell homeostasis and mediates effector differentiation. *Immunity*. 2013;39(6):1143-1157.
343. Kolev M, Dimeloe S, Le Friec G, et al. Complement Regulates Nutrient Influx and Metabolic Reprogramming during Th1 Cell Responses. *Immunity*. 2015;42(6):1033-1047.
344. Le Friec G, Sheppard D, Whiteman P, et al. The CD46-Jagged1 interaction is critical for human TH1 immunity. *Nat Immunol*. 2012;13(12):1213-1221.
345. Yamamoto H, Fara AF, Dasgupta P, Kemper C. CD46: the 'multitasker' of complement proteins. *Int J Biochem Cell Biol*. 2013;45(12):2808-2820.
346. Tsujimura A, Shida K, Kitamura M, et al. Molecular cloning of a murine homologue of membrane cofactor protein (CD46): preferential expression in testicular germ cells. *Biochem J*. 1998;330 ( Pt 1)(Pt 1):163-168.
347. Lyzogubov V, Wu X, Jha P, et al. Complement regulatory protein CD46 protects against choroidal neovascularization in mice. *Am J Pathol*. 2014;184(9):2537-2548.
348. Esposito P, Rodriguez C, Gandelman M, Liang J, Ismail N. CD46 expression in the central nervous system of male and female pubescent mice. *J Neuroimmunol*. 2023;385:578234.
349. Singh P, Kemper C. Complement, complosome, and complotype: A perspective. *Eur J Immunol*. 2023;53(12):e2250042.
350. Samstad EO, Niyonzima N, Nymo S, et al. Cholesterol crystals induce complement-dependent inflammasome activation and cytokine release. *J Immunol*. 2014;192(6):2837-2845.
351. Le Friec G, Kohl J, Kemper C. A complement a day keeps the Fox(p3) away. *Nat Immunol*. 2013;14(2):110-112.
352. Kerekes K, Prechl J, Bajtay Z, Jozsi M, Erdei A. A further link between innate and adaptive immunity: C3 deposition on antigen-presenting cells enhances the proliferation of antigen-specific T cells. *Int Immunol*. 1998;10(12):1923-1930.
353. Lalli PN, Strainic MG, Yang M, Lin F, Medof ME, Heeger PS. Locally produced C5a binds to T cell-expressed C5aR to enhance effector T-cell expansion by limiting antigen-induced apoptosis. *Blood*. 2008;112(5):1759-1766.
354. Strainic MG, Liu J, Huang D, et al. Locally produced complement fragments C5a and C3a provide both costimulatory and survival signals to naive CD4+ T cells. *Immunity*. 2008;28(3):425-435.

355. Sohn JH, Bora PS, Suk HJ, Molina H, Kaplan HJ, Bora NS. Tolerance is dependent on complement C3 fragment iC3b binding to antigen-presenting cells. *Nat Med*. 2003;9(2):206-212.
356. van der Touw W, Cravedi P, Kwan WH, Paz-Artal E, Merad M, Heeger PS. Cutting edge: Receptors for C3a and C5a modulate stability of alloantigen-reactive induced regulatory T cells. *J Immunol*. 2013;190(12):5921-5925.
357. Heeger PS, Kemper C. Novel roles of complement in T effector cell regulation. *Immunobiology*. 2012;217(2):216-224.
358. West EE, Kolev M, Kemper C. Complement and the Regulation of T Cell Responses. *Annu Rev Immunol*. 2018;36:309-338.
359. Clarke EV, Tenner AJ. Complement modulation of T cell immune responses during homeostasis and disease. *J Leukoc Biol*. 2014;96(5):745-756.
360. Dunkelberger JR, Song WC. Role and mechanism of action of complement in regulating T cell immunity. *Mol Immunol*. 2010;47(13):2176-2186.
361. Kolev M, Le Friec G, Kemper C. The role of complement in CD4(+) T cell homeostasis and effector functions. *Semin Immunol*. 2013;25(1):12-19.
362. Kemper C, Atkinson JP. T-cell regulation: with complements from innate immunity. *Nat Rev Immunol*. 2007;7(1):9-18.
363. Song WC. Crosstalk between complement and toll-like receptors. *Toxicol Pathol*. 2012;40(2):174-182.
364. Kopf M, Abel B, Gallimore A, Carroll M, Bachmann MF. Complement component C3 promotes T-cell priming and lung migration to control acute influenza virus infection. *Nat Med*. 2002;8(4):373-378.
365. Suresh M, Molina H, Salvato MS, Mastellos D, Lambris JD, Sandor M. Complement component 3 is required for optimal expansion of CD8 T cells during a systemic viral infection. *J Immunol*. 2003;170(2):788-794.
366. Kim AH, Dimitriou ID, Holland MC, et al. Complement C5a receptor is essential for the optimal generation of antiviral CD8+ T cell responses. *J Immunol*. 2004;173(4):2524-2529.
367. Gancevici GG. Role of complement inhibition in topical therapy of muco-cutaneous herpes simplex virus infections. *Roum Arch Microbiol Immunol*. 1993;52(4):293-303.
368. Zhou W, Peng Q, Li K, Sacks SH. Role of dendritic cell synthesis of complement in the allospecific T cell response. *Mol Immunol*. 2007;44(1-3):57-63.
369. Baudino L, Sardini A, Ruseva MM, et al. C3 opsonization regulates endocytic handling of apoptotic cells resulting in enhanced T-cell responses to cargo-derived antigens. *Proc Natl Acad Sci U S A*. 2014;111(4):1503-1508.
370. Tam JC, Bidgood SR, McEwan WA, James LC. Intracellular sensing of complement C3 activates cell autonomous immunity. *Science*. 2014;345(6201):1256070.
371. Li K, Anderson KJ, Peng Q, et al. Cyclic AMP plays a critical role in C3a-receptor-mediated regulation of dendritic cells in antigen uptake and T-cell stimulation. *Blood*. 2008;112(13):5084-5094.
372. Croker DE, Halai R, Kaeslin G, et al. C5a2 can modulate ERK1/2 signaling in macrophages via heteromer formation with C5a1 and beta-arrestin recruitment. *Immunol Cell Biol*. 2014;92(7):631-639.
373. Kastl SP, Speidl WS, Kaun C, et al. The complement component C5a induces the expression of plasminogen activator inhibitor-1 in human macrophages via NF-kappaB activation. *J Thromb Haemost*. 2006;4(8):1790-1797.
374. Grailer JJ, Bosmann M, Ward PA. Regulatory effects of C5a on IL-17A, IL-17F, and IL-23. *Front Immunol*. 2012;3:387.
375. Hashimoto M, Hirota K, Yoshitomi H, et al. Complement drives Th17 cell differentiation and triggers autoimmune arthritis. *J Exp Med*. 2010;207(6):1135-1143.
376. Li K, Fazekasova H, Wang N, et al. Functional modulation of human monocytes derived DCs by anaphylatoxins C3a and C5a. *Immunobiology*. 2012;217(1):65-73.

377. Karp CL, Grupe A, Schadt E, et al. Identification of complement factor 5 as a susceptibility locus for experimental allergic asthma. *Nat Immunol*. 2000;1(3):221-226.
378. Drouin SM, Sinha M, Sfyroera G, Lambris JD, Wetsel RA. A protective role for the fifth complement component (c5) in allergic airway disease. *Am J Respir Crit Care Med*. 2006;173(8):852-857.
379. Weaver DJ, Jr., Reis ES, Pandey MK, et al. C5a receptor-deficient dendritic cells promote induction of Treg and Th17 cells. *Eur J Immunol*. 2010;40(3):710-721.
380. Lajoie S, Lewkowich IP, Suzuki Y, et al. Complement-mediated regulation of the IL-17A axis is a central genetic determinant of the severity of experimental allergic asthma. *Nat Immunol*. 2010;11(10):928-935.
381. Cheng SC, Sprong T, Joosten LA, et al. Complement plays a central role in Candida albicans-induced cytokine production by human PBMCs. *Eur J Immunol*. 2012;42(4):993-1004.
382. Asgari E, Le Friec G, Yamamoto H, et al. C3a modulates IL-1beta secretion in human monocytes by regulating ATP efflux and subsequent NLRP3 inflammasome activation. *Blood*. 2013;122(20):3473-3481.
383. Vaknin-Dembinsky A, Murugaiyan G, Hafler DA, Astier AL, Weiner HL. Increased IL-23 secretion and altered chemokine production by dendritic cells upon CD46 activation in patients with multiple sclerosis. *J Neuroimmunol*. 2008;195(1-2):140-145.
384. Kurita-Taniguchi M, Fukui A, Hazeki K, et al. Functional modulation of human macrophages through CD46 (measles virus receptor): production of IL-12 p40 and nitric oxide in association with recruitment of protein-tyrosine phosphatase SHP-1 to CD46. *J Immunol*. 2000;165(9):5143-5152.
385. Wang X, Zhang D, Sjolinder M, Wan Y, Sjolinder H. CD46 accelerates macrophage-mediated host susceptibility to meningococcal sepsis in a murine model. *Eur J Immunol*. 2017;47(1):119-130.
386. Hakulinen J, Junnikkala S, Sorsa T, Meri S. Complement inhibitor membrane cofactor protein (MCP; CD46) is constitutively shed from cancer cell membranes in vesicles and converted by a metalloproteinase to a functionally active soluble form. *Eur J Immunol*. 2004;34(9):2620-2629.
387. Brodbeck WG, Kuttner-Kondo L, Mold C, Medof ME. Structure/function studies of human decay-accelerating factor. *Immunology*. 2000;101(1):104-111.
388. Ahearn JM, Fearon DT. Structure and function of the complement receptors, CR1 (CD35) and CR2 (CD21). *Adv Immunol*. 1989;46:183-219.
389. Ferreira VP, Pangburn MK. Factor H mediated cell surface protection from complement is critical for the survival of PNH erythrocytes. *Blood*. 2007;110(6):2190-2192.
390. Zipfel PF, Skerka C. Complement regulators and inhibitory proteins. *Nat Rev Immunol*. 2009;9(10):729-740.
391. Klos A, Tenner AJ, Johswich KO, Ager RR, Reis ES, Kohl J. The role of the anaphylatoxins in health and disease. *Mol Immunol*. 2009;46(14):2753-2766.
392. Klos A, Wende E, Wareham KJ, Monk PN. International Union of Basic and Clinical Pharmacology. [corrected]. LXXXVII. Complement peptide C5a, C4a, and C3a receptors. *Pharmacol Rev*. 2013;65(1):500-543.
393. Li R, Coulthard LG, Wu MC, Taylor SM, Woodruff TM. C5L2: a controversial receptor of complement anaphylatoxin, C5a. *FASEB J*. 2013;27(3):855-864.
394. Bokisch VA, Muller-Eberhard HJ. Anaphylatoxin inactivator of human plasma: its isolation and characterization as a carboxypeptidase. *J Clin Invest*. 1970;49(12):2427-2436.
395. Matthews KW, Mueller-Ortiz SL, Wetsel RA. Carboxypeptidase N: a pleiotropic regulator of inflammation. *Mol Immunol*. 2004;40(11):785-793.
396. Reis ES, Chen H, Sfyroera G, et al. C5a receptor-dependent cell activation by physiological concentrations of desarginated C5a: insights from a novel label-free cellular assay. *J Immunol*. 2012;189(10):4797-4805.

397. Sayah S, Jauneau AC, Patte C, Tonon MC, Vaudry H, Fontaine M. Two different transduction pathways are activated by C3a and C5a anaphylatoxins on astrocytes. *Brain Res Mol Brain Res*. 2003;112(1-2):53-60.
398. Verschoor A, Kemper C, Köhl J. Complement Receptors. Encyclopedia of Life Sciences:1-17.
399. Ames RS, Li Y, Sarau HM, et al. Molecular cloning and characterization of the human anaphylatoxin C3a receptor. *J Biol Chem*. 1996;271(34):20231-20234.
400. Crass T, Raffetseder U, Martin U, et al. Expression cloning of the human C3a anaphylatoxin receptor (C3aR) from differentiated U-937 cells. *Eur J Immunol*. 1996;26(8):1944-1950.
401. DiScipio RG, Daffern PJ, Jagels MA, Broide DH, Sriramarao P. A comparison of C3a and C5a-mediated stable adhesion of rolling eosinophils in postcapillary venules and transendothelial migration in vitro and in vivo. *J Immunol*. 1999;162(2):1127-1136.
402. Norgauer J, Dobos G, Kownatzki E, et al. Complement fragment C3a stimulates Ca2+ influx in neutrophils via a pertussis-toxin-sensitive G protein. *Eur J Biochem*. 1993;217(1):289-294.
403. Boulay F, Mery L, Tardif M, Brouchon L, Vignais P. Expression cloning of a receptor for C5a anaphylatoxin on differentiated HL-60 cells. *Biochemistry*. 1991;30(12):2993-2999.
404. Gerard NP, Gerard C. The chemotactic receptor for human C5a anaphylatoxin. *Nature*. 1991;349(6310):614-617.
405. Pease JE, Barker MD. N-linked glycosylation of the C5a receptor. *Biochem Mol Biol Int*. 1993;31(4):719-726.
406. Farzan M, Schnitzler CE, Vasilieva N, et al. Sulfated tyrosines contribute to the formation of the C5a docking site of the human C5a anaphylatoxin receptor. *J Exp Med*. 2001;193(9):1059-1066.
407. Ippel JH, de Haas CJ, Bunschoten A, et al. Structure of the tyrosine-sulfated C5a receptor N terminus in complex with chemotaxis inhibitory protein of Staphylococcus aureus. *J Biol Chem*. 2009;284(18):12363-12372.
408. Monk PN, Scola AM, Madala P, Fairlie DP. Function, structure and therapeutic potential of complement C5a receptors. *Br J Pharmacol*. 2007;152(4):429-448.
409. Ohno M, Hirata T, Enomoto M, Araki T, Ishimaru H, Takahashi TA. A putative chemoattractant receptor, C5L2, is expressed in granulocyte and immature dendritic cells, but not in mature dendritic cells. *Mol Immunol*. 2000;37(8):407-412.
410. Cain SA, Monk PN. The orphan receptor C5L2 has high affinity binding sites for complement fragments C5a and C5a des-Arg(74). *J Biol Chem*. 2002;277(9):7165-7169.
411. Okinaga S, Slattery D, Humbles A, et al. C5L2, a nonsignaling C5A binding protein. *Biochemistry*. 2003;42(31):9406-9415.
412. Scola AM, Johswich KO, Morgan BP, Klos A, Monk PN. The human complement fragment receptor, C5L2, is a recycling decoy receptor. *Mol Immunol*. 2009;46(6):1149-1162.
413. Gao H, Neff TA, Guo RF, et al. Evidence for a functional role of the second C5a receptor C5L2. *FASEB J*. 2005;19(8):1003-1005.
414. Monk PN, Partridge LJ. Characterization of a complement-fragment-C5a-stimulated calcium-influx mechanism in U937 monocytic cells. *Biochem J*. 1993;295 ( Pt 3)(Pt 3):679-684.
415. Skokowa J, Ali SR, Felda O, et al. Macrophages induce the inflammatory response in the pulmonary Arthus reaction through G alpha i2 activation that controls C5aR and Fc receptor cooperation. *J Immunol*. 2005;174(5):3041-3050.
416. Braun L, Christophe T, Boulay F. Phosphorylation of key serine residues is required for internalization of the complement 5a (C5a) anaphylatoxin receptor via a beta-arrestin, dynamin, and clathrin-dependent pathway. *J Biol Chem*. 2003;278(6):4277-4285.
417. la Sala A, Gadina M, Kelsall BL. G(i)-protein-dependent inhibition of IL-12 production is mediated by activation of the phosphatidylinositol 3-kinase-protein 3 kinase B/Akt pathway and JNK. *J Immunol*. 2005;175(5):2994-2999.

418. Perianayagam MC, Balakrishnan VS, King AJ, Pereira BJ, Jaber BL. C5a delays apoptosis of human neutrophils by a phosphatidylinositol 3-kinase-signaling pathway. *Kidney Int*. 2002;61(2):456-463.
419. Jiang H, Kuang Y, Wu Y, Smrcka A, Simon MI, Wu D. Pertussis toxin-sensitive activation of phospholipase C by the C5a and fMet-Leu-Phe receptors. *J Biol Chem*. 1996;271(23):13430-13434.
420. Mullmann TJ, Siegel MI, Egan RW, Billah MM. Complement C5a activation of phospholipase D in human neutrophils. A major route to the production of phosphatidates and diglycerides. *J Immunol*. 1990;144(5):1901-1908.
421. Buhl AM, Avdi N, Worthen GS, Johnson GL. Mapping of the C5a receptor signal transduction network in human neutrophils. *Proc Natl Acad Sci U S A*. 1994;91(19):9190-9194.
422. Daffern PJ, Pfeifer PH, Ember JA, Hugli TE. C3a is a chemotaxin for human eosinophils but not for neutrophils. I. C3a stimulation of neutrophils is secondary to eosinophil activation. *J Exp Med*. 1995;181(6):2119-2127.
423. Glovsky MM, Hugli TE, Ishizaka T, Lichtenstein LM, Erickson BW. Anaphylatoxin-induced histamine release with human leukocytes: studies of C3a leukocyte binding and histamine release. *J Clin Invest*. 1979;64(3):804-811.
424. Gutzmer R, Lisewski M, Zwirner J, et al. Human monocyte-derived dendritic cells are chemoattracted to C3a after up-regulation of the C3a receptor with interferons. *Immunology*. 2004;111(4):435-443.
425. Klos A, Bank S, Gietz C, et al. C3a receptor on dibutyryl-cAMP-differentiated U937 cells and human neutrophils: the human C3a receptor characterized by functional responses and 125I-C3a binding. *Biochemistry*. 1992;31(46):11274-11282.
426. Laumonnier Y, Karsten CM, Kohl J. Novel insights into the expression pattern of anaphylatoxin receptors in mice and men. *Mol Immunol*. 2017;89:44-58.
427. Zwirner J, Gotze O, Sieber A, et al. The human mast cell line HMC-1 binds and responds to C3a but not C3a(desArg). *Scand J Immunol*. 1998;47(1):19-24.
428. Quell KM, Karsten CM, Kordowski A, et al. Monitoring C3aR Expression Using a Floxed tdTomato-C3aR Reporter Knock-in Mouse. *J Immunol*. 2017;199(2):688-706.
429. Ischenko A, Sayah S, Patte C, et al. Expression of a functional anaphylatoxin C3a receptor by astrocytes. *J Neurochem*. 1998;71(6):2487-2496.
430. Monsinjon T, Gasque P, Chan P, Ischenko A, Brady JJ, Fontaine MC. Regulation by complement C3a and C5a anaphylatoxins of cytokine production in human umbilical vein endothelial cells. *FASEB J*. 2003;17(9):1003-1014.
431. Fregonese L, Swan FJ, van Schadewijk A, et al. Expression of the anaphylatoxin receptors C3aR and C5aR is increased in fatal asthma. *J Allergy Clin Immunol*. 2005;115(6):1148-1154.
432. Martin U, Bock D, Arseniev L, et al. The human C3a receptor is expressed on neutrophils and monocytes, but not on B or T lymphocytes. *J Exp Med*. 1997;186(2):199-207.
433. Karsten CM, Wiese AV, Mey F, et al. Monitoring C5aR2 Expression Using a Floxed tdTomato-C5aR2 Knock-In Mouse. *J Immunol*. 2017;199(9):3234-3248.
434. Hawksworth OA, Coulthard LG, Woodruff TM. Complement in the fundamental processes of the cell. *Mol Immunol*. 2017;84:17-25.
435. Manthey HD, Woodruff TM, Taylor SM, Monk PN. Complement component 5a (C5a). *Int J Biochem Cell Biol*. 2009;41(11):2114-2117.
436. Karsten CM, Laumonnier Y, Eurich B, et al. Monitoring and cell-specific deletion of C5aR1 using a novel floxed GFP-C5aR1 reporter knock-in mouse. *J Immunol*. 2015;194(4):1841-1855.
437. Dunkelberger J, Zhou L, Miwa T, Song WC. C5aR expression in a novel GFP reporter gene knockin mouse: implications for the mechanism of action of C5aR signaling in T cell immunity. *J Immunol*. 2012;188(8):4032-4042.
438. Murakami Y, Imamichi T, Nagasawa S. Characterization of C3a anaphylatoxin receptor on guinea-pig macrophages. *Immunology*. 1993;79(4):633-638.

439. Elsner J, Oppermann M, Czech W, Kapp A. C3a activates the respiratory burst in human polymorphonuclear neutrophilic leukocytes via pertussis toxin-sensitive G-proteins. *Blood*. 1994;83(11):3324-3331.
440. Kretzschmar T, Jeromin A, Gietz C, et al. Chronic myelogenous leukemia-derived basophilic granulocytes express a functional active receptor for the anaphylatoxin C3a. *Eur J Immunol*. 1993;23(2):558-561.
441. el-Lati SG, Dahinden CA, Church MK. Complement peptides C3a- and C5a-induced mediator release from dissociated human skin mast cells. *J Invest Dermatol*. 1994;102(5):803-806.
442. Takafuji S, Tadokoro K, Ito K. Effects of interleukin (IL)-3 and IL-5 on human eosinophil degranulation induced by complement components C3a and C5a. *Allergy*. 1996;51(8):563-568.
443. Fukuoka Y, Hugli TE. Demonstration of a specific C3a receptor on guinea pig platelets. *J Immunol*. 1988;140(10):3496-3501.
444. Aksamit RR, Falk W, Leonard EJ. Chemotaxis by mouse macrophage cell lines. *J Immunol*. 1981;126(6):2194-2199.
445. Ehrengruber MU, Geiser T, Deranleau DA. Activation of human neutrophils by C3a and C5A. Comparison of the effects on shape changes, chemotaxis, secretion, and respiratory burst. *FEBS Lett*. 1994;346(2-3):181-184.
446. Lett-Brown MA, Leonard EJ. Histamine-induced inhibition of normal human basophil chemotaxis to C5a. *J Immunol*. 1977;118(3):815-818.
447. Mastellos D, Papadimitriou JC, Franchini S, Tsonis PA, Lambris JD. A novel role of complement: mice deficient in the fifth component of complement (C5) exhibit impaired liver regeneration. *J Immunol*. 2001;166(4):2479-2486.
448. Strey CW, Markiewski M, Mastellos D, et al. The proinflammatory mediators C3a and C5a are essential for liver regeneration. *J Exp Med*. 2003;198(6):913-923.
449. Addis-Lieser E, Kohl J, Chiaramonte MG. Opposing regulatory roles of complement factor 5 in the development of bleomycin-induced pulmonary fibrosis. *J Immunol*. 2005;175(3):1894-1902.
450. Hillebrandt S, Wasmuth HE, Weiskirchen R, et al. Complement factor 5 is a quantitative trait gene that modifies liver fibrogenesis in mice and humans. *Nat Genet*. 2005;37(8):835-843.
451. Benard M, Gonzalez BJ, Schouft MT, et al. Characterization of C3a and C5a receptors in rat cerebellar granule neurons during maturation. Neuroprotective effect of C5a against apoptotic cell death. *J Biol Chem*. 2004;279(42):43487-43496.
452. Kemper C, Kohl J. Novel roles for complement receptors in T cell regulation and beyond. *Mol Immunol*. 2013;56(3):181-190.
453. Kordowski A, Reinicke AT, Wu D, et al. C5a receptor 1(-/-) mice are protected from the development of IgE-mediated experimental food allergy. *Allergy*. 2019;74(4):767-779.
454. Karsten CM, Pandey MK, Figge J, et al. Anti-inflammatory activity of IgG1 mediated by Fc galactosylation and association of FcγRIIB and dectin-1. *Nat Med*. 2012;18(9):1401-1406.
455. Engelke C, Wiese AV, Schmudde I, et al. Distinct roles of the anaphylatoxins C3a and C5a in dendritic cell-mediated allergic asthma. *J Immunol*. 2014;193(11):5387-5401.
456. Hawlisch H, Belkaid Y, Baelder R, Hildeman D, Gerard C, Kohl J. C5a negatively regulates toll-like receptor 4-induced immune responses. *Immunity*. 2005;22(4):415-426.
457. Schmudde I, Strover HA, Vollbrandt T, et al. C5a receptor signalling in dendritic cells controls the development of maladaptive Th2 and Th17 immunity in experimental allergic asthma. *Mucosal Immunol*. 2013;6(4):807-825.
458. Sheen JH, Strainic MG, Liu J, et al. TLR-Induced Murine Dendritic Cell (DC) Activation Requires DC-Intrinsic Complement. *J Immunol*. 2017;199(1):278-291.
459. Rittirsch D, Flierl MA, Nadeau BA, et al. Functional roles for C5a receptors in sepsis. *Nat Med*. 2008;14(5):551-557.
460. Krarup A, Wallis R, Presanis JS, Gal P, Sim RB. Simultaneous activation of complement and coagulation by MBL-associated serine protease 2. *PLoS One*. 2007;2(7):e623.

461. Suresh R, Chandrasekaran P, Sutterwala FS, Mosser DM. Complement-mediated 'bystander' damage initiates host NLRP3 inflammasome activation. *J Cell Sci*. 2016;129(9):1928-1939.
462. Triantafilou K, Hughes TR, Triantafilou M, Morgan BP. The complement membrane attack complex triggers intracellular Ca2+ fluxes leading to NLRP3 inflammasome activation. *J Cell Sci*. 2013;126(Pt 13):2903-2913.
463. Doyle SL, Campbell M, Ozaki E, et al. NLRP3 has a protective role in age-related macular degeneration through the induction of IL-18 by drusen components. *Nat Med*. 2012;18(5):791-798.
464. Benoit ME, Clarke EV, Morgado P, Fraser DA, Tenner AJ. Complement protein C1q directs macrophage polarization and limits inflammasome activity during the uptake of apoptotic cells. *J Immunol*. 2012;188(11):5682-5693.
465. Karsten CM, Kohl J. The immunoglobulin, IgG Fc receptor and complement triangle in autoimmune diseases. *Immunobiology*. 2012;217(11):1067-1079.
466. Rahman J, Bibby JA, Singh P, et al. A CD4(+) T cell-intrinsic complement C5aR2-prostacyclin-IL-1R2 axis orchestrates Th1 cell contraction. *Immunity*. 2025;58(6):1438-1455 e1410.
467. Schanzenbacher J, Kohl J, Karsten CM. Anaphylatoxins spark the flame in early autoimmunity. *Front Immunol*. 2022;13:958392.
468. Chang CH, Curtis JD, Maggi LB, Jr., et al. Posttranscriptional control of T cell effector function by aerobic glycolysis. *Cell*. 2013;153(6):1239-1251.
469. Cardone J, Le Friec G, Vantourout P, et al. Complement regulator CD46 temporally regulates cytokine production by conventional and unconventional T cells. *Nat Immunol*. 2010;11(9):862-871.
470. Ni Choileain S, Weyand NJ, Neumann C, Thomas J, So M, Astier AL. The dynamic processing of CD46 intracellular domains provides a molecular rheostat for T cell activation. *PLoS One*. 2011;6(1):e16287.
471. Ni Choileain S, Hay J, Thomas J, et al. TCR-stimulated changes in cell surface CD46 expression generate type 1 regulatory T cells. *Sci Signal*. 2017;10(502).
472. Arbore G, Kemper C. A novel "complement-metabolism-inflammasome axis" as a key regulator of immune cell effector function. *Eur J Immunol*. 2016;46(7):1563-1573.
473. Arbore G, West EE, Rahman J, et al. Complement receptor CD46 co-stimulates optimal human CD8(+) T cell effector function via fatty acid metabolism. *Nat Commun*. 2018;9(1):4186.
474. Ling GS, Crawford G, Buang N, et al. C1q restrains autoimmunity and viral infection by regulating CD8(+) T cell metabolism. *Science*. 2018;360(6388):558-563.
475. Fischer WH, Hugli TE. Regulation of B cell functions by C3a and C3a(desArg): suppression of TNF-alpha, IL-6, and the polyclonal immune response. *J Immunol*. 1997;159(9):4279-4286.
476. Fischer WH, Jagels MA, Hugli TE. Regulation of IL-6 synthesis in human peripheral blood mononuclear cells by C3a and C3a(desArg). *J Immunol*. 1999;162(1):453-459.
477. Paiano J, Harland M, Strainic MG, Nedrud J, Hussain W, Medof ME. Follicular B2 Cell Activation and Class Switch Recombination Depend on Autocrine C3ar1/C5ar1 Signaling in B2 Cells. *J Immunol*. 2019;203(2):379-388.
478. Kremlitzka M, Nowacka AA, Mohlin FC, Bompada P, De Marinis Y, Blom AM. Interaction of Serum-Derived and Internalized C3 With DNA in Human B Cells-A Potential Involvement in Regulation of Gene Transcription. *Front Immunol*. 2019;10:493.
479. Jimenez-Reinoso A, Marin AV, Subias M, et al. Human plasma C3 is essential for the development of memory B, but not T, lymphocytes. *J Allergy Clin Immunol*. 2018;141(3):1151-1154 e1114.
480. Cumpelik A, Heja D, Hu Y, et al. Dynamic regulation of B cell complement signaling is integral to germinal center responses. *Nat Immunol*. 2021;22(6):757-768.
481. Ratajczak MZ, Adamiak M, Abdelbaset-Ismail A, et al. Intracellular complement (complosome) is expressed in hematopoietic stem/progenitor cells (HSPCs) and regulates cell

trafficking, metabolism and proliferation in an intracrine Nlrp3 inflammasome-dependent manner. *Leukemia*. 2023;37(6):1401-1405.
482. Daniel E, Barlow HR, Sutton GI, et al. Cyp26b1 is an essential regulator of distal airway epithelial differentiation during lung development. *Development*. 2020;147(4).
483. Bernardo AS, Jouneau A, Marks H, et al. Mammalian embryo comparison identifies novel pluripotency genes associated with the naive or primed state. *Biol Open*. 2018;7(8).
484. Mach N, Gillessen S, Wilson SB, Sheehan C, Mihm M, Dranoff G. Differences in dendritic cells stimulated in vivo by tumors engineered to secrete granulocyte-macrophage colony-stimulating factor or Flt3-ligand. *Cancer Res*. 2000;60(12):3239-3246.
485. Karsunky H, Merad M, Cozzio A, Weissman IL, Manz MG. Flt3 ligand regulates dendritic cell development from Flt3+ lymphoid and myeloid-committed progenitors to Flt3+ dendritic cells in vivo. *J Exp Med*. 2003;198(2):305-313.
486. Vremec D, Segura E. The purification of large numbers of antigen presenting dendritic cells from mouse spleen. *Methods Mol Biol*. 2013;960:327-350.
487. Arora P, Porcelli SA. An Efficient and High Yield Method for Isolation of Mouse Dendritic Cell Subsets. *J Vis Exp*. 2016(110):e53824.
488. Onai N, Kurabayashi K, Hosoi-Amaike M, et al. A clonogenic progenitor with prominent plasmacytoid dendritic cell developmental potential. *Immunity*. 2013;38(5):943-957.
489. Onai N, Ohteki T. Isolation of Dendritic Cell Progenitor and Bone Marrow Progenitor Cells from Mouse. *Methods Mol Biol*. 2016;1423:53-59.
490. Griffiths JA, Richard AC, Bach K, Lun ATL, Marioni JC. Detection and removal of barcode swapping in single-cell RNA-seq data. *Nat Commun*. 2018;9(1):2667.
491. Lun ATL, Riesenfeld S, Andrews T, et al. EmptyDrops: distinguishing cells from empty droplets in droplet-based single-cell RNA sequencing data. *Genome Biol*. 2019;20(1):63.
492. Germain PL, Lun A, Garcia Meixide C, Macnair W, Robinson MD. Doublet identification in single-cell sequencing data using scDblFinder. *F1000Res*. 2021;10:979.
493. Satija R, Farrell JA, Gennert D, Schier AF, Regev A. Spatial reconstruction of single-cell gene expression data. *Nat Biotechnol*. 2015;33(5):495-502.
494. Butler A, Hoffman P, Smibert P, Papalexi E, Satija R. Integrating single-cell transcriptomic data across different conditions, technologies, and species. *Nat Biotechnol*. 2018;36(5):411-420.
495. Stuart T, Butler A, Hoffman P, et al. Comprehensive Integration of Single-Cell Data. *Cell*. 2019;177(7):1888-1902 e1821.
496. Hao Y, Hao S, Andersen-Nissen E, et al. Integrated analysis of multimodal single-cell data. *Cell*. 2021;184(13):3573-3587 e3529.
497. Hao Y, Stuart T, Kowalski MH, et al. Dictionary learning for integrative, multimodal and scalable single-cell analysis. *Nat Biotechnol*. 2024;42(2):293-304.
498. Mercer TR, Neph S, Dinger ME, et al. The human mitochondrial transcriptome. *Cell*. 2011;146(4):645-658.
499. Korsunsky I, Millard N, Fan J, et al. Fast, sensitive and accurate integration of single-cell data with Harmony. *Nat Methods*. 2019;16(12):1289-1296.
500. Finak G, McDavid A, Yajima M, et al. MAST: a flexible statistical framework for assessing transcriptional changes and characterizing heterogeneity in single-cell RNA sequencing data. *Genome Biol*. 2015;16:278.
501. Qiu X, Hill A, Packer J, Lin D, Ma YA, Trapnell C. Single-cell mRNA quantification and differential analysis with Census. *Nat Methods*. 2017;14(3):309-315.
502. Lutz MB, Rossner S. Factors influencing the generation of murine dendritic cells from bone marrow: the special role of fetal calf serum. *Immunobiology*. 2007;212(9-10):855-862.
503. Lehmann JS, Rughwani P, Kolenovic M, Ji S, Sun B. LEGENDplex: Bead-assisted multiplex cytokine profiling by flow cytometry. *Methods Enzymol*. 2019;629:151-176.
504. Nystedt J, Anderson H, Hirvonen T, et al. Human CMP-N-acetylneuraminic acid hydroxylase is a novel stem cell marker linked to stem cell-specific mechanisms. *Stem Cells*. 2010;28(2):258-267.

505. Rothenberg EV. Transcriptional control of early T and B cell developmental choices. *Annu Rev Immunol*. 2014;32:283-321.
506. Cool T, Worthington A, Poscablo D, Hussaini A, Forsberg EC. Interleukin 7 receptor is required for myeloid cell homeostasis and reconstitution by hematopoietic stem cells. *Exp Hematol*. 2020;90:39-45 e33.
507. Safavi S, Larouche A, Zahn A, et al. The uracil-DNA glycosylase UNG protects the fitness of normal and cancer B cells expressing AID. *NAR Cancer*. 2020;2(3):zcaa019.
508. Zhang C, Ni C, Lu H. Polo-Like Kinase 2: From Principle to Practice. *Front Oncol*. 2022;12:956225.
509. Xu H, Tan S, Zhao Y, et al. Lin(-) PU.1(dim) GATA-1(-) defines haematopoietic stem cells with long-term multilineage reconstitution activity. *Cell Prolif*. 2023;56(11):e13490.
510. Shafiq S, Hamashima K, Guest LA, et al. Competing dynamic gene regulatory networks involved in fibroblast reprogramming to hematopoietic progenitor cells. *Stem Cell Reports*. 2025;20(5):102473.
511. Yu X, Wang Y, Deng M, et al. The basic leucine zipper transcription factor NFIL3 directs the development of a common innate lymphoid cell precursor. *Elife*. 2014;3.
512. Han Y, Hu X, Yun X, et al. Nucleolar and spindle associated protein 1 enhances chemoresistance through DNA damage repair pathway in chronic lymphocytic leukemia by binding with RAD51. *Cell Death Dis*. 2021;12(11):1083.
513. Guo P, Liu Y, Geng F, et al. Histone variant H3.3 maintains adult haematopoietic stem cell homeostasis by enforcing chromatin adaptability. *Nat Cell Biol*. 2022;24(1):99-111.
514. Wu S, Su R, Jia H. Cyclin B2 (CCNB2) Stimulates the Proliferation of Triple-Negative Breast Cancer (TNBC) Cells In Vitro and In Vivo. *Dis Markers*. 2021;2021:5511041.
515. Bagadia P, Huang X, Liu TT, et al. An Nfil3-Zeb2-Id2 pathway imposes Irf8 enhancer switching during cDC1 development. *Nat Immunol*. 2019;20(9):1174-1185.
516. Elizondo DM, Brandy NZD, da Silva RLL, et al. Allograft Inflammatory Factor-1 Governs Hematopoietic Stem Cell Differentiation Into cDC1 and Monocyte-Derived Dendritic Cells Through IRF8 and RelB in vitro. *Front Immunol*. 2019;10:173.
517. Chauhan KS, Das A, Jaiswal H, et al. IRF8 and BATF3 interaction enhances the cDC1 specific Pfkfb3 gene expression. *Cell Immunol*. 2022;371:104468.
518. Murphy TL, Murphy KM. Dendritic cells in cancer immunology. *Cell Mol Immunol*. 2022;19(1):3-13.
519. Pereira da Costa M, Minutti CM, Piot C, et al. Interplay between CXCR4 and CCR2 regulates bone marrow exit of dendritic cell progenitors. *Cell Rep*. 2023;42(8):112881.
520. Liu TT, Zhang Z, Deng J, et al. CXCL16 knockout inhibit asthma airway inflammation by suppressing H2-DM molecular mediated antigen presentation. *Cell Death Discov*. 2025;11(1):90.
521. Gutierrez L, Nikolic T, van Dijk TB, et al. Gata1 regulates dendritic-cell development and survival. *Blood*. 2007;110(6):1933-1941.
522. Tsang AP, Visvader JE, Turner CA, et al. FOG, a multitype zinc finger protein, acts as a cofactor for transcription factor GATA-1 in erythroid and megakaryocytic differentiation. *Cell*. 1997;90(1):109-119.
523. Xu MM, Pu Y, Han D, et al. Dendritic Cells but Not Macrophages Sense Tumor Mitochondrial DNA for Cross-priming through Signal Regulatory Protein alpha Signaling. *Immunity*. 2017;47(2):363-373 e365.
524. He Y, Yang Z, Zhao CS, et al. T-cell receptor (TCR) signaling promotes the assembly of RanBP2/RanGAP1-SUMO1/Ubc9 nuclear pore subcomplex via PKC-theta-mediated phosphorylation of RanGAP1. *Elife*. 2021;10.
525. Cheung P, Schaffert S, Chang SE, et al. Repression of CTSG, ELANE and PRTN3-mediated histone H3 proteolytic cleavage promotes monocyte-to-macrophage differentiation. *Nat Immunol*. 2021;22(6):711-722.
526. Gaspar-Maia A, Qadeer ZA, Hasson D, et al. MacroH2A histone variants act as a barrier upon reprogramming towards pluripotency. *Nat Commun*. 2013;4:1565.

527. Jeon YJ, Khelifa S, Ratnikov B, et al. Regulation of glutamine carrier proteins by RNF5 determines breast cancer response to ER stress-inducing chemotherapies. *Cancer Cell*. 2015;27(3):354-369.
528. Larriba S, Sumoy L, Ramos MD, et al. ATB(0)/SLC1A5 gene. Fine localisation and exclusion of association with the intestinal phenotype of cystic fibrosis. *Eur J Hum Genet*. 2001;9(11):860-866.
529. Verhagen-Oldenampsen JH, Haanstra JR, van Strien PM, Valkhof M, Touw IP, von Lindern M. Loss of ercc1 results in a time- and dose-dependent reduction of proliferating early hematopoietic progenitors. *Anemia*. 2012;2012:783068.
530. Vroman H, Bergen IM, van Hulst JAC, et al. TNF-alpha-induced protein 3 levels in lung dendritic cells instruct T(H)2 or T(H)17 cell differentiation in eosinophilic or neutrophilic asthma. *J Allergy Clin Immunol*. 2018;141(5):1620-1633 e1612.
531. Lavoie S, Chun E, Bae S, et al. Expression of Free Fatty Acid Receptor 2 by Dendritic Cells Prevents Their Expression of Interleukin 27 and Is Required for Maintenance of Mucosal Barrier and Immune Response Against Colorectal Tumors in Mice. *Gastroenterology*. 2020;158(5):1359-1372 e1359.
532. Kingston D, Schmid MA, Onai N, Obata-Onai A, Baumjohann D, Manz MG. The concerted action of GM-CSF and Flt3-ligand on in vivo dendritic cell homeostasis. *Blood*. 2009;114(4):835-843.
533. Saha I, Chawla AS, Oliveira A, et al. Alloreactive memory CD4 T cells promote transplant rejection by engaging DCs to induce innate inflammation and CD8 T cell priming. *Proc Natl Acad Sci U S A*. 2024;121(34):e2401658121.
534. Meibers HE, Warrick KA, VonHandorf A, et al. Effector memory T cells induce innate inflammation by triggering DNA damage and a non-canonical STING pathway in dendritic cells. *Cell Rep*. 2023;42(10):113180.
535. Cabeza-Cabrerizo M, Cardoso A, Minutti CM, Pereira da Costa M, Reis e Sousa C. Dendritic Cells Revisited. *Annu Rev Immunol*. 2021;39:131-166.
536. Guermonprez P, Valladeau J, Zitvogel L, Théry C, Amigorena S. Antigen presentation and T cell stimulation by dendritic cells. *Annu Rev Immunol*. 2002;20:621-667.
537. Narni-Mancinelli E, Gauthier L, Baratin M, et al. Complement factor P is a ligand for the natural killer cell-activating receptor NKp46. *Sci Immunol*. 2017;2(10).
538. Cortes C, Ferreira VP, Pangburn MK. Native properdin binds to Chlamydia pneumoniae and promotes complement activation. *Infect Immun*. 2011;79(2):724-731.
539. Camous L, Roumenina L, Bigot S, et al. Complement alternative pathway acts as a positive feedback amplification of neutrophil activation. *Blood*. 2011;117(4):1340-1349.
540. Kemper C, Mitchell LM, Zhang L, Hourcade DE. The complement protein properdin binds apoptotic T cells and promotes complement activation and phagocytosis. *Proc Natl Acad Sci U S A*. 2008;105(26):9023-9028.
541. Nagamachi S, Ohsawa I, Suzuki H, et al. Properdin has an ascendancy over factor H regulation in complement-mediated renal tubular damage. *BMC Nephrol*. 2014;15:82.
542. O'Flynn J, van der Pol P, Dixon KO, Prohaszka Z, Daha MR, van Kooten C. Monomeric C-reactive protein inhibits renal cell-directed complement activation mediated by properdin. *Am J Physiol Renal Physiol*. 2016;310(11):F1308-1316.
543. Saggu G, Cortes C, Emch HN, Ramirez G, Worth RG, Ferreira VP. Identification of a novel mode of complement activation on stimulated platelets mediated by properdin and C3(H2O). *J Immunol*. 2013;190(12):6457-6467.
544. Xu W, Berger SP, Trouw LA, et al. Properdin binds to late apoptotic and necrotic cells independently of C3b and regulates alternative pathway complement activation. *J Immunol*. 2008;180(11):7613-7621.
545. Gaarkeuken H, Siezenga MA, Zuidwijk K, et al. Complement activation by tubular cells is mediated by properdin binding. *Am J Physiol Renal Physiol*. 2008;295(5):F1397-1403.

546. Zaferani A, Vives RR, van der Pol P, et al. Identification of tubular heparan sulfate as a docking platform for the alternative complement component properdin in proteinuric renal disease. *J Biol Chem*. 2011;286(7):5359-5367.
547. Chen Q, Manzke M, Hartmann A, et al. Complement Factor H-Related 5-Hybrid Proteins Anchor Properdin and Activate Complement at Self-Surfaces. *J Am Soc Nephrol*. 2016;27(5):1413-1425.
548. Ferreira VP, Cortes C, Pangburn MK. Native polymeric forms of properdin selectively bind to targets and promote activation of the alternative pathway of complement. *Immunobiology*. 2010;215(11):932-940.
549. Klop B, van der Pol P, van Bruggen R, et al. Differential complement activation pathways promote C3b deposition on native and acetylated LDL thereby inducing lipoprotein binding to the complement receptor 1. *J Biol Chem*. 2014;289(51):35421-35430.
550. Micklisch S, Lin Y, Jacob S, et al. Age-related macular degeneration associated polymorphism rs10490924 in ARMS2 results in deficiency of a complement activator. *J Neuroinflammation*. 2017;14(1):4.
551. O'Flynn J, Dixon KO, Faber Krol MC, Daha MR, van Kooten C. Myeloperoxidase directs properdin-mediated complement activation. *J Innate Immun*. 2014;6(4):417-425.
552. Zaferani A, Vives RR, van der Pol P, et al. Factor h and properdin recognize different epitopes on renal tubular epithelial heparan sulfate. *J Biol Chem*. 2012;287(37):31471-31481.
553. Kimura Y, Zhou L, Miwa T, Song WC. Genetic and therapeutic targeting of properdin in mice prevents complement-mediated tissue injury. *J Clin Invest*. 2010;120(10):3545-3554.
554. Kemper C, Atkinson JP, Hourcade DE. Properdin: emerging roles of a pattern-recognition molecule. *Annu Rev Immunol*. 2010;28:131-155.
555. Dixon KO, O'Flynn J, Klar-Mohamad N, Daha MR, van Kooten C. Properdin and factor H production by human dendritic cells modulates their T-cell stimulatory capacity and is regulated by IFN-gamma. *Eur J Immunol*. 2017;47(3):470-480.
556. Li K, Fazekasova H, Wang N, et al. Expression of complement components, receptors and regulators by human dendritic cells. *Mol Immunol*. 2011;48(9-10):1121-1127.
557. Reis ES, Barbuto JA, Isaac L. Human monocyte-derived dendritic cells are a source of several complement proteins. *Inflamm Res*. 2006;55(5):179-184.
558. Dembitzer FR, Kinoshita Y, Burstein D, et al. gC1qR expression in normal and pathologic human tissues: differential expression in tissues of epithelial and mesenchymal origin. *J Histochem Cytochem*. 2012;60(6):467-474.
559. Ghebrehiwet B, Lim BL, Kumar R, Feng X, Peerschke EI. gC1q-R/p33, a member of a new class of multifunctional and multicompartmental cellular proteins, is involved in inflammation and infection. *Immunol Rev*. 2001;180:65-77.
560. Eggleton P, Ghebrehiwet B, Sastry KN, et al. Identification of a gC1q-binding protein (gC1q-R) on the surface of human neutrophils. Subcellular localization and binding properties in comparison with the cC1q-R. *J Clin Invest*. 1995;95(4):1569-1578.
561. Peerschke EI, Ghebrehiwet B. The contribution of gC1qR/p33 in infection and inflammation. *Immunobiology*. 2007;212(4-5):333-342.
562. Soltys BJ, Kang D, Gupta RS. Localization of P32 protein (gC1q-R) in mitochondria and at specific extramitochondrial locations in normal tissues. *Histochem Cell Biol*. 2000;114(3):245-255.
563. van Leeuwen HC, O'Hare P. Retargeting of the mitochondrial protein p32/gC1Qr to a cytoplasmic compartment and the cell surface. *J Cell Sci*. 2001;114(Pt 11):2115-2123.
564. Dedio J, Jahnen-Dechent W, Bachmann M, Muller-Esterl W. The multiligand-binding protein gC1qR, putative C1q receptor, is a mitochondrial protein. *J Immunol*. 1998;160(7):3534-3542.
565. Soltys BJ, Gupta RS. Mitochondrial proteins at unexpected cellular locations: export of proteins from mitochondria from an evolutionary perspective. *Int Rev Cytol*. 2000;194:133-196.

566. Reis ES, Barbuto JA, Isaac L. Complement components, regulators and receptors are produced by human monocyte-derived dendritic cells. *Immunobiology*. 2007;212(3):151-157.
567. Sichien D, Lambrecht BN, Guilliams M, Scott CL. Development of conventional dendritic cells: from common bone marrow progenitors to multiple subsets in peripheral tissues. *Mucosal Immunol*. 2017;10(4):831-844.
568. Yanez A, Coetzee SG, Olsson A, et al. Granulocyte-Monocyte Progenitors and Monocyte-Dendritic Cell Progenitors Independently Produce Functionally Distinct Monocytes. *Immunity*. 2017;47(5):890-902 e894.
569. Prasher JM, Lalai AS, Heijmans-Antonissen C, et al. Reduced hematopoietic reserves in DNA interstrand crosslink repair-deficient Ercc1-/- mice. *EMBO J*. 2005;24(4):861-871.
570. Kool M, van Loo G, Waelput W, et al. The ubiquitin-editing protein A20 prevents dendritic cell activation, recognition of apoptotic cells, and systemic autoimmunity. *Immunity*. 2011;35(1):82-96.
571. Momtazi G, Lambrecht BN, Naranjo JR, Schock BC. Regulators of A20 (TNFAIP3): new drug-able targets in inflammation. *Am J Physiol Lung Cell Mol Physiol*. 2019;316(3):L456-L469.
572. Korkmaz B, Horwitz MS, Jenne DE, Gauthier F. Neutrophil elastase, proteinase 3, and cathepsin G as therapeutic targets in human diseases. *Pharmacol Rev*. 2010;62(4):726-759.
573. MacIvor DM, Shapiro SD, Pham CT, Belaaouaj A, Abraham SN, Ley TJ. Normal neutrophil function in cathepsin G-deficient mice. *Blood*. 1999;94(12):4282-4293.
574. Burgener SS, Leborgne NGF, Snipas SJ, Salvesen GS, Bird PI, Benarafa C. Cathepsin G Inhibition by Serpinb1 and Serpinb6 Prevents Programmed Necrosis in Neutrophils and Monocytes and Reduces GSDMD-Driven Inflammation. *Cell Rep*. 2019;27(12):3646-3656 e3645.
575. Bereshchenko O, Lo Re O, Nikulenkov F, et al. Deficiency and haploinsufficiency of histone macroH2A1.1 in mice recapitulate hematopoietic defects of human myelodysplastic syndrome. *Clin Epigenetics*. 2019;11(1):121.
576. Pasque V, Radzisheuskaya A, Gillich A, et al. Histone variant macroH2A marks embryonic differentiation in vivo and acts as an epigenetic barrier to induced pluripotency. *J Cell Sci*. 2012;125(Pt 24):6094-6104.
577. Yin X, Zeng D, Liao Y, Tang C, Li Y. The Function of H2A Histone Variants and Their Roles in Diseases. *Biomolecules*. 2024;14(8).
578. Sheshachalam A, Srivastava N, Mitchell T, Lacy P, Eitzen G. Granule protein processing and regulated secretion in neutrophils. *Front Immunol*. 2014;5:448.
579. Garg B, Mehta HM, Wang B, Kamel R, Horwitz MS, Corey SJ. Inducible expression of a disease-associated ELANE mutation impairs granulocytic differentiation, without eliciting an unfolded protein response. *J Biol Chem*. 2020;295(21):7492-7500.
580. Horwitz MS, Corey SJ, Grimes HL, Tidwell T. ELANE mutations in cyclic and severe congenital neutropenia: genetics and pathophysiology. *Hematol Oncol Clin North Am*. 2013;27(1):19-41, vii.
581. Alfarsi LH, Ansari RE, Erkan B, et al. SLC1A5 is a key regulator of glutamine metabolism and a prognostic marker for aggressive luminal breast cancer. *Sci Rep*. 2025;15(1):2805.
582. Hassanein M, Hoeksema MD, Shiota M, et al. SLC1A5 mediates glutamine transport required for lung cancer cell growth and survival. *Clin Cancer Res*. 2013;19(3):560-570.
583. Zou W, Han Z, Wang Z, Liu Q. Targeting glutamine metabolism as a potential target for cancer treatment. *J Exp Clin Cancer Res*. 2025;44(1):180.
584. Li Z, Deng J, Wang H, et al. Overview of glutamine metabolism in stromal components of the tumor microenvironment and potential anti-tumor therapies. *Genes & Diseases*. 2025:101834.
585. Liu H, Sun L, Zhao H, et al. Proteinase 3 depletion attenuates leukemia by promoting myeloid differentiation. *Cell Death Differ*. 2024;31(6):697-710.
586. Loison F, Zhu H, Karatepe K, et al. Proteinase 3-dependent caspase-3 cleavage modulates neutrophil death and inflammation. *J Clin Invest*. 2014;124(10):4445-4458.

587. Gao Y, Nish SA, Jiang R, et al. Control of T helper 2 responses by transcription factor IRF4-dependent dendritic cells. *Immunity*. 2013;39(4):722-732.
588. Scott CL, Soen B, Martens L, et al. The transcription factor Zeb2 regulates development of conventional and plasmacytoid DCs by repressing Id2. *J Exp Med*. 2016;213(6):897-911.
589. Pachocki CJ, Boes M, Affandi AJ. Comparing DC subsets in solid tumors: what about DC3s? *Immunother Adv*. 2025;5(1):ltaf021.
590. Lin Q, Chauvistre H, Costa IG, et al. Epigenetic program and transcription factor circuitry of dendritic cell development. *Nucleic Acids Res*. 2015;43(20):9680-9693.
591. Bosteels C, Scott CL. Transcriptional regulation of DC fate specification. *Mol Immunol*. 2020;121:38-46.
592. Lanca T, Ungerback J, Da Silva C, et al. IRF8 deficiency induces the transcriptional, functional, and epigenetic reprogramming of cDC1 into the cDC2 lineage. *Immunity*. 2022;55(8):1431-1447 e1411.
593. Lubin R, Patel AA, Mackerodt J, et al. The lifespan and kinetics of human dendritic cell subsets and their precursors in health and inflammation. *J Exp Med*. 2024;221(11).
594. Watowich SS, Liu YJ. Mechanisms regulating dendritic cell specification and development. *Immunol Rev*. 2010;238(1):76-92.
595. Sere KM, Lin Q, Felker P, et al. Dendritic cell lineage commitment is instructed by distinct cytokine signals. *Eur J Cell Biol*. 2012;91(6-7):515-523.
596. Cyran L, Serfling J, Kirschner L, et al. Flt3L, LIF, and IL-10 combination promotes the selective in vitro development of ESAM(low) cDC2B from murine bone marrow. *Eur J Immunol*. 2022;52(12):1946-1960.
597. Brasel K, De Smedt T, Smith JL, Maliszewski CR. Generation of murine dendritic cells from flt3-ligand-supplemented bone marrow cultures. *Blood*. 2000;96(9):3029-3039.
598. Lee J, Breton G, Oliveira TY, et al. Restricted dendritic cell and monocyte progenitors in human cord blood and bone marrow. *J Exp Med*. 2015;212(3):385-399.
599. Naik SH, Proietto AI, Wilson NS, et al. Cutting edge: generation of splenic CD8+ and CD8- dendritic cell equivalents in Fms-like tyrosine kinase 3 ligand bone marrow cultures. *J Immunol*. 2005;174(11):6592-6597.
600. Matthews W, Jordan CT, Gavin M, Jenkins NA, Copeland NG, Lemischka IR. A receptor tyrosine kinase cDNA isolated from a population of enriched primitive hematopoietic cells and exhibiting close genetic linkage to c-kit. *Proc Natl Acad Sci U S A*. 1991;88(20):9026-9030.
601. Kreisel FH, Blasius A, Kreisel D, Colonna M, Cella M. Interferon-producing cells develop from murine CD31(high)/Ly6C(-) marrow progenitors. *Cell Immunol*. 2006;242(2):91-98.
602. Kim S, Bagadia P, Anderson DA, 3rd, et al. High Amount of Transcription Factor IRF8 Engages AP1-IRF Composite Elements in Enhancers to Direct Type 1 Conventional Dendritic Cell Identity. *Immunity*. 2020;53(4):759-774 e759.
603. Inaba K, Inaba M, Romani N, et al. Generation of large numbers of dendritic cells from mouse bone marrow cultures supplemented with granulocyte/macrophage colony-stimulating factor. *J Exp Med*. 1992;176(6):1693-1702.
604. Sallusto F, Lanzavecchia A. Efficient presentation of soluble antigen by cultured human dendritic cells is maintained by granulocyte/macrophage colony-stimulating factor plus interleukin 4 and downregulated by tumor necrosis factor alpha. *J Exp Med*. 1994;179(4):1109-1118.
605. Hanada K, Tsunoda R, Hamada H. GM-CSF-induced in vivo expansion of splenic dendritic cells and their strong costimulation activity. *J Leukoc Biol*. 1996;60(2):181-190.
606. Anjuere F, Martin P, Ferrero I, et al. Definition of dendritic cell subpopulations present in the spleen, Peyer's patches, lymph nodes, and skin of the mouse. *Blood*. 1999;93(2):590-598.
607. Anjuere F, Martinez del Hoyo G, Martin P, Ardavin C. Langerhans cells acquire a CD8+ dendritic cell phenotype on maturation by CD40 ligation. *J Leukoc Biol*. 2000;67(2):206-209.

608. Cella M, Salio M, Sakakibara Y, Langen H, Julkunen I, Lanzavecchia A. Maturation, activation, and protection of dendritic cells induced by double-stranded RNA. *J Exp Med*. 1999;189(5):821-829.
609. De Smedt T, Pajak B, Muraille E, et al. Regulation of dendritic cell numbers and maturation by lipopolysaccharide in vivo. *J Exp Med*. 1996;184(4):1413-1424.
610. Inaba K, Steinman RM, Pack MW, et al. Identification of proliferating dendritic cell precursors in mouse blood. *J Exp Med*. 1992;175(5):1157-1167.
611. Luft T, Pang KC, Thomas E, et al. Type I IFNs enhance the terminal differentiation of dendritic cells. *J Immunol*. 1998;161(4):1947-1953.
612. Olweus J, BitMansour A, Warnke R, et al. Dendritic cell ontogeny: a human dendritic cell lineage of myeloid origin. *Proc Natl Acad Sci U S A*. 1997;94(23):12551-12556.
613. Paquette RL, Hsu NC, Kiertscher SM, et al. Interferon-alpha and granulocyte-macrophage colony-stimulating factor differentiate peripheral blood monocytes into potent antigen-presenting cells. *J Leukoc Biol*. 1998;64(3):358-367.
614. Pulendran B, Smith JL, Caspary G, et al. Distinct dendritic cell subsets differentially regulate the class of immune response in vivo. *Proc Natl Acad Sci U S A*. 1999;96(3):1036-1041.
615. Salomon B, Cohen JL, Masurier C, Klatzmann D. Three populations of mouse lymph node dendritic cells with different origins and dynamics. *J Immunol*. 1998;160(2):708-717.
616. Wu L, Vremec D, Ardavin C, et al. Mouse thymus dendritic cells: kinetics of development and changes in surface markers during maturation. *Eur J Immunol*. 1995;25(2):418-425.
617. Witmer-Pack MD, Olivier W, Valinsky J, Schuler G, Steinman RM. Granulocyte/macrophage colony-stimulating factor is essential for the viability and function of cultured murine epidermal Langerhans cells. *J Exp Med*. 1987;166(5):1484-1498.
618. Markowicz S, Engleman EG. Granulocyte-macrophage colony-stimulating factor promotes differentiation and survival of human peripheral blood dendritic cells in vitro. *J Clin Invest*. 1990;85(3):955-961.
619. Caux C, Dezutter-Dambuyant C, Schmitt D, Banchereau J. GM-CSF and TNF-alpha cooperate in the generation of dendritic Langerhans cells. *Nature*. 1992;360(6401):258-261.
620. Palucka KA, Taquet N, Sanchez-Chapuis F, Gluckman JC. Dendritic cells as the terminal stage of monocyte differentiation. *J Immunol*. 1998;160(9):4587-4595.
621. Lutz MB, Kukutsch N, Ogilvie AL, et al. An advanced culture method for generating large quantities of highly pure dendritic cells from mouse bone marrow. *J Immunol Methods*. 1999;223(1):77-92.
622. Helft J, Bottcher J, Chakravarty P, et al. GM-CSF Mouse Bone Marrow Cultures Comprise a Heterogeneous Population of CD11c(+)MHCII(+) Macrophages and Dendritic Cells. *Immunity*. 2015;42(6):1197-1211.
623. Saunders D, Lucas K, Ismaili J, et al. Dendritic cell development in culture from thymic precursor cells in the absence of granulocyte/macrophage colony-stimulating factor. *J Exp Med*. 1996;184(6):2185-2196.
624. Wada H, Noguchi Y, Marino MW, Dunn AR, Old LJ. T cell functions in granulocyte/macrophage colony-stimulating factor deficient mice. *Proc Natl Acad Sci U S A*. 1997;94(23):12557-12561.
625. Garrigan K, Moroni-Rawson P, McMurray C, et al. Functional comparison of spleen dendritic cells and dendritic cells cultured in vitro from bone marrow precursors. *Blood*. 1996;88(9):3508-3512.
626. Labeur MS, Roters B, Pers B, et al. Generation of tumor immunity by bone marrow-derived dendritic cells correlates with dendritic cell maturation stage. *J Immunol*. 1999;162(1):168-175.
627. Vremec D, Shortman K. Dendritic cell subtypes in mouse lymphoid organs: cross-correlation of surface markers, changes with incubation, and differences among thymus, spleen, and lymph nodes. *J Immunol*. 1997;159(2):565-573.
628. Poltorak MP, Schraml BU. Fate mapping of dendritic cells. *Front Immunol*. 2015;6:199.

629. Nutt SL, Chopin M. Transcriptional Networks Driving Dendritic Cell Differentiation and Function. *Immunity*. 2020;52(6):942-956.
630. Anderson DA, 3rd, Murphy KM. Models of dendritic cell development correlate ontogeny with function. *Adv Immunol*. 2019;143:99-119.
631. He Z, Zhu X, Shi Z, Wu T, Wu L. Metabolic Regulation of Dendritic Cell Differentiation. *Front Immunol*. 2019;10:410.
632. Konopko A, Lukomska A, Kucia M, Ratajczak MZ. The Different Responsiveness of C3- and C5-deficient Murine BM Cells to Oxidative Stress Explains Why C3 Deficiency, in Contrast to C5 Deficiency, Correlates with Better Pharmacological Mobilization and Engraftment of Hematopoietic Cells. *Stem Cell Rev Rep*. 2025;21(1):59-67.
633. Ratajczak MZ, Konopko A, Jarczak J, Kazek M, Ratajczak J, Kucia M. Complosome as a new intracellular regulatory network in both normal and malignant hematopoiesis. *Leukemia*. 2025;39(7):1571-1577.
634. Borkowska S, Suszynska M, Wysoczynski M, Ratajczak MZ. Mobilization studies in C3-deficient mice unravel the involvement of a novel crosstalk between the coagulation and complement cascades in mobilization of hematopoietic stem/progenitor cells. *Leukemia*. 2013;27(9):1928-1930.
635. Autio A, Wang H, Velázquez F, et al. SIRPα - CD47 axis regulates dendritic cell-T cell interactions and TCR activation during T cell priming in spleen. *PLoS One*. 2022;17(4):e0266566.
636. Per-Arne O. Role of CD47 and Signal Regulatory Protein Alpha (SIRPα) in Regulating the Clearance of Viable or Aged Blood Cells. *Transfus Med Hemother*. 2012;39(5):315-320.
637. Zhu S, Niu C, Chen J. Transcriptional divergence between cDC1s and cDC2s: an AP1-IRF composite element-dependent program. *Cell Mol Immunol*. 2021;18(7):1618-1619.
638. Bosteels C, Neyt K, Vanheerswynghels M, et al. Inflammatory Type 2 cDCs Acquire Features of cDC1s and Macrophages to Orchestrate Immunity to Respiratory Virus Infection. *Immunity*. 2020;52(6):1039-1056 e1039.
639. Heger L, Hofer TP, Bigley V, et al. Subsets of CD1c(+) DCs: Dendritic Cell Versus Monocyte Lineage. *Front Immunol*. 2020;11:559166.
640. West EE, Kemper C. Complosome — the intracellular complement system. *Nature Reviews Nephrology*. 2023;19(7):426-439.
641. Antoniou K, Ender F, Vollbrandt T, et al. Allergen-Induced C5a/C5aR1 Axis Activation in Pulmonary CD11b(+) cDCs Promotes Pulmonary Tolerance through Downregulation of CD40. *Cells*. 2020;9(2).
642. Wiese AV, Ender F, Quell KM, et al. The C5a/C5aR1 axis controls the development of experimental allergic asthma independent of LysM-expressing pulmonary immune cells. *PLoS One*. 2017;12(9):e0184956.
643. Strainic MG, Liu J, An F, et al. CD55 Is Essential for CD103(+) Dendritic Cell Tolerogenic Responses that Protect against Autoimmunity. *Am J Pathol*. 2019;189(7):1386-1401.
644. Ma C, Su M, Shen K, Chen J, Ning Y, Qi C. Key genes and pathways in tumor-educated dendritic cells by bioinformatical analysis. *Microbiol Immunol*. 2020;64(1):63-71.
645. Deeg J, Axmann M, Matic J, et al. T cell activation is determined by the number of presented antigens. *Nano Lett*. 2013;13(11):5619-5626.
646. Manz BN, Jackson BL, Petit RS, Dustin ML, Groves J. T-cell triggering thresholds are modulated by the number of antigen within individual T-cell receptor clusters. *Proc Natl Acad Sci U S A*. 2011;108(22):9089-9094.
647. Fischer UB, Jacovetty EL, Medeiros RB, et al. MHC class II deprivation impairs CD4 T cell motility and responsiveness to antigen-bearing dendritic cells in vivo. *Proc Natl Acad Sci U S A*. 2007;104(17):7181-7186.
648. Lavoie PM, McGrath H, Shoukry NH, Cazenave PA, Sékaly RP, Thibodeau J. Quantitative relationship between MHC class II-superantigen complexes and the balance of T cell activation versus death. *J Immunol*. 2001;166(12):7229-7237.

649. Sansom DM, Manzotti CN, Zheng Y. What's the difference between CD80 and CD86? *Trends Immunol*. 2003;24(6):314-319.
650. Lenschow DJ, Walunas TL, Bluestone JA. CD28/B7 system of T cell costimulation. *Annu Rev Immunol*. 1996;14:233-258.
651. Li JG, Du YM, Yan ZD, et al. CD80 and CD86 knockdown in dendritic cells regulates Th1/Th2 cytokine production in asthmatic mice. *Exp Ther Med*. 2016;11(3):878-884.
652. Fujii S, Liu K, Smith C, Bonito AJ, Steinman RM. The linkage of innate to adaptive immunity via maturing dendritic cells in vivo requires CD40 ligation in addition to antigen presentation and CD80/86 costimulation. *J Exp Med*. 2004;199(12):1607-1618.
653. Wang W, Li J, Wu K, Azhati B, Rexiati M. Culture and Identification of Mouse Bone Marrow-Derived Dendritic Cells and Their Capability to Induce T Lymphocyte Proliferation. *Med Sci Monit*. 2016;22:244-250.
654. Fu F, Li Y, Qian S, et al. Costimulatory molecule-deficient dendritic cell progenitors (MHC class II+, CD80dim, CD86-) prolong cardiac allograft survival in nonimmunosuppressed recipients. *Transplantation*. 1996;62(5):659-665.
655. van Rijt LS, Vos N, Willart M, et al. Essential role of dendritic cell CD80/CD86 costimulation in the induction, but not reactivation, of TH2 effector responses in a mouse model of asthma. *J Allergy Clin Immunol*. 2004;114(1):166-173.
656. Gao D, Mondal TK, Lawrence DA. Lead effects on development and function of bone marrow-derived dendritic cells promote Th2 immune responses. *Toxicol Appl Pharmacol*. 2007;222(1):69-79.
657. Carenza C, Calcaterra F, Oriolo F, et al. Costimulatory Molecules and Immune Checkpoints Are Differentially Expressed on Different Subsets of Dendritic Cells. *Front Immunol*. 2019;10:1325.
658. Del Prete A, Salvi V, Soriani A, et al. Dendritic cell subsets in cancer immunity and tumor antigen sensing. *Cell Mol Immunol*. 2023;20(5):432-447.
659. Sakurai S, Furuhashi K, Horiguchi R, et al. Conventional type 2 lung dendritic cells are potent inducers of follicular helper T cells in the asthmatic lung. *Allergol Int*. 2021;70(3):351-359.
660. Wang Y, Yu Z, Zhou Y, et al. Different doses of ovalbumin exposure on dendritic cells determine their genetic/epigenetic regulation and T cell differentiation. *Aging (Albany NY)*. 2020;12(24):25432-25451.
661. Leon B. Type 2 conventional dendritic cell functional heterogeneity: ontogenically committed or environmentally plastic? *Trends Immunol*. 2025;46(2):104-120.
662. Izumi G, Nakano H, Nakano K, et al. CD11b(+) lung dendritic cells at different stages of maturation induce Th17 or Th2 differentiation. *Nat Commun*. 2021;12(1):5029.
663. Ronchese F, Webb GR, Ochiai S, Lamiable O, Brewerton M. How type-2 dendritic cells induce Th2 differentiation: Instruction, repression, or fostering T cell-T cell communication? *Allergy*. 2025;80(2):395-407.
664. Park J, Bryers JD. Chemokine programming dendritic cell antigen response: part II - programming antigen presentation to T lymphocytes by partially maintaining immature dendritic cell phenotype. *Immunology*. 2013;139(1):88-99.
665. Block MS, Dietz AB, Gustafson MP, et al. Th17-inducing autologous dendritic cell vaccination promotes antigen-specific cellular and humoral immunity in ovarian cancer patients. *Nat Commun*. 2020;11(1):5173.
666. Bourque J, Hawiger D. Variegated Outcomes of T Cell Activation by Dendritic Cells in the Steady State. *J Immunol*. 2022;208(3):539-547.
667. Tatsumi N, Tjitropranoto A, Davila-Pagan A, Kumamoto Y. Functional Specialization and Collaboration of cDC2 Subsets in CD4+ T Cell Priming and Differentiation. *Immunol Rev*. 2025;336(1):e70069.
668. Khayrullina T, Yen JH, Jing H, Ganea D. In vitro differentiation of dendritic cells in the presence of prostaglandin E2 alters the IL-12/IL-23 balance and promotes differentiation of Th17 cells. *J Immunol*. 2008;181(1):721-735.

669. Dalod M, Scheu S. Dendritic cell functions in vivo: A user's guide to current and next-generation mutant mouse models. *Eur J Immunol*. 2022;52(11):1712-1749.
670. Segura E, Touzot M, Bohineust A, et al. Human inflammatory dendritic cells induce Th17 cell differentiation. *Immunity*. 2013;38(2):336-348.
671. Vroman H, van den Blink B, Kool M. Mode of dendritic cell activation: the decisive hand in Th2/Th17 cell differentiation. Implications in asthma severity? *Immunobiology*. 2015;220(2):254-261.
672. Nguyen H, Kuril S, Bastian D, et al. Complement C3a and C5a receptors promote GVHD by suppressing mitophagy in recipient dendritic cells. *JCI Insight*. 2018;3(24).
673. Lim H, Kim YU, Drouin SM, et al. Negative regulation of pulmonary Th17 responses by C3a anaphylatoxin during allergic inflammation in mice. *PLoS One*. 2012;7(12):e52666.
674. Kwan WH, van der Touw W, Paz-Artal E, Li MO, Heeger PS. Signaling through C5a receptor and C3a receptor diminishes function of murine natural regulatory T cells. *J Exp Med*. 2013;210(2):257-268.
675. Tu H, Burke TM, Oderup C, et al. Robust expansion of dendritic cells in vivo by hydrodynamic FLT3L-FC gene transfer. *J Immunol Methods*. 2014;413:69-73.
676. Regnier P, Vetillard M, Bansard A, et al. FLT3L-dependent dendritic cells control tumor immunity by modulating Treg and NK cell homeostasis. *Cell Rep Med*. 2023;4(12):101256.
677. D'Amico A, Wu L. The early progenitors of mouse dendritic cells and plasmacytoid predendritic cells are within the bone marrow hemopoietic precursors expressing Flt3. *J Exp Med*. 2003;198(2):293-303.
678. Pham TNQ, Meziane O, Miah MA, et al. Flt3L-Mediated Expansion of Plasmacytoid Dendritic Cells Suppresses HIV Infection in Humanized Mice. *Cell Rep*. 2019;29(9):2770-2782 e2775.
679. Aliazis K, Boussiotis VA. A four-cell pathway orchestrated by Flt3-L-dependent cDCs controls anti-tumor responses. *Cell Rep Med*. 2024;5(1):101378.
680. Sathaliyawala T, O'Gorman WE, Greter M, et al. Mammalian target of rapamycin controls dendritic cell development downstream of Flt3 ligand signaling. *Immunity*. 2010;33(4):597-606.
681. Schnare M, Barton GM, Holt AC, Takeda K, Akira S, Medzhitov R. Toll-like receptors control activation of adaptive immune responses. *Nat Immunol*. 2001;2(10):947-950.
682. Blander JM, Medzhitov R. Toll-dependent selection of microbial antigens for presentation by dendritic cells. *Nature*. 2006;440(7085):808-812.
683. Heras-Murillo I, Mananes D, Munne P, et al. Immunotherapy with conventional type-1 dendritic cells induces immune memory and limits tumor relapse. *Nat Commun*. 2025;16(1):3369.
684. Ng SL, Teo YJ, Setiagani YA, Karjalainen K, Ruedl C. Type 1 Conventional CD103(+) Dendritic Cells Control Effector CD8(+) T Cell Migration, Survival, and Memory Responses During Influenza Infection. *Front Immunol*. 2018;9:3043.
685. Lehmann CHK, Baranska A, Heidkamp GF, et al. DC subset-specific induction of T cell responses upon antigen uptake via Fcgamma receptors in vivo. *J Exp Med*. 2017;214(5):1509-1528.
686. Heger L, Hatscher L, Liang C, et al. XCR1 expression distinguishes human conventional dendritic cell type 1 with full effector functions from their immediate precursors. *Proc Natl Acad Sci U S A*. 2023;120(33):e2300343120.
687. Zaal A, Dieker M, Oudenampsen M, et al. Anaphylatoxin C5a Regulates 6-Sulfo-LacNAc Dendritic Cell Function in Human through Crosstalk with Toll-Like Receptor-Induced CREB Signaling. *Front Immunol*. 2017;8:818.
688. Hajishengallis G, Lambris JD. More than complementing Tolls: complement-Toll-like receptor synergy and crosstalk in innate immunity and inflammation. *Immunol Rev*. 2016;274(1):233-244.
689. Kwan WH, van der Touw W, Heeger PS. Complement regulation of T cell immunity. *Immunol Res*. 2012;54(1-3):247-253.

690. Raedler H, Heeger PS. Complement regulation of T-cell alloimmunity. *Curr Opin Organ Transplant*. 2011;16(1):54-60.
691. Senent Y, Remirez A, Reparaz D, et al. The C5a/C5aR1 Axis Promotes Migration of Tolerogenic Dendritic Cells to Lymph Nodes, Impairing the Anticancer Immune Response. *Cancer Immunol Res*. 2025;13(3):384-399.
692. Zaal A, Lissenberg-Thunnissen SN, van Schijndel G, Wouters D, van Ham SM, ten Brinke A. Crosstalk between Toll like receptors and C5a receptor in human monocyte derived DCs suppress inflammatory cytokine production. *Immunobiology*. 2013;218(2):175-180.
693. Raby AC, Holst B, Davies J, et al. TLR activation enhances C5a-induced pro-inflammatory responses by negatively modulating the second C5a receptor, C5L2. *Eur J Immunol*. 2011;41(9):2741-2752.
694. Zaal A, Nota B, Moore KS, Dieker M, van Ham SM, Ten Brinke A. TLR4 and C5aR crosstalk in dendritic cells induces a core regulatory network of RSK2, PI3Kbeta, SGK1, and FOXO transcription factors. *J Leukoc Biol*. 2017;102(4):1035-1054.
695. Petersen MS, Toldbod HE, Holtz S, Hokland M, Bolund L, Agger R. Strain-specific variations in the development of dendritic cells in murine bone-marrow cultures. *Scand J Immunol*. 2000;51(6):586-594.
696. Liu T, Matsuguchi T, Tsuboi N, Yajima T, Yoshikai Y. Differences in expression of toll-like receptors and their reactivities in dendritic cells in BALB/c and C57BL/6 mice. *Infect Immun*. 2002;70(12):6638-6645.
697. Lee JH, Yuk JM, Cha GH, Lee YH. Expression of cytokines and co-stimulatory molecules in the Toxoplasma gondii-infected dendritic cells of C57BL/6 and BALB/c mice. *Parasites Hosts Dis*. 2023;61(2):138-146.
698. Watanabe H, Numata K, Ito T, Takagi K, Matsukawa A. Innate immune response in Th1- and Th2-dominant mouse strains. *Shock*. 2004;22(5):460-466.
699. Kumar V, Lee JD, Clark RJ, Noakes PG, Taylor SM, Woodruff TM. Preclinical Pharmacokinetics of Complement C5a Receptor Antagonists PMX53 and PMX205 in Mice. *ACS Omega*. 2020;5(5):2345-2354.
700. Cui CS, Kumar V, Gorman DM, Clark RJ, Lee JD, Woodruff TM. In Vivo Pharmacodynamic Method to Assess Complement C5a Receptor Antagonist Efficacy. *ACS Pharmacol Transl Sci*. 2022;5(1):41-51.

# Abbreviations and Symbols

| | |
|---|---|
| -/- | knock-out |
| °C | degree Celsius |
| % | percent |
| Ab | antibody |
| ANOVA | analysis of variance |
| AP | alternative pathway |
| APC | antigen-presenting cell |
| BATF3 | Basic Leucine Zipper ATF-Like Transcription Factor 3 |
| BCR | B cell receptor |
| BM | bone marrow |
| BMDC | bone marrow-derived dendritic cells |
| BSA | bovine serum albumin |
| BST2 | BM stromal cell antigen 2 |
| C1-INH | C1 inhibitor |
| C3aR | C3a receptor |
| C4BP | C4b-binding protein |
| C5aR1 | C5a receptor 1 |
| C5aR2 | C5a receptor 2 |
| CD | cluster of differentiation |
| cDC | conventional dendritic cell |
| cDC1 | conventional dendritic cell type 1 |
| cDC2 | conventional dendritic cell type 2 |
| cDNA | Complementary DNA |
| CDP | common dendritic cell precursor |
| CFSE | carboxylfluorescein succinimidyl ester |
| CLP | common lymphoid progenitor |
| CLR | C-type lectin receptor |
| cMoP | common monocyte progenitor |
| CMP | common myeloid progenitor |
| CP | classical pathway |
| CR | complement receptor |
| CTL | cytotoxic T lymphocyte |

| | |
|---|---|
| CTSL | Cathepsin L |
| *Ctsg* | cathepsin G |
| D | day |
| DAF | decay-accelerating factor |
| DAMP | damage-associated molecular pattern |
| DC | dendritic cell |
| DEG | differentially expressed genes |
| DMEM | Dulbecco's Modified Eagle Medium |
| DNA | Deoxyribonucleic acid |
| DPBS | Dulbecco's Phosphate Buffered Saline |
| dsRNA | double-stranded RNA |
| ECS | extracellular |
| EDTA | Ethylenediaminetetraacetic acid |
| *Elane* | neutrophil elastase |
| ELISA | Enzyme-linked Immunosorbent Assay |
| ER | endoplasmic reticulum |
| ERK | extracellular signal-regulated kinases |
| et al. | et alia, and others |
| FACS | fluorescence activated cell sorting |
| Factor P | Properdin |
| FasL | Fas ligand |
| FBS | fetal bovine serum |
| FC | flow cytometry |
| FcγR | Fc receptors for IgG |
| FCS | fetal calf serum |
| FITC | fluorescein isiothiocyanate |
| Flt3L | Fms-like tyrosine kinase receptor-3 ligand |
| FFAR2 | free fatty acid receptor 2 |
| FH | factor H |
| FI | factor I |
| FMO | fluorescence minus one |
| FSC | Forward scatter |
| g | gram (unit) |

| | |
|---|---|
| GEMs | Gel Beads in emulsion |
| GC | Germinal center |
| GM-CSF | granulocyte-macrophage colony stimulating factor |
| GMDP | granulocytes, monocytes, and DC precursor |
| GPCR | G-protein–coupled receptor |
| GRK | GPCR kinases |
| GVHD | graft-versus-host disease |
| h | hour |
| HRP | Horse-radish-peroxidase |
| HSPC | hematopoietic stem and progenitor cell |
| HSC | hematopoietic stem cell |
| i.e. | In example |
| i.p. | intraperitoneal |
| IC | isotype control |
| ICS | intracellular |
| ID2 | inhibitor of DNA binding 2 |
| IL | interleukin |
| ILC | innate lymphoid cell |
| IMDM | Iscove’s Modified Dulbecc’s Medium |
| IRF | interferon regulatory factor |
| $Lin^-$ | lineage-negative |
| LP | lectin pathway |
| LPS | lipopolysaccharide |
| LTβR | lymphotoxin beta receptor |
| MAC | membrane attack complex |
| MACS | magnetic-activated cell sorting |
| MASP | MBL–associated serine proteases |
| MC | mast cell |
| MDP | monocyte and dendritic cell precursor |
| MFI | mean fluorescence intensity |
| mg | milligram |
| MHC | major histocompatibility complex |
| Min | minute |

| | |
|---|---|
| ml | milliliter |
| moDC | monocyte-derived dendritic cell |
| mTOR | mammalian target of rapamycin |
| µl | micro liter |
| NF-κB | nuclear factor kappa B |
| NK | natural killer cell |
| NKT | natural killer T cell |
| NLR | NOD-like receptor |
| NLRP | Nucleotide-binding Oligomerization domain (NOD) domain, a Leucine-rich Repeat (LRR) domain, and a PYD domain-containing protein |
| NO | nitric oxide |
| NSP | neutrophil serine protease |
| OPD | o-Phenylenediamine dihydrochloride |
| OVA | ovalbumin |
| p | pico |
| PAMP | pathogen-associated molecular pattern |
| PBS | phosphate buffered saline |
| pDC | plasmacytoid dendritic cell |
| PE | phycoerythrin |
| PFA | paraformaldehyde |
| PI3K | phosphatidylinositol-4,5-bisphosphate 3-kinase |
| PKB | protein kinase B |
| pMHC | peptide–MHC complexes |
| PRM | pattern-recognition molecule |
| PRR | pattern recognition receptor |
| *Prtn3* | proteinase 3 |
| Rag2 | Recombinase activating gene 2 |
| RBC | red blood cell |
| RCA | regulators of complement activation |
| RNA | Ribonucleic acid |
| ROS | reactive oxygen species |
| RT | room temperature |
| scRNA-seq | Single-cell RNA sequencing |

| | |
|---|---|
| SEM | Standard error of the mean |
| SiglecH | sialic acid–binding Ig-like lectin H |
| siRNA | small interfering RNA |
| SSC | Side scatter |
| TCC | terminal complement complex |
| TCM | central memory T cell |
| TCR | T cell receptor |
| TEFF | Effector T cell |
| TEM | Effector memory T cell |
| Tfh | T follicular helper cell |
| tg | transgenic |
| Th | T helper cell |
| TLR | Toll-like receptor |
| TMB | tetramethylbenzidine |
| TMP | memory precursors T cell |
| TP | terminal pathway |
| Treg | regulatory T cells |
| TRM | tissue-resident memory T cell |
| qPCR | quantitative polymerase chain reaction |
| UMAP | uniform manifold approximation and projection |
| vsRNA | virus-derived small RNA |
| WT | wild type |
| ZBTB46 | Zinc Finger and BTB Domain Containing 46 |
| Zeb2 | Zinc Finger E-Box Binding Homeobox 2 |

# List of figures

# List of tables

# Conference contributions

## Poster presentation

**Differential roles of C3aR and C5aR1 in hematopoietic stem cell differentiation and function of type 1 and 2 conventional dendritic cells**

Alicja A. Nowacka, Sven Geisler, Gabriele Köhl, Chandrashekhar Pasare, Jörg Köhl

19th EMCHD, Lubeck, Germany 2024

**Anaphylatoxin receptors regulate the differentiation and function of dendritic cells subsets from bone marrow-derived precursors**

Alicja A. Nowacka, Jörg Köhl

Immunology Retreat, College Corner, Ohio, USA 2022

## Oral presentation

**Anaphylatoxin receptors as regulators of dendritic cell differentiation and function**

Alicja A. Nowacka, Sven Geisler, Jörg Köhl

AKKS, Hamburg, Germany 2025

**Anaphylatoxin receptors as regulators of dendritic cell differentiation and function**

Alicja A. Nowacka, Jörg Köhl

CORVOS Symposium, Obergurgl, Austria 2025

**The role of anaphylatoxin receptors in the differentiation & function of dendritic cell subsets from BM-derived precursors**

Alicja A. Nowacka, Sven Geisler, Chandrashekhar Pasare, Jörg Köhl

AKKS, Tutzing, Germany 2024

**The role of anaphylatoxin receptors in the differentiation & function of dendritic cell subsets from BM-derived precursors**

Alicja A. Nowacka, Jörg Köhl

CORVOS Symposium, Obergurgl, Austria 2024

**C5a receptor 1 controls antigen and TLR-driven T cell proliferation and differentiation by splenic conventional type 2 dendritic cells**

Alicja A. Nowacka, Chandrashekhar Pasare, Jörg Köhl

29th International Complement Workshop (ICW), Newcastle, England 2023

**Anaphylatoxin receptors regulate the differentiation and function of dendritic cells subsets from bone marrow-derived precursors**

Alicja A. Nowacka, Sven Geisler, Chandrashekhar Pasare, Jörg Köhl

18th EMCHD, Bern, Switzerland 2022

**Anaphylatoxin-mediated regulation of conventional dendritic cell differentiation and function**

Alicja A. Nowacka, Sven Geisler, Chandrashekhar Pasare, Jörg Köhl

AKAI, Marburg, Germany 2022

**Anaphylatoxin-mediated regulation of conventional dendritic cell differentiation and function**

Alicja A. Nowacka, Jörg Köhl

AKKS, Tutzing, Germany 2022

**C5a/C5aR1 axis activation in conventional pulmonary dendritic cells as a regulator of pulmonary tolerance**

Alicja A. Nowacka, Dominika Stronczek, Konstantina Antoniou, Jörg Köhl

AKKS, Online, Germany 2021

## Awards

**ECN Poster Prize 2024** awarded by the European Complement Network Committee on the occasion of the 19th European Meeting on Complement in Human Disease (Lubeck, Germany) for an excellent poster

**ICW 2023 Travel Award** awarded by the Local Organizing Committee and the International Complement Society (ICS) and the ICS Council for outstanding scientific contribution to ICW2023 (Newcastle, England)

**EMCHD 2022 Travel Award** awarded by the Committee of the 18th European Meeting in Complement for Human Disease (Bern, Switzerland) for an oral presentation entitled *Anaphylatoxin receptors regulate the differentiation and function of dendritic cells subsets from bone marrow-derived precursors*

**Scholarship** from Lund University for students; 2017-2018, 2019-2020

**Best Students of the University of Gdansk**, Faculty of Chemistry (XIII Edition) 2017

**Scholarship** for Academic Merit from University of Gdansk 2015-2018

# List of publications

**Nowacka A. A**., Einwohlt P., Ohms M., Geisler S., Abdala Y., Fähnrich A., Köhl J. *C3a and C5a regulate DC progenitor homeostasis and their differentiation into cDC1 and cDC2 subsets.* (manuscript in preparation)

**Nowacka A. A,** Sordo Vieira L., Petr V., Fageräng B., Würzner R., Ohms M. *The grand escape – how pathogens outsmart the human complement system.* Immunobiol. 2025 230:153126 *https://doi.org/10.1016/j.imbio.2025.153126*

Laumonnier Y., Korkmaz R. U., **Nowacka A. A**., Köhl J. *Complement-mediated immune mechanisms in allergy.* Eur. J. Immunol. 2023 53: 2249979 *https://doi.org/10.1002/eji.202249979*

Kremlitzka, M., Colineau L., **Nowacka A. A.**, Mohlin F. C., Wozniak K., Blom A. M., King B. C. *Alternative translation and retrotranslocation of cytosolic C3 that detects cytoinvasive bacteria.* Cell. Mol. Life Sci. 2022 79: 291 *https://doi.org/10.1007/s00018-022-04308-z*

Kremlitzka, M., **Nowacka A. A.**, Mohlin F. C., Bompada P., Marinis Y. D., Blom A. M. *Interaction of Serum-Derived and Internalized C3 with DNA in Human B Cells – A Potential Involvement in Regulation of Gene Transcription.* Front. Immunol. 2019 10:493 *https://doi.org/10.3389/fimmu.2019.00493*

# Acknowledgement

This PhD has been a truly life-changing and often challenging journey, one that would not have been possible without the support and guidance of many people. Completing this work at ISEF has provided an environment in which I could grow both professionally and personally. I have been especially fortunate to collaborate with inspiring colleagues whose generosity, encouragement, and expertise have been indispensable for bringing this thesis to completion.

My heartfelt thanks go to:

**Prof. Dr. med. Jörg Köhl**, my doctoral advisor, for his unwavering support and mentorship throughout my PhD studies. His thoughtful guidance, combined with the freedom to pursue my own scientific questions, has profoundly shaped both my research and my approach to science. I am deeply grateful for the opportunity to work with him as part of the IRTG 1911 and for his trust in my work, which enabled me to present our findings at numerous national and international conferences, for which I am extremely thankful. I greatly value his encouragement, his immense knowledge, and the many quick scientific conversations that so often evolved into long, inspiring brainstorming sessions pushing me to think outside the box. His enthusiasm and endless ideas motivated me to keep learning and to venture into unexplored directions. I am especially thankful for all the support I received during my stay in Cincinnati; without his guidance and constant feedback, this PhD would not have been possible.

**Chandrashekhar Pasare, DVM PhD**, who served as my second supervisor within the IRTG 1911, for providing an outstanding research environment during my six-month stay in his laboratory in Cincinnati. His guidance, continuous feedback, regular weekly meetings, and even spontaneous lab discussions were invaluable, making the immunological work carried out there possible. I am especially grateful that he meticulously organized my research stay in the United States in advance, enabling me to begin experiments immediately upon arrival.

**Prof. Dr. rer. nat. Kathrin Kalies** for kindly accepting my invitation as a second referee and **Prof. Dr. rer. nat. Norbert Tautz** for accepting my invitation as the examination chair.

The six-month research stay at CCHMC was an exceptional experience, offering firsthand insight into how research is conducted in the United States. I was deeply impressed by the motivation, passion, and excitement-driven mindset of the scientists there, and by how they engaged with my project, often posing questions that, I must admit, had not even occurred to me before.

**Julie Rogers**, for expertly organizing my stay in Cincinnati and providing care once I arrived there.

**Ian P. Lewkowich, PhD** for generously providing *C5ar1*$^{-/-}$ mice essential to the research I conducted in Cincinnati.

**Sven Geisler, PhD** from CAnaCore, for performing my numerous cell sortings, without his help, this research would not have been possible. I also thank the Flow Core family

at CCHMC for FACS-sorting training, and **Irene Saha**, **PhD**, for her constant sorting support on a regular basis in Cincinnati.

**Anke Fähnrich, PhD** and members of her group, for conducting the scRNA-seq experiments and analyzing the data.

All former and current members of the **Köhl** lab for being fantastic friends throughout my PhD, for creating a warm working atmosphere in the lab and during social gatherings and joint activities outside of work. In particular, I would like to thank **Mareike Ohms, PhD,** for her unwavering support, scientific discussions on DC topics, brainstorming sessions, and encouragement during difficult times. **Janti Haj Ahmad**, my office mate and daily memes provider, for keeping my spirits high even in the toughest moments; and for his invaluable help during my unexpected hospital stay after a spontaneous accident, when he kindly brought my belongings home to the sixth floor. A very special thanks to **Philip Einwohlt, PhD**, for meticulously preparing the scRNA-seq figures exactly as I envisioned them. Finally, my sincere gratitude goes to all the technicians in the Köhl group: **Grabriele Köhl**, for establishing a safe working environment for everyone, managing mouse breeding and orders, and sharing her qPCR expertise; and **Sina Borus**, for keeping the lab running smoothly by solving technical issues and ensuring the seamless flow of experiments, for her joyful company in the lab, her understanding, her gentle reminders when lab time prevented tidying up, and her generous help with printing.

Members of the **Pasare** lab, for being fantastic friends during my stay in Cincinnati, for inspiring scientific discussions, rapid problem-solving, lab support, and the wonderful times we shared after experiments, hanging out and learning about each other's cultures. Special thanks to **Hannah Meibers, PhD**, and **Kiana Kawarizadeh** for excellent scientific discussions and assistance in the animal house. **Lisa Waggoner** for organizing my lab space Cincinnati, managing mouse breeding and care, and providing essential technical support with experiments; **Irene Saha, PhD,** for training me in B16-Flt3L melanoma cells injections and joining me as part of the night-shift crew during those long days of seemingly never-ending experiments; and **Kathy Warrick,** for her help with experiments during the Thanksgiving holiday, allowing me to visit and celebrate with my family in Chicago.

**My family and friends,** for their encouragement and advice throughout my studies. My parents, for their unfailing support and continuous encouragement during my years of study, research, and thesis writing; for always standing by my side, especially during difficult times. My lovely grandma, who never failed to ask how the research was going and motivated me throughout the dissertation writing process. My siblings, who work in completely different fields, were always curious about my experimental results and research conclusions. A special thank you to Ben, for his unconditional support, encouraging spirit, endless motivation, and care, celebrating successes together and lifting me up in times of need. Even though his field of expertise is entirely different, he always listened patiently to my scientific ideas and brainstorming sessions, offering suggestions with genuine happiness and excitement.